Investigating the regulation of APOBEC3A and APOBEC3B expression in keratinocytes

A thesis submitted to the University of Kent for the degree of

Ph.D Cell Biology in the Division of Natural Sciences

September 2021

Nicola Smith

School of Biosciences

I Declaration

No part of this thesis has been submitted in support of an application for any degree or qualification of the University of Kent or any other University or institute of learning.

Nicola Smith

September 2021

II Acknowledgements

First and foremost, I thank Tim Fenton for giving me the opportunity to embark on this project, and his endless support and guidance throughout.

I would also like to thank members of the Fenton, Ellis and Garrett labs, especially Maxmilan Jeyakumar for his friendship and all his much appreciated help; also Paige Policelli, for her enthusiastic assistance including near-industrial scale cell lysate preparations; our Erasmus student, Virginia Di-Bella, for numerous qPCR assays and contributions towards the A3B work; and Peter Ellis, Marie Claire Aquilina and Serena Torrini for their help and guidance with flow cytometry.

Thanks also to the Rosetree Trust for facilitating additional research, and to all our collaborators including Simak Ali and Manikandan Periyasamy at Imperial College London; Rémi Buisson and Pégah Jalil at the University of California; and John Maciejowski and Alexandra Danenberg at the Memorial Sloan Kettering Cancer Centre, New York.

Finally, a big thank you to my mum and my brother for all their support and encouragement throughout my studies, and to my children for all their patience and understanding.

III Contents

IV List of Figures

V Abbreviations

ACF	APOBEC1 complementation factor
ADAR	Adenosine deaminases acting on RNA
AP site	Apurinic/apyrimidinic site
APE-1	Apurinic-apyrimidinic endonuclease 1
APOBEC	Apolipoprotein B mRNA editing enzyme catalytic polypeptide-like
ATM	Ataxia-telangiectasia-mutated
ATR	Ataxia Telangiectasia and Rad3-related
BER	Base-excision repair
cc-DNA	Covalently closed circular DNA
CD	Cluster of differentiation
CDK	Cyclin-dependent kinase
CHK	Checkpoint kinase
cGAMP	Cyclic guanosine monophosphate–adenosine monophosphate
cGAS	Cyclic GMP-AMP synthase
CRM1	Chromosomal maintenance 1 (also known as exportin 1)
CSR	Class switch recombination
CTD	C-terminal catalytic domain
DAG	Diacylglycerol
DAI	DNA-dependent activator of interferon-regulatory factors
DAMP	Danger associated molecular pattern
DC	Dendritic cell
DSB	Double strand break
E2F1	E2F transcription factor 1
EBV	Epstein-Barr virus
EGF	Epidermal growth factor
EGFR	Epidermal growth factor receptor
ERK	Extracellular signal regulated kinase
GPCR	G-protein coupled receptor
HBV	Hepatitis B virus
HCMV	Human cytomegalovirus

He-PTP	Haematopoietic protein phosphatase
HIV	Human Immunodeficiency Virus
HNSCC	Head and neck squamous cell carcinoma
HSP	Heat shock protein
HSV	Herpes Simplex Virus
HPV	Human Papillomavirus
IFI16	IFN-γ-inducible protein 16
IFN	Interferon
IL	Interleukin
IP3	Inositol trisphosphate
IRF	Interferon-regulatory factor
ISG	Interferon-stimulated gene
ISRE	IFN-stimulated response element
JAK	Janus protein tyrosine kinases
JNK	c-Jun NH2-terminal protein kinase
LINE-1	Long interspersed nucleotide sequence-1
LPA	Lysophosphatidic acid
LPS	Lipopolysaccharide
MAPK	Mitogen-activated protein kinase
MAV	Mitochondrial anti-viral signalling
MDDC	Monocyte-derived dendritic cells
MEK	Mitogen-activated protein kinase kinase
MMTV	Mouse mammary tumour virus
mTORC1	Mammalian target of rapamycin complex 1
NIKS	Near-normal immortalised keratinocyte cells
NES	Nuclear export signal
NF-κB	Necrosis factor κB
NLS	Nuclear localisation signal
NTD	N-terminal catalytic domain
PAMP	Pathogen associated molecular pattern
PBMC	Peripheral blood mononuclear cells
PCR	Polymerase chain reaction

PD-L1	Programmed death-ligand 1
PI3K	Phosphoinositide-3-kinase
PKA	Protein Kinase A
PKC	Protein Kinase C
PLC	Phospholipase C
PMA	Phorbol 12-myristate 13-acetate
RAF	Rapidly accelerated fibrosarcoma
RAS	Rat sarcoma oncogene
Rb	Retinoblastoma tumour suppressor protein
RIG-I	Retinoic acid-inducible gene 1
SHM	Somatic hypermutation
STAT	Signal transducer and activator of transcription
STING	Stimulator of interferon gene
TBK1	TANK-binding kinase 1
TLR	Toll-like receptor
TNF	Tumour necrosis factor
TEAD	Transcriptional enhancer factor domain
TGF-β	Transforming growth factor-β
UNG	Uracil-DNA glycosylase
UTR	Untranslated region
VIF	Viral Infectivity Factor

VI Abstract

APOBEC3A (A3A) and APOBEC3B (A3B) can disrupt viral and retrotransposon replication through deamination, while off-target activity represents a major source of mutations in epithelial cancers. A3A additionally has an emerging role as an RNA editor within immune cells. To explore their function and regulation in normal epithelia, we used near-normal human keratinocyte cells (NIKS) in which CRISPR-Cas9 editing had been used to delete endogenous A3A, or to epitope-tag A3A or A3B. Having observed that A3A induction by known inducers (phorbol ester and interferon-α) occurs in a subset of cells and is sensitive to contact inhibition, we hypothesised cell cycle-dependent regulation and discovered striking induction upon cell cycle re-entry induced by Epidermal Growth Factor (EGF) in NIKS, primary keratinocytes (NHEK), and breast mammary epithelial cells (MCF10A). We found A3B was also cell-cycle related and specifically upregulated during G2/M phase of proliferating cells. Surprisingly, high A3A levels appear to persist through S-phase without overt genotoxic effects. Instead, we observe high levels of A3A-dependent RNA editing, the significance of which remains to be determined. A3A induction is blunted in cancer cell lines and in NIKS expressing human papillomavirus oncogenes, and A3A deletion significantly increased proliferation of NIKS. Together, our findings uncover EGF signalling as a potent inducer of A3A in epithelial cells with implications for cell cycle regulation and carcinogenesis.

1 Introduction

1.1 APOBEC cytosine deaminase family

1.1.1 Background

The first instance of RNA editing in a vertebrate was described in 1987, involving the post-transcriptional deamination of cytosine (C) to uracil (U) at position C666 and thus the introduction of a premature stop codon and formation of a truncated version of apolipoprotein B (apoB) messenger RNA (mRNA), a component of lipid transportation in the small intestine (Chen *et al.*, 1987; Powell *et al.*, 1987). The 27-kDa catalytic enzyme responsible, encoded at human chromosome 12p13, was later given the nomenclature: apolipoprotein B mRNA editing enzyme catalytic polypeptide-like (APOBEC1 (A1)) and forms the founding member of this cytosine deaminase family (Navaratnam *et al.*, 1993; Davidson *et al.*, 1995). The successive discoveries of APOBEC2 (A2), activation-induced deaminase (AID), the seven APOBEC3 (A3) genes, and APOBEC4 (A4) completed the eleven membered family, each with diverse physiological functions.

The APOBEC family members each have a conserved zinc-coordinating motif: His-X_1-Glu-$X_{23–28}$-Pro-Cys-$X_{2–4}$-Cys, in which X denotes any amino acid residue. The Zn^{2+} ion is required for catalytic activity and coordinated by the histidine (His) and cysteine (Cys) residues; whereas the catalytic residue, glutamic acid (Glu), functions as a proton shuttle during the deamination reaction (Betts *et al.*, 1994; Wedekind *et al.*, 2003).

AID, A1, A2, A3A, A3C, A3H and A4 each contain a single N-terminal catalytic domain (NTD), whereas A3B, A3D, A3F and A3G are double domain enzymes containing both a catalytically active C-terminal domain (CTD), and an N-terminal pseudocatalytic domain (Jarmuz *et al.*, 2002; Shandilya, Bohn and Schiffer, 2014). The catalytic domains of the APOBEC3 family are further subdivided into Z1, Z2 or Z3 (LaRue *et al.*, 2009), as shown in Figure 1-1.

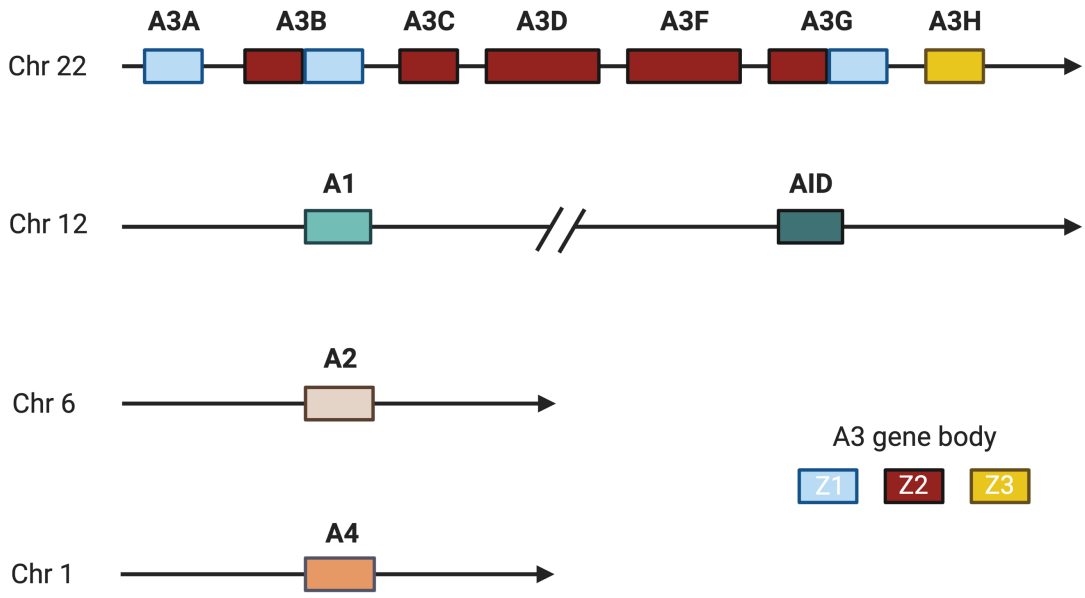

Figure 1-1 The APOBEC family of cytosine deaminases.
A schematic of the genes encoding the 11-member APOBEC family in humans. A3A-3H are encoded in tandem on chromosome (Chr) 22 of which A3A, A3C and A3H have single zinc (Z)-coordinating domains; whereas A3B, A3D and A3F are double domains enzymes. The A3 catalytic domains are subdivided into Z1, Z2, and Z3 domains, shown in blue, red, and yellow respectively. AID and A1 are single-domain enzymes and are encoded ~1 Mb apart on chromosome 12; A2 and A4 also contain single-domains and are encoded on chromosomes 6 and 1 respectively.

1.1.2 APOBEC1

Present only in mammals and well characterised for the apoB mRNA editing role in the small intestine (Mehta *et al.*, 2000), additional characteristics of A1 include its preference for AU-rich sequences in RNA (Anant, MacGinnitie and Davidson, 1995); the ability to deaminate single-stranded DNA (ssDNA) (Petersen-Mahrt and Neuberger, 2003) including that mouse A1 can induce somatic mutations in nuclear DNA (Caval *et al.*, 2019); and its capacity to inhibit endogenous retrovirus sequences and the transposition of long interspersed element-1 (LINE-1) (Ikeda *et al.*, 2011).

Paradoxically, despite apoB editing being a nuclear event, A1 is predominantly a cytoplasmic protein (Blanc *et al.*, 2001); editing is facilitated through nuclear shuttling due to an N-terminal nuclear localisation signal (NLS), a C-terminal nuclear export sequence (NES), as well as interactions with the chaperone proteins: APOBEC1 complementation factor (ACF) (Yang, Yang and Smith, 1997; Blanc, Kennedy and Davidson, 2003), or RBM47 (Fossat *et al.*, 2014).

Whilst A1 expression is mostly restricted to the small intestine where it is constitutively expressed, a study of herpes simplex virus (HSV-1), the causative agent of encephalitis, found A1 was also induced in neuronal cells during disease in a rat model and capable of both editing viral DNA and inhibiting viral replication (Lada *et al.*, 2011). Similarly, rat but not human A1 was found to be a potent inhibitor of the human immunodeficiency virus (HIV-1) (Bishop *et al.*, 2004), a finding that has since been extended to include A1s from a range of small mammals (Ikeda *et al.*, 2008).

These findings that A1 could deaminate ssDNA in addition to RNA suggested a potential role for mutagenic activity in the development of human cancers (Harris, Petersen-Mahrt and Neuberger, 2002), and A1s mutagenic potential has subsequently been demonstrated in that over-expression in transgenic mice or rabbits leads to the development of hepatocellular carcinoma (Yamanaka *et al.*, 1995).

Additionally, the upregulation of A1 together with its signature mutations has been seen in human esophageal adenocarcinomas, though the involvement of other APOBEC family members could not be excluded (Saraconi *et al.*, 2014).

Furthermore, A1 edits a cytidine to uridine in an arginine codon in the mRNA of neurofibromatosis type I (NF1) gene that encodes the neurofibromin tumour suppressor protein, creating an in-frame translation stop codon and inactivation of gene transcripts that potentiates a functional loss of tumour suppressor activity (Skuse *et al*., 1996). NF1 mRNA editing occurs at low levels in normal peripheral blood leukocytes, but was found to be upregulated in rat hepatoma and human neural tumour cell lines (Skuse *et al*., 1996).

A1 can also bind a consensus site at the 3' untranslated region (UTR) of the oncogene c-MYC, thereby increasing its mRNA stability (Anant and Davidson, 2000), and a transcriptome-wide comparative RNA sequencing screen validated 32 further APOBEC1 mRNA editing targets located in AU-rich segments at the 3'UTR of mRNAs (Rosenberg *et al.*, 2011).

1.1.3 APOBEC2

The cloning of APOBEC2 (A2) added an evolutionary related member to the cytosine deaminase family; this was mapped to human chromosome 6p21 and found to be exclusively expressed in heart and skeletal muscle (Liao *et al.*, 1999). Though not exhibiting RNA or DNA editing activity (Mikl *et al.,* 2005) and little is known about the function of this family member in humans, the zinc-coordinating domains of zebrafish A2a and A2b were found to be important for retina and optic nerve regeneration, a role that could be substituted using human A2 (Powell, Elsaeidi and Goldman, 2012; Powell, Cornblath and Goldman, 2014).

1.1.4 Activation induced deaminase (AID)

The same year as the discovering of A2, stimulation of a murine B-cell lymphoma line followed by cDNA library screening led to the identification of activation-induced cytidine deaminase (AID), the third family member (Muramatsu *et al.*, 1999).

Closely related to A1 and mapped to chromosome 12p13 (Muto *et al.,* 2000), abundant expression was found in lymphoid organs and specifically located in germinal centre B-cells (Muramatsu *et al.*, 1999). AID is also a nucleo-cytoplasmic shuttling protein, facilitated by its N-terminus NLS and C-terminal NES (Ito *et al.*, 2004). Though A1 was the first member of the cytosine deaminase family to be discovered and cloned, phylogenetic studies suggest that both A1 and A3 may have evolved from AID through gene duplication (Conticello *et al.,* 2005).

As opposed to A1s predominant function as an RNA editor, the DNA editing capacity of AID has a very important physiological role in antibody diversification (Muramatsu *et al.*, 2000; Revy *et al.*, 2000). The need to generate a repertoire of high-affinity antibodies has evolved as part of the immune response against infection and this is orchestrated through variable (V), diversity (D), joining (J) gene recombination (V(D)J recombination), class switch recombination (CSR), and somatic hypermutation (SHM) (Chi, Li and Qiu, 2020).

With the exception of V(D)J recombination, these processes rely on the activity of AID (Muramatsu *et al.*, 2000; Harris *et al.*, 2002). Following completion of V(D)J recombination, mature B lymphocytes express low-affinity IgM on their surface (Pham *et al.*, 2003); CSR allows for further diversification, enabling them to express IgA, IgG or IgE class antibodies which is facilitated through intrachromosomal DNA recombination of the N-terminal V region with a different C-terminal heavy chain constant (C_H) region (Milstein and Neuberger, 1996).

With the assistance of the enzymes uracil-DNA glycosylase (UNG) and apurinic-apyrimidinic endonuclease 1 (APE1) (Rada *et al.*, 2002; Masani, Han and Yu, 2013), AID initiates this process through deamination of deoxycytidine (dC) residues at target intronic sites called switch regions which are located upstream of each of the C_H region genes (Muramatsu *et al.*, 1999; Bross *et al.*, 2002). Patients defective in AID therefore have high levels of IgM-type antibody only (hyper-IgM syndrome 2), and thus have a weakened immune system and suffer from recurrent infections (Revy *et al.,* 2000).

SHM promotes antibody diversity through the accumulation of AID-mediated point mutations in the V genes, linked with positive selection for rare clones that have increased affinity for the antigen (Griffiths *et al.*, 1984; Lau and Brink, 2020); AID mediates this through its preference for deamination of cytosine residues within a WRC (W = A/T, R = A/G) consensus site with the formation of U:G lesions (Pham *et al.*, 2003).

Replication before removal of the resulting uracil leads to C-to-T transitions, whereas excision of the uracil by the UNG enzyme can cause both C-to-T transitions and C-to-G transversions at C:G pairs (Petersen-Mahrt and Neuberger, 2003; Henderson and Fenton, 2015).

However, deregulation of AID may lead to somatic mutations from which lymphocyte malignancies arise: it has been shown that constitutive expression of AID in transgenic mice leads to T-cell lymphomas and lung adenocarcinomas (Okazaki *et al*., 2003), and that AID mediates IgH–MYC translocations in B-cells that are characteristic in Burkitt's lymphomas (Ramiro *et al*., 2004).

Furthermore, high expression of AID is induced in gastric epithelial cells by *Helicobacter pylori* infection, leading to mutations in TP53, cyclin dependent kinase (CDK) inhibitor 2A (CDKN2A) and CDKN2B tumour suppressor genes and thus forms a potential mechanism that links these infections with gastric cancers (Matsumoto *et al.*, 2007, 2010).

1.1.5 APOBEC3 family

Psoriasis is a hyperproliferative inflammatory disease of the dermis with aberrant differentiation and an altered Protein Kinase C (PKC) signalling pathway (Raynaud and Evain-Brion, 1991). Stimulation of PKC signalling in normal primary keratinocytes using phorbol 12-myristate 13-acetate (PMA) and phorbol 12-13 dibutyrate (PDBu), led to the upregulation and identification of two proteins (and found also to be present in psoriatic lesions) that were consequently named phorbolin-1 and phorbolin-2 (Rasmussen and Celis, 1993).

Through molecular cloning and chromosomal mapping to position 22q13, phorbolin-1 and phorblin-2 were shown to have 44% similarity to A1 (Madsen *et al*., 1999). The subsequent discovery of a cluster of seven APOBEC related genes arranged in tandem on human chromosome 22, designated APOBEC3A to 3G (Jarmuz *et al.*, 2002), led to the renaming of phorbolin-1 and phorbolin-2 to APOBEC3A (A3A) and APOBEC3B (A3B) respectively. The number of A3 genes varies between vertebrate species (the mouse genome encodes only one A3 protein (mA3) for example) (Su *et al.*, 2004).

The APOBEC3 family are interferon (IFN) stimulated cytosine deaminase enzymes that have diverse functions including the restriction of mobile genetic elements, and prominent roles in innate immunity through the deamination of viral DNA which leads to genomic mutations that restrict replication (Koito and Ikeda, 2013; Harris and Dudley, 2015); of which the antiretroviral activity of A3G against HIV-1 is the most highly characterised example (Mangeat *et al.*, 2003).

1.1.6 APOBEC3 signature mutations

A potential consequence of APOBEC3-mediated immunoprotection is that aberrant induction of these enzymes exposes host-DNA to the risk of acquired mutations. Accordingly, APOBEC3 signature mutations (thought to be largely due to A3A and A3B) form the second-most prominent source of DNA mutagenesis (in ~15% of all sequenced tumours) and are present in 50% or more of certain cancer types including breast, lung, and those of human papillomavirus (HPV) associated cervix and head-and-neck cancers. Furthermore, sublethal levels of deamination by APOBEC3 enzymes may contribute to viral evolution, increase tumour heterogeneity, and drive chemotherapeutic resistance (Alexandrov *et al.*, 2013, 2020; Taylor *et al.*, 2013; Burns *et al.*, 2013; Burns, Temiz and Harris, 2013; Roberts *et al.*, 2013; Logue *et al.*, 2014; Swanton *et al.*, 2015; Henderson and Fenton, 2015; Buisson *et al.*, 2019; Petljak *et al.*, 2019; Jalili *et al.*, 2020).

A3A and A3B both deaminate ssDNA at thymidine-phosphate-cytosine (TpC) motifs preferentially located on the lagging-strand template of DNA replication (which undergoes longer exposure as ssDNA due to discontinuous replication) (Okazaki *et al.*, 1968; Haradhvala *et al.*, 2016), with an additional preference for non-methylated cytosines in the TpCpG context (Seplyarskiy *et al.*, 2016).

Their signature mutations are distinguishable in that A3B favours deamination of cytosines within an RTCA motifs (R denotes a purine), whereas A3A favours deamination at a YTCA sequence (Y denoting a pyrimidine) (Chan *et al.*, 2015).

Following cytosine deamination the resulting uracil (dU) is normally excised by UNG in the base excision repair (BER) pathway and the cytosine is replaced (Lindahl, 1982). However, if translesion synthesis polymerases (TLS) replicate over the abasic site before repair is completed, they most commonly insert a dA in the daughter strand (known as the 'A rule', as shown in Figure 1-2) resulting in fixation of a C-to-T transition in the subsequent round of replication (Henderson and Fenton, 2015). C-to-T transitions can also arise from replication that occurs before the uracil removal by UNG, resulting in dA incorporation into the daughter strand. An alternative low-fidelity TLS polymerase, Rev1, can instead insert dC at abasic sites which subsequently results in C-to-G transversions (Chan, Resnick and Gordenin, 2013; Taylor *et al.*, 2013); if deamination occurs in close proximity on both strands, double-strand breaks (DSBs) can arise (reviewed by Harris, 2015).

Whilst the majority of APOBEC3 mutations are dispersed across the genome (Nik-Zainal *et al.*, 2012; Burns *et al.*, 2013; Burns, Temiz and Harris, 2013; Roberts *et al.*, 2013; Seplyarskiy *et al.*, 2016), a fraction of APOBEC3 mutations occur in clusters termed "*kataegis*" which are more highly enriched within 10 kb from DNA double-strand breakpoints (Nik-Zainal *et al.*, 2012). The A3A mutation signature is most predominant within cervical, head and neck, lung, breast and endometrial tumours; whilst A3B mutations are predominant within tumours of the breast, kidney and sarcoma (Burns *et al.*, 2013). Furthermore, A3B mRNA is highly upregulated in the majority of oestrogen receptor-positive breast tumours which correlates with poorer clinical outcomes and promotes drug resistance (Sieuwerts *et al.*, 2014; Law *et al.*, 2016).

High A3B expression is additionally a poor prognostic factor for renal cancer and multiple myeloma patients (Walker *et al.*, 2015; Xu *et al.*, 2015), and a 29.5 kb germline deletion that creates a A3A_B hybrid (transcribed as the A3A coding region and the A3B 3'-UTR) is associated with an age related increased risk of lung and prostate cancer (<50 years) (Nik-Zainal *et al.*, 2014; Gansmo *et al.*, 2017).

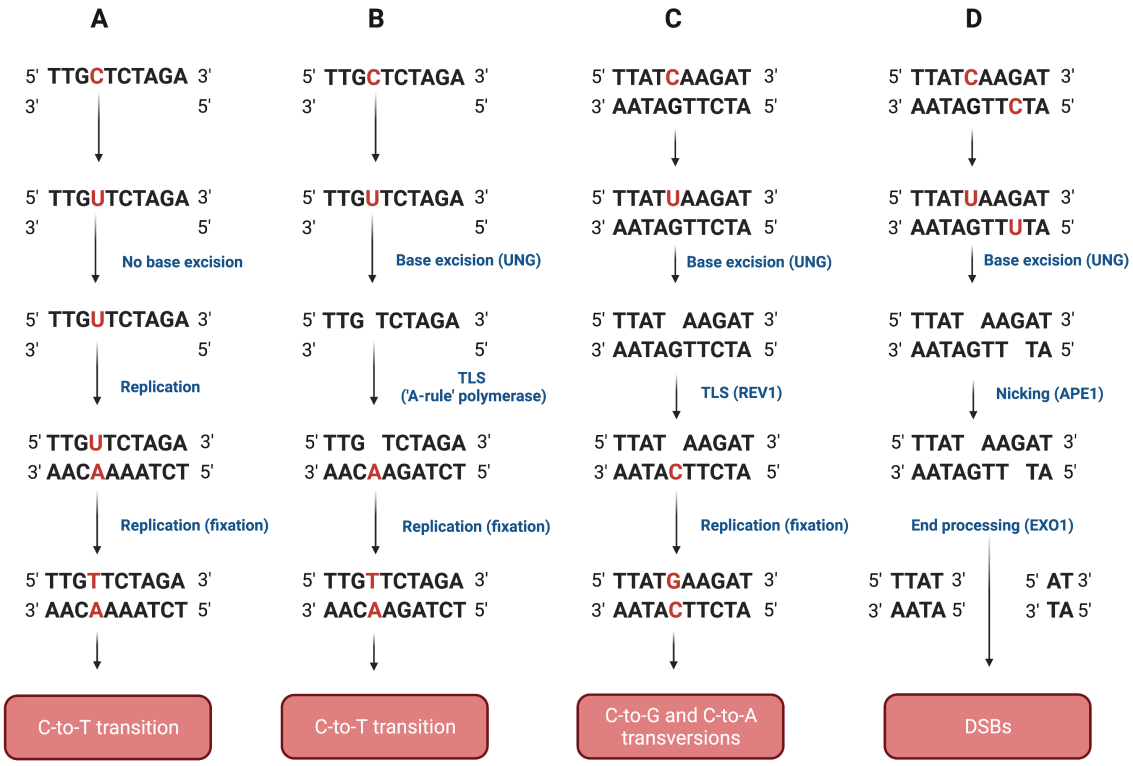

Figure 1-2 APOBEC3 signature mutations.
(A) Replication that occurs before the removal of uracil arising from APOBEC3-mediated cytosine deamination results in dA incorporation into the daughter strand and subsequent C-to-T transitions. **(B)** Uracils removed by uracil-DNA glycosylase (UNG) in the normal process of base excision repair yields an abasic site. Translesion synthesis polymerases (TLS) replicate over the site and most commonly insert a dA in the daughter strand (the 'A-rule') leading to a C-to-T transition. **(C)** Low fidelity TLS polymerase REV1 inserts dC at abasic sites which results in C-to-G transversions. **(D)** Deamination of bases on opposing strands can lead to DSBs.

1.1.7 Involvement of APOBEC3s in HPV associated cancers

HPVs are small, non-enveloped, dsDNA viruses from the *Papillomaviridae* family (Münger *et al.*, 2004). Infection is typically asymptomatic and most HPV infections are cleared naturally by host defence mechanisms within 12-18 months (Richardson *et al*., 2003; Bodily and Laimins, 2011), however, infection with high-risk (HR) types (of which there are at least twelve, including HPV-16 and -18) has been identified as a carcinogen in at least six types of human cancer including a great proportion of cervical squamous cell carcinomas (CESC) and a subset of head and neck squamous cell carcinoma (HNSCC), particularly of the oropharynx (Forman *et al.*, 2012; Henderson *et al.*, 2014; Beyazit *et al.*, 2018).

Hyper-editing of viral DNA by APOBEC3 has been found in HPV infected cells (Vartanian *et al*., 2008); additionally, higher rates of APOBEC3 mutational signatures are found in HPV positive cervical cancers and head and neck cancers in comparison to HPV negative cancers, together with APOBEC3 signature mutations discovered in potential cancer driver genes such as the PIK3CA proto-oncogene (Henderson *et al*., 2014; Warren *et al*., 2015). Taken together with highly elevated expression levels of A3A and A3B in skin keratinocytes (the primary host cell for HPV infection) seen during early stages of cancer progression (Warren *et al*., 2015) suggests a strong link between APOBEC3 mediated viral responses and off-target driver mutations in the host genome (D'Souza and Dempsey, 2011; Nik-Zainal *et al.*, 2012; Alexandrov *et al.*, 2013; Roberts *et al.*, 2013; Henderson *et al.*, 2014; Swanton *et al.*, 2015; Li *et al.*, 2017).

Regulation of APOBEC3 gene expression is important for limiting mutagenic activity, though this has been found to be disrupted by HR-HPV. HPV encodes two viral oncoproteins, E6 and E7: E6 overcomes p53-tumour suppressor protein mediated cell cycle control through binding and forming a heterodimer with the cellular ubiquitin ligase, E6AP, and subsequently recruiting p53 and instigating its proteasomal degradation (Scheffner *et al*., 1990; Huibregtse, Scheffner and Howley, 1991; Martinez-Zapien *et al*., 2016). The best known target of E7 is the cell cycle regulator and tumour suppressor protein, retinoblastoma (Rb), which has functions in cell cycle control, DNA damage response checkpoint inhibition, and in differentiation (Dyson *et al*., 1989). The hypo-phosphorylated forms of Rb block E2F-mediated induction of cell cycle genes required for the G1/S transition (Narasimha *et al*., 2014), and E7 disrupts this regulation through promoting the proteolytic degradation of Rb (Tzenov *et al*., 2013).

Two repressive E2F transcription factor complexes suppress A3B transcription: the E2F6/PRC1.6 complex (Roelofs *et al.*, 2020), and the E2F4/DP1/p107/p130-containing DREAM transcriptional repressor complex which is directed to the A3B promoter by p53 (Periyasamy *et al*., 2017). Thus E6 mediated p53 degradation also leads to derepression of the DREAM complex and subsequent A3B gene upregulation and activation (Ohba *et al*., 2014; Vieira *et al*., 2014; Mori *et al*., 2017). Furthermore, two functional regions in the A3B promoter have been identified, each containing E6-responsive elements: basal promoter activity can be activated by E6 in human keratinocytes at the distal region, and the proximal region exerts inhibition of gene expression which can be relieved by E6 (Mori *et al*., 2015).

Three further sites within the A3B promoter are also recognised by the TEAD family of transcription factors (TEAD1-4 in mammals) (Mori *et al*., 2017); these evolutionary conserved transcription factors also mediate expression of genes involved in cell proliferation, epithelial–mesenchymal transition and apoptosis evasion via TAZ (transcriptional co-activator with PDZ binding motif) and YAP (Yes-associated protein) (Zhu, Li and Zhao; Jacquemin *et al.*, 1996; Zhao *et al.*, 2008; Zhang *et al.*, 2009). E6-expressing keratinocytes show p53-degradation dependent increases in TEAD1/4 and induced A3B promoter activation, whilst exogenous expression of TEAD also leads to A3B promoter activation (Mori *et al*., 2017).

Thus p53 degradation by E6 also results in increased levels of TEAD, A3B promoter activation, cell growth, epithelial–mesenchymal transition, and potentiates oncogenic transformation (Henderson *et al.*, 2014; Vieira *et al.*, 2014; Warren *et al.*, 2017; Smith and Fenton, 2019).

1.1.8 APOBEC3 expression patterns in normal human tissues

Peripheral blood mononuclear leukocytes (PBMLs) include cells from the myeloid lineage (monocytes, macrophages, dendritic cells (DCs)), and peripheral blood lymphocyte (PBL) cells (B-cells, T-cells, natural killer cells). Circulating monocytes, originating from hematopoietic stem cells in the bone marrow, migrate into tissues where they differentiate into macrophages or DCs (Robinson *et al.*, 2021).

With the exception of A3A, basal expression levels of the different APOBEC3 family members remain relatively constant across PBMLs (Berger *et al.*, 2011): A3A expression is low in either quiescent or stimulated PBLs, moderate in monocyte-derived macrophages (MDMs) and DCs, and highly expressed in primary monocytes, specifically in those expressing the cell surface receptor, cluster of differentiation 14 ($CD14^+$) (Stenglein *et al.*, 2010; Berger *et al.*, 2011; Koning *et al.*, 2011). Whereas basal expression of A3B and A3H is lowest in primary monocytes but this increases upon differentiation into macrophages or DCs; and A3D/E, A3F, A3G and A3H are higher in PBLs, whether quiescent or activated, than in myeloid cells (Berger *et al.*, 2011). HIV-1 primarily infects $CD4^+$ T-cells and A3G has evolved as an important factor in the restriction of this virus (Sheehy *et al.*, 2002), accordingly A3G is found highly expressed in a cell line non-permissive to HIV-1 infection, CEM, as compared to its permissive counterpart, CEM-SS (Refsland *et al.*, 2010). Levels of A3C, A3D and A3F are also higher in two non-permissive cell lines, suggesting these may also contribute to HIV-1 restriction (Refsland *et al.*, 2010).

Comparing tissue expression of the APOBEC3 family: the thymus has low expression of A3A and A3B, and high expression of A3C, A3D, A3F and A3G; the spleen has relatively high levels of all seven APOBEC3s, though it is a major reservoir for undifferentiated monocytes (Refsland *et al.*, 2010). A3A expression is high in lung and adipose tissue, though these are both rich in resident and infiltrating $CD14^+$ macrophages; lung tissue additionally expresses increased levels of A3B, A3C, A3D and A3H, whereas A3C, A3F and A3G are observed to be elevated in ovarian tissue (Refsland *et al.*, 2010).

While nearly all cell types express multiple APOBEC3s, some immune privileged organs such as the brain and testes have very low levels (Refsland *et al.*, 2010), with few exceptions such as strong expression of A3B, A3C, A3F and A3G in primary human brain microvascular endothelial cells (these cells form part of the blood-brain barrier and central nervous system and are susceptible to HIV-1 infection), and this can be augmented by IFN-α and IFN-γ and restrict HIV-1 infection. Whereas A3A and A3D mRNA is undetectable in these cells (Argyris *et al.*, 2007).

Similarly, A3B, A3C, A3F and A3G expression is robust in astrocytes and differentiated post-mitotic mature neurons (Argyris *et al.,* 2007). Additionally, A3G (but not A3A) can be induced by IFN-γ in human retinal capillary endothelial cells, a component of the blood-retinal barrier (Lin *et al.*, 2009).

1.1.9 Protein Kinase C activation of APOBEC3A and APOBEC3B

Induction of A3A and A3B in normal primary keratinocytes can be stimulated using the phorbol ester, PMA, in a PKC-dependent manner (Madsen *et al.*, 1999); PMA is an analog of diacylglycerol (DAG) and strongly activates the PKC pathway and downstream signalling through the necrosis factor-κB (NF-κB) pathway (Holden *et al.*, 2008). Prolonged activation of PKC leads to the synthesis of pro-inflammatory cytokines such as tumour necrosis factor-α (TNF-α), the production of reactive oxygen species (ROS), and promotes tumour formation in mouse models (Nishizuka, 1988; Kazanietz *et al.*, 2000; Rundhaug and Fischer, 2010).

Inflammatory skin conditions such as psoriasis may have an increased cancer risk, and chronic inflammation following high-risk HPV infection is a contributary factor in oncogenesis (Pouplard *et al.*, 2013; Hammouda *et al.*, 2020; Hong *et al.*, 2020); the fact that A3A and A3B can be induced by PMA suggests a possible mechanism by which chronic inflammation could drive tumour development by causing APOBEC3-dependent mutagenesis.

However, cell type-dependent PMA induction of A3A and A3B is reported: quantifying mRNA levels of all APOBEC3 family members in a panel of cell lines following PMA induction found only A3B had detectable upregulation, most notably a 100-fold increase of A3B was seen in the immortalised normal breast epithelial cell line, MCF-10A (Leonard *et al.*, 2015). Conversely, PMA treatment in normal human oral keratinocytes instead found that induction of A3A mRNA and protein were more than 2-fold greater than that of A3B, and through combining PMA with the inflammation mediator, TNF-α (which can also induce the NF-κB pathway), they augmented A3A induction whereas there was only a slight increase in A3B (Siriwardena *et al.*, 2018).

The PMA induction of A3B can be dose-dependently suppressed through pre-incubation with either a broad spectrum inhibitor of PKC isoforms (Gö6983), a classical (cPKC) and novel (nPKC) selective inhibitor (BIM-1 and Sotrastaurin), and by a cPKC selective inhibitor (Gö6976), thus implicating the cPKC isoform in the PMA-mediated A3B upregulation (Leonard *et al.*, 2015).

Different PKC isoforms have distinct functions in the proliferation and differentiation of keratinocytes (Dlugosz and Yuspa, 1993; Denning *et al.*, 1995; Newton, 2003; Papp *et al.*, 2003): the E2F transcription factor 1 (E2F1) is required for normal proliferation and this is downregulated at the onset of Ca^{2+} induced differentiation through the nPKC pathway, modulated by the activity of the mitogen-activated protein kinase (MAPK) p38β (Ivanova, D'Souza and Dagnino, 2006). Furthermore, both A3A and A3B mRNA and protein have been found to be upregulated in the cervical intraepithelial neoplasia-1 (CIN1) keratinocyte cell line, W12, when cultured in differentiating conditions using high extracellular Ca^{2+} stimulation (Wakae *et al.*, 2018), and the E5 protein of HPV has been shown to activate the PKC pathway in mouse fibroblasts (Crusius *et al.*, 1999).

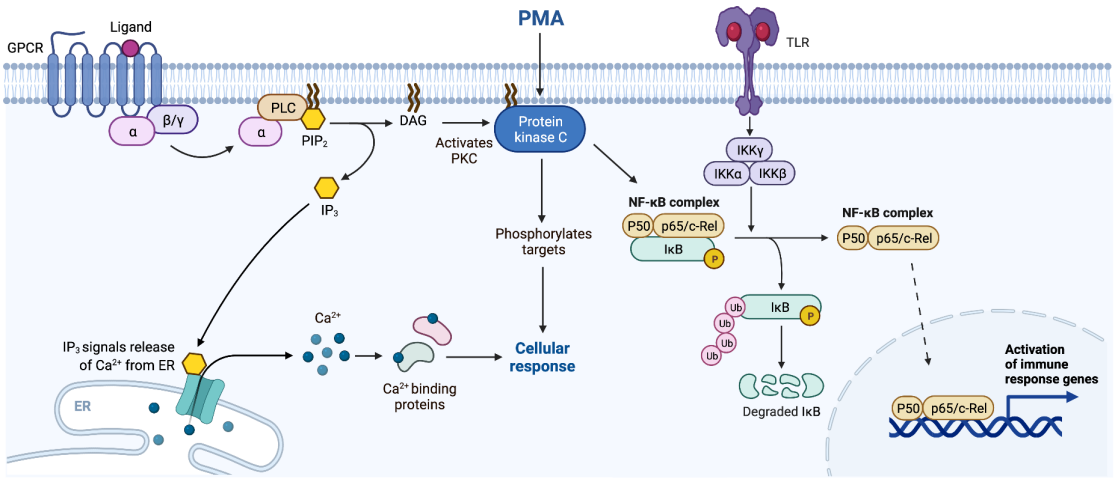

Figure 1-3 Phorbol ester (PMA) activates the PKC signalling pathway.
G-protein coupled receptor (GPCR) activation or phorbol ester (PMA) stimulation activates PKC and induces downstream signalling pathways through activation of phospholipase C (PLC). PLC mediates the hydrolysis of phosphatidylinositol 4,5-bisphosphate (PIP2), into diacylglycerol (DAG) and inositol trisphosphate (IP3) and the release of intracellular Ca^{2+}. PKC is maintained in an inactive form in the cytoplasm, but through DAG and Ca^{2+} activity it is recruited to the plasma membrane and activated.

Chronic exposure to the A3A inducer, TNF-α, has also been shown to promote increased proliferation, anchorage-independent growth and calcium resistance in HPV16-immortalised keratinocytes, but not HPV16 negative keratinocytes, together with the self-renewal capacity of a cancer stem cell population through the suppression of stemness-inhibiting microRNAs miR-203 and miR-200c (Hong *et al.*, 2020).

Finally, interleukin-1α (IL-1α) and TNF-α upregulate an autocrine epidermal growth factor receptor (EGFR) ligand, amphiregulin, which promotes tissue repair and homeostasis following acute or chronic inflammation, but can also increase the proliferation of HPV-immortalized oral keratinocytes and HPV-infected cervical carcinoma cell lines (Woodworth *et al.*, 1995; Zaiss *et al.*, 2015). Subsequently, the activation of PKC and TNF-α signalling in keratinocytes is a further means by which A3A and A3B can become upregulated during HPV-infection.

1.1.10 APOBEC3 gene activation during innate immune responses

1.1.10.1 Viral nucleic acid sensing and interferon signalling pathways

Viral infections trigger the induction of type-1 IFNs (IFN-β, IFN-ε, IFN-κ, IFN-ω, and 12 subtypes of IFN-α) that elicit autocrine and paracrine signalling to promote an antiviral state through the induction of IFN-stimulated genes (ISGs) (Honda, Takaoka and Taniguchi, 2006).

ISGs, including APOBEC3s, mediate several mechanisms of viral restriction such as the degradation of viral nucleic acids and inhibition of replication, the recruitment and enhancement of adaptive immune responses, and the induction of pro-inflammatory cytokines such as TNF-α and TNF-related apoptosis-inducing ligand (TRAIL) that trigger cell growth arrest or apoptosis (Kornbluth *et al.*, 1989; Yarilina *et al.*, 2008; Mehta *et al.*, 2012; Yan, Zheng and Xu, 2018).

The innate immune system employs mechanisms to sense foreign DNA: a subset of toll-like receptors (TLRs) recognise nucleic acids that have been internalised in endosomal compartments, of which TLR9 recognises unmethylated cytosine–phosphate–guanine (CpG) dinucleotide motifs in ssDNA, including a region from the HPV16 E6 gene (Lebre *et al*., 2007; Suspène *et al*., 2017); however HPV16 mitigates this viral recognition by downregulating TLR9 (Hasan *et al*., 2007). TLR3 activation in keratinocytes can be potently stimulated by polyinosinic-polycytidylic (poly [I:C]), an analog of dsRNA, triggering the NF-κB pathway (Lian *et al*., 2012; Suri, Verma and Schmidtchen, 2018; Voccola *et al.*, 2020).

Cytosolic viral RNA can be detected by the retinoic acid-inducible gene 1 (RIG-I) proteins which sense RNA molecules with a 5′-triphosphate group (5’-ppp-RNA) and short double-stranded RNA (dsRNA), but not 5’-capped host mRNA; RIG-I forms oligomers around the viral RNA which allows interactions with effector protein kinases (Baum and García-Sastre, 2011; Peisley *et al*., 2013). Additionally, the RIG-I-like receptors, melanoma differentiation-associated protein 5 (MDA5) and the laboratory of genetics and physiology 2 (LGP2), work cooperatively to form an antiviral response (Kato *et al*., 2006; Bruns *et al*., 2014).

Sensors of cytoplasmic DNA can either activate effector proteins directly or via second messenger molecules: the nucleic acid receptor Z-DNA binding protein 1 (ZBP1), also known as DNA-dependent activator of IFN-regulatory factors (DAI), or tumour stroma and activated macrophage protein (DLM-1), interacts with dsDNA and dsRNA in the left-handed Z-conformation (Schwartz *et al.*, 2001); this directly activates both type-I IFN production through the stimulator of IFN gene (STING) pathway (Takaoka *et al.*, 2007), and virus induced regulated necrotic cell death (Upton, Kaiser and Mocarski, 2012).

RNA polymerase-III (RNAPIII) acts indirectly by binding to viral DNA and producing 5'-ppp-RNA which then serves as a ligand for RIG-I binding (Chiu, MacMillan and Chen, 2009). Cytoplasmic DNA has also been found to induce A3A in an RNA Pol III / RIG-I dependent manner in a human acute monocytic leukaemia cell line (Suspène *et al*., 2017).

Cyclic GMP-AMP synthase (cGAS) binding to dsDNA generates the second messenger, cyclic guanosine monophosphate–adenosine monophosphate (cGAMP), which binds to and activates STING in the endoplasmic reticulum which causes its rapid translocation to the Golgi apparatus (Saitoh *et al.*, 2009; Sun *et al.*, 2013); cytosolic cGAS can also be triggered by DNA:RNA hybrids and by mitochondrial DNA fragments (mtDNA) which resemble bacterial DNA in that they also contain unmethylated CpG motifs (Mankan *et al.*, 2014; Suspène *et al.*, 2017).

Another important viral DNA sensor, IFN-γ-inducible protein 16 (IFI16), recognises ssDNA from a number of viruses in both the nucleus and cytoplasm (Kerur *et al.*, 2011; Li *et al.*, 2019); IFI6 acts synergistically with cGAS to activate STING in keratinocyte cells, but is not required for cGAMP production (Almine *et al.*, 2017).

Binding of bacterial lipopolysaccharide (LPS) to the TLR4/myeloid differentiation factor 2 (MD-2) receptor complex causes the dimerisation of TLR4 and the activation of the myeloid differentiation primary response gene 88 (MyD88) and toll-interleukin 1 receptor (TIR) domain-containing adaptor inducing IFN-beta (TRIF) pathways (Burns *et al.*, 1998; Fitzgerald *et al.*, 2003).

Downstream signalling via NF-κB and the Janus protein tyrosine kinases (JAK) and signal transducer and activator of transcription (STAT) pathways (Yamamoto *et al.*, 2002) leads to the production of IFN-β and TNF-α (Toshchakov *et al.*, 2002; Wang *et al.*, 2002). Additionally activated are the extracellular signal regulated kinase (ERK), p38, and c-Jun NH2-terminal protein kinase (JNK) in the MAPK pathways (Schmidt, Caron and Hall, 2001; Xu *et al.*, 2003). IFN-α also activates the p38 MAPK pathway which is associated with cellular stress responses, this then coordinates with the JAK-STAT pathway to facilitate transcription of ISGs (Uddin *et al.*, 1999).

Following DNA detection, signal transduction and cytokine production is mediated predominantly through two adapter kinases, the STING pathway and the mitochondrial anti-viral signalling (MAVS) protein (Liu *et al.*, 2015).

Activated STING translocation to the Golgi apparatus allows for the recruitment, phosphorylation and nuclear translocation of the IFN-regulatory factor 3 (IRF3) transcription factor (Liu *et al.*, 2015); MAVS localise to the mitochondrial outer membrane and activate IRF3 (Liu *et al.*, 2015). STING and MAV activation also lead to signalling through the NF-κB pathway (Abe and Barber, 2014; Liu *et al.*, 2015).

Type-I IFNs act in an autocrine and paracrine manner, signalling to neighbouring cells through a heterodimeric IFN-α cell surface receptor (IFNAR) consisting of IFNAR1 and IFNAR2 and activation of the JAK/STAT pathway (Uzé, Lutfalla and Gresser, 1990; Novick, Cohen and Rubinstein, 1994); the activation of receptor-associated JAK1 and tyrosine kinase 2 (TYK2) (Plataniassj, Uddins and Colamonicin, 1994) in turn phosphorylate and activate STAT1 and STAT2, enabling their dimerisation (Shuai *et al.*, 1994). STAT1 and STAT2 then assemble with cytoplasmic IRF9 to form the IFN-stimulated gene factor 3 (ISGF3) complex which then translocates to the nucleus and stimulates transcription of many ISGs through binding to IFN-stimulated response elements (ISREs) (Levy *et al.*, 1989; Darnell, Kerr and Stark, 1994; Cohen *et al.*, 1995; Domanski *et al.*, 1995).

Negative regulators of IFN-signalling pathways include a host three prime repair exonuclease 1 (TREX1), also known as DNase III, that resides on the endoplasmic reticulum and digests ssDNA and dsDNA to limit autoimmunity from self-recognition; it can also facilitate clearance of viral DNA such as HIV-1, though this self-limiting mechanism can also lead to suppression of type-I IFN responses to HIV-1 infection (Stetson *et al.*, 2008; Yan *et al.*, 2010).

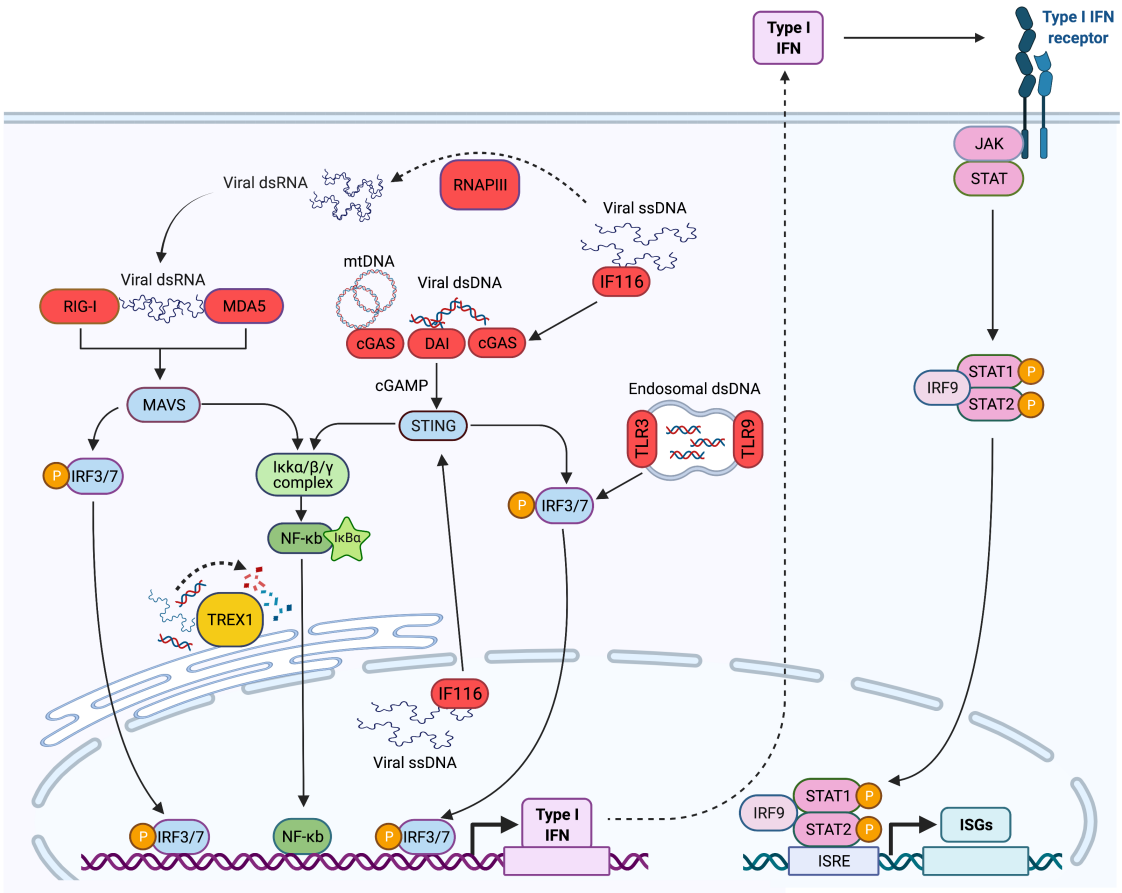

Figure 1-4 Viral nucleic acid sensing in the innate immune response.
Foreign DNA and RNA is detected in the nucleus and cytoplasm by nucleic acid sensors (red). Signal transduction proceeds through effector proteins (blue), either directly or via second messenger molecules, with activation of the NF-κB signalling pathway (green). Production of type-I IFNs provides a positive feedback mechanism, acting on the JAK/STAT pathway (pink) to induce transcription of ISGs. Negative regulators include TREX1 in the endoplasmic reticulum that digests ssDNA and dsDNA.

Another mechanism of self-tolerance is through the immunosuppressive type-I transmembrane glycoprotein named programmed death ligand 1 (PD-L1) (also known as B7-H1 or CD274), which is expressed on macrophages, T-cells, B-cells, monocytes, DCs, as well as a variety of non-haematopoietic tissues including endothelial and epithelial cells (Keir *et al.*, 2008). PD-L1 binds to the complementary surface receptor on T-cells (programmed death-1 (PD-1)), leading to down-modulation of T-cell effector responses (Blank *et al.*, 2006; Karwacz *et al.*, 2011).

PD-L1 is also expressed on the cell surface of multiple tumour types, facilitating immune evasion (Eppihimer *et al*., 2002; Schreiner *et al*., 2004; Garcia-Diaz *et al*., 2017). PD-L1 expression can be induced by type I IFNs, though primarily is upregulated by type II IFN-γ via the JAK/STAT pathway (Lee *et al*., 2006; Garcia-Diaz *et al*., 2017), or by TNF-α or IFN-γ activation of the NF-κB pathway (Gowrishankar *et al*., 2015). Inducible A3A expression was found to lead to deaminase-dependent transcriptional upregulation of PD-L1 in cancer cells, which was shown to be independent of IFN signalling but dependent on replication-associated DNA damage and JNK/c-Jun signalling (Zhao *et al*., 2021). A pan-cancer analysis also identified a correlation between overexpression of PD-L1 and several of the APOBEC3s, together with their signature mutational pattern of *kataegis* (Boichard, Tsigelny and Kurzrock, 2017; Zhao *et al.*, 2021), with increased A3A expression found to correlate most strongly with increased PD-L1 expression in urothelial carcinoma cells (Mullane *et al*., 2016).

Myeloid cells are crucial for host immune defence and have many roles including the clearance of pathogens through phagocytosis (Aderem and Underhill, 1999), and tissue-resident macrophages respond rapidly to infection, assisted by the recruitment of circulating monocytes that undergo differentiation into macrophages and DCs (Robinson *et al.*, 2021). Myeloid cells express surface receptors that recognise apoptotic cells, damage-associated molecular patterns (DAMPs) and pathogen-associated molecular patterns (PAMPs). One such receptor, CD14, is expressed by monocytes and macrophages and acts as a co-receptor with TLR4, facilitating LPS recognition and downstream NF-κB signalling (Chow *et al.*, 1999).

Macrophages and DCs are also professional antigen presenting cells, activating naïve $CD4^+$ T-cells to initiate an adaptive immune response (Kashem, Haniffa and Kaplan, 2017). Several APOBEC3 family members are upregulated through pathogen-associated stimulation in many cell types, and IFN-stimulated response elements (ISRE) have been found in the promoter regions of A3F and A3G, and in a putative promoter region of A3A (Peng *et al.*, 2006). Each of these APOBEC3s have been shown to be IFN-α inducible in both macrophages (Peng *et al.*, 2006; Fransje A Koning *et al.*, 2009), and DCs (Fransje A Koning *et al.*, 2009; Mohanram *et al.*, 2013). Furthermore, detection of cytoplasmic RNA by RIG-I or MDA5 promotes the expression of A3A via a MAVS / IRF3 / IFN and STAT2 signalling pathway (Oh *et al.*, 2021).

A3A is strongly induced by both IFN-γ and Human Cytomegalovirus (HCMV) in human decidual tissues (Weisblum *et al.*, 2017); and A3G restricts HIV-1 in $CD4^+$ T-cells through incorporating into budding virions within newly infected cells and causing mutations in the viral genome (Sheehy *et al.*, 2002), a defence that HIV-1 has evolved to overcome via its viral infectivity factor (Vif) protein that mediates the proteasomal degradation of A3G. Similarly, A3D, A3F and A3H are encapsulated in budding virions in Vif deficient HIV-1 positive cells (Hultquist *et al*., 2011).

A3G can be induced by IFN-α, IFN-β and IFN-γ in $CD14^+$ MDMs (Stopak *et al.*, 2007) and by IFN-α in resting, but not immortalised, $CD4^+$ T-cells (Rose *et al.*, 2004; K. Chen *et al.*, 2006). Subsequently, A3A and A3F have also been found upregulated by IFN-α in naïve $CD4^+$ T-cells (F A Koning *et al.*, 2009).

Furthermore, A3B, A3F and A3G induction by IFN-α in human primary hepatocytes can inhibit hepatitis B virus (HBV) replication (Bonvin *et al.*, 2006; Tanaka *et al.*, 2006). A3A was found to be strongly induced by IFN and CpG DNA in $CD14^+$, but not $CD14^-$ monocytes and macrophages (Stenglein *et al.*, 2010); by IFN-α in activated and quiescent PBLs, monocytes, MDMs and DCs (Berger *et al.*, 2011); and by IFN-α and IL-2 in peripheral blood mononuclear cells (PBMLs) (Refsland *et al.*, 2010; Aynaud *et al.*, 2012), in which A3A can inhibit early stages of HIV-1 infection (Berger *et al.*, 2011). Moreover, IFN-β induces A3A in keratinocyte (NIKS) cells, repressing HPV replication ; it also induces A3A, A3F and A3G in the HPV16+ W12 keratinocyte line, originally isolated from a low-grade cervical intraepithelial neoplasia (Stanley *et al.*, 1989) causing hypermutation of HPV16 early 2 (E2) gene (Wang *et al.*, 2014).

Alternative IFN species that upregulate expression of APOBEC3 family members include IFN-ε, which is constitutively expressed in mucosal tissue and induces A3A, A3F and A3G in MDMs, protecting primary macrophages against HIV-1 infection (Tasker *et al.*, 2016); and IFN-ω that upregulates A3A and A3B in HPV11 expressing immortalised keratinocyte cells (HaCaT) (Wang *et al.*, 2017). LPS and IFN-α both stimulate mA3 upregulation, leading to the restriction of mouse mammary tumour virus (MMTV) *in vivo,* and in DCs (Okeoma *et al*., 2009). Vesicular stomatitis virus (VSV) induces transient IFN-β-dependent expression of mA3 in a murine melanoma cell line, inhibiting viral infection; and A3B knockdown reduces resistance to oncolytic VSV therapy in human melanoma cells (Huff *et al.*, 2018).

1.1.10.2 NF-κB signalling pathway

The NF-κB signalling pathway is activated downstream of the PKC and viral nucleic acid sensing pathways and plays many important regulatory roles in immune responses and inflammation, though inappropriate immune responses via NF-κB signalling have also been implicated in carcinogenesis and tumour progression (Tilborghs *et al.,* 2017).

Diversity in NF-κB transcriptional activity results from a combination of complexes that are formed of homo- or heterodimers comprised of RelA (p65), RelB, c-Rel, NF-κB1 (p105) which gives rise to p50, and NF-κB2 (p100) which gives rise to p52, that can act as either transcriptional activators or repressors. The most common complex in cells is the p65-p50 heterodimer, referred to as NF-κB (Sen and Baltimore, 1986; Baeuerle and Baltimore, 1989; Ballard *et al.*, 1990; Ghosh *et al.*, 1990; Matthews *et al.*, 1993; Plaksin, Baeuerle and Eisenbach, 1993; Betts and Nabel, 1996).

NF-κB subunits are regulated by IκB inhibitory proteins, sequestering them in an inactive form in the cytoplasm (Plaksin, Baeuerle and Eisenbach, 1993). Through inducing stimuli, this inhibition is relieved by the IκB kinase (IKK) complex (IKKα and IKKβ, and a non-catalytic accessory protein, NF-κB Essential Modulator (NEMO)) via the rapid phosphorylation and subsequent proteasomal degradation of IκBs, which facilitates the release of NF-κB dimers and consequently their nuclear translocation and transcriptional activation of target genes (Yamaoka *et al.*, 1998).

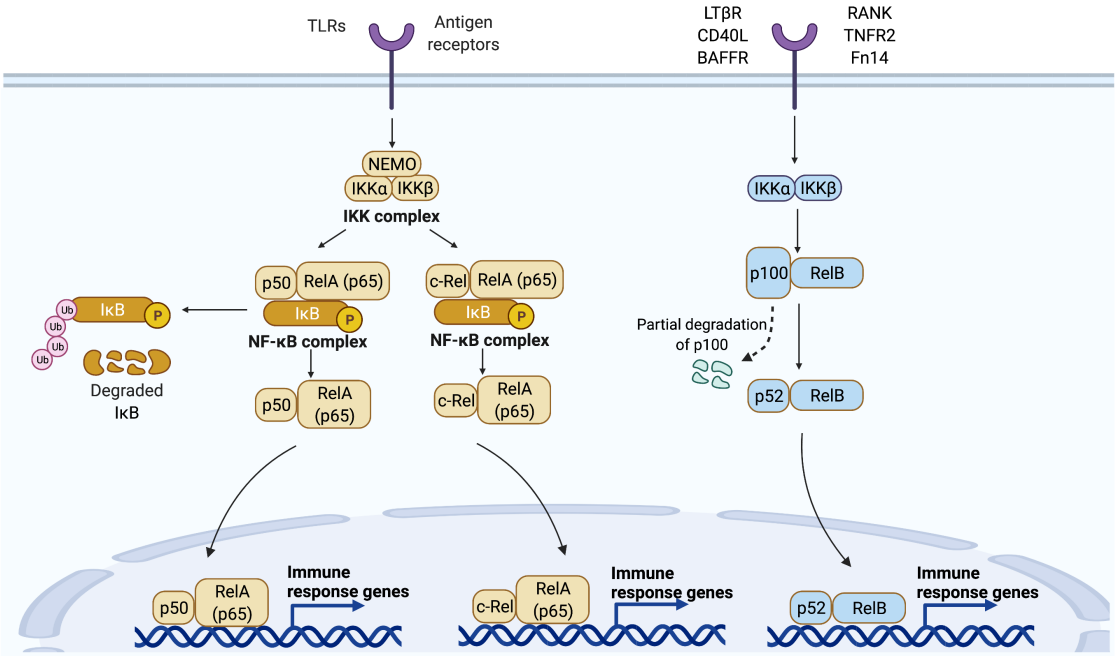

Figure 1-5 The NF-κB signalling pathway.
Signalling through the canonical NF-κB pathway (yellow) downstream of PKC and viral nucleic acid sensing pathways leads to activation of the IKK complex which phosphorylates inhibitory IκBs, initiating proteasomal degradation and the release of NF-κB dimers (c-Rel/ RelA(p65) and p50/RelA(p65)) which translocate to the nucleus and activate their target genes. The non-canonical pathway (blue) can occur through ligation of receptors such as lymphotoxin β-receptor (LTβR), CD40L, B-cell activation factor (BAFFR), receptor activator for nuclear factor kappa B (RANK), tumour necrosis factor (TNF) receptor-associated factor 2 (TNFR2), and the TWEAK receptor Fn14, and predominantly activates the p52/RelB complex through the inducible processing of p100 (a RelB inhibitor and precursor of p52).

The non-canonical NF-κB pathway can be activated through ligation of receptors such as lymphotoxin β-receptor (LTβR), CD40L, B-cell activation factor (BAFFR), receptor activator for nuclear factor kappa B (RANK), tumour necrosis factor (TNF) receptor-associated factor 2 (TNFR2), and the TWEAK receptor Fn14 (Sun, 2011). PMA induction of A3B has been found to be either via the non-canonical NF-κB pathway, through RelB/p52 heterodimer recruitment to the A3B promoter region (Leonard *et al.*, 2015), or via the classical pathway through p65/p50 and p65/c-Rel recruitment to A3B promoter (Maruyama *et al.*, 2016).

The HR-HPV E6 oncoprotein also activates NF-κB complexes during the development of cervical cancer, which could also contribute to the high A3B expression found in HPV-associated tumours (Nees *et al.*, 2001; James, Lee and Klingelhutz, 2006; Da Costa *et al.*, 2016; Tilborghs *et al.*, 2017). Furthermore, A3A can also be transiently induced through genotoxic stress in a p65/IkBα-dependent manner (Oh *et al.*, 2021).

1.1.11 APOBEC3A

1.1.11.1 Cellular localisation

Though lacking a NLS, A3A is a small single-domain enzyme (~23 kDa) so does not exceed the nuclear pore exclusion limit (Görlich and Kutay, 1999), enabling its traversal via passive diffusion. It has been found to be excluded from condensed DNA during early mitosis, and resumes a cell-wide distribution upon reaching telophase (Lackey *et al.*, 2013).

A3A is a hypermutator of ssDNA and therefore very important to understand its proximity to genomic DNA. Generally, subcellular localisation has been analysed using ectopically expressed epitope-tagged A3A in HeLa or 293T cells (both having little or no endogenous expression of A3A), with evidence suggesting it is diffuse in both the cytoplasm and the nucleus throughout interphase (Muckenfuss *et al.*, 2006; Goila-Gaur *et al.*, 2007; Kinomoto *et al.*, 2007; Niewiadomska *et al.*, 2007; Hultquist *et al.*, 2011; Lackey *et al.*, 2013).

A3A has additionally been seen to form small focal points that colocalise with cytoplasmic P-bodies (ribonucleoprotein granules involved in mRNA decay) (Niewiadomska *et al*., 2007; Luo, Na and Slavoff, 2018); and cellular stress caused by arsenite treatment causes the majority of cytosolic A3A (but not nuclear A3A) to accumulate within stress granules (granules formed and arising from mRNAs stalled in translation initiation) (Marin *et al.*, 2008; Protter and Parker, 2016). These localisation properties have also been seen for A3G (Gallois-Montbrun *et al.*, 2007).

1.1.11.2 Catalytic activity

The human A3A sequence gives rise to two functional, enzymatically active isoforms (F A Koning *et al.*, 2009; Trapp *et al.*, 2009) through translation initiation at two alternative start sites, methionine 1 (Met^1; long-form) and Met^{13} (short-form). The Met^1 transcript is the most commonly seen form (Thielen *et al.*, 2010).

The binding affinity of A3A to ssDNA substrates is 50 to 100-fold less than that of high affinity A3G (Iwatani *et al.*, 2006; Love, Xu and Chelico, 2012; Byeon *et al.*, 2013; Mitra *et al.*, 2014); conversely, A3A potently deaminates ssDNA with amongst the highest catalytic activity (~10-fold greater than A3G), and is unique in also efficiently deaminating 5-methylcytosines (though ~5-fold less than unmethylated) (Carpenter *et al.*, 2012; Wijesinghe and Bhagwat, 2012; Siriwardena, Guruge and Bhagwat, 2015). It is additionally proposed that A3A can form a higher affinity cooperative dimer (Bohn *et al*., 2015).

As visualised through γ-H2AX staining, a marker of DNA damage signalling, ectopic induction of A3A caused UNG-dependent DNA DSBs, Ataxia Telangiectasia Mutated (ATM) mediated signalling (which responds to DSB formation), leading to activation of the G1/S checkpoint, cell cycle arrest, and consequently cell death (Landry *et al.*, 2011; Mussil *et al.*, 2013). Following replication stress, Replication Protein A (RPA) binds exposed ssDNA and stimulates the activation of Ataxia Telangiectasia and Rad3-related (ATR) kinase, in turn activating Checkpoint Kinase (Chk1) and the G2/M checkpoint (Mognato, Burdak-Rothkamm and Rothkamm, 2021). In addition to ATM signalling, ATR has also been shown to be activated by A3A induction with an enrichment of DSBs in S-G2 phase cells that suggested cells are susceptible to A3A-mediated DNA damage at exposed replication forks (Green *et al.*, 2016). Furthermore, in addition to editing nuclear DNA (including segments of c-MYC and TP53 in an UNG-deficient background), human mitochondrial DNA is also susceptible to hypermutation by A3A (Suspène *et al.*, 2011).

A3A specifically deaminates ssDNA (not dsDNA or DNA:RNA hybrids) (Chen *et al.*, 2006) and early studies of A3As enzymatic activity concluded it was unable to deaminate short RNA sequences (Madsen *et al.*, 1999), though it exhibited higher binding affinity for longer ssRNA than equivalent length ssDNA substrates (Byeon *et al.*, 2013; Mitra *et al.*, 2014). It subsequently became the second family member (in addition to A1) shown capable of also editing RNA transcripts, including IFN-inducible deamination of succinate dehydrogenase B (SDHB) in normal PBMLs and MDMs, which was greatly augmented by hypoxia treatment (Sharma *et al.*, 2015).

These A3A-mediated host-RNA editing events were found in multiple transcripts within monocytes and macrophages, and have been linked to pro-inflammatory M1 polarisation in the latter (Sharma *et al.*, 2015, 2017; Alqassim *et al.*, 2021). The majority of editing of RNA targets are found within stem-loop structures, preferentially at sites flanked by short palindromic sequences (Sharma *et al.*, 2015; Sharma and Baysal, 2017), and consistent with observations that A3A also favours deamination of DNA and RNA stem-loop structures within sequenced tumours (Buisson *et al.*, 2019; Jalili *et al.*, 2020).

1.1.11.3 Viral restriction

The ability of A3A to restrict viral replication is variable and can either be deaminase-dependent (generally involving viral genome editing), or deaminase-independent via an alternative mechanism. To confer antiretroviral effects against the lentivirus HIV-1, A3G proteins are incorporated into virions and transferred into newly infected cells; here they cause C-to-U mutations in viral cDNA upon minus-strand synthesis, and consequently G-to-A hypermutations in the positive strand of the proviral sequence (Chiu and Greene, 2008). A3A was amongst the ISGs that was found to be upregulated (7-fold) in MDMs by Viral Protein R (Vpr), a HIV-1 protein that induces G2 arrest by activating the ATR-mediated G2/M checkpoint (Zimmerman *et al.*, 2004; Zahoor *et al.*, 2014). Yet unlike A3G, A3A is not incorporated into virions and has little effect on HIV-1 replication, though it can maintain viral latency through interactions with the 5′ long terminal repeat region of proviral DNA leading to the recruitment of repressive histone molecules and epigenetic silencing (Taura *et al.*, 2019).

A3A can restrict retroviruses other than HIV-1: the human T-cell leukaemia virus type I (HTLV-1) retrovirus primarily infects $CD4^+$ T cells and a fraction of carriers can go on to develop adult T-cell leukaemia (Takatsuki, 2005). Though A3A expression is low in T-cells (Refsland *et al.*, 2010), mutations in the HTLV-1 genome can arise through co-transfection with A3A expression plasmids in 293T cells, accompanied by potent, deaminase-dependent viral inhibition (Ooms *et al.*, 2012); A3A can also moderately inhibit the Rous sarcoma virus in a quail cell line (Qcl-3) (Wiegand and Cullen, 2007).

The herpesvirus family are a large family of dsDNA viruses, of which only a few infect humans (including: herpes simplex virus (HSV) -1 and -2, Epstein-Barr virus (EBV) and human cytomegalovirus (HCMV)) (Cheng *et al.*, 2021). Overexpressed A3A can edit the genomes of HSV-1 and EBV, though this activity was found to have little suppression of infection *in vitro* (Suspene *et al.*, 2011; Cheng, Moraes, *et al.*, 2019), or *in vivo* (Nakaya *et al.*, 2016).

Conversely, A3A (but not A3B, A3C, A3F, or A3G) dramatically inhibits replication of adeno-associated virus in 293T cells, a small ssDNA virus from the parvovirus family (H. Chen *et al.*, 2006). Yet as opposed to direct editing of the viral genome, inhibition occurs through blocking viral replication centres in an active site-dependent, deaminase-independent mechanism (Chen *et al.*, 2006; Narvaiza *et al.*, 2009). Overexpression or upregulation of A3A can also inhibit the infectivity of HPV though without overt editing of the viral genome (Ahasan *et al.*, 2015; Warren *et al.*, 2015).

Furthermore, A3A can be packaged within HBV virions in a deaminase-independent mechanism (Nair and Zlotnick, 2018), whereas its upregulation by IFN-α or LTβR agonists and subsequent deaminase activity facilitate the degradation of HBV covalently closed circular (ccc)-DNA and prevents viral reactivation (Lucifora *et al.*, 2014). A3A is also upregulated through HCMV infection and found to restrict viral replication in decidual cell cultures with evidence of viral genome editing (that is additionally detected in clinical amniotic fluid samples from foetuses congenitally infected with HCMV) (Weisblum *et al.*, 2017).

1.1.11.3.1 Retrotransposon inhibition

Transposable elements make up greater than 40% of the human genome (Craig Venter *et al.*, 2001), and the mobility of retrotransposons (such as LINE-1) occurs through the transcription of an RNA intermediate, the reverse transcription into cDNA (making a RNA/DNA hybrid), and the reintegration of the cDNA at a new location (Dombroski *et al.*, 1991; Zhang, Zhang and Yu, 2020).

LINE-1 elements contain a 5′ UTR, three open reading frames (ORF0, OFR1 and ORF2) and a 3′ UTR (Dombroski *et al.*, 1991; Denli *et al.*, 2015). It is estimated ~500,000 exist in the human genome (Lander *et al.*, 2001) and whilst the vast majority are truncated at the 5’ end or alternatively inactive due to internal rearrangements or mutations (Cordaux and Batzer, 2009), ~80-100 remain retrotransposition-competent (Brouha *et al.*, 2003) and thus pose a risk of disruption to essential genes.

Preceding their viral restriction activities, APOBEC3s additionally had the ability to inhibit LINE-1 retrotransposition and with the exception of A3A, restriction is largely independent of their deaminase activity (Bogerd *et al.*, 2006; Muckenfuss *et al.*, 2006; Mitra *et al.*, 2014; Richardson *et al.*, 2014; Feng *et al.*, 2017; Renner *et al.*, 2018). A3A is the only APOBEC3 member able to deaminate the LINE-1 cDNA, which occurs when it is temporarily exposed as ssDNA by the action of RNase-H (Richardson *et al.*, 2014; Renner *et al.*, 2018). In contrast, the RNA/DNA hybrid intermediate is found to be protected from APOBEC3 activity (Richardson *et al.*, 2014).

1.1.12 APOBEC3B

1.1.12.1.1 Cellular localisation

Of the APOBEC3 family, A3B is unique in that it is the only member that is constitutively nuclear (Pak *et al.*, 2011; Lackey *et al.*, 2012, 2013). With the exception that (similar to A3A) it is also excluded from condensed chromosomes during mitosis but is actively reimported back to the daughter cell nuclei following cell division (Lackey *et al.*, 2012, 2013). Though it lacks a classical NLS, A3B is actively transported into the nucleus, an activity which is dependent on two sets of residues within its NTD and thought that it may utilise the importin-α dependent pathway (Lackey *et al.*, 2012; Salamango *et al.*, 2018). Alternatively, it is proposed that A3B may have a yet unidentified import partner analogous to that used by the cyclin D1-CDK4 complex: neither components contain their own NLS, yet import is facilitated through binding to the NLS-containing p21 or p27 proteins (Bockstaele *et al.*, 2006; Salamango *et al.*, 2018).

1.1.12.1.2 Catalytic activity

A3B is a double domain enzyme consisting of a catalytically active CTD which alone is sufficient for DNA editing (Shi *et al.*, 2015); and an NTD that although catalytically inactive, facilitates enzyme activity as the CTD alone is 10-fold less active than full-length A3B (Bogerd *et al.*, 2007; Fu *et al.*, 2015; Adolph *et al.*, 2017).

Some double-domain enzymes of the APOBEC3 family have been shown to form high-molecular weight (HMW) complexes: A3G for example has been shown to exist in an inactive, HMW complex in the cytoplasm that dissociates into an active, low-molecular weight (LMW) species following RNase A treatment (Huthoff *et al.*, 2009; Li *et al.*, 2014). A3B can form HMW complexes which yield far greater deaminase activity following RNase A treatment, suggesting that A3B activity is attenuated in an RNA-dependent manner; yet in contrast to A3G this does not lead to the conversion of a LMW form of A3B (Xiao *et al.*, 2017; Cortez *et al.*, 2019).

Full-length recombinant A3B was shown to have similar catalytic activity against ssDNA substrate as that of A3G (Adolph *et al.*, 2017). A3B also has a very weak ability to deaminate 5-methylcytosines to uracil, though at least 10-fold less efficient than that of A3A (Siriwardena, Guruge and Bhagwat, 2015; Fu *et al.*, 2015).

1.1.12.1.3 Viral restriction

Whilst the upregulation of A3B by the HPV E6 oncoprotein has been well characterised (Vieira *et al.*, 2014), it does not appear to restrict viral replication, though A3B was shown to potently inhibit both WT- and Vif deficient HIV-1 replication in co-transfection studies in 293T cells (whereas A3G only inhibits Vif deficient HIV-1) (Doehle, Schäfer and Cullen, 2005). Yet conversely, A3B expression was low and did not restrict HIV-1 in a permissive human T-cell line (the host-cell for HIV-1 infection) (Hultquist *et al.*, 2011; Vieira *et al.*, 2014). HTLV-1 replication is inhibited by exogenous A3B expression in 293T cells (though more so by A3A and A3H Haplotype II), an activity that was dependent on both domains (Ooms *et al.*, 2012). Furthermore, a long-term HTLV-1 infection in a humanised mouse model suggested a correlation between A3B expression and the development of adult T-cell leukaemia/lymphoma (Yao *et al.*, 2019).

Despite low A3B protein expression in 293T cells, endogenous A3B was initially identified in co-immunoprecipitation studies as a binding partner of an expressed EBV viral protein (BORF2), and subsequently also in gastric carcinoma cells (Cheng, Yockteng-Melgar, *et al.*, 2019). Knockdown of BORF2 led to A3B mediated viral mutations and limited viral replication, suggesting that the BORF2-A3B interaction is necessary to limit its EBV antiviral effects (Cheng, Yockteng-Melgar, *et al.*, 2019). IFN-α and LTβR activation also up-regulate A3B (in addition to A3A) in HBV-infected cells and primary hepatocytes, and though A3B-knockdown does not limit LTβR-mediated reduced viral replication, it reversed the A3B-mediated degradation of HBV ccc-DNA (Lucifora *et al*., 2014) which occurs through DNA editing during reverse transcription (Chen *et al.*, 2018).

A3B is also upregulated by the polyomavirus large T antigen in different epithelial cell types (Starrett *et al.*, 2019), though this was in a p53-independent mechanism which is in contrast with the model of A3B overexpression by HPV oncoproteins through p53 inactivation (Vieira *et al.*, 2014). This study further showed that A3B correlated with expression of cell-cycle related genes (Starrett *et al.*, 2019).

1.1.13 APOBEC4

APOBEC4 (A4) was the most recently discovered member of the cytosine deaminase family and found encoded on chromosome 1q25 (Rogozin *et al.*, 2005). It has cytoplasmic and nuclear localisation, though only weakly associates with ssDNA and lacks cytosine deaminase activity (Marino *et al.*, 2016). Originally thought to be expressed primarily in the testis (Rogozin *et al.*, 2005; Marino *et al.*, 2016), a transcriptomic study subsequently identified high expression of A4 in nasal, bronchiolar, lung, and tracheal epithelium cells, all of which are targets of severe acute respiratory syndrome coronavirus 2 (SARS-CoV-2) infection (Meshcheryakova *et al.*, 2021). Though co-expression of A4 and HIV-1 found that instead of inhibiting viral replication, it instead enhanced it in a dose-dependent manner (Marino *et al.*, 2016).

Interestingly, a sequencing study of APOBEC mutations in multiple myeloma patients found translocation associated upregulation of A4, which was abrogated through knockdown of a transcription factor, MafB, (Walker *et al.*, 2015); MafB is associated with poorer prognosis in multiple myeloma patients and also a negative regulator of type I IFN production (Kim and Seed, 2010; Liu *et al.*, 2019).

1.2 The cell cycle

The cell cycle is a highly orchestrated and regulated process in which a proliferating cell replicates its contents and genetic material and prepares for cell division, producing two identical daughter cells (Vermeulen, Van Bockstaele and Berneman, 2003). It consists of four distinct phases: gap 1 (G1), synthesis (S), gap 2 (G2), and mitosis (M) as shown in Figure 1-6.

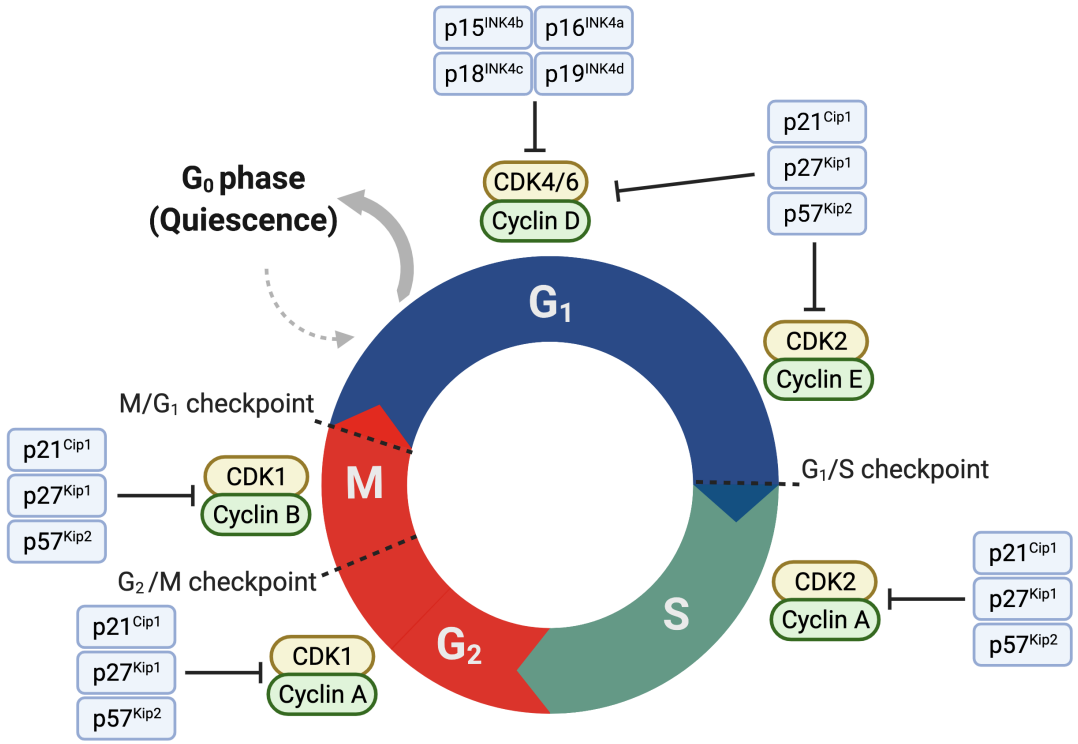

Figure 1-6 Schematic diagram of cell cycle phases and key regulators.
The transition through cell-cycle phases is regulated by cyclin-CDK complexes, which in turn are negatively regulated by CDK inhibitors of the INK4, Cip and Kip family of proteins.

Progression is dependent on the phosphorylation of key targets by heterodimers of cyclins (A, B, D, E) and CDKs (1, 2, 4, 6), which in turn are negatively regulated by two families of proteins: INK4 (p15, p16, p18, p19) that specifically interact with and inhibit CDK4 and CDK6, and Kip/Cip (p21, p27, p57) which can inhibit all cyclin-CDK complexes (Sherr and Roberts, 1999).

CDK activity is additionally regulated by phosphorylation of threonine and tyrosine residues (Lew and Kornbluth, 1996). To secure genomic integrity, progression through each phase requires the passing through major cell-cycle checkpoints at G1/S, G2/M, and the spindle checkpoint in mitosis (M/G1) (Vermeulen, Van Bockstaele and Berneman, 2003).

1.2.1 Quiescence (G_0)

Cells can exit the cell cycle during early G1 (prior to a point at which cells were bound to continue even in the absence of stimulation known as the restriction point), and enter a temporary and reversible proliferation arrest known as quiescence (or G0 phase), where they can remain until stimulated to resume growth and cell division (Yao, 2014). This balance between quiescent and proliferative cells is crucial for whole body maintenance such as the renewal of epithelia, haematopoiesis, and tissue regeneration after injury: keratinocytes within the suprabasal layer of the dermis are mostly quiescent and can be re-stimulated by injury which promotes proliferation and migration to facilitate wound healing (Levy *et al.*, 2005).

Unlike cyclin A, B and E which are expressed periodically, cyclin D is synthesised constitutively in the presence of growth factors (Sherr, 1994). The E2F1 transcriptional activator is required for S-phase entry, and is negatively regulated by Rb; the cyclin D-CDK4/6 complexes promote G1/S progression by phosphorylating and inactivating Rb (Sherr and Roberts, 1999; Marescal and Cheeseman, 2020). Entry into quiescence is tightly regulated through expression of the CDK inhibitors p21, p27 and p57 which inactivate cyclin D-CDK4/6 complexes, thus preventing the phosphorylation and inactivation of Rb (Sherr and Roberts, 1999; Marescal and Cheeseman, 2020).

Confluent, contact-inhibited cells also exit the cell cycle, initiated by down-regulation of cyclin D1 prior to mitosis and the p27-mediated inhibition of cyclin A-CDK1/2 (Chassot *et al.*, 2008). Cells can additionally be induced into this resting state through limitations of nutrient availability (serum starvation) as a cell survival mechanism under adverse conditions (Pirkmajer and Chibalin, 2011).

1.2.2 G0-to-G1 transition

The balance between quiescence and proliferation is controlled by an Rb-E2F1 bistable switch (Yao *et al.*, 2008): growth factors activate signal transduction through transcription factors such as c-MYC (Hanson *et al.*, 1994), leading to decreased CDK inhibitor expression and increased levels of cyclins; this allows the cyclin D-CDK4/6 complex to phosphorylate and inactivate Rb, which causes the depression of E2F1 and induces cell-cycle re-entry (Marescal and Cheeseman, 2020).

G1 is the first gap phase in which the cell synthesises cellular components in preparation for S-phase entry. Phosphorylation of Rb by cyclin D-CDK4/6 leads to the dissociation of histone deacetylases (HDAC) from Rb and depression of cyclin A, cyclin E, and CDK1 gene expression, promoting their transcription (Zhang *et al.*, 2000). G1 to S-phase progression is driven by cyclin A-CDK2 and cyclin E-CDK2 complexes (Ohtsubo *et al.*, 1995), facilitated by removal of inhibitory phosphorylation by Cdc25a phosphatase (Bertoli, Skotheim and de Bruin, 2013). During the G1/S transition, phosphorylation and inactivation of CDK inhibitors and transcriptional repressors facilitates activation of G1/S genes (Montagnoli *et al.*, 1999).

Progression can be stalled at the G1/S checkpoint by detection of DNA DSBs that activate the ATM kinase, leading to phosphorylation of p53 and checkpoint kinase 2 (Chk2) (Matsuoka, Huang and Elledge, 1998). Phosphorylation and stabilisation of p53 also leads to transcriptional activation of the CDK inhibitor, p21 (Shieh *et al.*, 1997). Activated Chk2 inhibits Cdc25a, preventing the dephosphorylation of cyclin A-CDK2 and cyclin E-CDK2 and therefore blocks S-phase entry (Falck *et al.*, 2001).

1.2.3 S-phase

The cyclin E-CDK complex is the primary initiator of DNA replication in early S-phase (Jackson *et al.*, 1995), and cyclin A-CDK2 has roles in both the initiation of DNA synthesis (Pagano *et al.*, 1992) and is additionally required during the progression through S-phase (Furuno, den Elzen and Pines, 1999).

DNA lesions that occur in S-phase are detected by ATR at an intra-S checkpoint, leading to activation of Chk1 which then mediates the proteosomal degradation of Cdc25a, preventing further progression through S-phase until DNA repair processes are complete (Xiao *et al.*, 2003).

1.2.4 G2-phase and mitosis

G2 is the second gap phase in which there is further cellular growth before mitosis, regulated by the cyclin B1-CDK1 complex (Miyazaki and Arai, 2007). CDK1 is inactivated by phosphorylation at Tyr15 by Wee1 and at Thr14 by Wee1 and Myt1, and dephosphorylated at these residues at the G2/M transition by the Cdc25 phosphatase (Smits and Medema, 2001). Dephosphorylation by Cdc25 enables the full activation of CDK1 to be initiated through subsequent phosphorylation at Thr161 by the CDK kinase activating kinase (CAK) complex (Lolli and Johnson, 2005).

Mitosis is a highly regulated process by which a tetraploid cell divides its genetic and cellular material into two identical diploid cells and consists of distinct phases: prophase, prometaphase, metaphase, anaphase, telophase, and cytokinesis (Nurse, 1994). Cyclin B1 has a cytoplasmic retention signal (CRS) (Pines and Hunter, 1994) and a nuclear export signal (NES); though it lacks a canonical NLS, it is imported by a non-canonical importin-β mechanism (Takizawa, Weis and Morgan, 1999) and the cyclin B1-CDK1 complex continuously shuttles between the nucleus and the cytoplasm (Takizawa and Morgan, 2000).

During interphase, the rate of export of the inactive cyclin B1-CDK complex exceeds the rate of import and therefore is predominantly cytoplasmic (Takizawa and Morgan, 2000). Cyclin B1 levels increase in G2, peaking in mitosis, and the activated cyclin B-CDK1 complex rapidly accumulates in the nucleus in prophase where it initiates nuclear envelope breakdown, chromosome condensation and mitotic spindle formation (Gong and Ferrell, 2010).

The accumulation is mediated in part through phosphorylation of cyclin B1 which disrupts the interaction between the CRS and exporter, CRM1, thus decreasing the rate of export (Takizawa and Morgan, 2000). Rapid degradation of cyclin B1 and subsequent inactivation of CDK1 occurs in metaphase, necessary for the initiation of spindle elongation and cytokinesis, and is mediated by the anaphase promoting complex/cyclosome (APC/C^{Cdc20}) (Clijsters *et al.*, 2014).

The cyclin A-CDK1 complex activity is also required in late G2 phase and has roles including regulating cyclin B1-CDK1 activation and nuclear import, histone H3 phosphorylation, and driving entry into mitosis (Furuno, den Elzen and Pines, 1999).

The G2/M checkpoint prevents cells entering mitosis with damaged DNA, facilitated by Wee1 phosphorylation and inhibition of cyclin B1-CDK1 (Smits and Medema, 2001), and ATR phosphorylation and activation of Chk1 which then phosphorylates and inhibits Cdc25 (preventing the dephosphorylation of cyclin B1-CDK1) (Smith *et al.*, 2020).

1.3 Project outline

The aim of this project was to gain a better understanding of the physiological function and regulation of A3A and A3B in normal epithelial cells from which cancers displaying APOBEC3 signature mutation arise. This study utilised near-normal immortalised human keratinocyte (NIKS) cells in which a CRISPR/Cas9 knock-in strategy had been employed to express HA-epitope tags on the endogenous A3A and A3B genes, and to generate a homozygous deletion of A3A (A3A KO NIKS).

Specific aims:

1) To stimulate A3A and A3B expression in NIKS (using known inducers: phorbol ester and interferon) and study protein expression and subcellular localisation using immunofluorescence microscopy (using an HA-epitope specific antibody).

2) To investigate APOBEC3 mRNA expression by known inducers in WT-NIKS and compare against expression in A3A KO NIKS.

3) To investigate A3A and A3B function and regulation in the absence of viral infection (using A3A KO NIKS for comparison of A3A activity).

2 Materials and Methods

2.1 Materials

2.1.1 General Materials

General Materials	Company	Product Code
Amersham Hyperfilm ECL	Fisher Scientific	10094984
Ampicillin	Melford	A0104
10X Blue Juice Loading Buffer	Invitrogen	10816015
Bacteriological Agar	Thermo-Fisher	LP011
Benzonase Nuclease	Sigma-Aldrich	E1014
Bovine Serum Albumin	Sigma-Aldrich	A2153
Bromophenol Blue	Sigma-Aldrich	114405
cOmplete Mini Protease Inhibitor	Roche	04693116001
Dimethyl Sulfoxide (DMSO)	Fisher Scientific	10103483
DNA Ladder, 1 Kb	Invitrogen	10787018
Dithiothreitol (DTT)	Melford	MB1095
DNAzol	Fisher Scientific	10503027
Donkey Serum	Sigma-Aldrich	D9663
Ethylenediaminetetraacetic Acid Tetrasodium Salt Dihydrate (EDTA)	Fisher Scientific	D/0700/53
Ethylene glycol-bis(2-aminoethylether)-N,N,N′,N′-tetraacetic acid (EGTA)	Sigma-Aldrich	03777
Ethidium Bromide	Thermo-Fisher	17898
Ethanol	Fisher Scientific	E/06500F/17
Formaldehyde, 16% (w/v), Methanol-Free	Fisher Scientific	10751395
Glacial Acetic Acid	Fisher Scientific	A/0360/PB17
Glycerol	Fisher Scientific	G/0650/17
Glycine	Fisher Scientific	G/0800/60
HEPES Free Acid	Melford	B2001
Kanamycin	Sigma-Aldrich	K4000

NucBlue Fixed Cell Ready Probes Reagent (DAPI)	Thermo-Fisher	R37606
PageRuler Plus Prestained Protein Ladder, 10 to 250 kDa	Thermo-Fisher	26620
Phenylmethylsulfonyl fluoride (PMSF)	Sigma-Aldrich	78830
Phosphate Buffered Saline (PBS) Tablets (100X)	Fisher Scientific	BR0014G
PhosSTOP Phosphatase Inhibitors	Roche	04906837001
Potassium Chloride (KCl)	Sigma-Aldrich	P9541
ProLong Gold Antifade Mountant	Invitrogen	P36934
Ribonuclease A (RNase A) from Bovine Pancreas	Sigma	R6513
Skimmed Milk Powder	Oxoid	LP0031
Sodium Chloride (NaCl)	Fisher Scientific	S/3160/60
Sodium Dodecyl Sulphate (SDS)	Fisher Scientific	S/P530/53
Tris-Base	Fisher Scientific	BTP63001
Triton X-100	Sigma-Aldrich	T8787
Tryptone	Thermo-Fisher	LP0042
Tween-20	Fisher Scientific	10485733
Yeast Extract	Thermo-Fisher	LP0021

2.1.2 Buffer Compositions

General Buffers	Composition
Agar Plates	1% Tryptone, 1.2% Bacteriological Agar 0.5% Yeast Extract, 1% NaCl
Agarose Gel	2% Agarose in TAE Buffer, 0.5 μg/ml Ethidium Bromide
Laemmli Sample Buffer	10% Glycerol, 60 mM Tris-HCL (pH 6.8), 2% SDS, 0.01% Bromophenol Blue
LB Medium	1% Tryptone, 1% NaCl, 0.5% Yeast Extract
PBS (Tablets), pH 7.4	137 mM NaCl, 10 mM Na_2HPO_4, 1.8 mM KH_2PO_4, 2.7 mM KCl

SOC Media	2% Tryptone, 0.05% NaCl, 0.5% Yeast Extract, 20 mM Glucose
Tris-Acetate-EDTA (TAE)	40 mM Tris-Base, 20 mM Glacial Acetic Acid, 1 mM EDTA
TE Buffer	10 mM Tris-HCl, pH 7.5, 1 mM EDTA
Tris Buffered Saline (TBS) pH 7.6	20 mM Tris-Base, 150 mM NaCl
TBS-T	TBS, 0.1% Tween-20
Tris-Glycine SDS running buffer	25 mM Tris-Base, 192 mM Glycine, 0.1% SDS, pH 8.3
Tris-Glycine SDS transfer buffer	25 mM Tris-Base, 192 mM Glycine, 0.1% SDS, 20% Methanol

2.1.3 Mammalian Tissue Culture

2.1.3.1 Cell lines

WT-NIKS	Wild-type keratinocytes arising from the BC-1-Ep strain of normal human neonatal foreskin keratinocytes
HA-A3A NIKS	NIKS with HA-epitope tag on endogenous A3A
HA-A3B NIKS	NIKS with HA-epitope tag on endogenous A3B
A3A KO NIKS	NIKS with a homozygous deletion of A3A
MCF-10A	Normal breast epithelial cells
NHEK	Normal primary human epidermal keratinocytes from pooled adult donors (Sigma, C-12006)
BFTC-905	Urinary bladder carcinoma cells

2.1.3.2 Media reagents

Reagents	Source	Product Code
Adenine	Sigma	A2786
Cholera Toxin	Merck Millipore	227036
Dulbecco's Modified Eagle Medium (DMEM) with 4.5 g/L Glucose, 3.7 g/L $NaHCO_3$, with L-Glutamine, without Sodium Pyruvate	Pan Biotech	P04-03550
Earle's Balanced Salt Solution (EBSS) 10X	Sigma	E7510
Epidermal Growth Factor (EGF) from murine submaxillary gland	Sigma	E1257
Recombinant Human EGF	R&D Systems	AFL236
Foetal Bovine Serum	Pan Biotech	P30-3031
Ham's F12 Medium, with 1.176 g/L $NaHCO_3$ and L-Glutamine	Pan Biotech	P04-14500
HEPES Solution, 1M, pH 7.4-7.6	Sigma	H0887
Horse Serum	Gibco	26050-070
Hydrocortisone	Sigma	H0888
Insulin	Sigma	I6634
Iscove's Modified Dulbecoo's Medium (IMDM) with 25 mM Hepes, 3.024 g/L $NaHCO_3$ and L-Glutamine	Pan Biotech	P04-20150
Keratinocyte Growth Medium 2 Kit (Basal Medium and Supplement Pack)	Sigma	C-20111
Mitomycin C from *Streptomyces caespitosus*	Sigma	M4287
Penicillin / Streptomycin (containing 10,000 U/ml Penicillin and 10 mg/ml Streptomycin)	Pan Biotech	P06-07100
Trypsin 0.05% / ethylene-diamine-tetra acetic acid (EDTA) 0.02% in PBS	Pan Biotech	P10-0235SP

2.1.3.3 NIKS media preparation (FC media)

Stocks	Concentration	Preparation
Ham's F12 Medium	66.7%	Filter sterilised
DMEM	22.3%	Filter sterilised
FBS	5 %	Filter sterilised
Penicillin-Streptomycin	1 %	Filter sterilised
Adenine	24 μg/ml	121 mg of adenine dissolved in 50 ml of 0.05N HCl to make a 2.42 mg/ml (100X) stock solution. Stirred for 1 hr and stored at -20°C. Filter sterilised
Cholera Toxin	8.3 ng/ml	Resuspended at 10 μM in sterile dH_2O and stored at -20°C, from which 50 μl dissolved in 50 ml of HBES containing 0.1% BSA to make a 0.83 μg/ml (100X) solution and stored at 4°C. Filter sterilised
EGF from murine submaxillary gland	10 ng/ml	100 μg of EGF dissolved in 10 ml of sterile dH_2O then 90 ml of HBES containing 0.1% BSA added to make a 1 μg/ml (100X) stock solution and stored at -20°C. Filter sterilised
Hydrocortisone	0.4 μg/ml	25 mg of hydrocortisone dissolved in 5 ml of cold 100% ethanol to make a 5 mg/ml solution, from which 0.8 ml added to 100 ml of HBES with 5% FBS to make a 40 μg/ml (100X) stock solution and stored at -20°C. Filter sterilised
Insulin	5 μg/ml	Resuspended at 500 μg/ml (100X) with 0.05N HCl and stored at 4°C. Filter sterilised with a filter pre-wet with FBS
HEPES-Buffered Earles' Salts (HBES)		10% EBSS, 260 mM $NaHCO_3$, 25 mM HEPES. Filter sterilised, stored at 4°C

2.1.3.4 MCF-10A media preparation

Stocks	Concentration	Preparation
Ham's F12 Medium	47%	Filter sterilised
DMEM	47%	Filter sterilised
Horse Serum	5 %	Filter sterilised
Penicillin-Streptomycin	1 %	Filter sterilised
Cholera Toxin	100 ng/ml	Resuspended as a 10 μM (8300X) stock solution in sterile dH_2O and stored at -20°C. Filter sterilised
Recombinant Human EGF	20 ng/ml	Resuspended at 100 μg/ml (5000X) in sterile dH_2O and stored at -20°C. Filter sterilised
Hydrocortisone	0.5 μg/ml	25 mg of hydrocortisone dissolved in 5 ml of cold 100% ethanol to make a 5 mg/ml (10,000X) stock solution and stored at -20°C. Filter sterilised
Insulin	10 μg/ml	Resuspended at 10 mg/ml (1000X) in dH_2O containing 1% glacial acetic acid and stored at 4°C. Filter sterilised with a filter pre-wet with FBS

2.1.3.5 NHEK media preparation

Keratinocyte growth media 2 kit (basal media and supplement pack, Sigma) reconstituted as per supplier's instructions with a final concentration as follows: 0.4% bovine pituitary extract, 0.125 ng/ml recombinant human EGF, 5 μg/ml insulin, 0.33 μg/ml hydrocortisone, 0.39 μg/ml epinephrine, 10 μg/ml transferrin and 0.06 mM $CaCl_2$. Supplemented with 1% Penicillin-Streptomycin.

2.1.3.6 Materials

Consumables	Source	Product Code
6-well plates	Sarstedt	83.3920.300
96-well plates	Sarstedt	82.1582.001
T-25 Culture Flasks	Sarstedt	83.3910.002
T-75 Culture Flasks	Sarstedt	83.3911.002
T-175 Culture Flasks	Sarstedt	83.3912.002

2.1.4 Drugs and Inhibitors

Compound	Inhibitor target	Supplier	Product code
Afatinib	EGFR	Fisher Scientific	16463748
Bleocin, from *S. verticillus*	-	Sigma-Aldrich	203048
Capivasertib (AZD5363)	AKT	Selleck Chemicals	S8019
Cisplatin	-	Sigma-Aldrich	P4394
Erlotinib hydrochloride	EGFR	Sigma-Aldrich	SML2156
5-ethynyl-2´-deoxyuridine (EdU)		Invitrogen	C10634
Everolimus	mTOR	Fluka Analyticals	57-55-6
Gö6983	PKC	Sigma-Aldrich	G1918
MK2206	AKT	Selleck Chemicals	S1078
Nocodazole	-	Sigma-Aldrich	M1404
Pictilosib (GDC0941)	PI3K	Selleck Chemicals	S1065
Ravoxertinib (GDC0994)	ERK1/2	Selleck Chemicals	S7554
SB203580	p38 α/β	Abcam	ab120162
Thymidine	-	Sigma-Aldrich	T1895
Trametinib (GSK1120212)	MEK1/2	Selleck Chemicals	NC0991754

2.1.5 Kits and assays

Kit/Assay	Supplier	Product Code
CellTiter Cell Proliferation Assay (MTS)	Promega	G3580
Clarity Western ECL	Bio-Rad	1705060
Criterion TGX Midi Protein Gel, Any kD	Bio-Rad	5671124/ 5671125
Hot StarTaq Plus Master Mix	Qiagen	203643
KAPA HiFi HotStart ReadyMix PCR Kit	Roche	07958919001
LunaScript RT Supermix (Reverse Transcriptase)	New England BioLabs	E3010
Monarch Total RNA Miniprep	New England BioLabs	T2010
Oxiselect Oxidative DNA Damage Quantitation Kit	Cell Biolabs	STA-324
PageRuler Plus Prestained Ladder	Thermo Scientific	26619
Pierce BCA Protein Assay Kit	Thermo Scientific	23225
Plasmid Miniprep Kit	Monarch	T1010
PowerUp SYBR Green 2X MasterMix	Applied Biosystems	A25741
Trans-Blot Turbo RTA Midi Transfer Kit	Bio-Rad	1704273
Zero Blunt TOPO PCR Cloning Kit	Invitrogen	450245

2.1.6 Antibodies

2.1.6.1 Primary antibodies

Target antigen	Supplier	Species	Code	Lot number
β-Actin-HRP (AC15)	Sigma-Aldrich	Mouse monoclonal	A3854	-
APOBEC3A	Sigma-Aldrich	Rabbit polyclonal	HPA043237	
APOBEC3A	J.Maciejowski	Mouse monoclonal	-	-
Cyclin B1 (GNS1)	Santa Cruz	Mouse monoclonal	sc-245	G1818
DDOST	Abcam	Rabbit polyclonal	ab204314	GR3200777
HA-epitope (C29F4)	Cell Signalling	Rabbit monoclonal	3724S	
γ-H2AX	MerckMillipore	Mouse monoclonal	05-636	
γ-H2AX	PTM Biolabs	Mouse monoclonal	P.E	
pH3	Cell Signalling	Rabbit monoclonal	9701	17

2.1.6.2 Secondary antibodies

Target antigen	Species	Supplier	Product Code
Anti-Rabbit IgG (H+L) Cross-Absorbed, HRP conjugated	Donkey	Invitrogen	A16023
Anti-Mouse IgG (H+L) Cross-Absorbed, HRP conjugated	Donkey	Invitrogen	A16011
Anti-mouse Alexa Fluor-488	Donkey	Invitrogen	A21202
Anti-rabbit Alexa Fluor-488	Donkey	Invitrogen	A21206
Anti-mouse Alexa Fluor-594	Donkey	Invitrogen	A21203
Anti-rabbit Alexa Fluor-594	Donkey	Invitrogen	A21207

2.1.7 qPCR Primers

All primer sequences were synthesised by Integrated DNA Technologies (IDT):

Name of Primer	Sequence
APOBEC3A (Forward)	5'- GAGAAGGGACAAGCACATGG -3'
APOBEC3A (Reverse)	5'- TGGATCCATCAAGTGTCTGG -3'
APOBEC3B (Forward)	5'- GACCCTTTGGTCCTTCGAC -3'
APOBEC3B (Reverse)	5'- GCACAGCCCCAGGAGAAG -3'
APOBEC3C (Forward)	5'- AGCGCTTCAGAAAAGAGTGG -3'
APOBEC3C (Reverse)	5'- AAGTTTCGTTCCGATCGTTG -3'
APOBEC3D (Forward)	5'- ACCCAAACGTCAGTCGAATC -3'
APOBEC3D (Reverse)	5'- CACATTTCTGCGTGGTTCTC -3'
APOBEC3F (Forward)	5'- CCGTTTGGACGCAAAGAT -3'
APOBEC3F (Reverse)	5'- CCAGGTGATCTGGAAACACTT -3'
APOBEC3G (Forward)	5'- CCGAGGACCCGAAGGTTAC -3'
APOBEC3G (Reverse)	5'- TCCAACAGTGCTGAAATTCG -3'
APOBEC3H (Forward)	5'- AGCTGTGGCCAGAAGCAC -3'
APOBEC3H (Reverse)	5'- CGGAATGTTTCGGCTGTT -3'
Cyclin A2 (Forward)	5'- TCCTCCTTGGAAAGCAAACA -3'
Cyclin A2 (Reverse)	5'- GGGCATCTTCACGCTCTATT -3'
Cyclin B1 (Forward)	5'- GGTGTCACTGCCATGTTTATTG -3'
Cyclin B1 (Reverse)	5'- TCTGTCTGATTTGGTGCTTAGT -3'
Cyclin D1 (Forward)	5'- GGTTCAACCCACAGCTACTT -3'
Cyclin D1 (Reverse)	5'- CAGCGCTATTTCCTACACCTATT-3'
Cyclin E1 (Forward)	5'- CTGGATGTTGACTGCCTTGA -3'
Cyclin E1 (Reverse)	5'- CTCTATGTCGCACCACTGATAC -3'
CDKN1A/p21 (Forward)	5'- GAGCGATGGAACTTCGACTT -3'
CDKN1A/p21 (Reverse)	5'- CGGGATGAGGAGGCTTTAAATA -3'
DDOST (Forward)	5'- CTGAAGAAGAAAGGTGGCAAATAC -3'
DDOST (Reverse)	5'- GTAGCCTAGCCGGTTGTAATC -3'
GAPDH (Forward)	5'- GTCATCCATGACAACTTTGGTA -3'
GAPDH (Reverse)	5'- GGATGATGTTCTGGAGAGC -3'
TBP (Forward)	5'- TTGAGGAAGTTGCTGAGAAGAG -3'
TBP (Reverse)	5'- CAGATAGCAGCACGGTATGAG -3'

2.2 Methods

2.2.1 Cell culture

2.2.1.1 Freezing cells

Proliferating cells of no greater than 80% confluency were detached using 0.05% trypsin / 0.02% EDTA, pelleted by centrifugation at 500 x g for 5 mins (with the exception of NHEK cells: 220 x g for 5 mins), and resuspended at 1 x 10^6 per ml in freezing media composed of DMEM with 10% FBS and 10% DMSO. Cells were frozen slowly before transfer to a -80^{o}C freezer for at least 24 hr, then transferred to a liquid nitrogen cryostat.

2.2.1.2 Thawing cells

Vials were taken from liquid nitrogen storage and kept on dry ice until ready to thaw. At which point they were thawed quickly in a water bath at 37^{o}C and the contents transferred to greater than 4-times volume of DMEM containing 10% FBS. Cells were then pelleted by centrifugation at 500 x g, following which the supernatant was removed and the pellet resuspended in cell-line specific media before transferring to a tissue culture flask. NHEK primary cells were instead transferred directly to a cell culture flask containing NHEK media (without centrifugation), and the media changed 4 hr later when cells had attached to remove the DMSO component of the freezing medium.

2.2.1.3 NIH 3T3-J2 feeder cells preparation

NIH 3T3-J2 (3T3) murine embryonic fibroblast feeder cells were maintained in DMEM supplemented with 10% FBS, and incubated at 37 °C and 5% CO_2. Cells were grown to -80% confluency before treating for 3-4 hr with 4 μg/ml of the proliferation inhibitor, mitomycin C (Sigma-Aldrich). Following which, cells were washed twice with PBS and detached using 0.05% trypsin / 0.02% EDTA and either plated immediately or frozen for future use.

2.2.1.4 Near-normal keratinocyte cells (NIKS)

The near-normal keratinocyte (NIKS) cell line is a spontaneously immortalised human cell line that was derived from the BC-1-Ep strain of neonatal foreskin keratinocytes (Allen-Hoffmann *et al.*, 2000). NIKS were maintained on a layer of mitomycin C treated 3T3 feeder cells (at a density of ~12,000 cells cm^{-2}), in FC media containing 3 parts F12 media, 1 part DMEM, supplemented with 5% FBS, 10 ng/ml of EGF from murine submaxillary gland, 24 μg/ml adenine, 5 μg/ml insulin, 8.3 ng/ml cholera toxin, 0.4 μg/ml hydrocortisone, and 1% penicillin/streptomycin. Cells were incubated at 37 °C and 5% CO_2, the media replaced every two days, and grown to -80% confluency before passaging which as follows: differential trypsinisation (using 0.05% trypsin / 0.02% EDTA, for 1 - 2 mins) to first remove the 3T3 cells. NIKS were then washed with PBS followed by the addition of fresh trypsin (10-15 min). The Trypsin was neutralised using DMEM containing 10% FBS and the cells collected and pelleted by centrifugation at 500 x g for 5 mins.

2.2.1.5 Primary keratinocyte cells (NHEK)

Normal Human Epidermal Keratinocytes (NHEK) from pooled adult donors were purchased from Sigma (PromoCell). These were thawed (passage number 2) and cultured for no more than two further passages in either: (1) serum-free, feeder-free, in keratinocyte growth media (Sigma) containing 0.4% bovine pituitary extract, 0.125 ng/ml recombinant human EGF, 5 μg/ml insulin, 0.33 μg/ml hydrocortisone, 0.39 μg/ml epinephrine, 10 μg/ml transferrin and 0.06 mM $CaCl_{2,}$ and 1% Penicillin-Streptomycin, or (2) with 3T3 feeder cells and FC media (3 parts F12 media, 1 part DMEM, supplemented with 5% FBS, 10 ng/ml of EGF from murine submaxillary gland, 24 μg/ml adenine, 5 μg/ml insulin, 8.3 ng/ml cholera toxin, 0.4 μg/ml hydrocortisone, and 1% penicillin/streptomycin). Cells were incubated at 37 °C and 5% CO_2, the media replaced every two days, and grown to -80% confluency before passaging.

2.2.1.6 Breast epithelial cells (MCF-10A)

Normal breast epithelial cells (MCF-10A) were maintained in media containing a 1:1 ratio of F12 media and DMEM, supplemented with: 5% horse serum, 20 ng/ml of recombinant human EGF, 100 ng/ml cholera toxin, 10 μg/ml insulin, 0.5 μg/ml hydrocortisone, and 1% penicillin/streptomycin. Cells were cultured at 37°C and 5% $CO_{2.}$ Media was refreshed every two days, and cells grown to -80% confluency before passaging.

2.2.1.7 Retinal pigment epithelial cells (RPE-1)

RPE-1 cells were maintained in F12:DMEM media (1:1) containing 10% FBS and 1% penicillin/streptomycin. Cells were sub-cultured as described before.

2.2.1.8 Cervical cancer cell lines

SiHa and HeLa cells were maintained in DMEM media containing 10% FBS and 1% penicillin/streptomycin. Cells were sub-cultured as described before.

2.2.1.9 Urinary bladder carcinoma cells (BFTC-905)

BFTC-905 cells were maintained in IMDM media containing 10% FBS and 1% penicillin/streptomycin. Cells were sub-cultured as described before.

2.2.2 Cell viability / proliferation assays

For proliferation assays: cells were plated in 96-well plates with NIKS at a density of 3 x 10^3 cells per well together with mitomycin C treated 3T3 feeder cells at a density of 1 x 10^3 cells per well, in FC media with six technical repeats and cultured at 37°C and 5% CO_2. Cell proliferation was quantified on days 2 to 4 through the addition of MTS reagent (Promega) and incubation at 37^{o}C for 2 hr. Media was removed and replaced every second day on each remaining 96-well plate.

The assay involves the conversion of the MTS tetrazolium compound in metabolically active cells, through the activity of NAD(P)H-dependent dehydrogenase enzymes to generate a coloured formazan dye. The formazan dye conversion was quantified on a microplate absorbance reader at 490 nm. For cell viability assays conducted with DNA damaging drugs, cells were plated and quantified as above with the exception of having three technical repeats and NIKS at a density of 5 x 10^3 cells per well. Cells were incubated with a dose range of drug on day one at plating, then either: (1) half of the media removed each subsequent day and replaced with same volume of media containing fresh drug (over a 4-day period), or (2) Incubated in the same media (and drug) for the duration.

2.2.3 Cell synchronisation

2.2.3.1 G1/S arrest (single thymidine block)

Cell synchronisation at the G1/S boundary can be reversibly achieved with high concentrations of thymidine, which interrupts the deoxynucleotide metabolism pathway through competitive inhibition (Galavazi, Schenk and Bootsma, 1966). NIKS were plated in 6-well plates at a density of 3 x 10^5 cells per well in 2 ml of FC media (208 μl/cm^2), together with mitomycin C treated 3T3 feeder cells at a density of 1 x 10^5 cells per well, and cultured at 37°C and 5% CO_2. The next day, the media was aspirated from each well and replaced with 2 ml of FC media containing 2 mM of thymidine, and incubated at 37°C for 18 hr.

Cells were then released from G1/S blockade through aspiration of the media containing thymidine, the cells washed twice with pre-warmed PBS, followed by incubation in 2 ml of fresh FC media and samples collected samples at the time intervals shown.

2.2.3.2 G1/S arrest (double thymidine block)

A double thymidine block may achieve a more uniform blockade in early S-phase. To achieve this, NIKS were plated in 6-well plates at a density of 2.5 x 10^5 cells per well in 2 ml of FC media with mitomycin treated 3T3 feeder cells as above, and cultured at 37°C and 5% CO_2. The next day, synchronisation at the G1/S boundary was performed by either:

(1) First thymidine block (2 ml of FC media/ 2 mM thymidine per well (208 $\mu l/cm^2$) for 18 hr, then media removed, cells washed twice with PBS and incubated with 2 ml of fresh FC media for 9 hr. Media then removed and replaced with 2 ml of fresh media containing 2 mM of thymidine for a further 16 hrs. Cells were released from the second thymidine block through washing as before followed by the addition of 2 ml of fresh FC media.

(2) First thymidine block, except using 1 ml of FC media / 2 mM thymidine per well (104 $\mu l/cm^2$), for 18 hr. Cells then washed twice with PBS and incubated with 1 ml of fresh FC media for 9 hr.

Then, without removing media, 1 ml of fresh media containing 4 mM (2X) thymidine added to existing 1 ml media, making 1X final concentration, and incubation for a further 16 hrs. Cells were released from the second block through washing as before and adding 1 ml of fresh FC media.

(3) NIKS were plated in T175 flasks in 20 ml of FC media (114 $\mu l/cm^2$) at a density of 1.5 x 10^6 cells per flask, with mitomycin C treated 3T3 feeder cells at a density of 1 x 10^6. The next day, media was removed and replaced with 20 ml of FC media containing 2 mM of thymidine and incubated for 18 hr. After which, media containing thymidine removed, cells washed twice with PBS and incubated with 20 ml of fresh FC media for 9 hr. Followed by removal and replacement with 20 ml of fresh media containing 2 mM of thymidine for a further 16 hrs. Cells were released from the second thymidine block through washing as before, followed by the addition of 20 ml of fresh FC media.

2.2.3.3 Synchronisation in G0 / quiescence through serum starvation

To induce quiescence through growth factor withdrawal, a protocol used in NIKS by Matrka *et al.*, (2015) was adapted and used as follows: cells were plated in 6-well plates at a density of 2 x 10^5 cells per well in 2 ml of FC media (208 $\mu l/cm^2$), with mitomycin C treated 3T3 feeder cells at a density of 1 x 10^5 cells per well and incubated at 37°C and 5% CO_2. The next day, the media was aspirated from each well and cells washed twice with pre-warmed PBS.

This was followed by incubation in 2 ml of media containing: F-12/DMEM, 0.3% FBS, 8.3 ng/ml cholera toxin and 0.4 μg/ml hydrocortisone (no EGF, insulin or adenine), and cells incubated for 40 hr. For re-stimulation, starvation media was replaced with FC media (5% FBS and all growth factors).

NHEK primary cells were either: (1) plated in 6-well plates at a density of 2 x 10^5 cells per well in 2 ml of NHEK media (208 μl/cm^2). The next day, the media was removed, cells washed twice PBS, followed by incubation for either 18 hr, 24 hr or 48 hr in 2 ml of starvation media consisting of either: (a) DMEM containing 0.3% FBS, (b) NIKS starvation media (as described above), or (c) NHEK basal media, 0.3% FBS, 0.39 μg/ml epinephrine and 0.33 μg/ml hydrocortisone (no hEGF, insulin or transferrin). For re-stimulation, starvation media was replaced with NHEK media (0.4% BPE and all NHEK cell growth factors); or (2) plated as above, in 2 ml of NIKS FC media together with mitomycin C treated 3T3 feeder cells, and incubated in NIKS starvation media for 18 hr, 24 hr or 48 hr, followed by re-stimulation with FC media.

2.2.3.4 G1 arrest through CDK4/6 inhibition

When a cell commits to replication by passing the restriction point in G1, levels of D-type cyclins (D1-D3) increase and form complexes with CDK4 and CDK6; these complexes enter the nucleus and promote the G1-S transition by phosphorylating Rb which leads to the derepression of E2F transcription factor activity and an increase in S-phase gene activity (reviewed by Goel *et al*., 2018).

To achieve G1 arrest in NIKS, cells were first synchronised in G0/quiescence by incubation in starvation media as previously described. Following which, starvation media was removed and replaced with FC media containing 200 nM of the CDK4/6 inhibitor, Palbociclib, and samples collected over the subsequent 24 hr time-period.

2.2.3.5 Mitotic arrest with nocodazole

Nocodazole is a chemical agent that disrupts microtubule disassembly, causing cell cycle arrest during mitosis (Vasquez *et al.*, 1997). To arrest NIKS in mitosis, cells were treated with nocodazole by either: (1) a double thymidine block as previously described, after which cells were released from G1/S arrest by adding fresh FC media for 2 hr, then the media was removed and replaced with FC media containing 100 ng/ml of nocodazole for a further 10 hr, or (2) cells synchronised in G0/quiescence by serum starvation as previously described, then released back into the cell cycle for 18 hr to traverse through G1-S-into early G2, before adding 100 ng/ml of nocodazole and incubating cells for a further 6 hr.

2.2.4 Preparation of total cell lysate

Cells were either: (1) washed with PBS and detached using trypsin (differential trypsinisation of 3T3 feeder cells to remove first). Trypsin was then neutralised and cells collected using DMEM containing 10% FBS, pelleted by centrifugation at 500 x g for 5 mins, the supernatant removed and cell pellets flash frozen at -80^{o}C.

Following which, cell pellets were defrosted on ice and resuspended in MPER lysis buffer containing protease and phosphatase inhibitor cocktails, and 0.2 U/μl of benzonase (an endonuclease), for 15 mins on ice with agitation, or (2) cells washed twice with PBS, the PBS removed and the tissue culture dish flash frozen at -80^{o}C.

Tissue culture plates were defrosted on ice, lysis buffer (as above) added directly to each well, and cells scraped and collected into 1.5 ml Eppendorf tubes which were then placed on ice for 15 mins with agitation. Lysates from both methods were then centrifuged at 14,000 g for 20 mins to separate soluble proteins from the insoluble fraction, the supernatant then transferred to fresh 1.5 ml Eppendorf tubes and flash frozen. Lysates were stored at -80^{o}C.

2.2.5 SDS-PAGE and western blot analysis

Protein concentration was quantified using a colourimetric bicinchoninic acid (BCA) assay according to the manufacturer's instructions. Whole cell lysates. (20 – 25 μg) were prepared in Laemmli buffer containing 100 mM of DTT and heated to 70^{o}C for 10 mins before separation by Sodium Dodecyl Sulphate Polyacrylamide Gel Electrophoresis (SDS-PAGE).

SDS-PAGE was performed using Criterion Tris-Glycine (TGX) pre-cast midi polyacrylamide gels (any kD, that separate polypeptides from ~10–200 kD), with Tris-Glycine SDS running buffer.

Electrophoresis was performed at a constant voltage of 200v for 45 min, after which proteins were transferred to a methanol-activated 0.2 μm Polyvinylidene Difluoride (PVDF) membrane using Tris-Glycine SDS transfer buffer, and a Trans-Blot Turbo transfer system (BioRad) at 2.5 A and up to 25v for 7 min. Non-specific proteins were blocked using TBS-T and 5% skimmed milk for 1 hr, then incubated with primary antibody in TBS containing 2% BSA, overnight at 4°C.

The next day, membranes were washed three times with TBS-T for 10 min each, then incubated with horseradish peroxidase (HRP)-conjugated secondary antibody (1:10,000) raised against the primary antibody species, for 1 hr at room temperature with agitation. Finally, the PVDF membrane was washed three times with TBS-T for 10 min each, then incubated with enhanced luminol-based detection (ECL) reagent before exposure either on a Syngene G:Box-fluorescence imager, or an X-Ray film developer using Amersham Hyperfilm ECL.

2.2.6 Extraction of RNA

RNA purification was performed using the Monarch Total RNA Miniprep Kit (NewEngland BioLabs) according to the manufacturer's instructions. An optional component of the kit, on-column DNase digestion, was used to remove genomic DNA. Purified RNA was stored at -80^{o}C.

2.2.7 cDNA synthesis

The concentration of RNA samples was determined using a ND-1000 NanoDrop Spectrophotometer, from which up to 1 μg was used to synthesise cDNA using LunaScript Reverse Transcriptase (RT) SuperMix Kit (NewEngland BioLabs), which contains random hexamer and oligo-dT primers, dNTPs, murine RNase inhibitor, and Luna reverse transcriptase enzyme. Reactions were incubated in a thermocycler at 25°C for 2 mins (primer annealing step), 55°C for 10 mins (cDNA synthesis step), and 95°C for 1 min (heat inactivation step), and then diluted in RNase-free water prior to use in qPCR.

2.2.8 Quantitative real-time PCR (qPCR)

Reactions were performed in 96-well plates on a QuantStudio 3 Real-Time PCR system (Applied Biosystems), with two technical repeats for each sample and a 10 μl total volume comprised of: 5 μl of PowerUp SYBR Green 2X Master Mix, 0.3 μl (0.3 μM) each of forward and reverse primer, 0.4 μl of nuclease-free water, and 4 μl of diluted cDNA (10 ng). Additionally, PowerUP SYBR Green and nuclease-free water only (no template control) was performed in duplicate for each primer pair. Reactions were incubated at 50°C for 2 mins and 95°C for 10 min (hold step), then forty cycles at 95°C for 15 sec and 60°C for 1 min (PCR step), then 95°C for 15 sec, 60°C for 1 min and 95°C for 1 sec (melt curve step). The number of PCR cycles at which amplification was detectable above a background threshold (threshold cycle, or Ct) was determined by the QuantStudio cycler software.

2.2.9 Standard curve generation for qPCR

Standard curves are used to measure absolute amounts of target copies by qPCR. As basal levels of A3A are low, TATA-box binding protein (TBP) was chosen as the housekeeping gene for quantifying A3A mRNA values due to its lower expression compared to that of GAPDH. Plasmids pRH3097-A3A, pRH3097-A3C, and pRH3097-A3H were kindly provided by Professor Reuben Harris (HHMI, University of Minnesota); pCMV4-A3B, pCMV4-A3D, pCMV4-A3F, pCMV4-A3G were provided by Professor Mike Malim (Kings College London). These were then transformed into competent cells from which plasmid DNA was extracted (described below) and serial dilutions made to generate standard curves.

2.2.9.1 Bacterial cell transformation

Agar was heated to dissolve then left to cool to ~50-55°C before the addition of selection antibiotic (ampicillin at 100 μg/ml, or kanamycin at 50 μg/ml), mixed and poured onto plates to set. 10 ng of plasmid DNA was added to 50 μl of competent *E.coli* cells, samples mixed and incubated on ice for 30 min. The *E.coli* cells were next heat-shocked at 42^{o}C for 45 sec, placed on ice for 2 min, 250 μl of SOC media added, and cells then incubated at 37^{o}C for 1 hr with shaking at 150 rpm. After which, 10 μl and 50 μl of the transformed cells were streaked onto agar plates with the appropriate selection antibiotic and incubated overnight at 37^{o}C.

2.2.9.2 KAPA Taq PCR and TOPO-cloning

For generation of plasmids for TBP and DDOST, PCR was first performed with cDNA reverse transcribed from RNA extracted from WT-NIKS, using KAPA Taq PCR to produce blunt-end PCR products, as follows: 10 μl of 2X KAPA master mix, 0.3 μl (0.3 μM) each of forward and reverse primer, 100 ng of cDNA, and nuclease-free water to a total 20 μl volume. Reactions were incubated at 95°C for 3 mins (initial denaturation), then thirty cycles at 98°C for 20 sec (denaturation), 62°C for 15 sec (annealing), 72°C for 30 sec (extension); and a final extension at 72°C for 1 min.

PCR products were separated on a 1% agarose gel by electrophoresis to verify that a single, discrete band of the correct size was obtained: 2 μl of each PCR product was mixed with 1 μl 10x Blue Juice Loading Buffer and 8 μl of nuclease-free water. PCR products were loaded alongside a 1 kb Plus DNA Ladder, the gel run at 100V for 1 hr, and DNA bands visualised on a Syngene G:Box imager.

Amplified fragments (TBP: 650 bp; DDOST: 301 bp) were then subcloned into Topoisomerase I–activated plasmid vectors (pCR-Blunt II-TOPO) as follows: 4 μl of PCR product incubated with 1 μl of TOPO vector and 1 μl of salt solution (200 mM NaCl, 10 mM $MgCl_2$) for 5 min at room temperature. 2 μl of the TOPO reaction was then transformed into competent *E.coli* cells as previously described. After which, colony PCR was performed using Hot StarTaq Plus Master Mix followed by agarose gel electrophoresis to again verify amplification of a single product.

Colonies were subsequently grown in an overnight culture of LB medium containing the appropriate selection antibiotic, at 37°C with shaking at 300 rpm. The following day, glycerol stocks were made in cryovials by adding 500 µl of 50% glycerol and 500 µl of culture (25% final concentration). Cryovials were then stored at -80°C.

2.2.9.3 Plasmid isolation

Plasmid DNA was extracted from cultures using a Monarch Plasmid Miniprep Kit, according to the manufacturer's instructions. Briefly, cells were harvested by centrifugation at 16,000 x g for 30 sec, the supernatant removed and cells resuspended in lysis buffer. Lysis buffer was neutralised and lysates clarified by centrifugation for 2 minutes at 16,000 x g. Plasmid DNA was washed to remove RNA, protein, and endotoxin, and eluted using DNA elution buffer.

2.2.9.4 Standard curves

Plasmid DNA was quantified using a Nano-Drop Spectrophotometer, from which 5-fold serial dilutions, from 5.12 up to 1 x 10^7 copy numbers, were made to generate standard curves. Each dilution was run in triplicate technical repeats with no-template controls. qPCR melt curves additionally confirmed amplification of a single product, an example of which (DDOST) is shown in Figure 2-1.

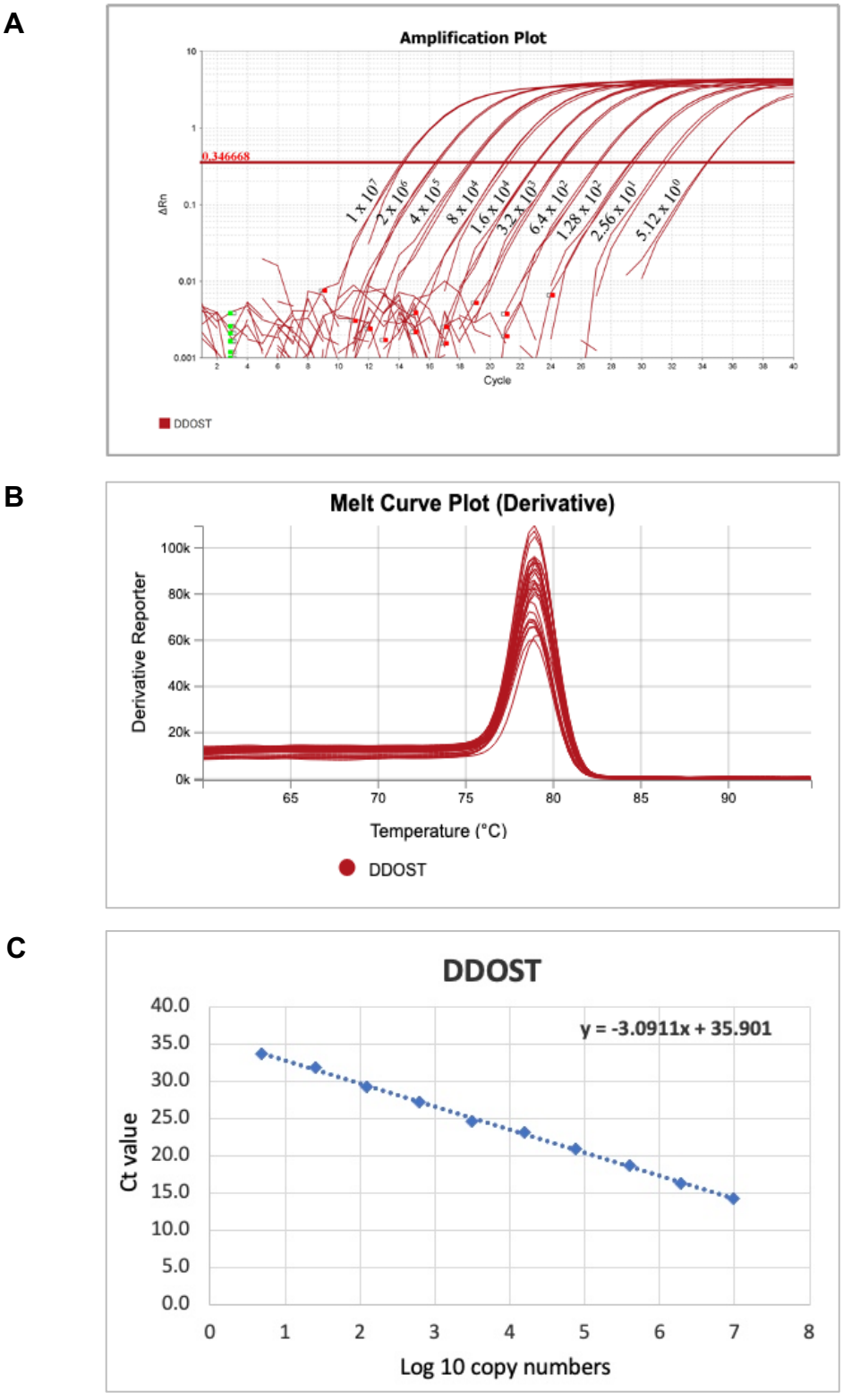

Figure 2-1 Standard curves for absolute quantification of mRNA levels.
Example of standard curve generation (DDOST). **(A)** qPCR amplification plot with serial dilutions from 5.12 x 100 - 1 x 107 copy numbers. **(B**) Melt curve plot of dilutions showing amplification of a single product. **(C)** Plot of Ct values against Log 10 copy numbers to generate equation for quantifying sample copy numbers.

2.2.10 Cell cycle analysis by flow cytometry

Propidium iodide (PI) staining of cells allows for DNA content to be measured by its relative fluorescent intensity, enabling quantification of populations at different cell cycle stages (G2 cells have 4n DNA content so will have double the fluorescent intensity of G0/G1 cells that have 2n DNA content. Cells in S-phase have variable DNA content between 2n-to-4n).

Following serum starvation, NIKS were collected for flow cytometry analysis by differential trypsinisation to first remove the 3T3 feeder cells, then the trypsin neutralised and cells collected using DMEM containing 10% FBS. The cells were pelleted by centrifugation at 500 x g, the supernatant removed, and washed once in PBS before fixation in either: (1) 70% ice-cold ethanol while gently vortexing, then overnight at -20^{o}C, or (2) 4% formaldehyde for 15 min at room temperature, followed by centrifugation at 300 x g, the supernatant then removed followed by two washes with PBS containing 1% BSA, and stored at 4^{o}C before commencing PI staining.

For PI staining, cells were pelleted by centrifugation at 300 x g followed by washing with PBS. Cell pellets were resuspended in 250 μl of PBS to which 5 µl of 10 mg/ml RNase A was added and cells incubated at 37°C for 1 hour (200 μg/ml final concentration). Cells were then stained using 5 µl of a 1 mg/ml PI solution (20 μg/ml final concentration) and kept in the dark on ice for 30 min before analysing on a BD Accuri C6 Plus Flow Cytometer. Cells were excited using a laser line at 488 nm, and a 585/40 nm optical emission filter.

2.2.11 Immunofluorescence

Prepared coverslips (autoclaved, washed in 70% ethanol, followed by two washes with sterile distilled water) were placed in 6-well plates on which NIKS and 3T3 feeder cells were plated and treated as previously described. For fixation, the media was aspirated and cells washed twice with PBS before incubating them in 4% formaldehyde in PBS for 15 mins at room temperature. Cells were then washed three times with PBS and stored in PBS at 4°C until staining.

For staining, cell membranes were permeabilised with TBS containing 0.3% Triton X-100 for 10 mins, then coverslips washed twice with TBS. To minimise background staining from non-specific antibody binding, cells were blocked in either: (1) TBS containing 2% BSA and 0.05% Tween-20, or (2) TBS containing 10% donkey serum and 0.05% Tween-20, for 1 hr at room temperature. Coverslips were then incubated in primary antibody diluent (TBS with 2% BSA and 0.05% Tween-20) and either: anti-HA (Cell Signalling) 1:500; A3A (Sigma) 1:100; A3A (gift from J.Maciejowski); γ-H2AX mouse monoclonal antibody (PTM Biolabs; 1:350), 1:200, overnight at 4°C in a humidity chamber.

The next day, coverslips were washed three times with TBS containing 0.1% BSA and 0.05% Tween-20, for 10 mins each then incubated in secondary antibody diluent (TBS with 0.1% BSA and 0.05% Tween-20) with Alexa Fluor-conjugated secondary antibodies raised against the primary antibody species, at room temperature for 1 hr in a humidity chamber.

Coverslips were again washed three times with TBS containing 0.1% BSA and 0.05% Tween-20, for 10 mins each, then either: (1) incubated with NucBlue Fixed Cell Ready Probes Reagent (DAPI) before mounting on a glass microscope slide with Prolong Gold mounting medium, or (2) mounting directly using Prolong Gold mounting medium containing DAPI (4',6-diamidino-2-phenylindole hydrochloride). Imaging was conducted on either a Zeiss LSM 880 Elyra confocal microscope, or by using an Olympus BX-60 or Olympus BX-61 epifluorescence microscope equipped with DAPI, FITC, and Cy5 filters.

2.2.12 Oxidative DNA damage quantitation

Abasic sites arising from base loss (apurinic/apyramidic (AP) sites) were detected in NIKS using an Oxiselect Oxidative DNA Damage Quantitation Kit (Cell Biolabs) according to the manufacturer's instructions. DNA was first extracted from ~5-10 x 10^6 cells using DNAzol (a guanidine-detergent lysing solution), followed by precipitation with ethanol and solubilisation of the DNA pellet in TE buffer. Cells were treated with 10 mM of hydrogen peroxide (H_2O_2) for 1 hr as a positive control.

A biotinylated aldehyde reactive probe (ARP) in the AP site assay reacts with an aldehyde group on the open ring form of AP sites. The biotin was detected with a Streptavidin-Enzyme conjugate and absorbance read on a microplate reader at 450 nm. This absorbance was then compared to a standard curve that was generated from DNA containing predetermined AP sites.

2.2.13 Chromatin Immunoprecipitation

Cell pellets were prepared for chromatin immunoprecipitation (ChIP) from asynchronously growing populations of WT-NKS, as well as those that had been synchronised in G0/quiescence through serum starvation followed by re-stimulation, as previously described.

To prepare cell pellets, NIKS were plated in T175 tissue culture flasks in 30 ml of FC media, at a density of 4 x 10^6 cells per flask together with 3T3 feeder cells as a density of 1.5 x 10^6 per flask. For covalent fixation of the protein-DNA complexes, 1/10 volume of fixative solution containing 11% formaldehyde, 50 mM HEPES-KOH, 100 mM NaCl, 1 mM EDTA, 0.5 mM EGTA (1% final concentration of formaldehyde) was added to flasks, swirled briefly and incubated at room temperature for 10 min. The formaldehyde was then quenched by the addition of 1/20 volume of 2.5 M glycine (125 mM final concentration) for 5 min at room temperature. Cells were washed twice with ice-cold PBS then scraped for collection into falcon tubes using cold PBS containing 0.5 mM of PMSF (protease inhibitor). Cell pellets were obtained by centrifugation at 2000 x rpm for 10 min, the supernatant removed and cell pellets flash frozen and stored at −80°C.

3 Characterisation of APOBEC3 expression in NIKS

3.1 Introduction

The APOBEC3 family of cytosine deaminases have diverse functions, of which they are best known for their ability to cause C-to-T mutations in viral DNA as a mechanism of innate immunity. However, their roles in the absence of viral infection are largely undefined and APOBEC3 signature mutations (particularly A3A and A3B) are frequently found in the cellular genome of sequenced tumours due to their deregulation or off-target effects (Alexandrov *et al.*, 2013; Roberts *et al.*, 2013).

High sequence homology between some family members has made studying their endogenous activity and cellular localisation problematic (for example, A3A shares >90% sequence identity with the CTD of A3B) (Ng and Fraternali, 2020). To gain a better understanding of the physiological roles of A3A and A3B in normal human keratinocytes (a cell type from which HPV-driven cancers arise) and to allow specific recognition of either A3A or A3B protein, CRISPR/Cas9 gene edited keratinocytes (NIKS) were used in which haemagglutinin (HA) epitope tags were expressed on the endogenous A3A and A3B protein. NIKS that had been generated containing a homozygous deletion of A3A (A3A KO) enabled a comparison of activity against wild-type (WT)-NIKS. The expression levels of HA-A3A and HA-A3B NIKS could then be validated using known inducers of their expression (PMA and IFN-α); this additionally allowed us to determine whether the gene knockout (A3A) caused any perturbation to the expression of the other A3 genes.

3.2 Generation of cell lines

The HA-epitope tagged A3A and A3B, and the A3A knockout cell lines were generated previously in the lab (T.Fenton, unpublished data) by employing the 'split nickase' approach (Ran *et al.*, 2013), using a pX335-U6-Chimeric_BB-CBh-hSpCas9n(D10A) plasmid from the Feng Zhang lab (Addgene #42335) to express sgRNA pairs, and the Cas9 D10A nickase. Targeting plasmids were used to introduce either an N-terminal HA-tag or translation and transcription termination sequences into the first exon. Single-cell clones were then generated following confirmation of successful targeting.

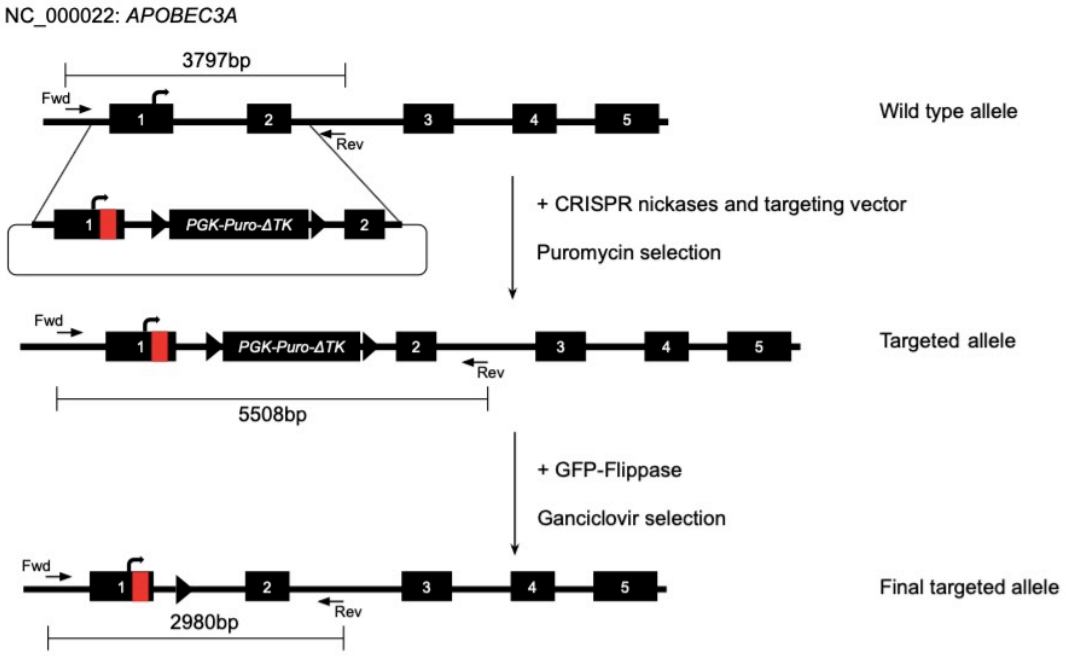

Figure 3-1 A3A targeting vector.
Schematic of the targeting vector for A3A and its incorporation into the locus. The encoding sequence (red box) inserts a bpA site immediately following the start codon in exon 1 (HA-tagged cells) or translational stop codons in all three reading frames (A3A deletion). A 'PGK-Puro-D-TK' dual selection cassette inserts between exons 1 and 2 to allow for positive selection with puromycin. This is flanked by Flippase Recognition Target (FRT) sites for the removal of the selection cassette by flippase recombinase.

3.3 Validation of HA-tagged and A3A deletion NIKS

3.3.1 A3A protein is strongly induced by PMA and IFN-α treatment

Basal levels of endogenous A3A are barely detectable in NIKS by qPCR, and undetectable by western blot analysis, though some APOBEC3 family members (in particular A3A and A3B) are induced in a cell type dependent manner by PMA through the PKC/NF-kB pathway, and by type-1 IFNs (Rasmussen and Celis, 1993; Madsen *et al.*, 1999; Mehta *et al.*, 2012). Additionally, it has been shown that co-treatment of PMA and TNF-α augments A3A induction in oral keratinocytes (Siriwardena *et al.*, 2018).

To validate the activity of HA-tagged A3A, as well as to establish optimal induction for further study, starting concentrations of PMA were based on those used in literature. With the exception of a dose range (10 ng/ml to 1 μg/ml) all other PMA treatments were at 100 ng/ml; IFN-α was used at 1000 IU/ml, and equal amounts of DMSO (0.002%) used as a vehicle-only control for PMA.

HA-A3A NIKS were plated with 3T3 feeder cells and 48 hr later (when cells were ~60% confluent) were treated with PMA for 3, 6, 24 and 48 hr, or for 6 hr with either: PMA, IFN-α, a co-treatment of PMA and IFN-α, or a dose range of PMA. Additionally, to corroborate that PMA induction of A3A occurred via the PKC pathway in NIKS, cells were pre-incubated with 100 nM of a pharmacological inhibitor of PKC, Gö6983, for 15 mins prior to and during treatment. WT-NIKS were used as a negative control.

As seen in Figure 3-2, western blot analysis (using an HA-epitope specific antibody) shows endogenous A3A protein induction at 3 hr and 6 hr post-PMA treatment, most abundantly at 24 hr, and receding by 48 hr. NIKS showed morphological changes at 24 hr post-treatment hence 6 hr induction was chosen for subsequent treatments. Importantly, whilst IFN-α treatment alone led to minimal detection of A3A, it acted synergistically with PMA and greatly augmented induction through co-treatment. Consistent with previous findings, the PKC inhibitor abrogated PMA-mediated A3A induction, but did not completely eliminate A3A induced by co-treatment with IFN-α, indicating that IFN-α stimulation proceeds through an alternative pathway, most likely JAK/STAT signalling (Mehta *et al.*, 2012).

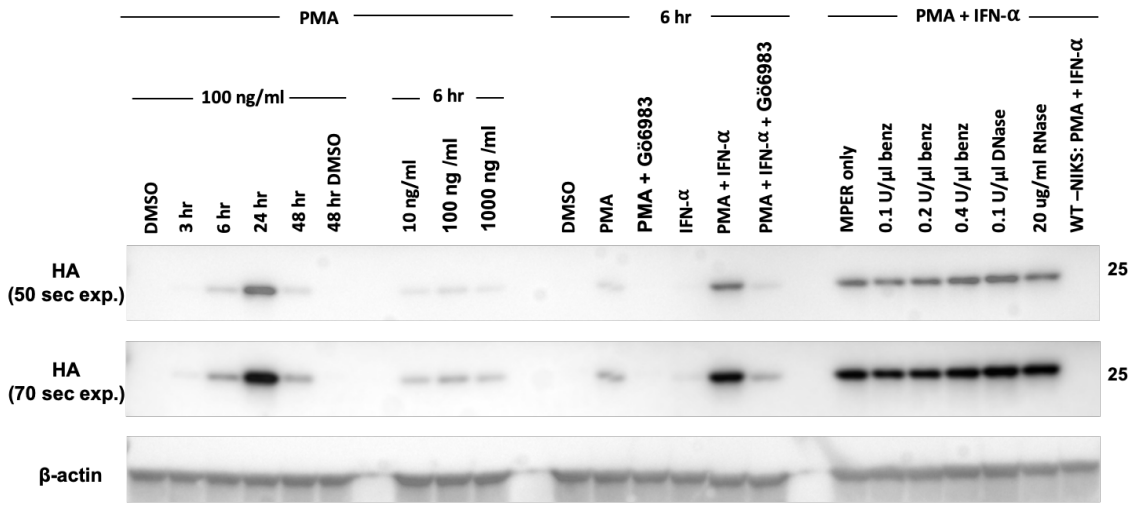

Figure 3-2 PMA and IFN-α have a synergistic effect on A3A induction.
HA-A3A tagged NIKS were plated at a density of 2.5 x 10^5 cells per well in 6-well plates and two days later (~60% confluent), media was removed and replaced with fresh media containing either: 10-1000 ng/ml of PMA for 3 to 48 hr; or 100 ng/ml of PMA, 1000 IU/ml of IFN-α, PMA and IFN-α together, or PMA +/- IFN-α following PKC pathway inhibition with 100 nM of Gö6983. Proteins were extracted using mammalian protein extraction reagent (MPER), with or without 0.1-0.4 U/µl of benzonase, 0.1 U/µl DNase, or 20 µg/ml of RNase. Whole cell lysate separated by SDS-PAGE was probed with HA-tag mAb (Cell Signalling). WT-NIKS were used as a negative control for the HA-epitope tag; β-actin shown as a loading control.

Furthermore, lysates prepared with the addition of either 0.4 U/μl of benzonase (an endonuclease), or 0.1 U/μl DNase in the cell lysis buffer (MPER) yielded slightly more A3A than the lysis buffer alone.

3.3.2 A3B is not induced under the same conditions as A3A

A3A and A3B have shown variable responses to PMA in different human cell lines: A3A induction by PMA was not detected in a normal breast epithelial cell line, MCF10A (Leonard *et al.*, 2015), primary human neonatal keratinocyte cells (HEKn), or in a squamous cell carcinoma-derived cell line (A431) (Siriwardena *et al.*, 2018), though was strongly induced by PMA (and TNF-α) in normal oral keratinocytes (Siriwardena *et al.*, 2018). A3B, on the other hand, was induced in all of the above (most notably ~100-fold in MCF10As) as well as a panel of cancer cell lines (Leonard *et al.*, 2015), though there was less A3B induction than A3A in the oral keratinocytes (Siriwardena *et al.*, 2018).

To compare the expression of A3A and A3B in NIKS, HA-A3A and HA-A3B tagged cells were treated for 6 hr with combinations of either PMA, IFN-α, or co-treated in the presence or absence of PKC inhibitor (as previously described). Whole cell lysate was separated by SDS-PAGE and probed with an anti-HA antibody. A3A is a single-domain enzyme and has a molecular weight of ~23 kDa; A3B is a double-domain enzyme of ~46 kDa. As seen in Figure 3-3, A3A was again induced by PMA, and more strongly by co-treatment with PMA and IFN-α.

Unlike other studies, both the A3A and A3B gene share the same epitope tag (HA) in this system, allowing a direct comparison of their protein levels. Surprisingly, A3B protein was undetectable indicating that A3A is more strongly induced by PMA (+/- IFN-α) in NIKS under these conditions. Verifying that the A3B cells are expressing the HA-epitope tag, (HA)-A3B protein was detectable under alternative conditions that are shown subsequently in section 3.4.

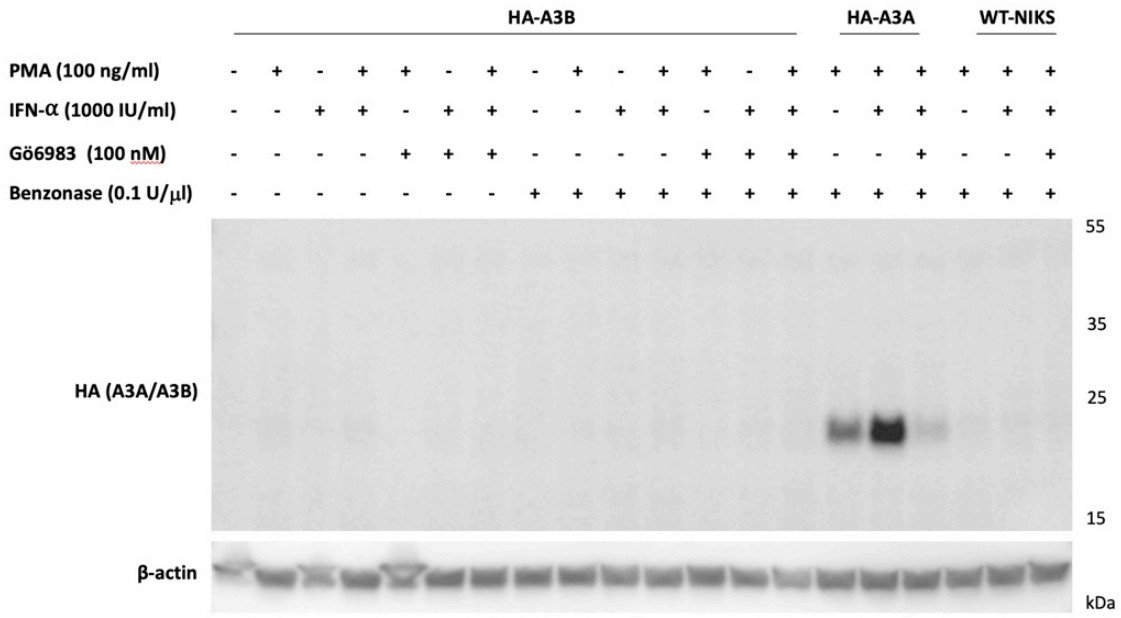

Figure 3-3 A3A, but not A3B, is strongly induced by PMA (and IFN-α).
HA-A3A, HA-A3B tagged NIKS (and WT-NIKS as a negative control for the HA-epitope) were treated 48 hr post-seeding (~60% confluent), with either 100 ng/ml of PMA, 1000 IU/ml of IFN-α, or 100 ng/ml of PMA and 1000 IU/ml of IFN-α for 6 hrs, with or without pre-treatment with 100 nM of PKC inhibitor, Gö6983. Proteins were extracted using MPER lysis buffer containing 0.1 U/μl of benzonase. Whole cell lysate was separated by SDS-PAGE and probed with HA-tag mAb (Cell Signalling). β-actin shown as a loading control.

3.3.3 PMA and IFN-α induction is restricted to sub-confluent cells

Thus far A3A induction had been investigated in sub-confluent, therefore presumed to be actively proliferating cells. To verify whether induction would also occur in cells that had been growth arrested through contact inhibition, samples were additionally prepared from cells that had been allowed to reach full confluency prior to treatment (receiving a daily media change). Consistent with previous findings, A3A was induced by PMA and IFN-α in the sub-confluent cell cultures, though it was not detected in the confluent cells. Again, A3B protein was not induced under either of these conditions.

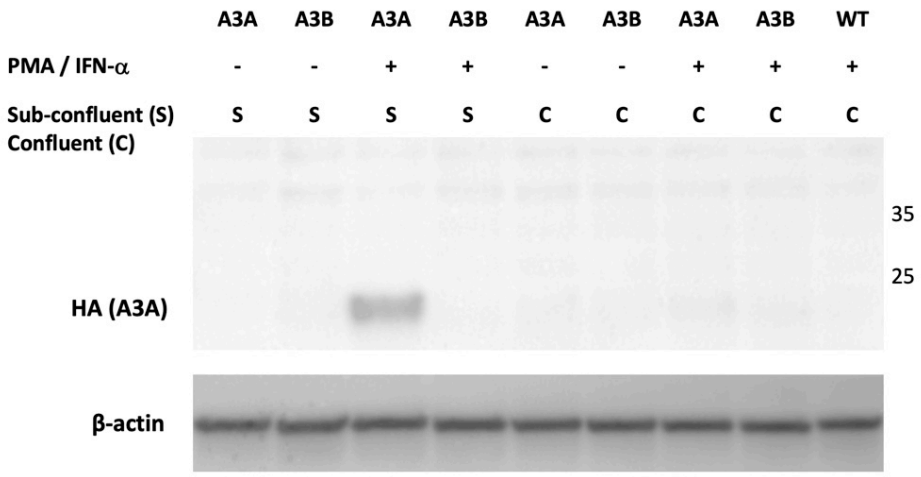

Figure 3-4 A3A is not induced by PMA and IFN-α in confluent cells.
HA-A3A and HA-A3B and WT-NIKS were plated at density of 5 x 10^5 cells in 6-well plates. The next day, media was removed from the sub-confluent samples (~70% confluent) and replaced with fresh media containing 100 ng/ml of PMA and 1000 IU/ml of IFN-α for 6 hrs. Media was refreshed on the confluent samples daily, and three days after plating (when they had reached ~95-100% confluency) were treated in the same manner. Proteins were extracted using RIPA buffer containing 0.2 U/ml of benzonase. Whole cell lysate was separated by SDS-PAGE and probed with HA-tag mAb (Cell Signalling). β-actin shown as a loading control.

3.3.4 PMA induces expression of A3A in a subset of cells

Varying subcellular localisation patterns have been reported for A3A, and its localisation may also differ between cell types: for example, it would seem there is a regulatory mechanism that causes it to be retained in the cytoplasm in macrophages (Land *et al.*, 2013), whereas when ectopically expressed in 293T cells (which have no endogenous expression of A3A), it enters the nucleus and causes DNA breaks (Land *et al.*, 2013). Pan-cellular (or even nuclear) localisation in keratinocytes (NOK) has been shown (Siriwardena *et al.*, 2018), though the limitation with that study is that they use an antibody that cross-reacts with A3B, so it can't be certain that they were detecting A3A in their immunofluorescence experiments.

Having established conditions in which it was possible to induce sufficient endogenous A3A expression (PMA and IFN-α) for visualisation by immunofluorescence, we next sought to validate the subcellular localisation of endogenous A3A protein.

HA-A3A and WT-NIKS were treated with PMA with/without IFN-α for 6 hrs and labelled with anti-HA antibody (and AlexaFluor488). Confocal microscopy imaging (in Figure 3-5) demonstrates that A3A is induced strongly in both the cytoplasm and nucleus in NIKS. Though surprisingly, the A3A induction appeared to be restricted to a subpopulation of cells, and this observation was consistent regardless of whether they were treated with PMA alone or in combination with IFN-α, motivating the hypothesis that A3A may be induced in a cell-cycle phase dependent manner.

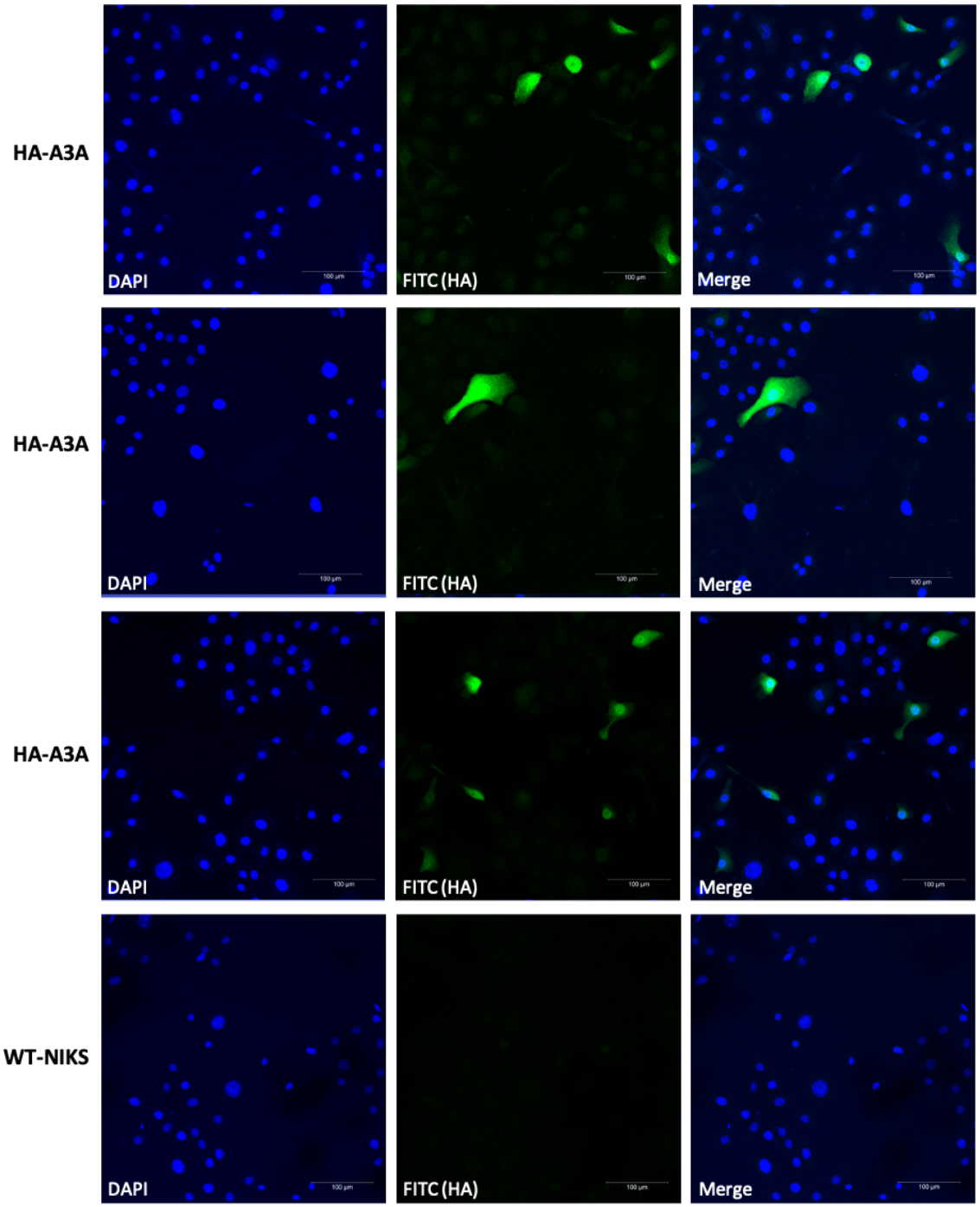

Figure 3-5 HA-A3A NIKS show expression of A3A in a subset of cells following PMA induction. HA-tagged A3A NIKS (HA-A3A) showing multiple fields of the same conditions, and WT-NIKS as a negative control for the HA-tag. Cells were grown on coverslips in a 6-well plate at a density of 4 x 10^5 cells per well and the next day, upon reaching 60-70% confluency, were treated with 100 ng/ml of PMA for 6 hrs. Immunofluorescence staining was performed using HA-tag mAb (Cell Signalling). Anti-HA was labelled with AlexaFluor488 secondary antibody (Invitrogen). Nuclei were counterstained with DAPI and imaging was performed on a confocal microscope. Signal intensity was normalised to the WT-negative control; the scale bar represents 100 μm.

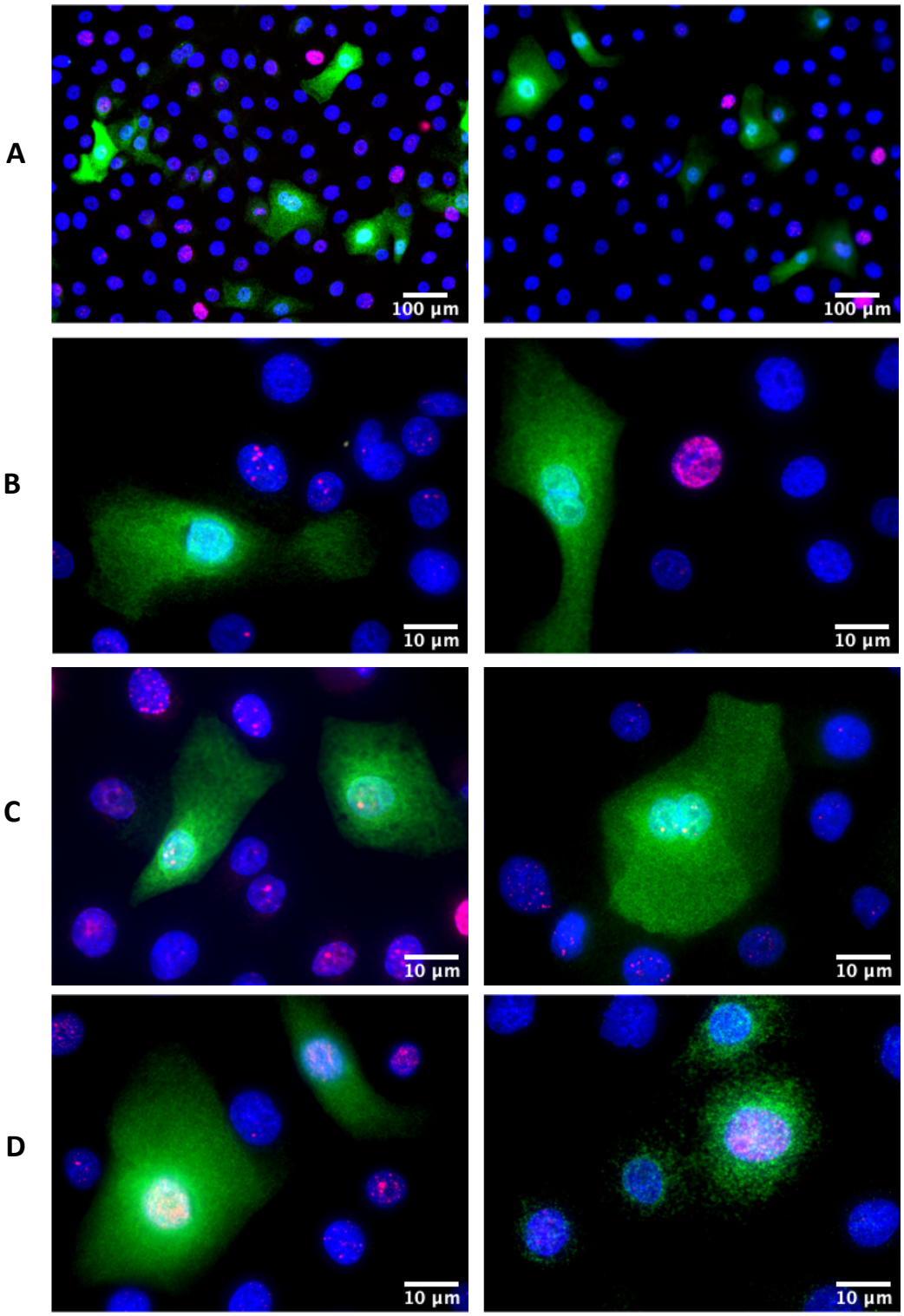

Figure 3-6 A3A induction does not correlate with DNA double-strand break formation.
A3A induction in cells (labelled in green) and DSB formation (γ-H2AX labelled in red). **(A)** Overview at 20X magnification; **(B)** A3A expressing cells with no DSBs (60X); **(C)** A3A together with 2-4 DSB foci per nuclei (60X); **(D)** A3A together with multiple DSBs (pan-nuclear) (60X). HA-A3A NIKS were grown in 6-well plates at a density of 5 x 10^5 cells per well, and the next day treated with PMA and IFN-α for 6 hr. A3A was detected using HA-tag mAb (Cell Signalling) then labelled with AlexaFluor488 secondary antibody (Invitrogen); DSBs were detected using anti-γ-H2AX mouse mAb (MerckMillipore) then labelled with AlexaFluor594 (Invitrogen). Nuclei were counterstained with DAPI and imaging performed on an epifluorescent microscope.

Previous studies show that overexpressing A3A leads to DNA DSBs and cell-cycle arrest (Landry *et al.*, 2011; Mussil *et al.*, 2013), however we found no correlation between A3A induction and DSB formation (through γ-H2AX co-staining, shown in Figure 3-6.

PMA can induce DNA DSBs through the production of reactive oxygen species (Tanaka *et al.*, 2006) and as such a number of cells displayed γ-H2AX foci formation following treatment. NIKS strongly expressing A3A had varying quantities of foci (panel C: 2-4 per nuclei; panel D: pan-nuclear foci; panel B: strong A3A induction but no visible DSBs); this suggests that either A3A induction does not occur in S-phase cells (where ssDNA substrate would be exposed), or that endogenous A3A induction in NIKS is non-genotoxic.

3.3.5 Induction of other APOBEC3 genes by PMA and IFN-α treatment

To quantify the mRNA induction of the remaining APOBEC3 family members, WT-NIKS were induced with the same combinations of treatment as previously described. RNA was extracted from which cDNA was synthesised for qPCR analysis, using primers specific for each of the A3A – A3H transcripts. Copy numbers were calculated relative to copy numbers of the housekeeping gene, TATA-box binding protein (TBP), and the results are shown collectively in Figure 3-7 (A), and on a Log 10 scale in Figure 3-7 (B). A3C was found to have the highest basal level under these conditions, followed by A3B and then A3A. Basal levels of A3A (DMSO) from three independent experiments had a mean of 0.21 ± 0.04 copies/copy TBP (standard error of the mean (SEM)).

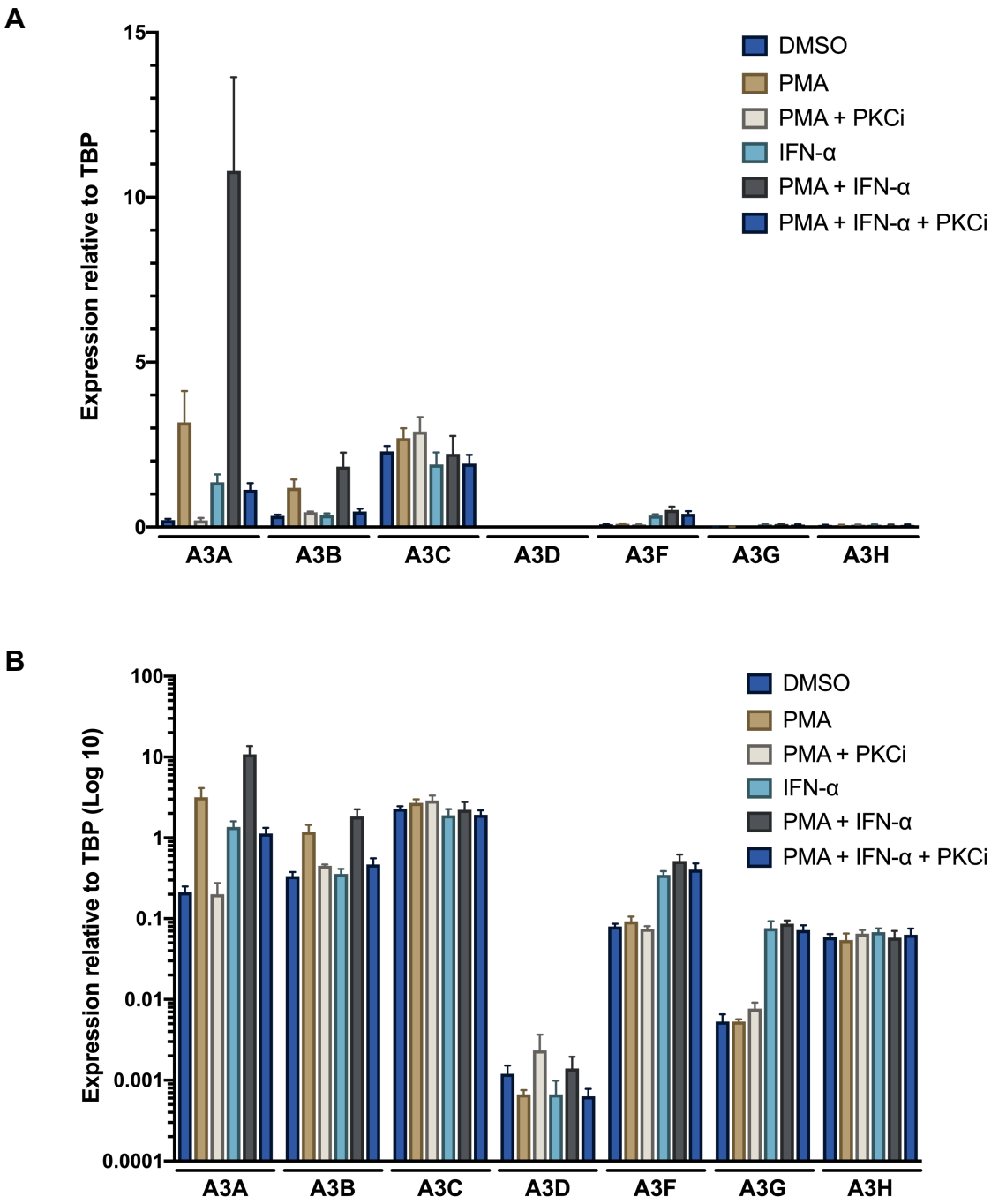

Figure 3-7 Comparing mRNA induction of all APOBEC3 family members.
(A) Linear scale expression of all seven APOBEC3 family in WT-NIKS. **(B)** Log 10 scale of APOBEC3 expression. WT-NIKS were plated at a density of 2.5 x 10^5 cells per well in 6-well plates. 48 hr later (when cells were ~60% confluent), media was removed and replaced with fresh media containing either 100 ng/ml of PMA; 1000 IU/ml of IFN-α; PMA and IFN-α simultaneously; or PMA +/- IFN-α following inhibition of the PKC pathway with 100 nM of Gö6983. RNA was extracted and converted to cDNA for qPCR analysis. mRNA copy numbers are shown relative to TBP copies. Mean $\pm$ SEM from three independent experiments.

PMA treatment increased A3A expression to 3.17 ± 0.95 copies/copy TBP which was abrogated by the PKC inhibitor; induction by IFN-α alone was 1.36 ± 0.24. Supporting the western blot findings, there was strong synergistic induction of A3A through co-treatment with PMA and IFN-α, with a mean expression of 10.98 ± 2.85 copies/copy TBP: equating to a ~50-fold change compared to basal levels. Although basal levels of A3B were slightly higher under these conditions (mean 0.34 ± 0.04), it was less potently induced by PMA and IFN-α (5.5-fold: mean 1.83 ± 0.43). A3A and A3B are unique in their induction by PMA, and though A3C has the highest basal level in NIKS (mean 2.29 ± 0.17) it is not induced by PMA or IFN-α. A3F and A3G basal levels are both very low, though could be increased by IFN-α treatment.

3.3.6 A3A deletion does not lead to compensatory upregulation of other APOBEC3s

As the A3A KO NIKS were to be subsequently used for characterising A3A activity, we wanted to verify that the deletion did not have any influence on the expression of other APOBEC3 genes; for example: the 29.5 kB germline deletion of A3B of in the APOBEC3 cluster that generates a hybrid gene (A3A_A3B) can negatively correlate with A3A expression in certain tissue types (Klonowska *et al.*, 2017). To investigate this, three separate clones of A3A KO NIKS were treated as previously described, followed by qPCR analysis on all seven family members (which also verified there was no A3A mRNA induction), and results were compared to those from WT-NIKS (shown in Figure 3-8).

Notwithstanding slight increases in A3B and A3C by PMA treatment in the A3A KO cells, there was no cooperativity through co-treatment with IFN-α and thus appears that deletion of A3A does not result in compensation by other family members. These minor differences could potentially be related to other cell-cycle related alterations in the KO cells (discussed later).

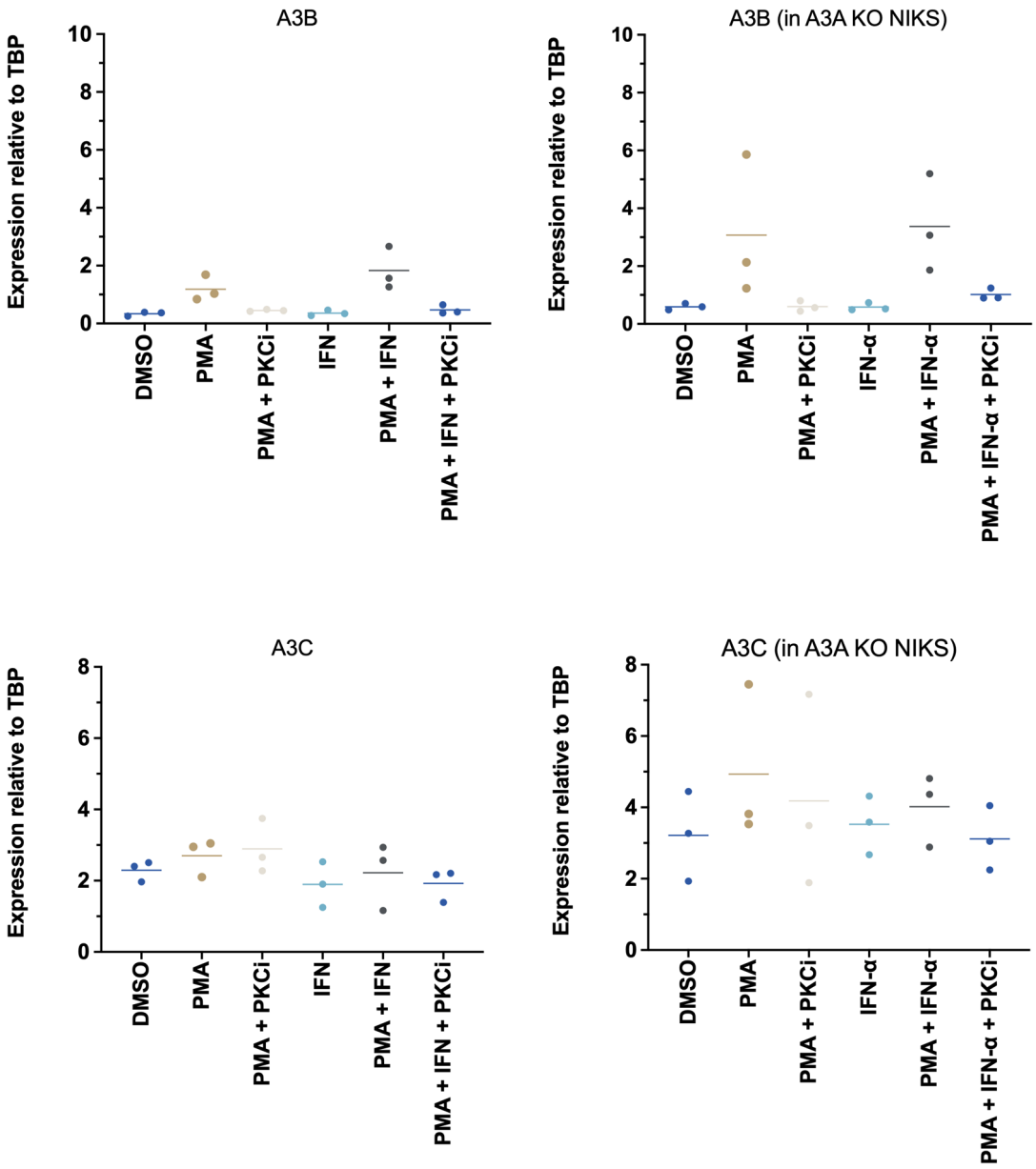

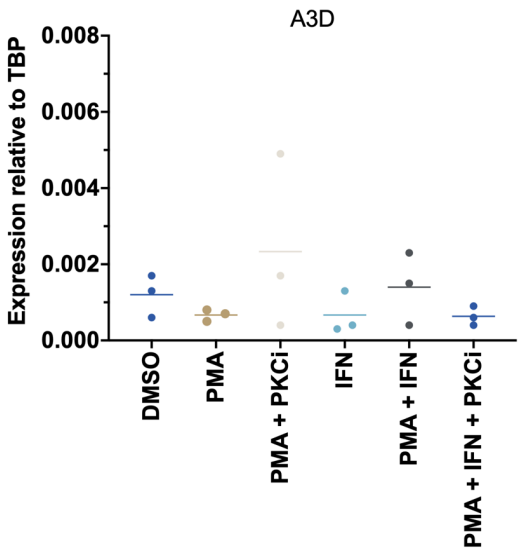
A3D
Expression relative to TBP
0.008
0.006
0.004
0.002
0.000
DMSO
PMA
PMA + PKCi
IFN
PMA + IFN
PMA + IFN + PKCi

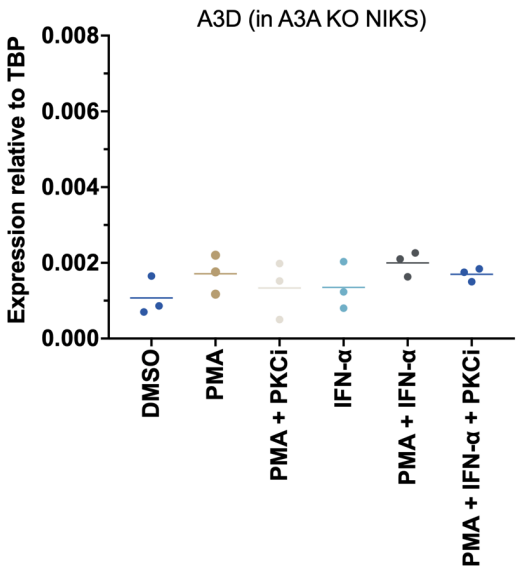
A3D (in A3A KO NIKS)
Expression relative to TBP
0.008
0.006
0.004
0.002
0.000
DMSO
PMA
PMA + PKCi
IFN-α
PMA + IFN-α
PMA + IFN-α + PKCi

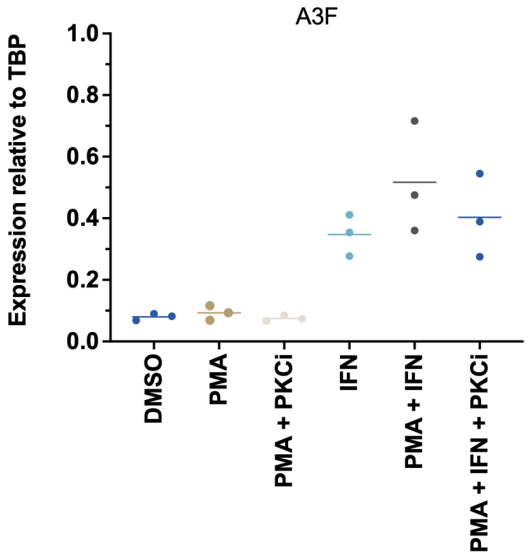
A3F
Expression relative to TBP
1.0
0.8
0.6
0.4
0.2
0.0
DMSO
PMA
PMA + PKCi
IFN
PMA + IFN
PMA + IFN + PKCi

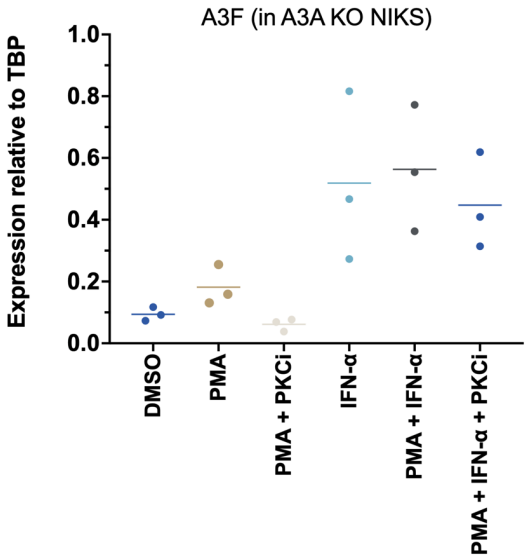
A3F (in A3A KO NIKS)
Expression relative to TBP
1.0
0.8
0.6
0.4
0.2
0.0
DMSO
PMA
PMA + PKCi
IFN-α
PMA + IFN-α
PMA + IFN-α + PKCi

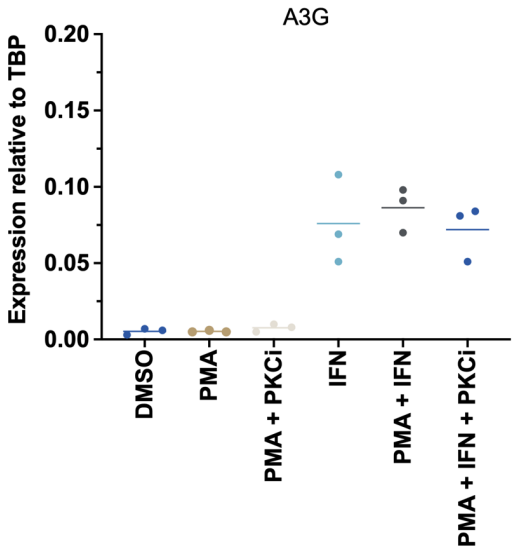
A3G
Expression relative to TBP
0.20
0.15
0.10
0.05
0.00
DMSO
PMA
PMA + PKCi
IFN
PMA + IFN
PMA + IFN + PKCi

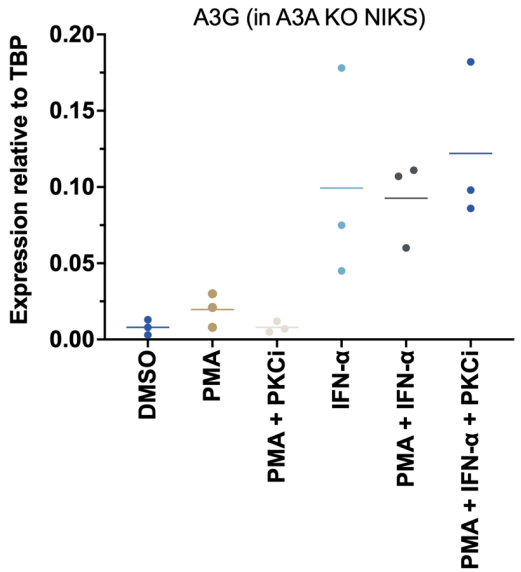
A3G (in A3A KO NIKS)
Expression relative to TBP
0.20
0.15
0.10
0.05
0.00
DMSO
PMA
PMA + PKCi
IFN-α
PMA + IFN-α
PMA + IFN-α + PKCi

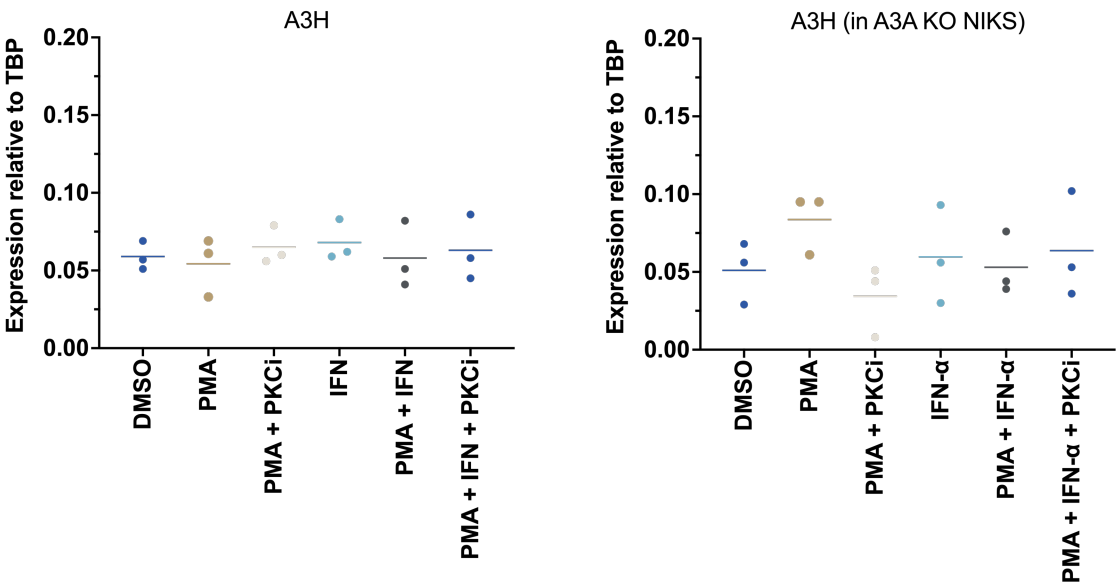

Figure 3-8 Comparison of A3B-A3H mRNA induction in WT-NIKS vs A3A deletion cells.
WT-NIKS and three separate clones of A3A homozygous deletion (KO) cells were treated with combinations of PMA, IFN-α, and PKC inhibitor as previously described. mRNA expression is shown as copy numbers relative to TBP copies (line at mean; n=3).

3.4 A3B is detected during G2/M phase of the NIKS cell cycle

Despite A3B being the APOBEC3 family member reported to be the most transcriptionally activated by PMA treatment in many cell types, we found instead that its induction was less than that of A3A in NIKS both at the mRNA level (Figure 3-7), and undetectable at the protein level (Figure 3-3 and Figure 3-4). However, Kanu *et al*. found a correlation between HER2 amplified breast cancers (from The Cancer Genome Atlas samples) with elevated APOBEC3 signature mutations, together with higher A3B mRNA expression. Coupling HER amplification with increased replicative stress, they further showed that A3B could be induced by DNA damaging drugs and oncogenes that induced replication stress *in vitro*, particularly hydroxyurea (Kanu *et al*., 2016).

Furthermore, A3B transcription is repressed by the G1/S related Rb/E2F pathway (Starrett *et al.*, 2019; Roelofs *et al.*, 2020), and expression of A3B correlates with both mitotic gene expression in highly proliferative breast tumours (Cescon, Haibe-Kains and Mak, 2015), and with DNA repair and G2/M cell cycle genes from a pan-cancer analysis (Ng *et al.*, 2019).

Synchronisation can enrich proteins that are specific to distinct cell-cycle stages: through incubating cells with an excess of thymidine they arrest at the G1/S boundary which can be reversed through washing off the thymidine and releasing them in fresh culture media. We were therefore interested in determining whether synchronising NIKS at the G1/S boundary could induce A3B in a cell-cycle dependent manner. HA-A3B NIKS were synchronised using a single thymidine block, and asynchronously growing cells (18 hr post-media change) were treated with PMA and IFN-α as a comparison.

As shown by the western blot results in Figure 3-9 (A), A3B was greatly upregulated at 8 hr post-release from G1/S blockade. Furthermore, A3B expression corresponded to an increase in cyclin B1 that is expected during the G2/M phase of the cell cycle. RNA was extracted from WT-NIKS that were treated simultaneously for qPCR analysis: there was a modest increase in A3B mRNA (Figure 3-9(B)) though less than that induced by PMA and IFN-α treatment (in which A3B protein was not detected). This suggests that existing A3B protein may either be stabilised during G2/M phase, or that A3B mRNA is preferentially translated at this time.

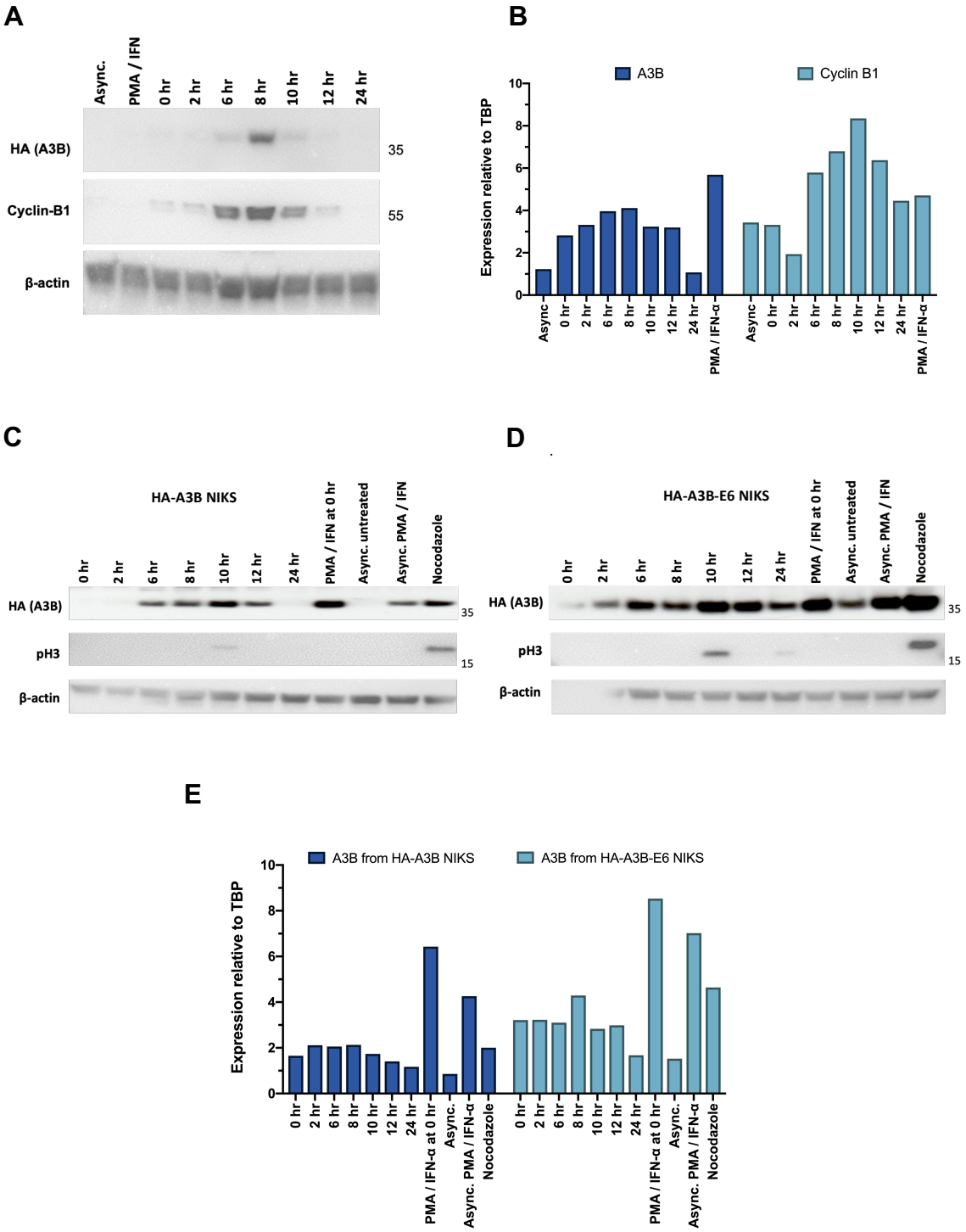

Figure 3-9 A3B protein is expressed at G2/M phase of the cell cycle.
(A-B) A3B protein and mRNA increases during G2/M following a single thymidine block (RNA extracted from WT-NIKS). **(C-D)** A3B protein induction at both G2/M and by PMA and IFN-α following a double thymidine block in HA-A3B NIKS (left) and HA-A3B-E6 NIKS (right). **(E)** A3B mRNA induction (in HA-A3B and HA-A3B-E6 NIKS) corresponding to (C) and (D) respectively. Asynchronous (async.) and G1/S arrested NIKS (0 hr) were treated with 100 ng/ml PMA and 1000 U/ml IFN-α for 6 hr. Nocodazole was added at 2 hr post-release from G1/S blockade for a further 10 hr. A3B mRNA copy numbers are shown relative to TBP copies (n=1).

Cells were next synchronised in G1/S using a double thymidine block (using protocol (1), pg. 2-75) or blocked in G2/M with 100 ng/ml of nocodazole (a microtubule inhibitor). Additionally, HA-A3B-E6 NIKS (stably expressing HPV16 E6) were used to compare A3B expression in the presence of the E6 oncogene, which is known to upregulate A3B (Vieira *et al.*, 2014).

Phospho-(Ser10)-Histone H3 (pH3) antibody was used as a specific marker for mitosis and corroborating that A3B is G2/M specific, A3B was strongly expressed both at 10 hr post-release and in nocodazole treated samples (Figure 3-9 (C)), corresponding with pH3 expression. A3B expression was higher in all E6 expressing samples as expected (Figure 3-9 (D-E)), though was also preferentially expressed at G2/M.

Interestingly, though A3B could not previously be detected by PMA and IFN-α treatment when cells were treated 48 hr after plating, it was detected using this alternative protocol involving frequent media changes prior to treatment (shadowing the media changes that are made during the synchronisation protocol (a schematic is shown later in Figure 4-2). However, the increase in protein expression was not accompanied by a greater increase in mRNA than that seen previously (Figure 3-9 (B) (E)), further suggesting that A3B may be preferentially stabilised or translated in actively proliferating/media enriched cells.

3.5 Discussion / Conclusions

NIKS were chosen for this project to gain an understanding of the physiological regulation and function of A3A in normal tissue from which HPV-driven cancers arise, and how its induction following viral infections might lead to deregulation and APOBEC3 driven mutations. To combat the antibody cross-reactivity with other APOBEC3 family members, NIKS were used that had been engineered to express an HA-epitope tag on the endogenous A3A and A3B proteins. A3A KO NIKS were validated by qPCR analysis which verified there was no disruption to the gene expression of the remaining APOBEC3s.

Consistent with the finding of others, A3A could be induced by PMA treatment via the PKC pathway, though was greatly augmented by a co-treatment of PMA and IFN-α. This provided a means by which endogenous A3A subcellular localisation could be verified by immunofluorescence and we found that A3A was strongly expressed in a sub-population of cells suggesting a possible cell-cycle specific induction. A3B mRNA was upregulated by PMA (and IFN-α) treatment, though to a lesser extent than A3A and was not detectable at the protein level under the same conditions as A3A. Characterisation of all A3 members showed A3C to have the highest basal levels, followed by A3B then A3A. Importantly, whilst A3B protein was not initially detected by PMA and IFN-α induction, it was specifically expressed during the G2/M phase of the cell cycle in both normal NIKS as well as those stably expressing the HPV16 E6 oncogene. Furthermore, it was subsequently detected by PMA/IFN-α treatment in actively proliferating cells (after multiple media changes).

4 Cell cycle and growth factor stimulation of A3A

4.1 Introduction

The epidermis is the outermost layer of skin; it consists of over 90% keratinocytes and tissue homeostasis is maintained by a subpopulation of small keratinocyte stem cells that remain in the basal layer of the epidermis. These cells are mainly quiescent but can produce new progenitor cells for self-renewal and as new basal cells are formed, existing cells become transit amplifying cells, migrating upwards through the layers and arrest cell growth at the onset of terminal differentiation, eventually being shed as squames (Le Roy *et al.*, 2010; Schlüter *et al.*, 2011). However, the keratinocyte life cycle is complicated and it is possible that terminal differentiation may be initiated from any point within the cell cycle (not just G0), whilst retaining the ability to replicate DNA as they do so (Gandarillas, Davies and Blanchard, 2000). Thus, cells arresting in S-phase or G2/M can undergo endoreplication: DNA synthesis without undergoing mitosis, resulting in polyploid or multinucleated cells.

Although keratinocyte stem cells have increased EGFR expression and this becomes progressively lower through the suprabasal layer, a subpopulation of epidermal stem-like cells with low expression of EGFR have the highest proliferative capabilities (Fortunel *et al.*, 2003). Spontaneously immortalised keratinocytes (NIKS) used in this study express very similar levels of EGFR, transforming growth factor (TGF)-β1, and the proto-oncogene c-MYC to their primary cell line, and maintain a dependency on growth factors for proliferation (Allen-Hoffmann *et al.*, 2000).

4.2 A3A increases early after release from the G1/S boundary

We previously found A3B is G2/M specific and that A3A induction by PMA/IFNα was restricted to a sub-population of cells. To determine whether A3A expression is also cell-cycle stage specific, HA-A3A and WT-NIKS were synchronised with a double thymidine block (as described in the methods section (protocol (1), pg. 2-75). In addition, asynchronous and synchronised samples were treated with PMA and IFN-α, or blocked at the G2/M boundary by the addition of nocodazole.

As shown in Figure 4-1 (A), A3A was detected in PMA and IFN-α treated cells, though it was additionally detected (albeit less strongly) in the G1/S arrested samples (0 hr) and up to 6 hr post-release; however qPCR analysis of A3A mRNA expression (Figure 4-1 (B)) showed only a small increase at 2 hr post-release (similar to basal level). A3A protein preceded the increased expression of cyclin B1 and suggested that A3A may have a function for which it is upregulated or stabilised in late-G1 into S-phase. Alternatively, A3A induction might rather be a consequence of cellular stress resulting from the G1/S blockade.

Furthermore, due to the much higher relative expression of A3A in PMA/IFN-α treated cells, it was not clear from the western blot whether A3A was induced at 24 hr and in the nocodazole treated cells, or whether the signal was from adjacent lanes. Hence, these factors were subjected to further investigation (shown in the next section).

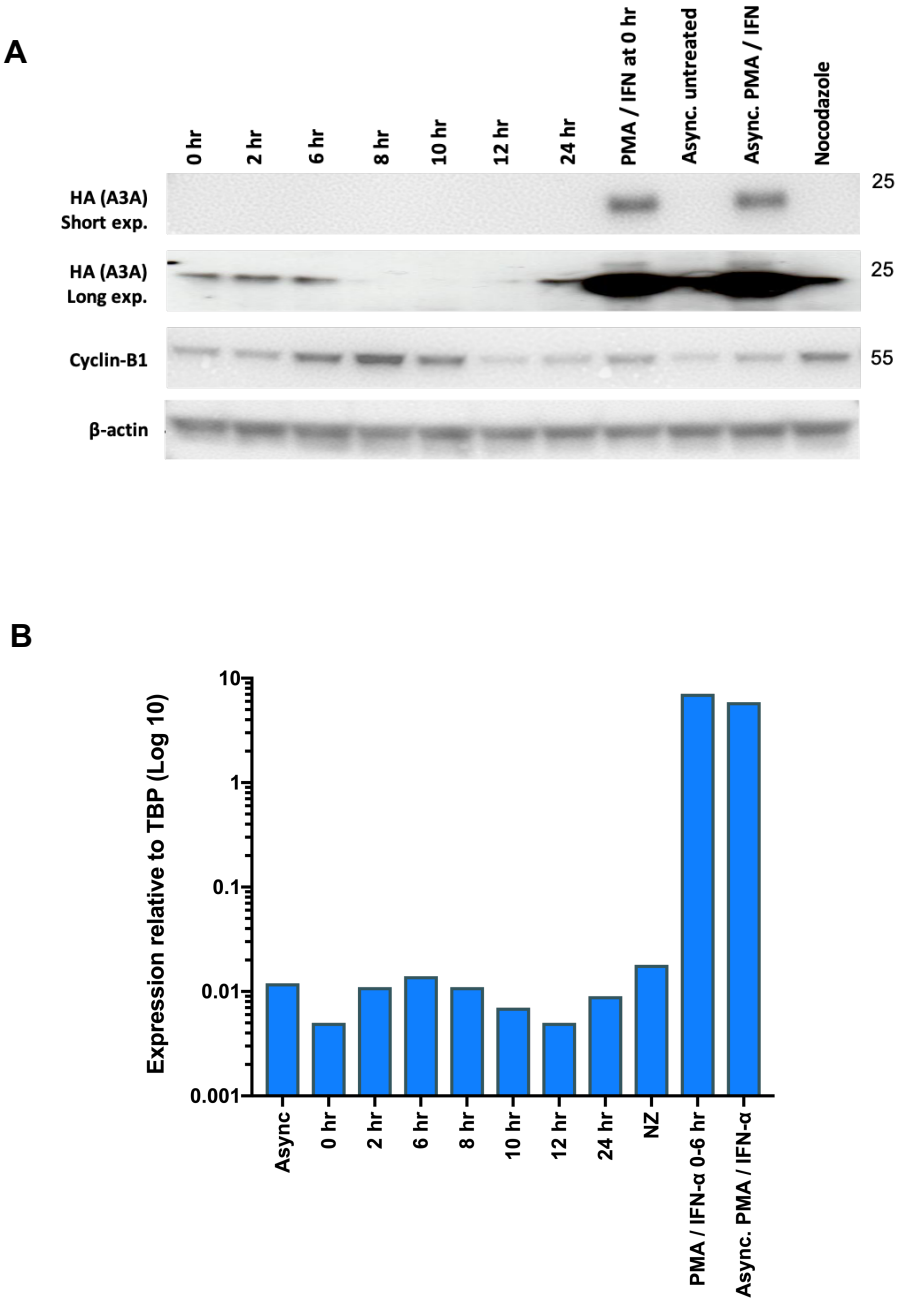

Figure 4-1 A3A expression during G1/S phase of the cell cycle.
(A) Western blotting shows induction of A3A protein following release from G1/S. **(B)** A3A mRNA levels by qPCR. WT-NIKS and HA-A3A NIKS were plated at a density of 2.5 x 10^5 cells/well in 6-well plates. The next day, cells were synchronisation at the G1/S boundary with a double thymidine block (protocol (1)), or in G2/M using 100 ng/ml of nocodazole for 10 hrs at 2 hr post-release from thymidine. Asynchronous (async.) samples were 18 hr post-media change and were either untreated or treated with 100 ng/ml PMA and 1000 U/ml IFN-α. G1/S arrested cells (0 hr) were treated with PMA and IFN-α for 6 hrs (0-6 hr). A3A mRNA levels from HA-A3B NIKS are expressed as copy numbers relative to TBP copy numbers (n=1, Log 10 scale).

Interestingly however, the levels of A3A in the asynchronous population this time were far lower (barely detectable at 0.01 copies/copy TBP) than that seen during the protocol used for inducing with PMA/IFN-α induction (in which mean basal (DMSO) expression of A3A (from three independent experiments) was 0.21 ± 0.04 copies/copy TBP (Figure 3-7). Furthermore, PMA and IFN-α induction in asynchronous cells was also almost 2-fold less (5.89 as compared to 10.98 ± 2.85 previously). Represented in Figure 4-2, the higher basal (and PMA/IFN-α) expression arose from cells that had been incubated in the same media for 48 hr later prior to a media change containing either PMA/IFN-α, or equal volumes of DMSO (as a negative control).

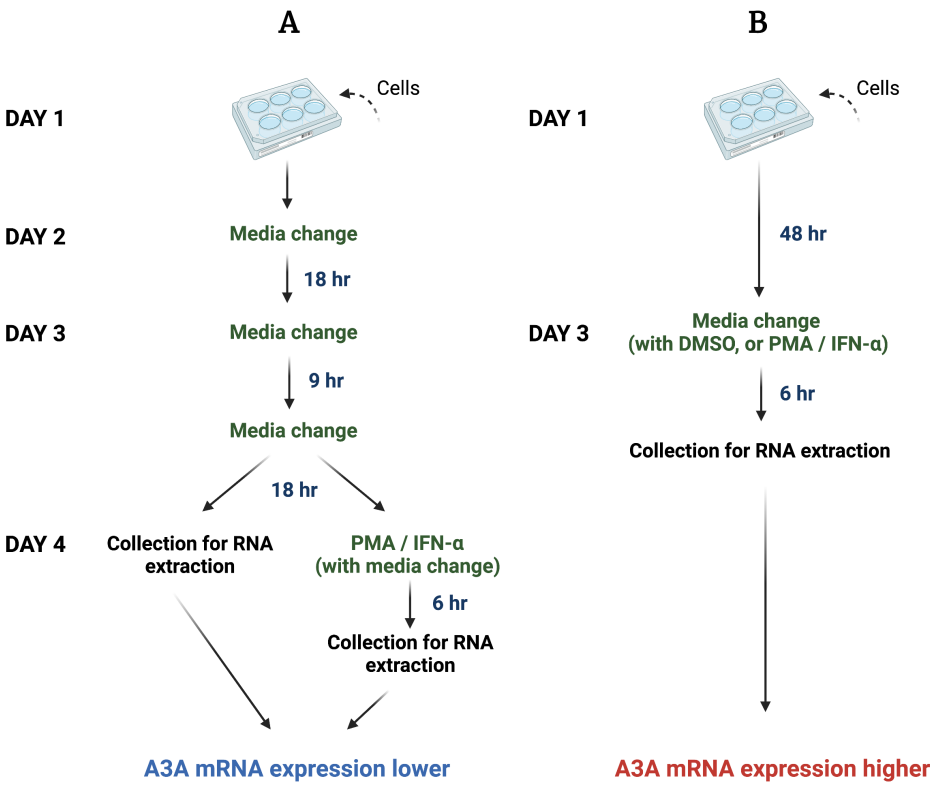

Figure 4-2 Cell culture conditions influence A3A basal mRNA expression.
(A) A3A mRNA is less in basal cells (and induced to a lower degree lower by PMA/IFN-α) when NIKS are collected for RNA extraction (or treated with PMA/IFN-α) at 18 hr post-media change. **(B)** A3A mRNA expression increases in NIKS when cultured in the same media for 48 hr followed by 6 hr stimulation with fresh media (containing 0.002% DMSO) or treated with PMA/IFN-α.

The lower basal (and PMA/IFN-α) expression arose from cells that had media changed 18 hr prior to collection/induction, thus it appears that basal/induced A3A is lower in actively cycling cells/or states of high nutrient availability, and higher during times that cells may have exited the cell cycle due to lower nutrient availability (48 hr post-media change) but subsequently re-activated following a media change.

4.3 A3A increases at G1 in the subsequent cell cycle

Cells may remain synchronised as they proceed through the next round of the cell cycle, therefore if A3A was specifically upregulated during G1/S phase one would expect to see a similar increase in protein when cells enter the subsequent G1/S phase (22-24 hr post-release). To determine whether A3A is in fact G1/S specific or rather that it is induced by cellular stress, the thymidine block was repeated (protocol (2), pg. 2-75), and sample collection time-points extended to 30 hr post-release.

Seen in Figure 4-3 (A), endogenous A3A protein expression was found to be surprisingly high at 28-30 hr post-release, at levels similar to that achieved previously by PMA and IFN-α induction. qPCR analysis was performed on WT-NIKS (as the HA-epitope tag on HA-A3A NIKS makes them unsuitable for qPCR analysis) and correspondingly shows that A3A mRNA and protein expression are both elevated at the same time-points (Figure 4-3 (B)): 4.66 copies/copy TBP at 28 hr post-release (as compared to 3.17 $\pm$ 0.95 by PMA induction, Figure 3-7).

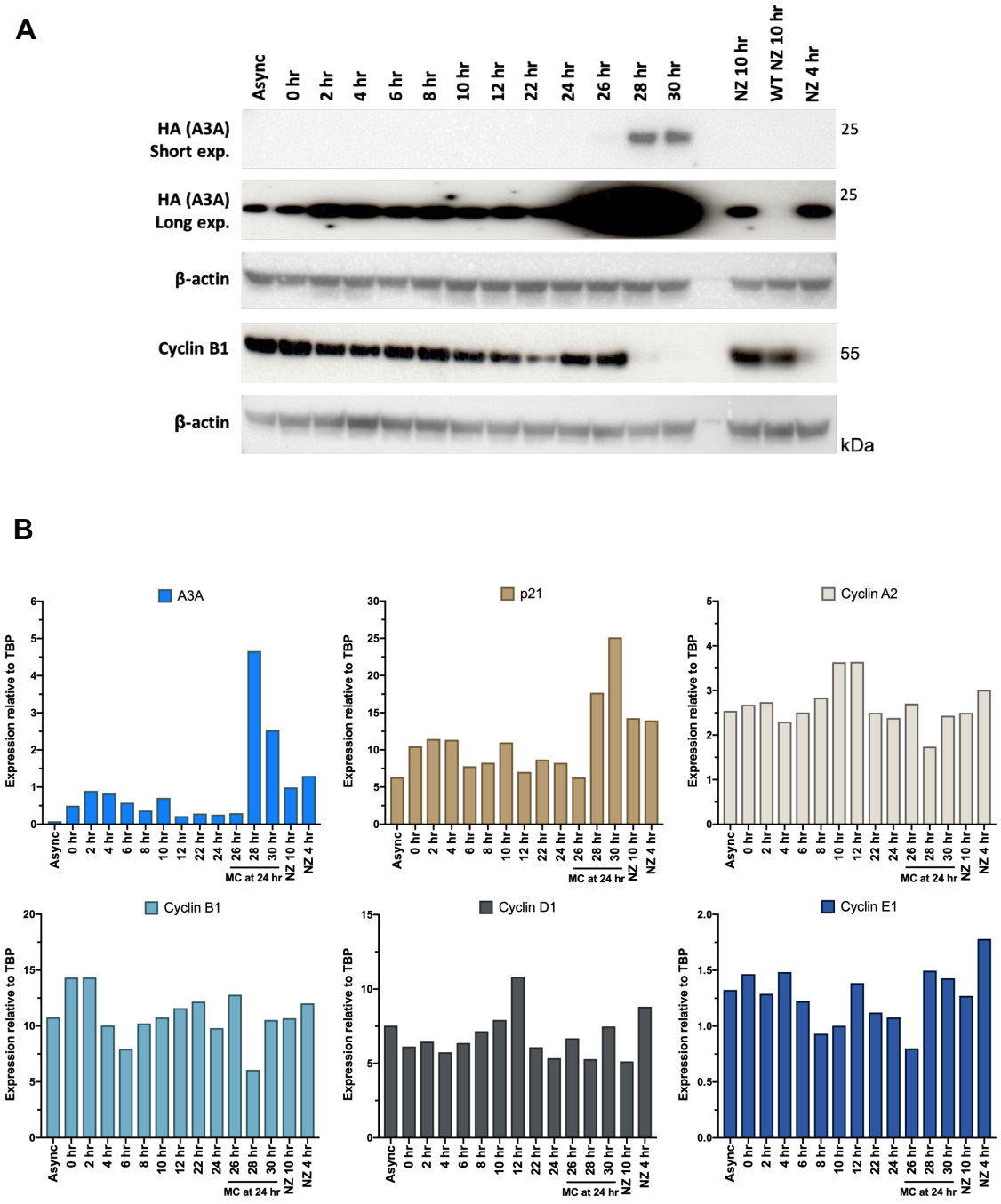

Figure 4-3 A3A is strongly induced at 28 hr and 30 hr post-release from a double thymidine block.

(A) Strong induction of A3A is seen at 28 hr and 30 hr post-release seen by western blot. **(B)** mRNA levels of A3A, p21 and cyclins A2, B1, D1 and E1. HA-A3A and WT-NIKS were plated at 2.5 x 10^5 cells/well in 6-well plates and synchronised at the G1/S boundary with a double thymidine block (protocol (2)), or at G2/M using 100 ng/ml of nocodazole (NZ) for either 4 hr or 10 hr at 2 hr post-release (PR). Asynchronous (async.) samples were collected at 18 hr post-media change (MC). At 24 hr PR, media was refreshed on remaining samples. RNA was extracted from WT-NIKS and mRNA copy numbers are shown relative to TBP copies (n=1).

The expression of p21 and cyclins A2, B1, D1, E1 mRNA are also shown in Figure 4-3 (B), and corresponding to the increase in A3A mRNA (at 28-30 hr) there was an increase in the cell-cycle inhibitor, p21 (~4-fold at 30 hr compared to asynchronous).

Cyclin B1 levels increase during S-phase and G2, and peak in mitosis, and its proteolysis during anaphase is required for mitotic exit (Holder, Mohammed and Barr, 2020). The decrease in cyclin B1 mRNA (Figure 4-3 (B): ~2-fold less at 28 hr compared to asynchronous), was accompanied by a more dramatic decrease at the protein level (Figure 4-3 (A): 28-30 hr). Although there is not accompanying flow cytometry analysis, these observations might suggest that the majority of cells were likely in the subsequent G1-phase at this point.

Additionally, to verify the observations seen previously as to whether A3A was induced by nocodazole (Figure 4-1) and if so, whether this induction was a consequence of cellular stress or a G2/M specific induction, cells were treated with nocodazole at 2 hr post-release for either 10 hr (to cause mitotic arrest), or for 4 hr so that cells would be in S-G2 phase but may still induce A3A if it was a response to cellular stress. Both methods resulted in small increases in A3A mRNA but not protein (although A3A can be detected in all HA-A3A cells with a long exposure).

Notably, at 24 hr post-release, the media was refreshed on the 26 hr, 28 hr and 30 hr samples in order to ensure that they had sufficient nutrient availability to continue actively cycling.

Therefore, it is possible that the A3A induction seen in the 28 hr and 30 hr time points was either directly cell-cycle attributable (G1/S specific), or as suspected from earlier observations, was a consequence of the media change, potentially stimulating cell cycle re-entry in a population of cells that may have exited the cell-cycle due to lower nutrient availability.

In order to establish whether the A3A induction was as a result of G1 specific cell cycle expression or a consequence of the media change at 24 hr post-release, NIKS were next plated in T175 flasks and the G1/S synchronisation repeated (protocol (3), pg. 2-75), both with and without a media change at 24 hr. Cells were collected from HA-A3B NIKS and divided into fractions for protein and RNA extraction (not WT-NIKS as we wanted to investigate both A3A and A3B activity by western blot and qPCR analysis, and they are suitable for both). Lysates were probed with an anti-A3A antibody (Sigma) which we verified is specific for A3A in the next section (in Figure 4-5). Interestingly, there was a failure to detect A3A in the HA-A3A NIKS that were grown simultaneously, though in 6-well plates with a higher volume of media (208 μl cm^{-2} instead of 114 μl cm^{-2} (data not shown)).

Using pH3 as a marker of mitosis, the western blot analysis (Figure 4-4 (A)) shows that cells were traversing through mitosis at 10-12 hr post-release from G1/S arrest. At 24 - 26 hr post-release, in the absence of a media change (a point at which the cells would likely be in the next G1/S-phase), A3A protein expression was detected though with only a moderate increase in A3A mRNA seen at 26 hr. A3A protein (but not mRNA) is again elevated at 34 hr, where it would appear from cyclin B1 protein expression that a proportion of cells were in G2/M.

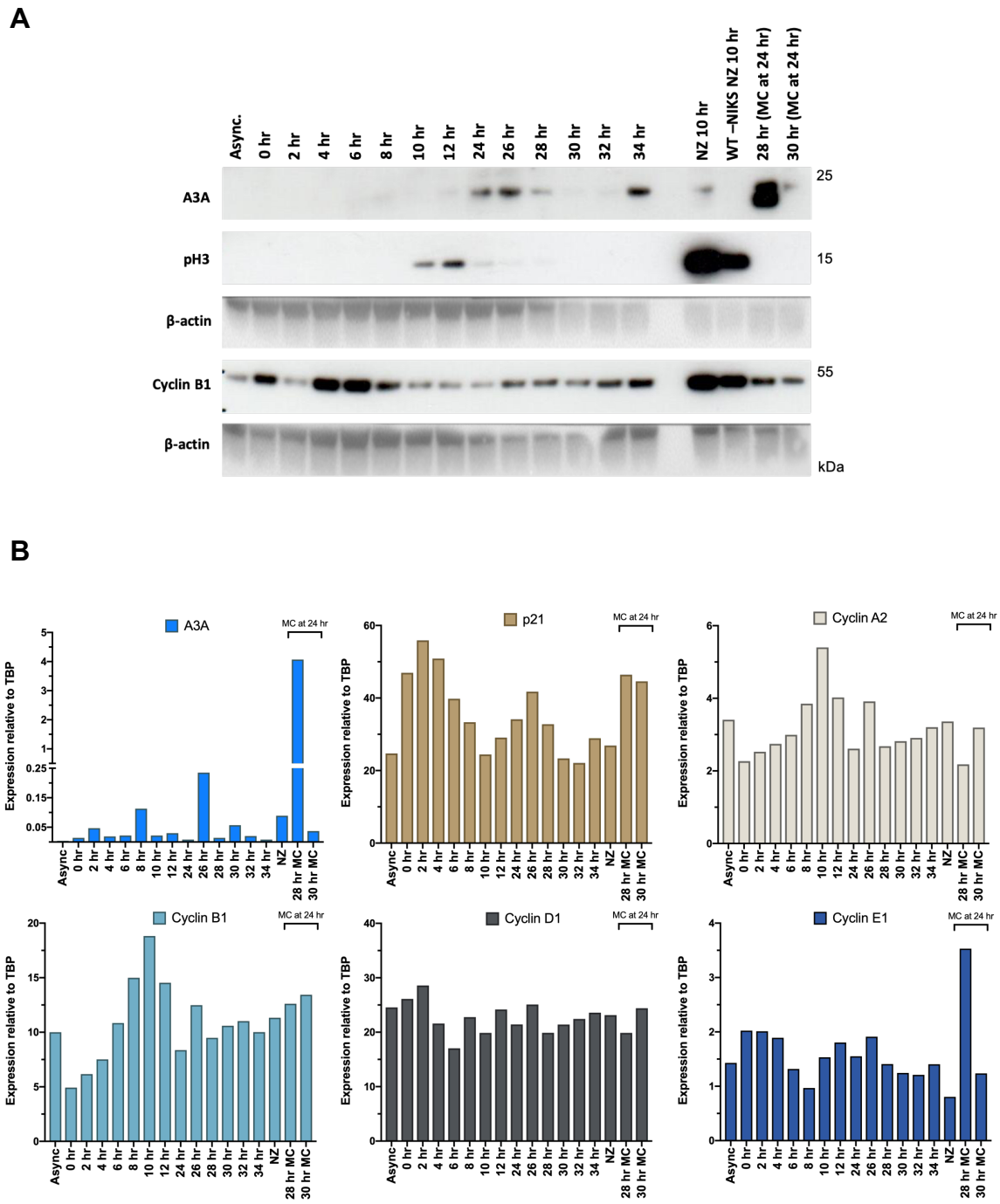

Figure 4-4 A3A is induced through media replenishment in G1 phase.
(A) A3A protein levels following release from a double thymidine block. **(B)** mRNA levels by qPCR of A3A, p21, cyclins A2, B1, D1 and E1**.** HA-A3B NIKS were synchronised in G1/S with a double thymidine block (protocol (3)) or synchronised in G2/M using 100 ng/ml of nocodazole (NZ) for 10 hr at 2 hr post-release. Asynchronous (async.) samples were 18 hr post-media change. Cells were released up to 34 hr, with or without a media change (MC) at 24 hr. RNA was extracted from HA-A3B NIKS and mRNA copy numbers are shown relative to TBP copies (n=1).

A3A protein was most strongly induced at 28 hr post-release in cells that had media refreshment at 24 hr, which coincides with an increase in mRNA to levels 4.07 times that of TBP (similar to that seen previously in Figure 4-3 (4.66)). Expression of p21 and cyclin A-E are also shown (Figure 4-4 (B)), and there was a 2.5-fold increase in the G1/S-phase specific cyclin E1 at 28 hr (compared to asynchronous levels) which corresponds with the A3A increase.

4.4 A3A is induced by serum starvation and re-stimulation

4.4.1 A3A mRNA is rapidly induced by re-stimulation of starved cells

Keratinocytes can be induced to enter their resting state of quiescence (G0/G1) through withdrawal of growth factors, and sub-confluent cells can be stimulated to re-enter the cell-cycle through their replacement. This method of synchronisation facilitates enrichment in early-G1 and would allow us to observe whether A3A was most strongly induced prior to the late-G1/S thymidine block.

Having previously established that the anti-A3A antibody could detect endogenous A3A protein, WT-NIKS were used hereafter, together with A3A KO to validate the specificity of the antibody. NIKS are grown in a complex (FC) media containing F-12, DMEM, 5% FBS, EGF, insulin, cholera toxin, adenine, and hydrocortisone (full details in method section); to induce quiescence but not terminal differentiation or excessive cell death, a protocol was used based on an adaptation by Matrka *et al.*, (2015): 40 hr incubation in F-12/DMEM, 0.3% FBS, cholera toxin and hydrocortisone (no EGF, insulin or adenine) and hereafter referred to as “starvation” media.

For re-stimulation of quiescent cells, the starvation media was removed and replaced with FC media (5% FBS and all growth factors). To ensure cells were sub-confluent and still actively cycling after 24 hr re-stimulation, WT-NIKS were plated at 2 x 10^5 cells/ well in 6-well plates with 3T3 feeder cells; A3A KO NIKS grow faster (shown later, at section 5.2) so were plated at 1.5 x 10^5 cells/ well.

Samples for western blot, flow cytometry and qPCR analysis were collected until 24 hr post re-stimulation, and the mean A3A mRNA level in starved cells (0 hr) was already ~50-fold higher than asynchronously growing cells: 0.94 $\pm$ 0.23 copies / copy TBP (Figure 4-5 (A)). However, following 3 hr of re-stimulation the mean A3A copy numbers (from seven independent experiments) increases a further ~100-fold to 92.75 $\pm$ 15.15 copies / copy TBP (~30-times greater than PMA induction, and ~10-times greater than PMA and IFN-α induction). Shown in Figure 4-5 (B), A3A protein could also be detected at 3 hr post-release, though most strongly between 9-18 hr, and still detectable at 24 hr.

Most cells in an asynchronous population will be in G1, and with normal diploid chromosomes, will have a 2n DNA content; as cells progress through S-phase there will a range of DNA content from 2n-to-4n. G2 phase cells will have 4n content, which gets shared between daughter cells during mitosis. DNA can therefore be stained with propidium iodide (PI) which allows for DNA content to be measured by flow cytometry. To verify that cells had arrested in G0/G1 through serum starvation as well as to analyse the cell cycle stages at each time-point, cells were collected (following removal of 3T3 feeder cells), then fixed and stained with PI.

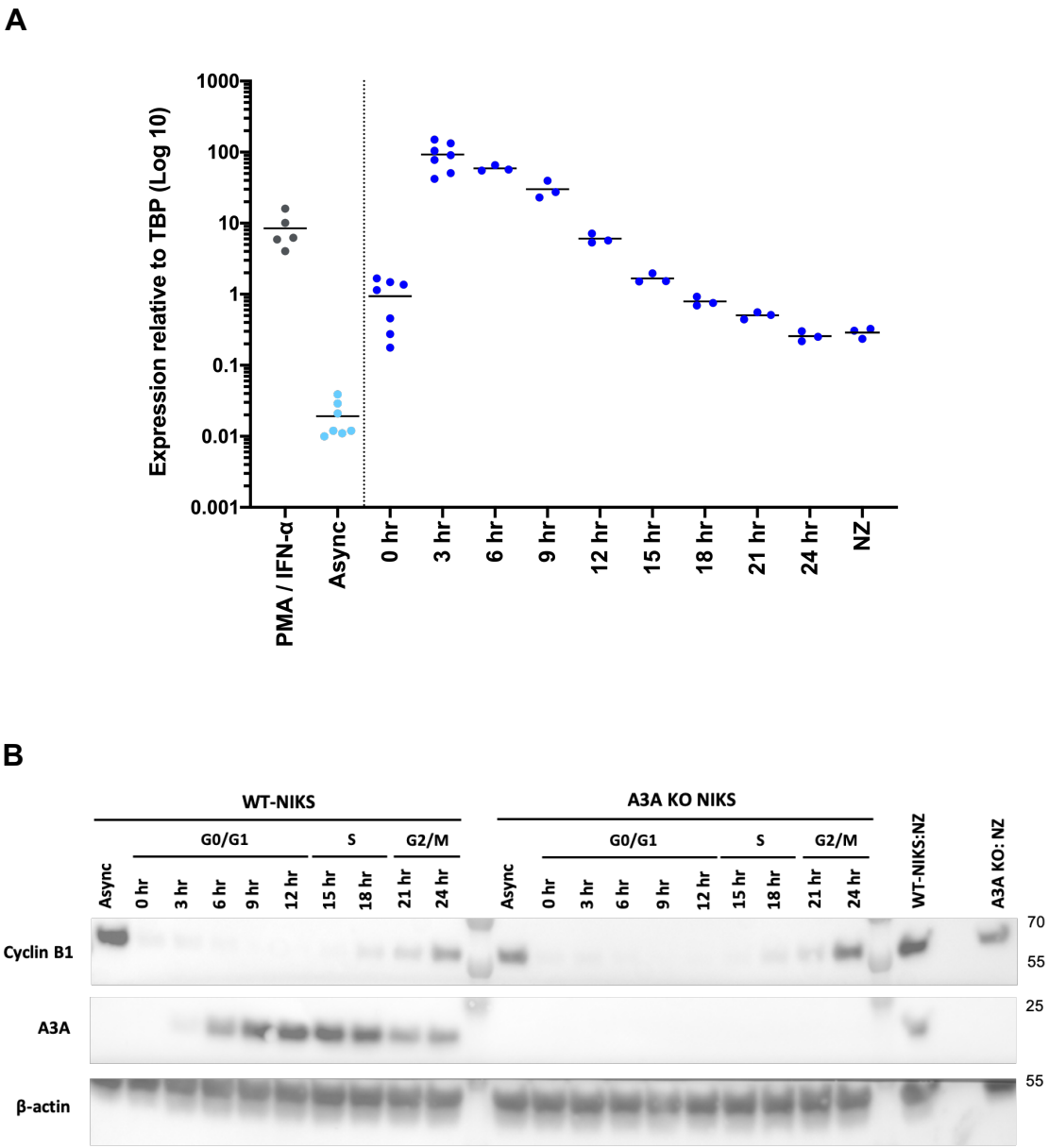

Figure 4-5 A3A is strongly induced by re-stimulation of quiescent cells.
(A) A3A mRNA peaks at 3 hr post re-stimulation of G0/G1 arrested cells. **(B)** A3A protein peaks between 9-18 hr post-release. WT-NIKS and A3A KO NIKS were synchronised in G0/G1 through incubation in starvation media for 40 hr, then re-stimulated with FC media. Asynchronous cells were 18 hr post-media change. 100 ng/ml of nocodazole (NZ) was added at 18 hr post-release for a further 6 hrs to arrest cells in G2/M. RNA was extracted from 3-8 biological repeats of WT-NIKS for qPCR analysis; mRNA copy numbers are shown relative to TBP copies; PMA and IFN-α induction is plotted for comparison (line at mean). Protein levels were detected with either anti-A3A antibody (Sigma), or anti-cyclin B1 antibody (Santa Cruz). β-actin shown as a loading control.

The results of the flow cytometry analysis are seen in Figure 4-6, and show that the majority of cells were in S-phase at 18 hr post-release. This implies that there is abundant expression of A3A during DNA replication, in which ssDNA could be vulnerable to A3A-mediated deamination.

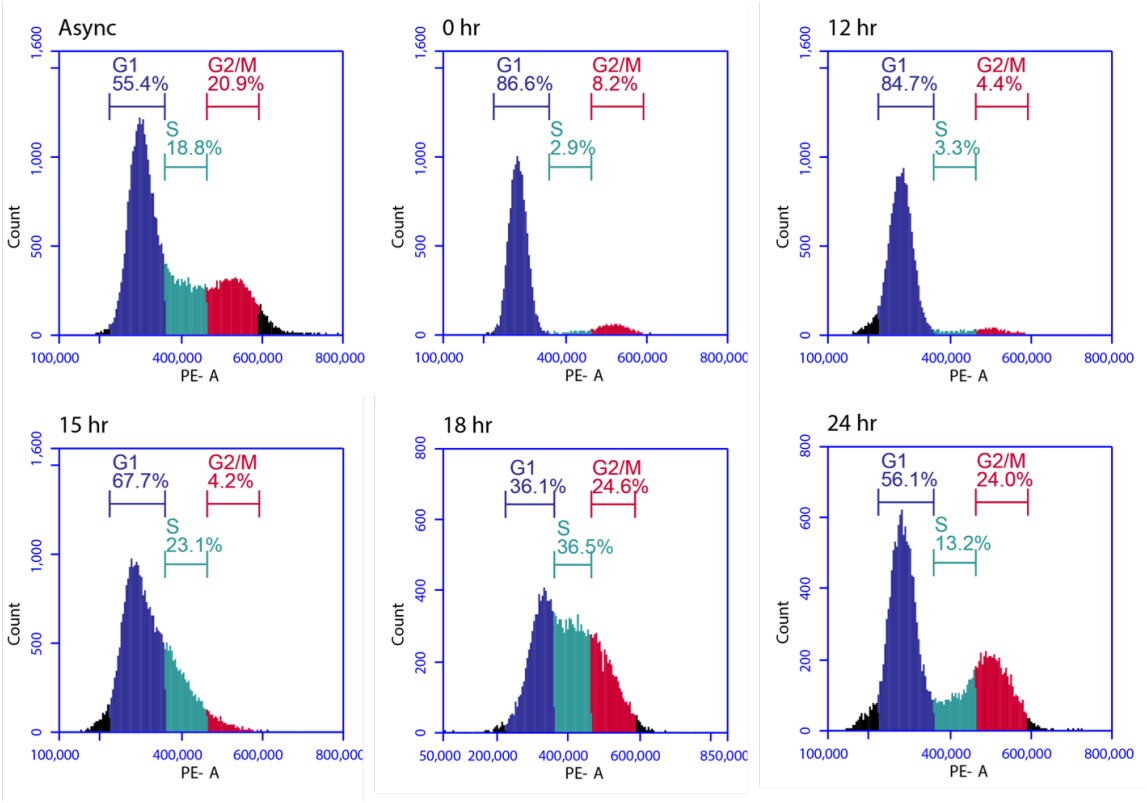

Figure 4-6 GO/G1 arrested NIKS reach S-phase at 15/18 hr post-release.
WT-NIKS were synchronised in G0/G1 through serum starvation for 40 hrs, then re-stimulated with FC media. Asynchronous cells were 18 hr post-media change. Cells were collected and stained with propidium iodide. Quantification of DNA content was performed on a BD Accuri™ C6 Plus Flow Cytometer.Cell-cycle analysis of DNA content confirmed that the majority of starved cells (0 hr) had a 2n DNA content and therefore were in G0/G1. There were no S-phase cells, though a proportion had a 4n DNA content and so had arrested in G2/M.

The results further show that a fraction of cells had progressed through to S-phase by 15 hr post-release, with the majority of the remaining cells having done so by 18 hr. By 24 hr post-release, a proportion of cells had 2n DNA content indicating that they had completed mitosis and had entered the subsequent G1-phase.

For immunofluorescent detection of A3A following starvation and re-stimulation, WT-NIKS were grown on coverslips and fixed with 4% PFA at 8 hr post-release (a time at which A3A protein levels were seen to be abundant) and the results are shown in Figure 4-7.

Immunofluorescent labelling with the A3A antibody used for western blot detection (Sigma) had previously led to high background staining in the A3A KO cells, therefore cells were labelled with an alternative A3A antibody (gift from J. Maciejowski, Memorial Sloan Kettering Cancer Center, New York).

Specific detection of endogenous A3A could be seen at 8 hr post re-stimulation of quiescent cells. Once again, A3A staining was detectable throughout the cytoplasm and nucleus, with very minimal background staining present in the A3A KO cells. Interestingly, despite synchronising cells into a mostly uniform population, it appears that strong A3A staining was still restricted to a sub-population of cells (although with longer exposure A3A appears to be in the majority of cells but at considerably lower abundance). Therefore, it remains to be established what is unique about these strongly expressing cells.

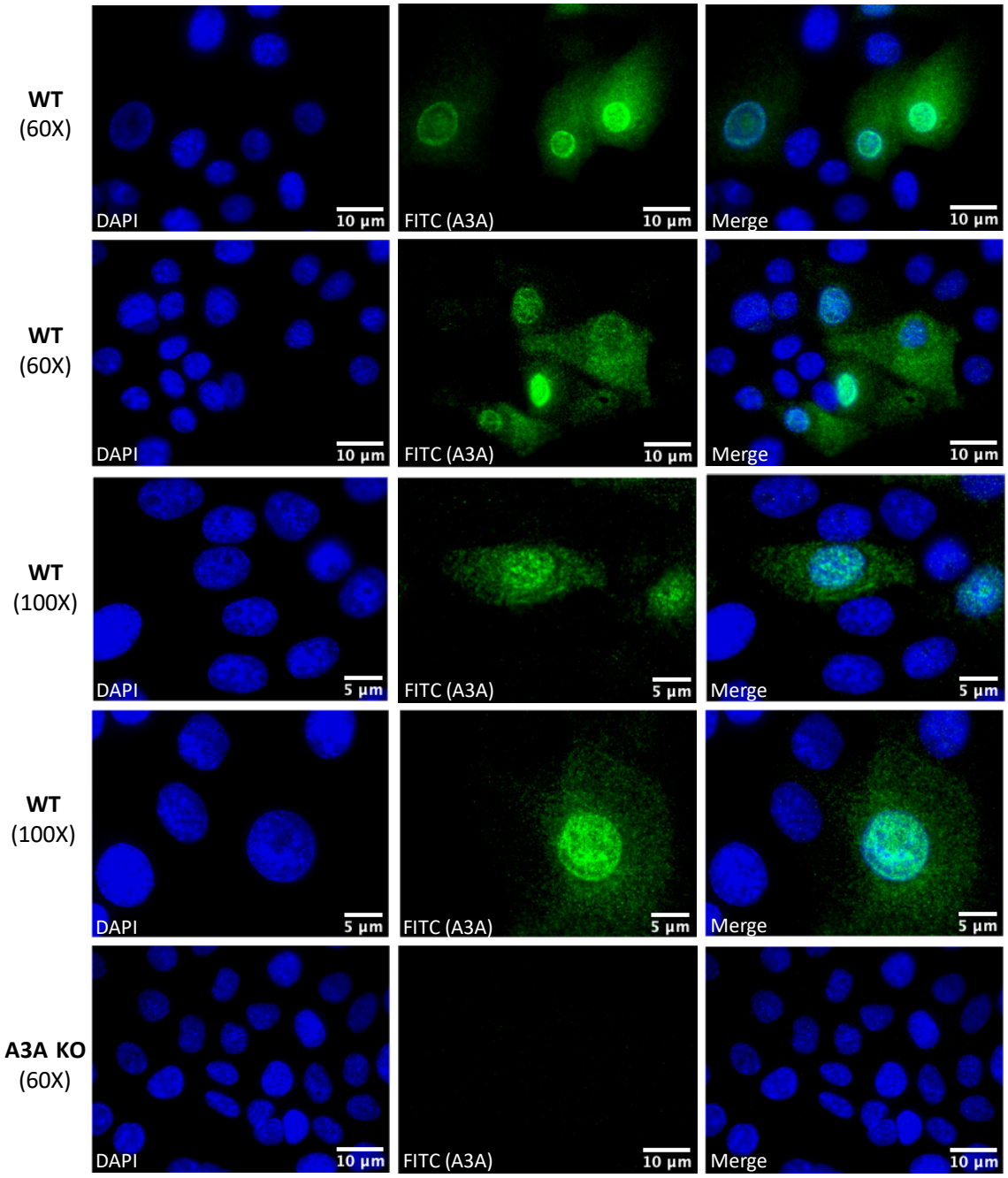

Figure 4-7 Endogenous A3A protein is specifically detected following starvation / re-stimulation.

WT-NIKS and A3A KO NIKS were grown on coverslips, serum starved for 40 hr as previously described, and re-stimulated for 8 hr with FC media. Cells were probed with A3A mouse monoclonal antibody (J. Maciejowski). Anti-A3A was labelled with AlexaFluor488 conjugated secondary antibody (Invitrogen). Nuclei were counterstained with DAPI and imaging was performed on an epifluorescent microscope at 60X or 100X magnification (as shown).

4.4.2 A3A induction is not dependent upon G1/S progression

We have found that A3A transcripts increase in serum starved cells and that both A3A mRNA and protein are potently induced upon their re-stimulation. Elevated levels persist over a prolonged period (greater than 21 hr), during which time cells re-enter the cell-cycle, replicate their DNA and progress through mitosis. We next wanted to address whether passage into S-phase is required for sustained A3A expression, and whether the kinetics of A3A induction and subsequent reduction back to baseline levels change if we block cell cycle progression. Mammalian cell-cycle entry relies on the formation of cyclin D-CDK4/6 complexes that phosphorylate and inactivate Rb, leading to the derepression of the E2F transcription factor and an increase in S-phase gene activity (reviewed by Goel *et al*., 2018).

Thus, pharmacological inhibition of CDK4/6 activity arrests cell cycle progression at the restriction point in G1, prior to cell cycle commitment (Trotter and Hagan, 2020). Palbociclib specifically inhibits CDK4/6 at nanomolar concentrations, and induces G1 arrest in an Rb-dependent manner (Knudsen *et al.*, 2017). NIKS were synchronised in G0/quiescence by incubation in starvation media as previously described, following which starvation media was removed and replaced with FC media, either with or without the addition of 200 nM Palbociclib. Samples were collected for RNA extraction, protein extraction, and flow cytometry (as well as DNA extraction (shown later at section 4.4.4)) over the subsequent 24 hr time-period. Additionally, fresh media containing palbociclib was added to asynchronously growing NIKS and collected 18 hr later.

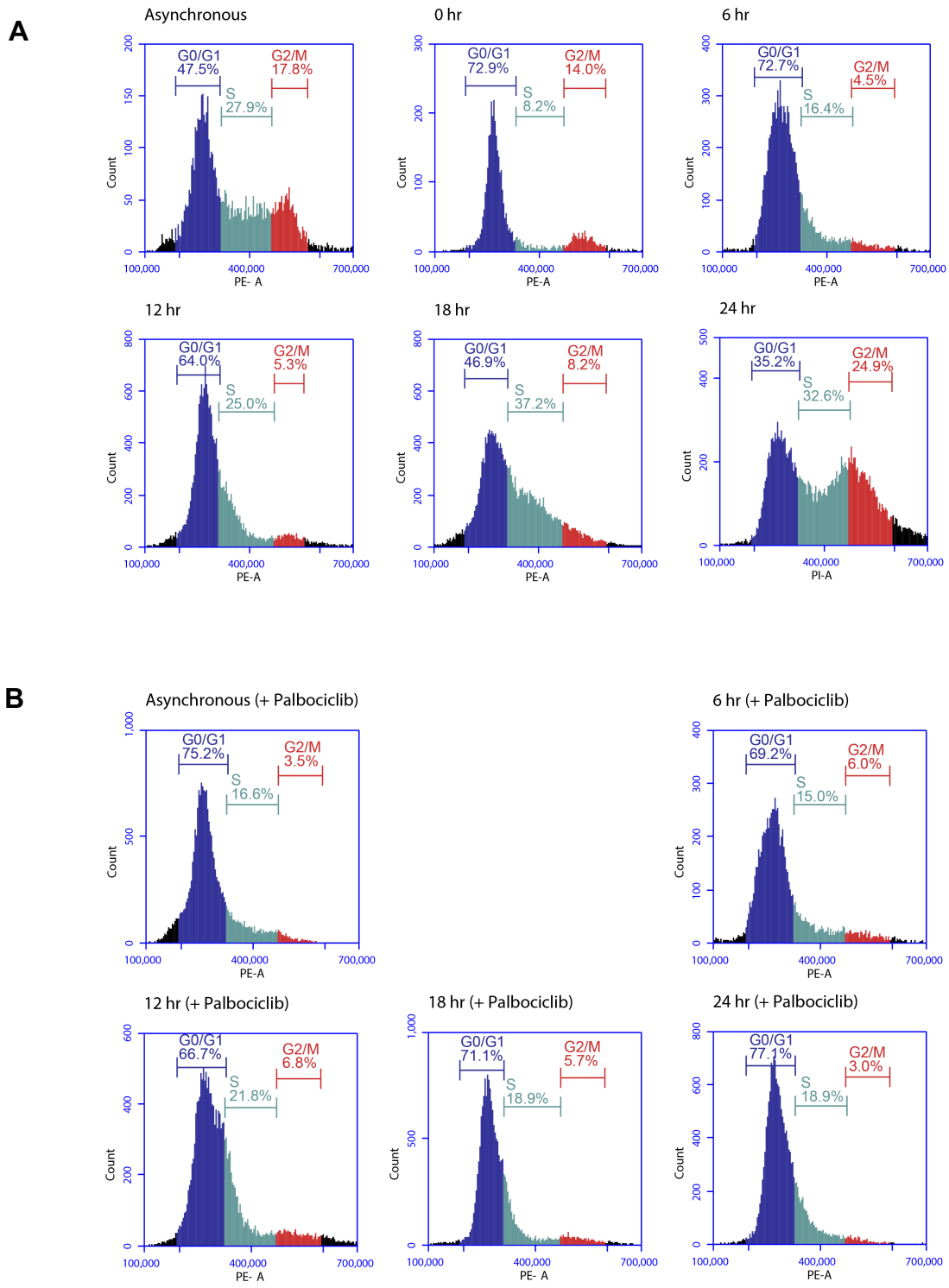

Figure 4-8 Palbociclib induces G1 arrest in re-stimulated NIKS.
(A) Cell cycle profile of WT-NIKS released from serum starvation over 24 hr. **(B)** Palbociclib induces arrest in G1. WT-NIKS were synchronised in G0/G1 through incubation in starvation media for 40 hr then re-stimulated with FC media. To inhibit G1 exit, 200 nM of CDK4/6 inhibitor, palbociclib, was included in the FC media upon re-stimulation. Asynchronous cells were 18 hr post-media change (+/- Palbociclib for 18 hr). Cells were collected and stained with propidium iodide. Quantification of DNA content was performed on a BD Accuri™ C6 Plus Flow Cytometer.

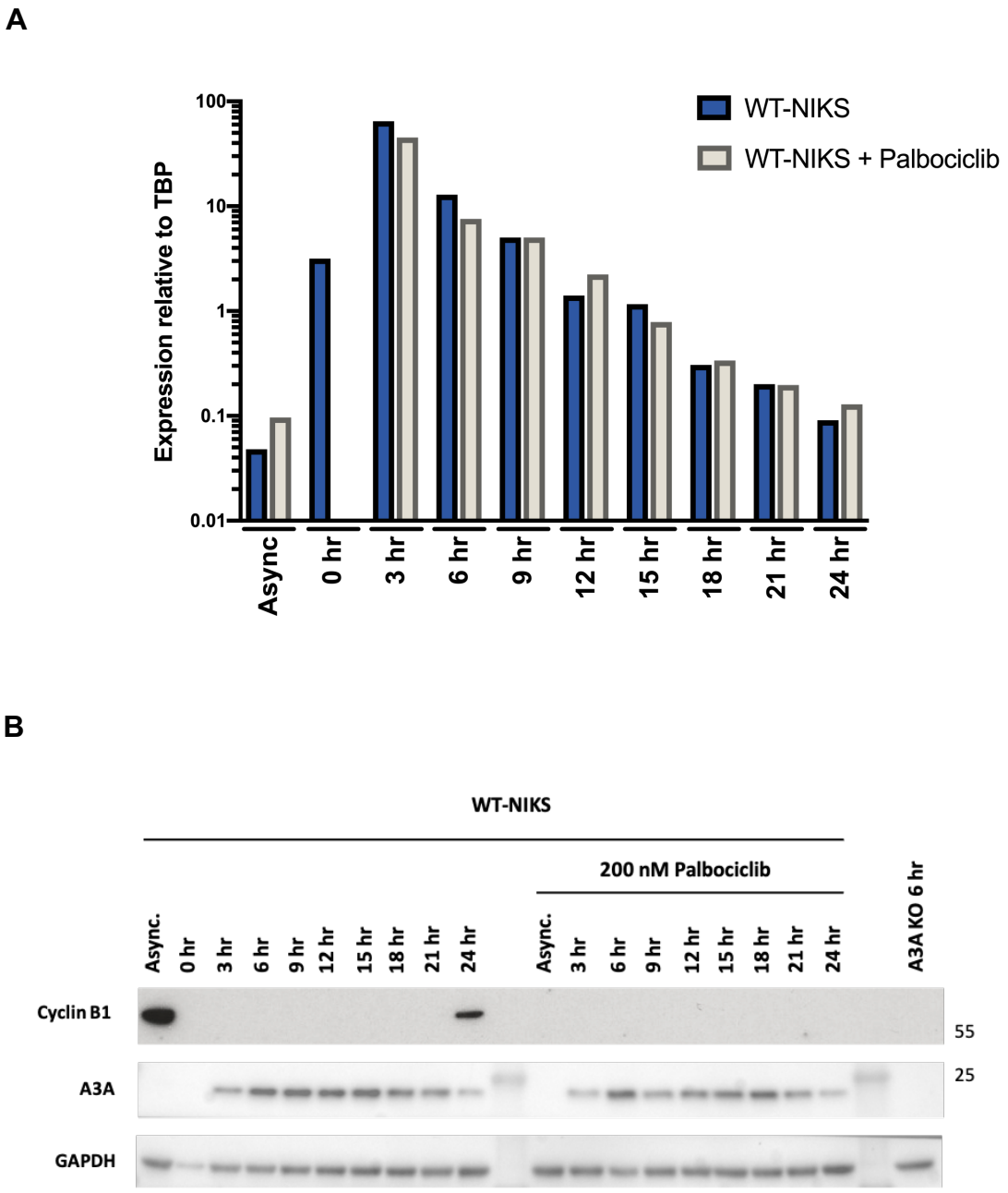

Figure 4-9 A3A expression persists with similar kinetics following G1 arrest.
(A) A3A mRNA following re-stimulation of starved cells with/without G1 arrest by palbociclib. **(B)** A3A protein levels (+/- palbociclib) by western blot analysis. WT-NIKS (and A3A KO) were synchronised in G0/G1 through incubation in starvation media for 40 hrs, then re-stimulated with FC media. To inhibit G1 exit, 200 nM of CDK4/6 inhibitor, Palbociclib, was included in the FC media upon re-stimulation. Asynchronous cells were 18 hr post-media change (+/- Palbociclib for 18 hr). RNA was extracted WT-NIKS for qPCR analysis; mRNA copy numbers are shown relative to TBP copies (n=1). Protein levels were detected by probing with anti-A3A antibody (Sigma); GAPDH shown as a loading control.

Flow cytometry analysis confirmed that the DNA content of palbociclib treated samples did not alter significantly post- re-stimulation and therefore had been blocked from G1 exit (Figure 4-8 (B)).

As seen in Figure 4-9 (A), peak A3A mRNA induction was again at 3 hr post-stimulation and the kinetics of induction and subsequent decline were unchanged in the presence of Palbociclib; though there was a slight increase in asynchronous cells which we can speculate is due to enrichment of the G1 population. Corroborating that seen previously (in Figure 4-5 (B)), peak A3A protein expression was first visible subsequent to peak mRNA expression, at 6 hr post-release. This was also consistent in the palbociclib treated cells (though with possibly slightly less expression). A3A protein persisted in both sets of samples at 24 hr, and there was no accumulation of A3A by preventing cells exiting G1.

4.4.3 A3A induction does not increase DNA DSB formation

Expression and enzymatic activity of the nuclear base excision repair enzyme, uracil-DNA glycosylase (UNG), increases during late-G1/S phase (Haug *et al.*, 1998) and it co-localises at ssDNA in replication foci with proliferating cell nuclear antigen (PCNA) and the p34 subunit of replication protein A (RPA2) (Nagelhus *et al.*, 1997; Otterlei *et al.*, 1999; Ko and Bennett, 2005). A3A primarily deaminates cytosines to uracil at exposed ssDNA sites in the lagging strand of replication forks (Haradhvala *et al.*, 2016).

UNG cleaves the resulting uracils creating AP (apurinic/apyrimidinic) sites, which unless correctly repaired can stall replication, convert a C:G pair into a U:A pair prior to replication, or lead to DNA DSB formation. Accordingly, ectopically induced overexpression of A3A has been found to cause DNA breaks and S-phase arrest in multiple cell types (Green *et al.*, 2016).

We saw that A3A protein was abundant at 18 hr post-release, a time at which a large proportion of cells were transiting through S-phase (as shown by flow cytometry analysis) and thus ssDNA substrate might be vulnerable to A3A-mediated deamination. We were therefore interested to see whether the abundance of A3A protein also led to an increase in DSBs.

By using γ-H2AX as a marker of DNA DSB foci and comparing their formation with A3A KO NIKS, cells were re-stimulated for 18 hr and then fixed and stained for imaging on an epifluorescent microscope. Although several cells displayed γ-H2AX foci indicative of DNA DSBs (an example is shown in Figure 4-10 (A)), there was no apparent increase in the WT-NIKS populations as compared to the A3A KO NIKS.

This was quantified by counting the number of γ-H2AX foci per nuclei which showed that the majority of cells had no foci, and there was no significant difference between the two cell lines (shown in Figure 4-10 (B)). This is also consistent to the earlier observations that A3A induction by PMA/IFN-α treatment did not correlate with an increase in DSB formation (Figure 3-6).

However, whilst ~37% of the cell population were in S-phase at 18 hr post-release (Figure 4-6, Figure 4-8), between 36-46% were still in G1-phase. These findings therefore indicate that either endogenous A3A is tightly regulated in such a way that it does not access or deaminate genomic DNA during S-phase (such as exclusion from the nucleus), making it non-genotoxic under these conditions; alternatively, that it is expressed in a sub-population of cells that do not enter S-phase (G1 or G2 arrested), or have not yet reached S-phase by 18 hr post-release.

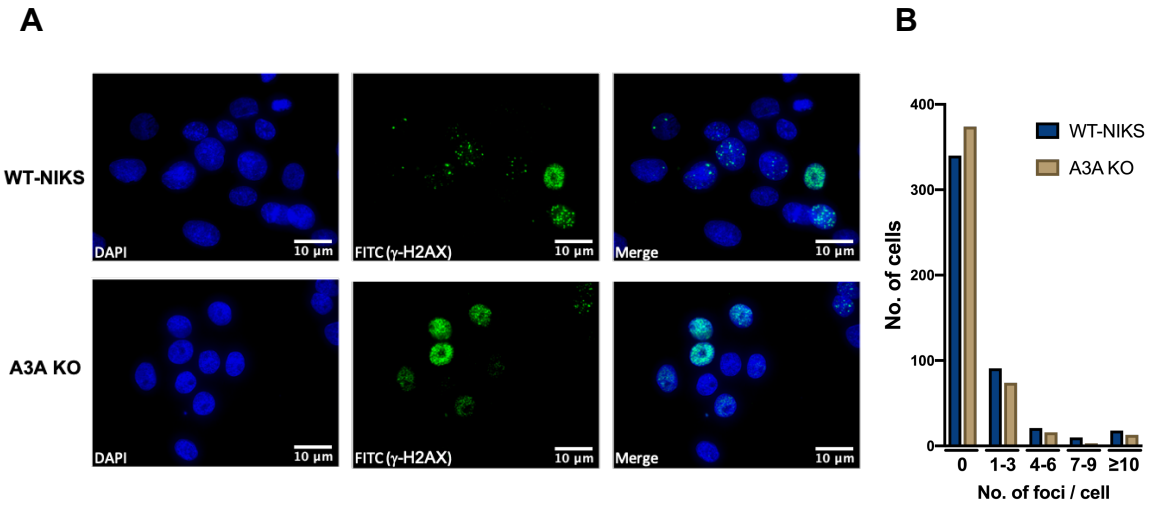

Figure 4-10 A3A induction during S-phase does not increase γ-H2AX foci.
(A) Representative images of γ-H2AX foci in WT-NIKS and A3A KO NIKS at 18 hr post-release from re-stimulation. (**B)** Quantification of γ-H2AX foci shows no significant difference between WT-NIKS and A3A KO NIKS. Cells were grown on coverslips and serum starved for 40 hr, then re-stimulated for 18 hr in FC media. Cells were stained with γ-H2AX antibody and AlexaFluor488 conjugated secondary antibody. Nuclei were counterstained with DAPI and imaging performed on an epifluorescent microscope at 60X magnification. γ-H2AX foci were counted from 500 nuclei/cell line (n=1; WT-NIKS mean: 45.18; A3A KO mean: 40.0; two-way ANOVA <0.9999).

4.4.4 A3A induction does not appear to increase AP site formation

Uracils created by cytosine deamination are cleaved by UNG, generating apurinic/apyrimidinic (AP) sites which are processed by excision and repair in the BER pathway (Helleday, Eshtad and Nik-Zainal, 2014); prior to repair, AP sites exist in an equilibrium of open-ring and closed ring forms (Beger and Bolton, 1998). An aldehyde reactive probe (ARP) contains an aminoxy group that will react with the aldehyde group on the open ring form of AP sites (Kubo *et al.*, 1992); ARP is biotinylated, thereby facilitating an interaction with a streptavidin-enzyme conjugate and quantification of AP sites in genomic DNA.

Thus far, it appears that A3A induction does not increase DNA DSB formation; we were therefore interested to see whether it might instead lead to an increase in AP sites. DNA was isolated from WT-NIKS and A3A KO NIKS that had been starved and re-stimulated for 24 hr (from same fraction of cells shown previously in Figure 4-9, in which A3A induction was confirmed to be robust by qPCR and western blot analysis).

The Oxiselect Oxidative DNA Damage Quantitation Kit ((Cell Biolabs) containing ARP and streptavidin-enzyme conjugate) was used to quantify AP sites per 100,000 bp (compared to a standard curve of predetermined AP sites), and as shown in Figure 4-11 (A), AP sites from two technical repeats for each time-point ranged between ~20-40 per 100,000 bp, and did not significantly change during S-phase (18 hr) or subsequently in either cell line.

Furthermore, there was no difference in the overall quantity of AP sites following induction of A3A in the WT-NIKS over the course of 24 hr, as compared to the A3A KO NIKS (Figure 4-11 (B)). Hydrogen peroxide (H_2O_2) was used (at 10 mM) as a positive control and since we saw a similar quantity of AP sites in our samples to the positive control, this is preliminary data that requires further quantification.

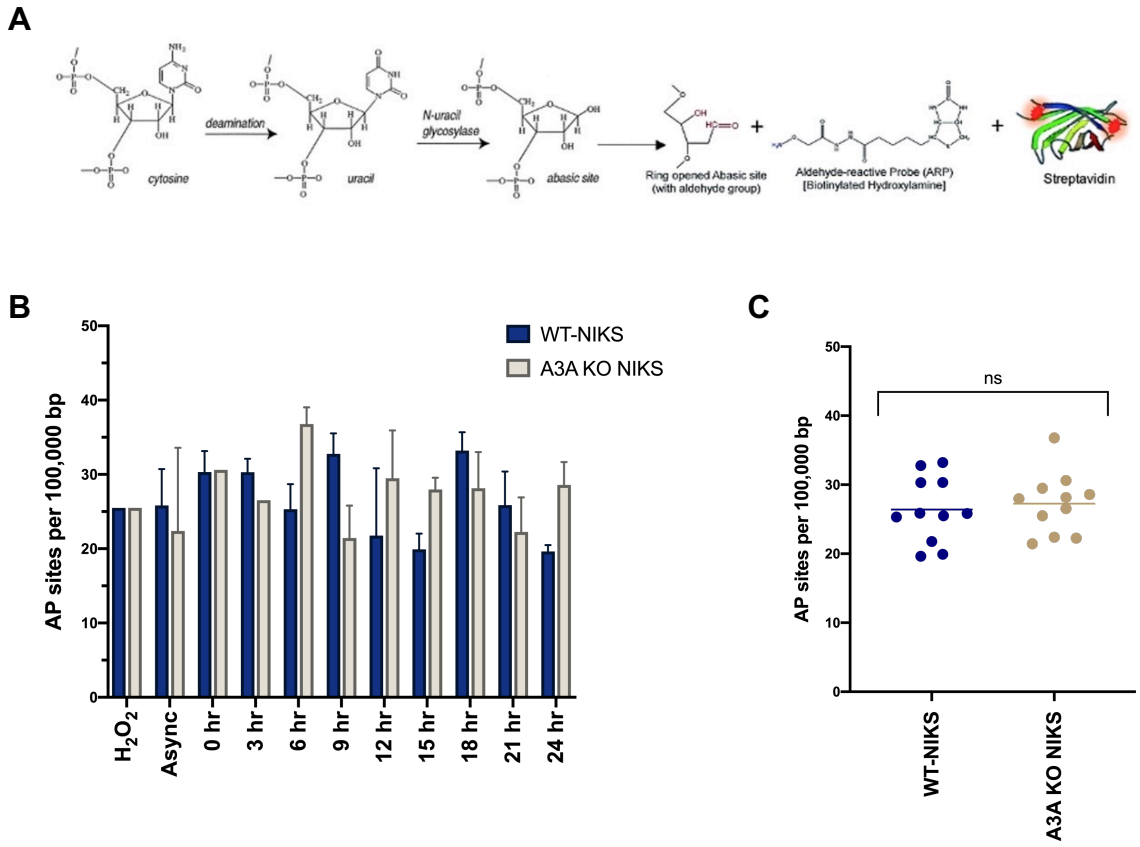

Figure 4-11 Induction of endogenous A3A does not increase AP sites formation in genomic DNA.

(A) An aldehyde reaction probe (ARP) reacts with an aldehyde group on the open-ring form of AP sites, allowing quantification with a streptavidin-enzyme conjugate (Vaidyanathan *et al.*, 2021). **(B)** Quantification of AP sites in genomic DNA of WT-NIKS and A3A KO at each time-point following re-stimulation. **(C)** Grouped results from quantification shown at (A). WT-NIKS and A3A KO NIKS were serum starved for 40 hr, then re-stimulated with FC media for 24 hr. Asynchronous cells (async) were 18 hr post-media change. DNA was extracted from ~5-10 x 10^6 cells per time-point. AP sites were detected using Oxiselect Oxidative DNA Damage Quantitation Kit (Cell Biolabs) and a standard curve generated from DNA containing predetermined AP sites. H_2O_2 used as a positive control (n=1). Mean and SEM (n=2 from technical repeats). Each point at (B) represents the mean of each time-point from (A)) (line at mean, two-way ANOVA <0.7131).

4.4.5 HPV oncoproteins suppress A3A expression following starvation / re-stimulation of NIKS

HPV-positive cervical tissues show elevated expression of A3A and A3B during early stages of cancer progression (in low-grade and high-grade intraepithelial lesions), in a mechanism that may involve the HPV oncoprotein E7 (Warren *et al.*, 2015). Furthermore, it was proposed that increased expression of A3A mRNA found within HPV-positive keratinocytes (NIKS) was through E7-dependent stabilisation of A3A protein and inhibiting A3A protein degradation (Westrich *et al.*, 2018). Though whilst A3A signature mutations are high within cervical cancer tissues, its mRNA expression is low, and exogenous A3A was found able to inhibit cervical cancer cell migration and proliferation (Chen *et al.*, 2015).

We were therefore interested to see the effect of HPV16 and its oncoproteins on A3A expression in NIKS following starvation/re-stimulation. To do this, we used NIKS that were stably transfected with either: E6 (NIKS-E6), E7 (NIKS-E7), both E6 and E7 (NIKS-E6/E7), or the whole HPV16 genome (NIKS-HPV16) and these were compared against NIKS containing the empty plasmid employed for generating the stable expression (NIKS-pLXSN).

Cells were synchronised through serum starvation as before, then re-stimulated for 3 hr and 6 hr with FC media, and collected for western blot and qPCR analysis (shown in Figure 4-12).

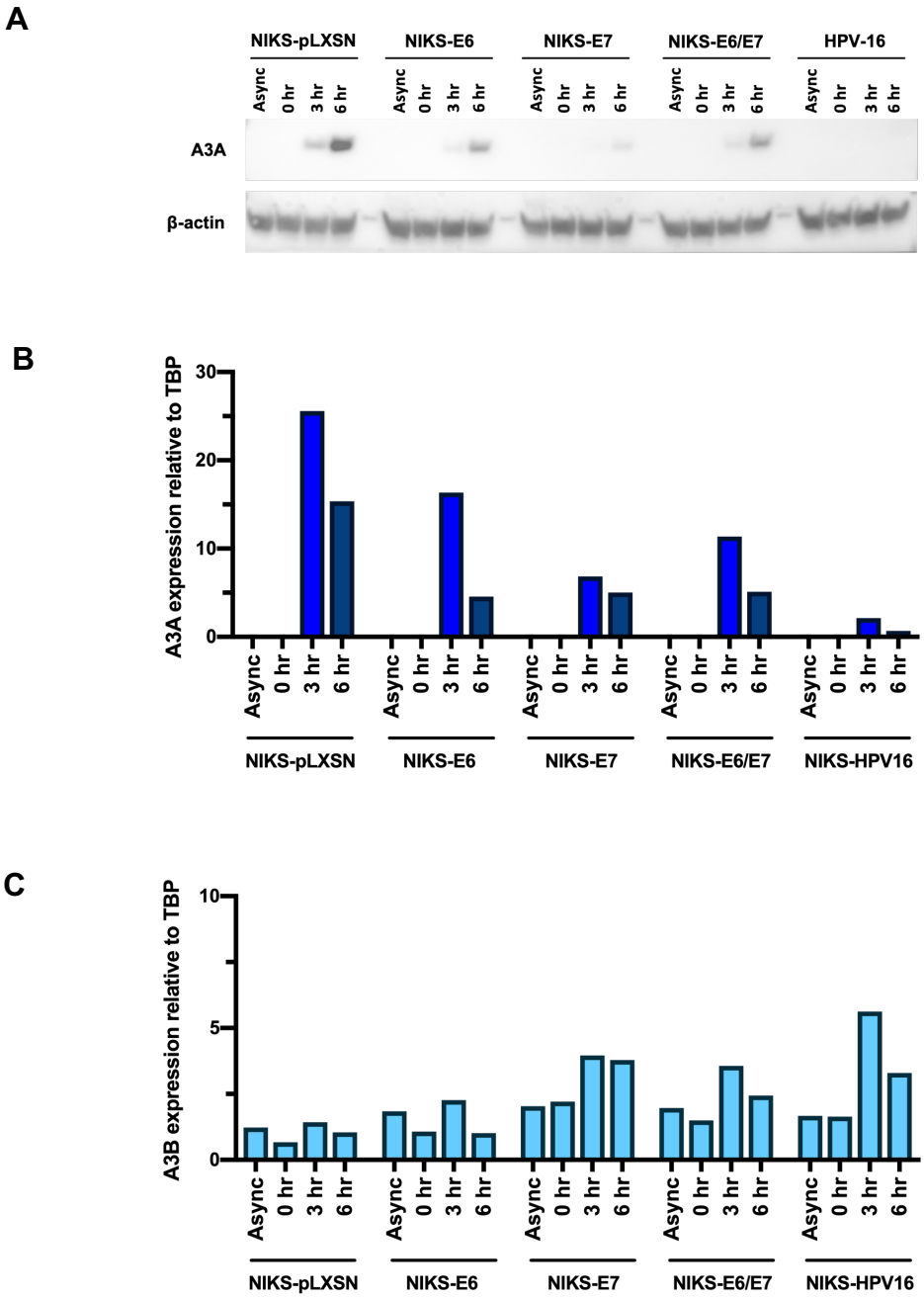

Figure 4-12 HPV oncoproteins disrupt A3A mRNA and protein expression.
(A) A3A protein induction in HPV16 oncoprotein containing NIKS upon starvation/re-stimulation. **(B)** A3A mRNA expression. **(C)** A3B mRNA expression. NIKS stably expressing either empty plasmid (NIKS-pLXSN), HPV16 E6 (NIKS-E6), E7 (NIKS-E7), both E6 and E7 (NIKS-E6/E7), or the whole HPV16 genome (NIKS-HPV16) were serum starved for 40 hrs, then re-stimulated with FC media for 3 hr and 6 hr. Asynchronous cells were 6 hr post-media change. mRNA copy numbers are shown relative to TBP copies (n=1). Protein levels were detected with anti-A3A antibody (Sigma); β-actin-HRP shown as a loading control.

The kinetics of A3A induction in the control cells (NIKS-pLXSN) was consistent with that seen previously in WT-NIKS, with peak mRNA induction elicited at 3 hr post-stimulation (Figure 4-12 (B)), followed by peak protein expression at 6 hr (Figure 4-12 (A)).

A3A protein was lower in NIKS-E6 and NIKS-E6/E7, and significantly more so in NIKS-E7. Moreover, A3A protein was undetectable at 6 hr post-stimulation in NIKS containing the whole HPV16 genome. Corroborating this, mRNA levels show that A3A transcripts are also lower at 3 hr and 6 hr in E6, E7 and HPV16-containing NIKS: expression of 25.59 copies/copy TBP at 3 hr in NIKS-pLXSN, as compared to 2.14 in NIKS-HPV16 (~12-fold less). In contrast, there was a ~4-fold increase in A3B expression at 3 hr post-stimulation in NIKS-HPV16 (Figure 4-12 (C)): 1.43 copies/copy TBP in NIKS-pLXSN, as compared to 5.63 in NIKS-HPV16.

However, although A3A mRNA is less at 3/6 hr post-stimulation in HPV16/E6/E7-NIKS, they also contain fewer A3A transcripts in asynchronous cells: pLXSN (0.088), E6 (0.029), E7 (0.033), E6/E7 (0.031), HPV16 (0.006) copies/copy TBP. The fold-change in A3A expression between asynchronous, starved, and re-stimulated (3 hr) cells is therefore in fact greater in all except NIKS-E7 (Figure 4-13 (B-C)), suggesting that the overall decrease may arise through disruption of the process that mediates transcriptional activity of A3A at the basal level.

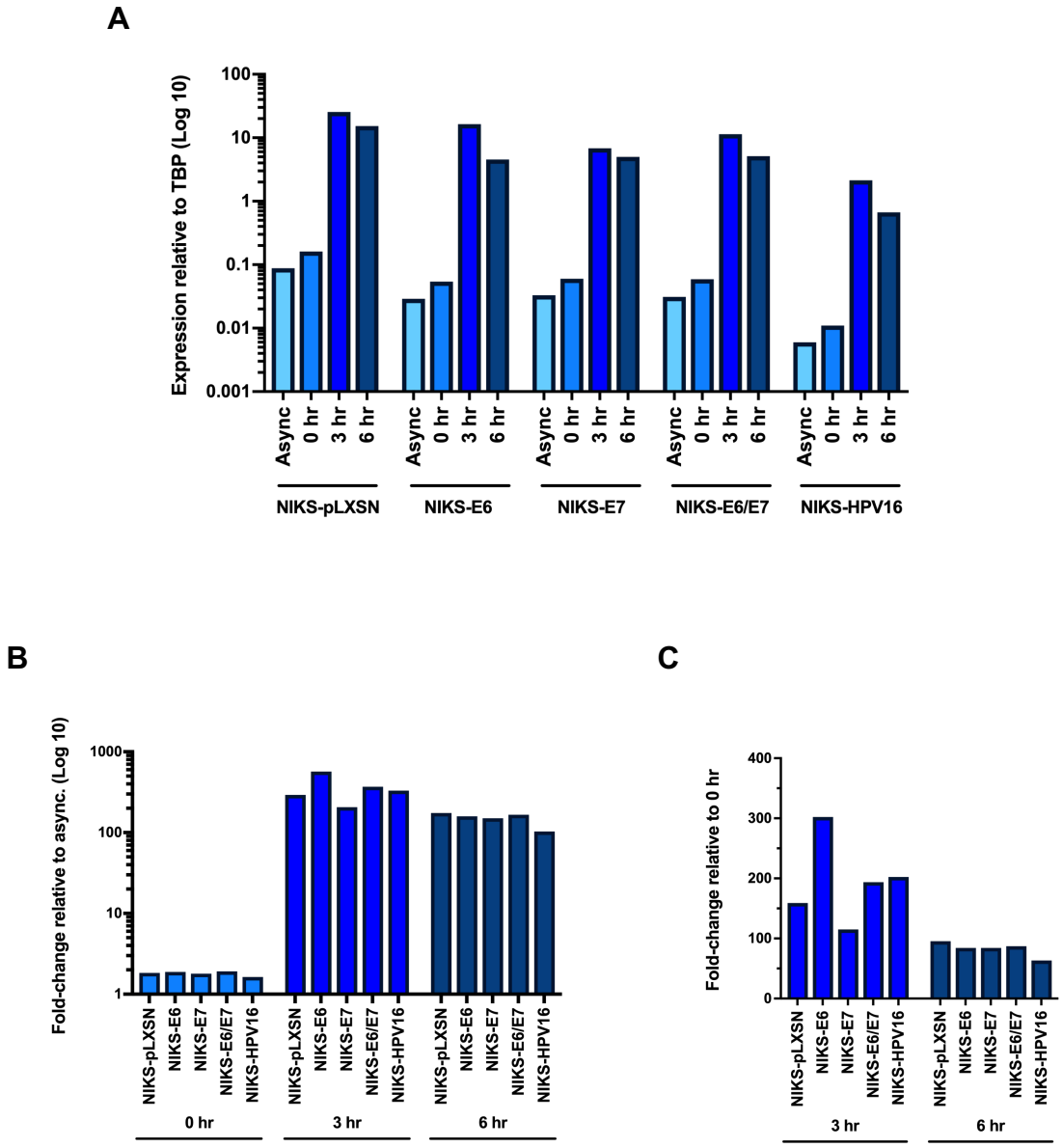

Figure 4-13 A3A induction by HPV16 (Log10 and fold-change).
(A) Comparison of A3A mRNA levels in NIKS expressing HPV16 oncoproteins (Log 10 scale of graph shown at Figure 4-12(B)). **(B-C)** A3A mRNA in NIKS containing HPV16 oncoproteins: expressed as a fold-change of induction compared to asynchronous (B), or 0 hr (C).

4.4.6 Sustained induction by growth factors is unique to A3A among the APOBEC3 family

A3A mRNA is ~50-fold higher than asynchronous levels in serum starved, quiescent NIKS and this rapidly increases a further ~100-fold upon re-stimulation with FBS and growth factors. Comparing this induction profile to the remaining APOBEC3s, no other family member was similarly induced (Figure 4-14). A3C and A3H are ~1.3-fold and ~5-fold higher respectively in starved cells (0 hr), though A3C rapidly declines to lower than basal levels by 6 hr post-release; and A3H increases very slightly upon re-stimulation yet declines to basal levels by 9 hr.

A3G is unique among the A3 genes in that there is ~90% reduction at all time-points compared to asynchronous levels. A3D and A3F mRNA levels are both slightly lower in starved cells; A3D levels then decline rapidly to about ~20% of asynchronous levels upon restimulation (by 3 hr), with a similar level of decline in A3F seen by 6 hr. A3B mRNA is ~90% lower in starved cells; there is a ~7-fold increase upon re-stimulation, yet this is less than half of asynchronous levels and quickly diminishes. Surprisingly there is no increase of A3B at G2/M (21 hr / 24 hr) following re-activation from quiescence, in contrast to that seen following release from thymidine block (Figure 3-9). Though interestingly, under these growth conditions (18 hr post-media change), asynchronous levels of all APOBEC3s (except A3A and A3H) are higher than seen previously (48 hr post-media change / 6 hr FC/DMSO, Figure 3-7). Moreover, A3B and A3C basal levels are similar under these conditions and equally the mostly abundantly expressed (previously A3C was ~6-fold greater than A3B).

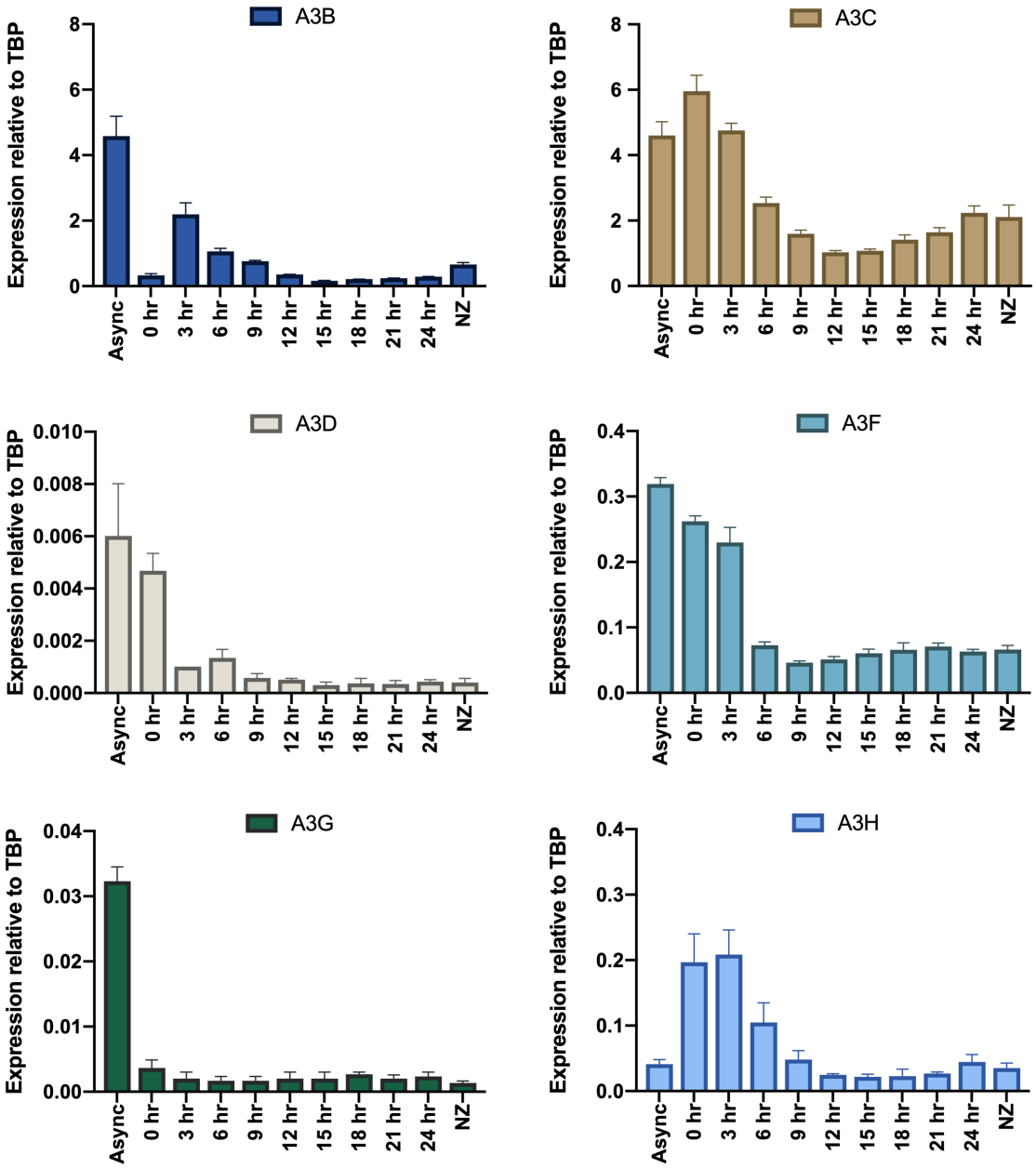

Figure 4-14 A3B-A3H levels during quiescence and re-stimulation.
WT-NIKS which were plated in 6-well plates at 2 x 10^5 per well. The next day, cells were serum starved for 40 hr then re-stimulated with FC media; asynchronous samples were 18 hr post media-change. 100 ng/ml of nocodazole (NZ) was added at 18 hr post-release for a further 6 hr to arrest cells in G2/M. mRNA copy numbers are shown relative to TBP copies (n=3).

4.4.7 A3A increases in confluent starved cells

We previously found A3A to be strongly induced by PMA and IFN-α in sub-confluent, asynchronous populations of NIKS, but not fully confluent NIKS (Figure 3-4). To validate whether A3A induction upon release from quiescence was similarly restricted to sub-confluent cultures, WT-NIKS were plated at either 7 x 10^4 (sub-confluent) or 5 x 10^5 per well (confluent) in 12-well plates. The next day, cells were washed twice and incubated in starvation media for 40 hr, then re-stimulated for 3 hr with FC media (all growth factors).

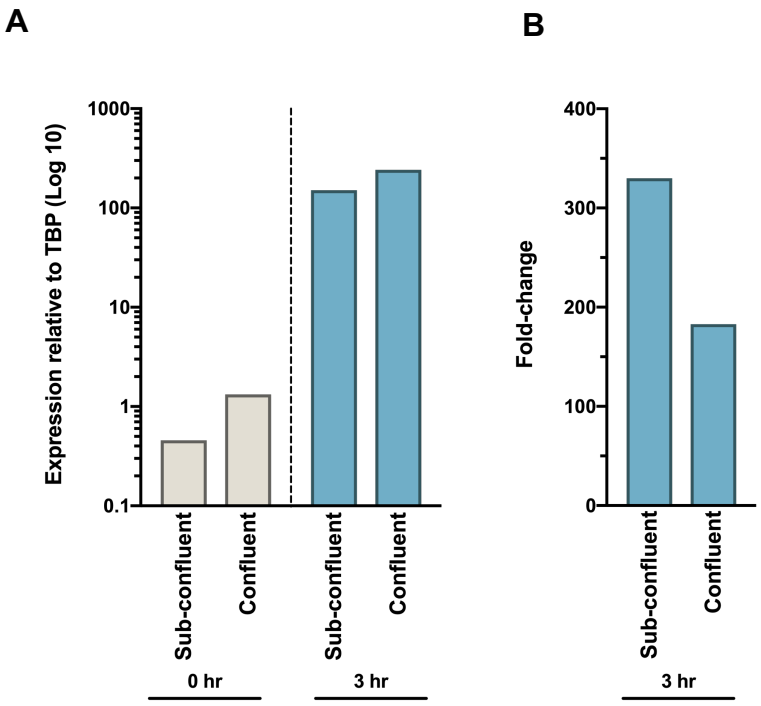

Figure 4-15 A3A increases in confluent starved cells.
(A) A3A induction in sub-confluent vs confluent cell cultures. **(B)** A3A induction expressed as fold-change relative to starved (0 hr). WT-NIKS were synchronised in G0/G1 through incubation in starvation media for 40 hrs, followed by re-stimulation for 3 hr with FC media. A3A mRNA copy numbers are shown relative to TBP copies (n=1).

The expression of A3A in sub-confluent starved cells (0 hr) was 0.46 copies/copy TBP; this was ~3-fold higher in confluent starved cells: 1.32 (Figure 4-15). Re-stimulation of sub-confluent starved cells for 3 hr increased A3A ~330-fold. Despite the lack of induction seen previously by PMA and IFN-α treatment in confluent cells following daily media replenishment, re-stimulation of confluent starved cells led to an even greater quantity of A3A mRNA (241.75 copies/copy TBP). However, despite the increased absolute level, the relative fold-change compared to 0 hr (~180-fold) was only ~55% of that seen in sub-confluent cells. It would appear therefore, that A3A induction by starvation is greater in confluent cells, however the subsequent induction by growth factor stimulation is reduced.

4.4.8 A3A is rapidly induced and increases with duration of starve

To investigate how long serum withdrawal takes to initiate A3A induction, cells were incubated in starvation media for a range of times between 6 hr and 60 hr. In addition, to determine how quickly A3A is induced upon re-stimulation, samples were collected between 1 hr and 6 hr post-stimulation. Furthermore, to validate whether A3A is normally induced in cultured cells upon each media change, samples were collected between 1 hr and 6 hr post-media change in asynchronously growing cells. Shown in Figure 4-16 (A), A3A is rapidly induced: within 1 hr of re-stimulation, the expression of A3A increases ~6-fold, from 0.94 ± 0.23 copies/copy TBP to 5.51 ± 0.31. This escalates to ~90-fold by 2 hr, and peaks at ~115-fold by 3 hr. There was no induction of A3A mRNA seen following a media change in asynchronous cells.

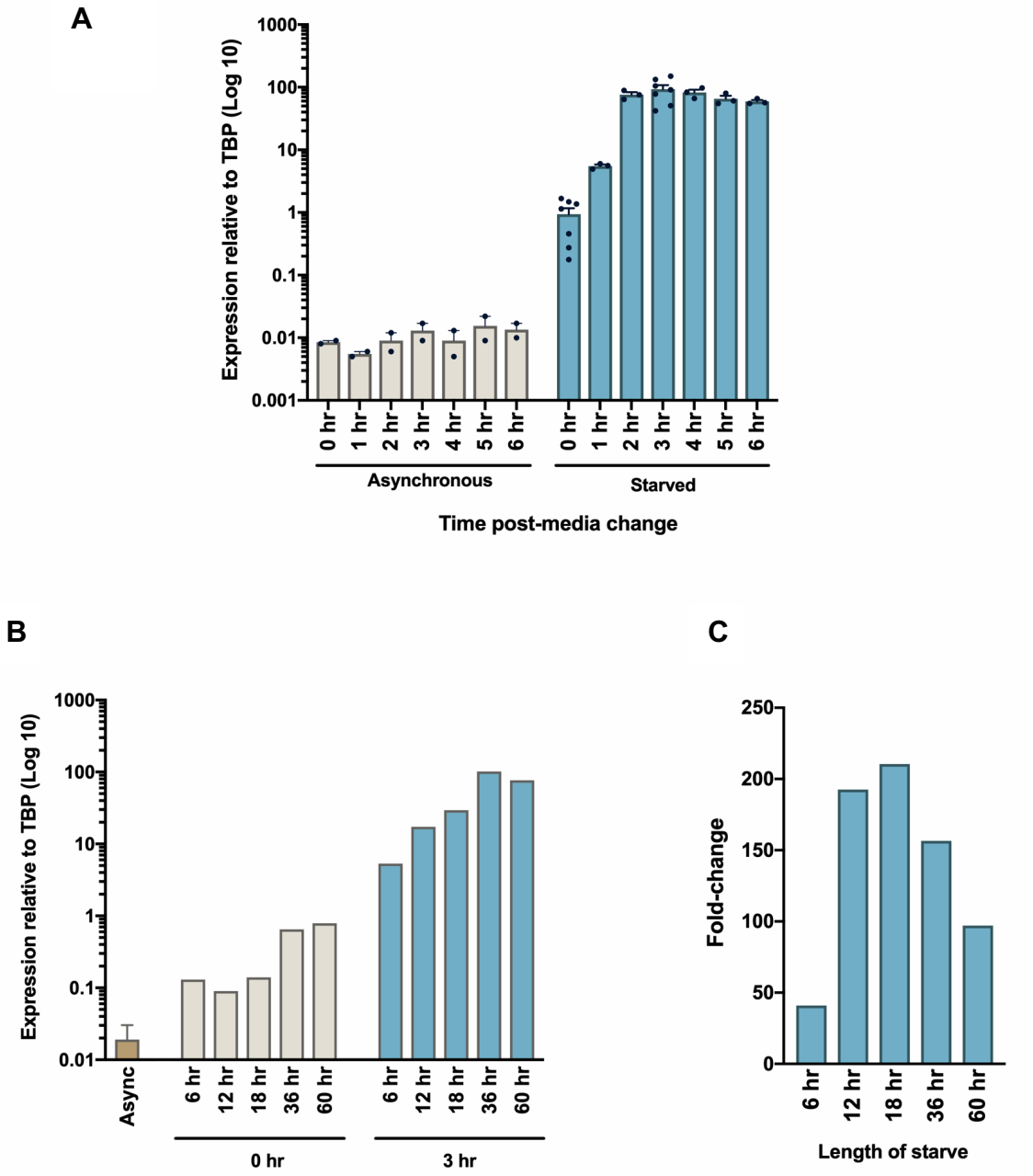

Figure 4-16 A3A is rapidly induced and increases with length of starvation.
(A) A3A is rapidly induced by media replenishment in starved, but not asynchronous (async.) cells. **(B)** A3A increases in starved cells and re-stimulation with increased duration of growth factor withdrawal. **(C)** Fold-change of induction upon restimulation remains similar between 12 hr to 36 hr starvation. WT-NIKS were serum starved for either: 40 hrs (A), or 6 – 60 hr (B-C). This was followed by re-stimulation with FC media for either: 1 to 6 hr (A), or 3 hr (B-C). Asynchronous cells were 18 hr post media change (prior to fresh media added and cells collected 1-6 hr later). A3A mRNA copy numbers are shown relative to TBP copies (n=1 for (B-C) and async. media change (0 -6 hr); n= 3-7 for async. and starved cells).

In Figure 4-16 (B), you can see that A3A mRNA is already significantly elevated at just 6 hr post-incubation in starvation media, though incrementally increases with the duration of incubation up to 36 hr. After which point it starts to decline (seen also in the fold-change in Figure 4-16 (C)), likely due to the substantial cell death that was evident from visual inspection of the cells after such prolonged starvation periods. Interestingly, despite the increase in induction between the 12 hr and 36 hr starvation period, the relative fold-change between starved and re-stimulated remains similar.

4.4.9 PMA/IFN-α augments A3A in quiescent and re-stimulated NIKS

A3A was the most abundantly expressed APOBEC3 in NIKS by PMA and IFN-α treatment of an asynchronous population (with a mean mRNA expression level of 10.98 ± 2.85 copies/copy TBP). We were additionally interested in how starved cells would respond to PMA/IFN-α treatment and whether co-stimulation with these inducers (in addition to serum/media stimulation) would mediate an even greater response than when added to asynchronous cells.

Firstly, WT-NIKS were serum starved (for 40 hr), after which they were treated with the same combinations of inducers as described previously. When PMA was added directly to the existing starvation media for 3 hr, this alone induced A3A ~40-fold (from a mean expression of 1.18 ± 0.25 copies/copy TBP in starved cells (n=9), to 49.9 ± 4.63 (n=3)), which was attenuated through PKC inhibition (shown in Figure 4-17(A)). IFN-α alone led to a ~2-fold induction.

Though PMA and IFN-α added together induced A3A ~50-fold (62.4 ± 8.0) and as expected this induction was greatly amplified through re-stimulation with full media and co-treatment with PMA or IFN-α (Figure 4-17 (B)). PMA treatment alone induced A3A ~130-fold as compared to starved cells (152.28 ± 15.78), which was ~2-fold greater than media only (DMSO: 72.31 ± 12.15). PMA treatment together with PKC inhibition reduced A3A to less than DMSO levels, suggesting that the PKC pathway may have some role in the induction through media/serum re-stimulation.

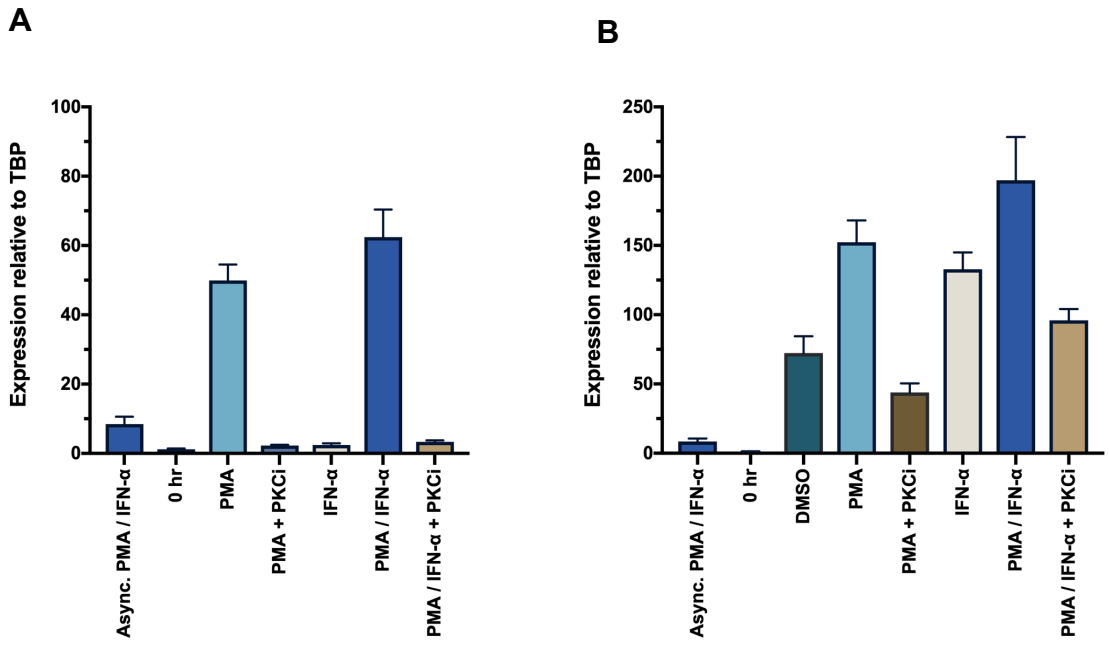

Figure 4-17 A3A is robustly induced by PMA and IFN-α in quiescent cells.
(A) PMA and IFN-α induction in starved, un-stimulated NIKS **(B)** PMA and IFN-α induction through co-stimulation with full media. WT-NIKS were serum starved for 40 hr, at which point (0 hr), either 100 ng/ml of PMA, 1000 IU/ml of IFN-α, or PMA and IFN-α together or following pre-treatment with 100 nM of PKC inhibitor (Gö6983) was added directly to the starvation media for 3 hr (A); or included in FC media (B) for 3 hr. A3A mRNA copy numbers are shown relative to TBP copies (n=3). Induction from asynchronous (async.) cells treated with PMA and IFN-α induction are shown for comparison (n=5).

IFN-α caused a 1.8-fold upregulation in addition to that seen through the addition of FC media, very similar to its effect in isolation (Figure 4-17 (A) and (B)). Co-treatment of PMA and IFN-α induced A3A ~170-fold (197.0 ± 31.31) compared to starved cells, and 2.7-fold greater than media only: resulting in ~18-fold more A3A than through PMA and IFN-α induction in an asynchronous population. The clear additive effects of PMA, IFN-α and serum/growth factor addition to starved cells strongly suggests that they all act via independent, parallel pathways to induce A3A expression.

4.4.10 A3A induction in starved cells is p38 MAPK dependent

The p38 mitogen activated protein kinase (MAPK) signalling pathway leads to phosphorylation of transcriptional regulators in response to a variety of stresses, and activation of p38 through serum deprivation can lead to either cell cycle arrest or apoptosis. Conversely, mitogen activation of p38 via GTPases is required for cell cycle re-entry of quiescent cells through the activation of cyclin D1 and phosphorylation of pRb (Faust *et al*., 2012). It is additionally involved in the wound healing response in epithelial cells (Harper, Alvares and Carter, 2005).

We have found that A3A is ~50-fold higher in starved cells than in asynchronous, proliferating cells, therefore we next sought to identify signalling pathways that may mediate this induction.

WT-NIKS were incubated in starvation media for 40 hr containing kinase inhibitors (their primary kinase targets are stated in parentheses: 20 μM SB203580 (p38α/β MAPK), 500 nM afatinib (EGFR), 10 μM pictilisib (PI3K), 500 nM Gö6983 (PKC), 2 μM trametinib (MEK), or 10 μM ravoxertinib (ERK). Inhibitors were initially used at higher concentrations than their biochemical potency and were chosen from published literature in which complete inhibition of their target was shown in epithelial cells (Solca *et al.*, 2012; Leonard *et al.*, 2015; Lulli, Carbone and Pastore, 2017; Meng *et al.*, 2018; Mi *et al.*, 2018; Salvadori *et al.*, 2021). However, target inhibition requires verification in NIKS through western blot analysis, and repeating to establish the minimum dose required to exert their inhibitory effect.

SB203580 selectively inhibits the p38 MAPK α and β isoforms with no effect on p38δ or p38γ due to differences in the ATP binding pocket, and shown in Figure 4-18 (A-B), 20 μM of SB203580 largely abrogated A3A induction in starved cells. This was repeated with a dose range (2 μM - 20 μM), which showed incremental decreases in A3A with increasing concentrations of inhibitor (Figure 4-18 (C)).

Interestingly, despite EGF not being included in the starvation media, 500 nM of Afatinib also decreased A3A induction by ~60%, though there was also a visible increase in cell death through both EGFR and PI3K inhibition over the incubation period, thus it is impossible to say whether the effect on A3A induction seen with these inhibitors is specific or is a non-specific effect due to toxicity of the inhibitors in starved cells.

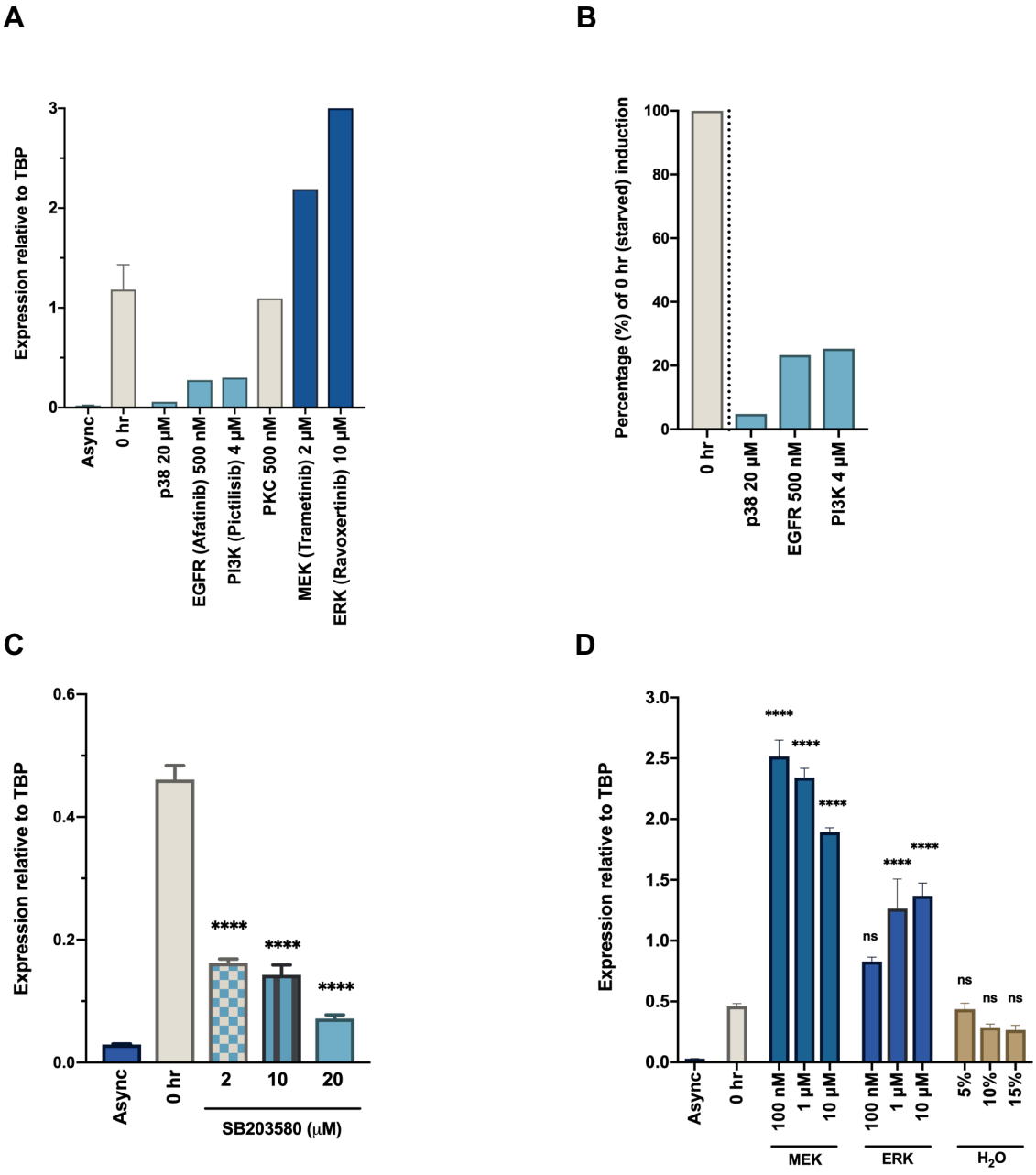

Figure 4-18 Induction in starved cells in attenuated by p38 MAPK inhibition.
(A) Asynchronous (async.) and starved (0 hr) cells (n=7) compared to cells starved with the following inhibitors (n=1): 20 µM SB203580 (p38 MAPK); 500 nM afatinib (EGFR), 10 µM pictilisib (PI3K), 500 nM Gö6983 (PKC), 2 µM trametinib (MEK), 10 µM ravoxertinib (ERK). **(B)** Percentage of inhibition (from (A)): p38 (~95%), EGFR (~77%), and PI3K (~75%). **(C)** A3A inhibition using dose range of p38 inhibitor, SB203580 (n=3, one-way ANOVA compared to 0 hr $p<0.0001$)). **(D)** MEK (trametinib) and ERK (ravoxertinib) inhibition increases A3A mRNA in staved cells (n=3, one-way ANOVA compared to 0 hr $p<0.0001$ (except 100 nM ravoxertinib). A3A copy numbers are shown relative to TBP copies. Error bar representing SEM.

Furthermore, 500 nM of Gö6983 (PKC) abrogates PMA induction of A3A in asynchronous cells (and somewhat the re-stimulation (Figure 4-17 (B)), but has no inhibitory effect on the A3A increase in starved cells. Interestingly, 2 μM of trametinib (MEK) and 10 μM of ravoxertinib (ERK) inhibitors increased A3A in starved cells (to 2.19 and 3.0 respectively (n=1)), as did dose ranges (100 nM, 1 μM, 10 μM) of MEK and ERK inhibitors (Figure 4-18 (D)).

4.4.11 A3A is induced by Epidermal Growth Factor

As NIKS are dependent on a complex combination of growth factors for survival in culture, we next sought to establish whether particular factor(s) may be principally responsible for A3A induction upon re-stimulation. WT-NIKS were serum starved as before, then re-stimulated for 3 hr with F-12/DMEM containing either 0.3% or 5% FBS, and the addition of only one media component in each sample (at the concentration in which they are cultured).

Each sample was normalised as a percentage of the maximum (max.) A3A copy numbers that were induced using the complete FC media. Shown in Figure 4-19 (A), 0.3% FBS alone led to slight induction of A3A (~13-fold compared to starved, but only ~4% of max.), and marginally more so with the addition of either hydrocortisone or insulin. Though the greatest singular increase was through the inclusion of EGF (~50-fold / 17% of the max.).

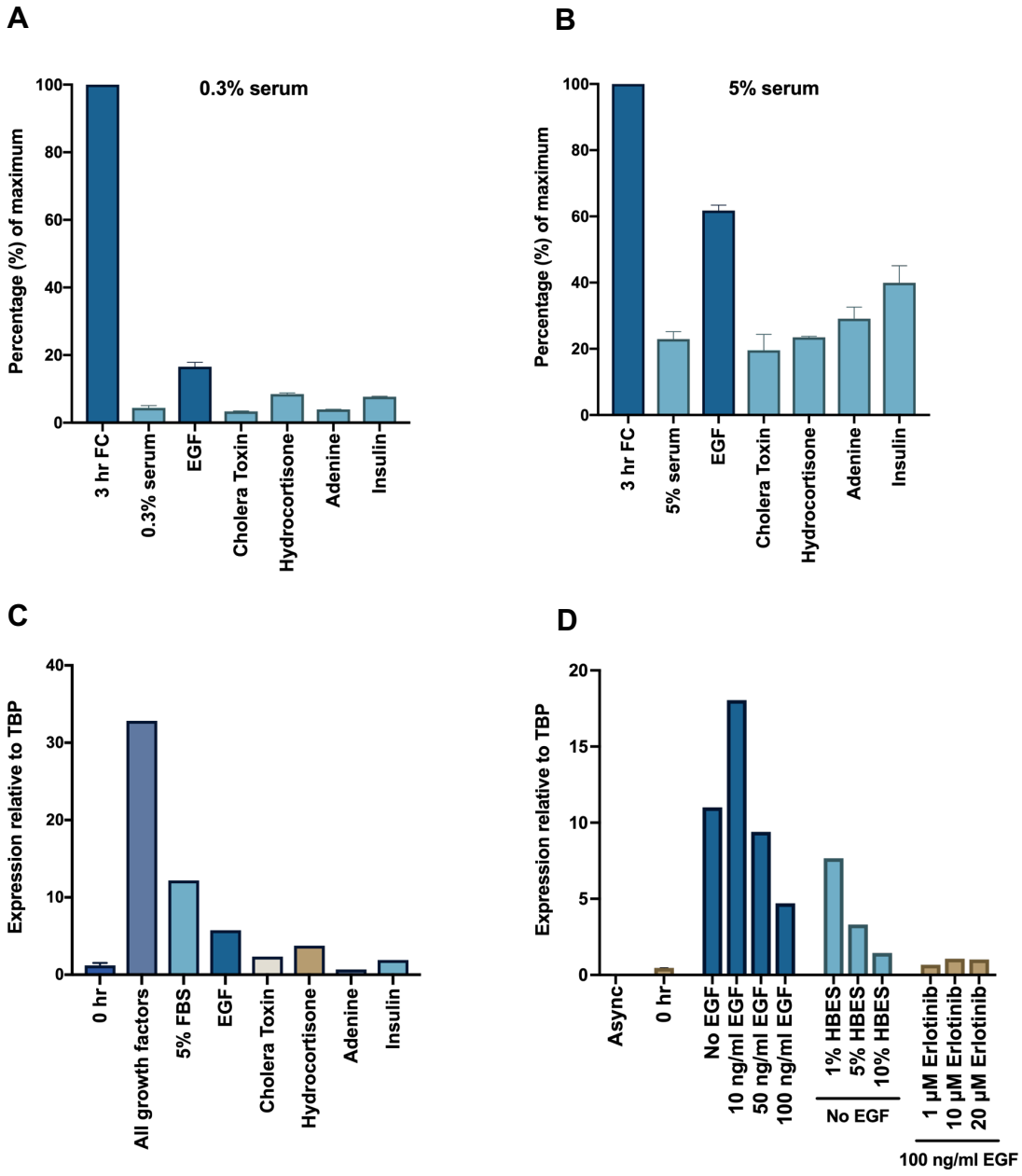

Figure 4-19 Effect of individual growth factors on A3A induction.
(A) Individual growth factors added in media containing 0.3% FBS. **(B)** Individual growth factors added in media containing 5% FBS. **(C)** Growth factors added directly to existing starvation media. **(D)** Re-stimulation with FC media and increasing concentrations of EGF (HBES vehicle-only control); or 100 ng/ml EGF with 1-20 μM of erlotinib. WT-NIKS were plated at a density of 2.5 x 10^5 cells per well in 6-well plates. The next day, they were serum starved for 40 hr then re-stimulated for 3 hr with either DMEM, F-12/DMEM (0.3 or 5% FBS) together with either: 10 ng/ml EGF, 8.3 ng/ml cholera toxin, 0.4 μg/ml hydrocortisone, 24 μg/ml adenine, or 5 μg/ml insulin. A3A mRNA copy numbers are shown relative to TBP copies. Induction expressed as a percentage of full induction achieved through FC media (n=1, error bars and SEM in (A-B) from 2 technical replicates).

Seen in Figure 4-19 (B), the increased concentration of serum enhanced A3A induction (~70-fold / 23% of max.), which was amplified by adenine and insulin. Once again, EGF was the single component responsible for the greatest A3A induction (~180-fold / 62% of max.). Furthermore, adding EGF directly to starved cells (in pre-existing starvation media), there was ~5-fold increase in A3A mRNA (Figure 4-19 (C)), inducing it to similar levels as found by PMA induction in asynchronous cells (though less potently than 5% serum). A3B mRNA levels were also analysed by qPCR from the same cDNA and in contrast to A3A induction, A3B was not induced by EGF or any other individual media component following serum starvation and the re-stimulation of NIKS (shown in Supplementary Figure 8-1).

.

To determine whether A3A induction increases according to EGF concentration, WT-NIKS were re-stimulated with F media containing either 0, 10, 50 or 100 ng/ml of EGF (Figure 4-19 (D)): the concentration of EGF that elicited the strongest induction was 10 ng/ml (the concentration in which they are cultured). To further corroborate whether A3A induction is via the EGF/EGFR signalling pathway, cells were re-stimulated in the presence of either 1, 10, or 20 μM of an EGFR inhibitor, erlotinib, each of which largely abrogated A3A induction.

EGF stock solutions are prepared in Hepes-buffered Earles' Salts (HBES) containing 10% EBSS, 260 mM $NaHCO_3$ and 25 mM HEPES, thus cells were treated with equal volumes of HBES as a vehicle-only control for each concentration of EGF. Interestingly, there is also some inhibitory effect on A3A induction (as compared to no EGF) with increasing concentrations of HBES.

We additionally tested a panel of inhibitors to see if alternative signalling pathways may contribute to A3A induction upon re-stimulation (Figure 4-20). A3A inhibition was normalised as a percentage of 3 hr induction through FC media and as expected, there was a potent increase in A3A expression which was reduced by ~44% in the presence of PKC inhibitor.

Notably, the EGFR inhibitor afatinib almost totally abrogated A3A induction by FC media, supporting our earlier observations suggesting a key role for EGF/EGFR signalling. The suppression of A3A induction by MEK inhibition and to a lesser extent, by ERK inhibition implicates the RAS/RAF MAPK pathway in mediating transcriptional activation of A3A downstream of EGFR but this requires further investigation.

The p38 kinase has been identified as a determining factor in whether EGF stimulation promotes migration or proliferation in epithelial cells: p38 inhibition blocks migration but promotes EGF-stimulated proliferation via the Src family tyrosine kinase signalling pathway (Frey, Golovin and Brent Polk, 2004). The p38 inhibitor, SB203580, inhibited A3A induction upon re-stimulation by ~79%.

Interestingly, although 500 nM of Src inhibitor SU-6656 led to a ~60% decrease in A3A induction (not shown), 5 μM led to an almost 2-fold increase. We additionally verified that the PI3K/AKT/mTOR cascade was not responsible for A3A induction: although there was some suppression with pictilisib (PI3K inhibitor), there was no inhibition using MK2206 (AKT inhibitor). Whereas mTORC1 inhibition (everolimus) led to slightly greater A3A induction.

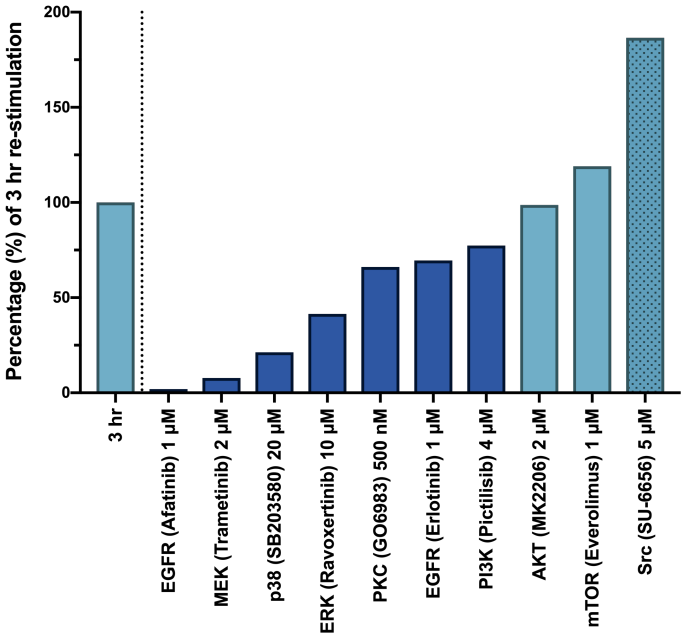

Figure 4-20 A3A induction is inhibited by afatinib.
WT-NIKSs were synchronised in G0/G1 by serum starvation, then pre-incubated with inhibitor before re-stimulated with FC media (and inhibitor) for 3 hr. A3A induction was suppressed as follows: EGFR (1 μM Afatininb: 98.2%); MEK (2 μM Trametinib: 92.2%); p38 (20 μM SB203580: 78.7%); ERK (10 μM Ravoxertinib: 58.5%); PKC (500 nM Gö6983: 33.9%); EGFR (1 μM Erlotinib: 30.5%); PI3K (4 μM Pictilisib: 22.5%); and AKT (2 μM MK2206: 1.2%). A3A induction increase through: mTOR (1 μM Everolimus: 119.3%); and Src (5 μM SU-6656: 186.5%) A3A mRNA copies were calculated relative to TBP copies and inhibition shown as a percentage of the maximum at 3 hr by FC media (n=1).

4.4.12 Starvation induces chromatin remodelling and RNA pol II recruitment to the A3A promoter

Differential gene expression is regulated through DNA-protein interactions and histone modifications. Tri-methylation of lysine 3 of histone 3 (H3K4me3) promotes the binding of positive transcription factors at promoter regions and rapid activation of genes (Lauberth *et al.*, 2013); acetylation on lysine 27 of histone 3 (H3K27ac) is mediated by the p300 histone acetyltransferase (p300) transcriptional co-activator and distinguishes active enhancers (Creyghton *et al.*, 2010).

Serum starved and re-activated WT-NIKS were therefore prepared for ChIP-qPCR analysis of the histone modifications (which was performed by collaborators: Mani Periyasamy and Simak Ali, Imperial College London). A3A has three potential regulatory regions located -33, -15 and -4 kb upstream from the transcription start site.

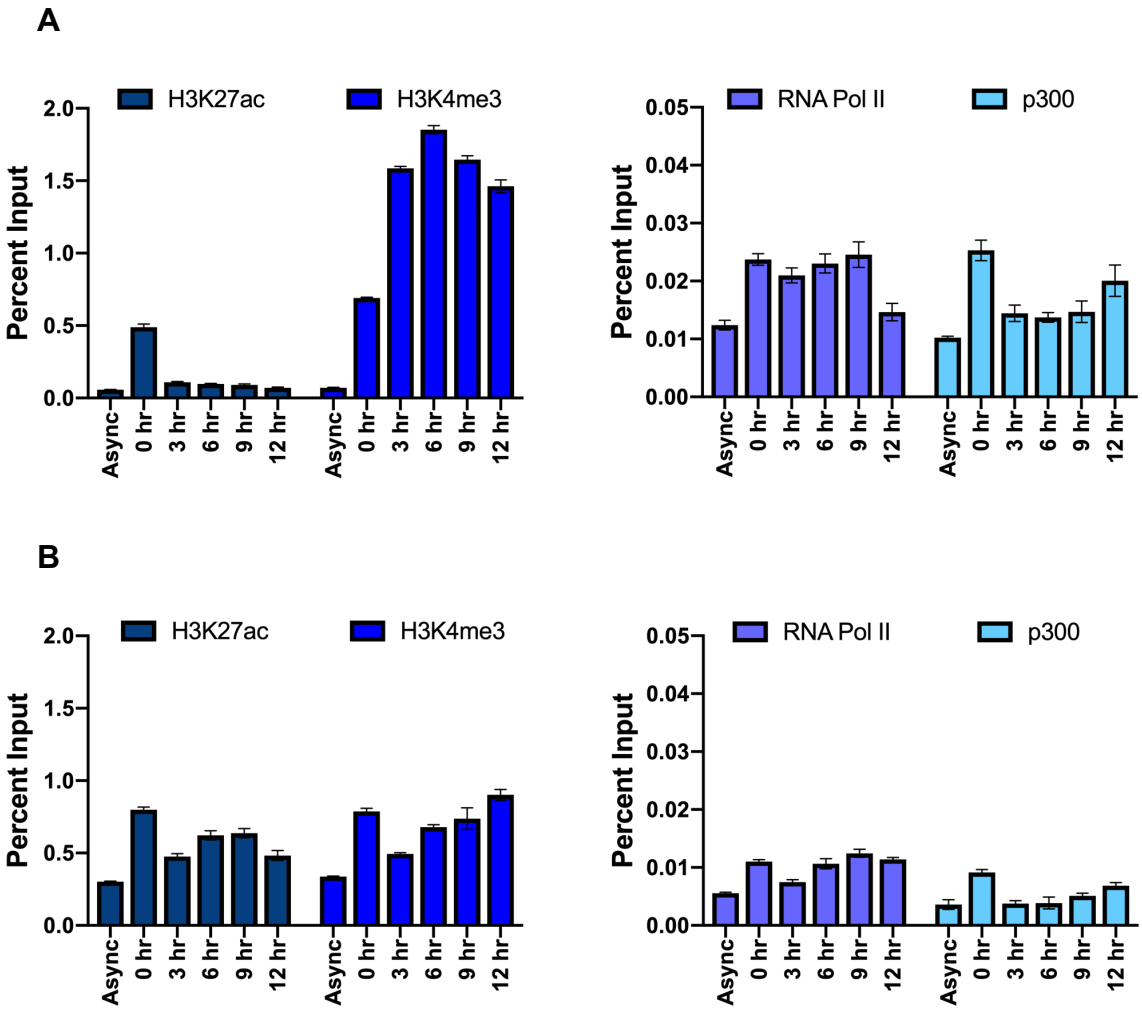

Figure 4-21 A3A transcriptional regulation during cell cycle exit and re-entry.
(A) A3A promoter **(B)** A3A predicted enhancer (-33 kb upstream). ChIP was performed for transcriptionally active chromatin marks (H3K27ac & H3K4me3) and RNA polymerase II (Pol II) and p300 using asynchronous (async), starved (0 hr) and NIKS re-stimulated with FC media over a 12 hr time course. ChIP DNA was purified, and qPCR was performed using A3A promoter or predicted enhancer specific primers. Percent input was calculated by normalising to input DNA (n=3).

Following starvation (0 hr), there was an increase in H3K4me3, H3K27ac, binding of the p300 and the RNA Polymerase II (RNA Pol II) transcription factor at both the transcription start site and the -33 kb upstream enhancer (Figure 4-21), consistent with the increased A3A expression observed in starved cells. Interestingly however, the potent induction of A3A observed following subsequent growth factor stimulation is not accompanied by further increases in these active chromatin marks at the enhancer, or by increased RNA pol II recruitment to the transcriptional start-site (TSS).

Based on these observations, we speculate that promoter-proximal pausing of RNA pol II (Li and Gilmour, 2011; Core and Adelman, 2019) in starved cells may "prime" cells for the rapid transcription of A3A upon stimuli. Upon re-stimulation, there is an increase in H3K4me3 at the transcription start site of A3A, consistent with the subsequent activation of A3A transcription.

4.4.13 A3A edits the RNA of host-protein DDOST in NIKS

Amino acid changes generated by A-to-I and C-to-U editing of mRNAs can aid proteomic adaptation to various stimuli (Yablonovitch *et al.*, 2017); synonymous edits do not change protein sequences but instead produce alternative codons that can affect mRNA stability or the speed and efficiency of ribosomal translation (Tuller *et al.*, 2010; Novoa and Ribas de Pouplana, 2012). ADAR catalyses the A-to-I deamination of a vast number of RNA transcripts, the majority of which occur in non-coding sequences (Nishikura, 2016).

Until 2015, APOBEC1 was the only known C-to-U RNA editing enzyme, a process that takes place predominantly in the nucleus and in contrast to A-to-I editing occurs largely in coding exons (Lau *et al.*, 1991; Yang, Sowden and Smith, 2000). A3A was subsequently also found to edit a large number of transcripts in macrophages during M1 polarisation, as well as widespread editing in monocyte-enriched PBMCs both independent of and upregulated by hypoxia and IFN treatment (Sharma *et al.*, 2015).

Overexpression of A3G showed that it is also capable of C-to-U editing of RNA transcripts, and though these were mostly distinct from those edited by A3A, both were found to edit RNA that encode proteins which may impact viral pathogenesis (Sharma *et al.*, 2016). A3A editing most commonly occurs within a CCAUCG sequence motif and has a preference for stem-loop structures consisting of 4-nucleotides (Sharma *et al.*, 2015; Jalili *et al.*, 2020).

Analysis of RNA editing in A3A positive tumours identified C-to-U editing in stem loops that correlated with A3A mRNA levels: the highest frequency of editing was within dolichyl-diphosphooligosaccharide-protein glycosyltransferase (DDOST), a component of the glycosylation machinery in the endoplasmic reticulum (~8% edited). Through use of an $A3A^{E27A}$ mutant this was found to be dependent on the catalytic domain (Jalili *et al.*, 2020).

We were therefore interested in whether endogenous A3A activity following re-stimulation from quiescence in NIKS also led to C-to-U editing of the DDOST transcript.

The RNA editing assay developed by Buisson and colleagues for this study (Jalili *et al.*, 2020) uses fluorescent TaqMan probes and droplet digital PCR (ddPCR) to determine the ratio of edited (U) vs non-edited (C) RNA at position 558 of DDOST. RNA extracted from three biological repeats of WT-NIKS and A3A KO cells (as used for qPCR analysis in Figure 4-5) was sent for conversion to cDNA and ddPCR analysis (by Pegah Jalili and Remi Buisson, at The University of California Irvine).

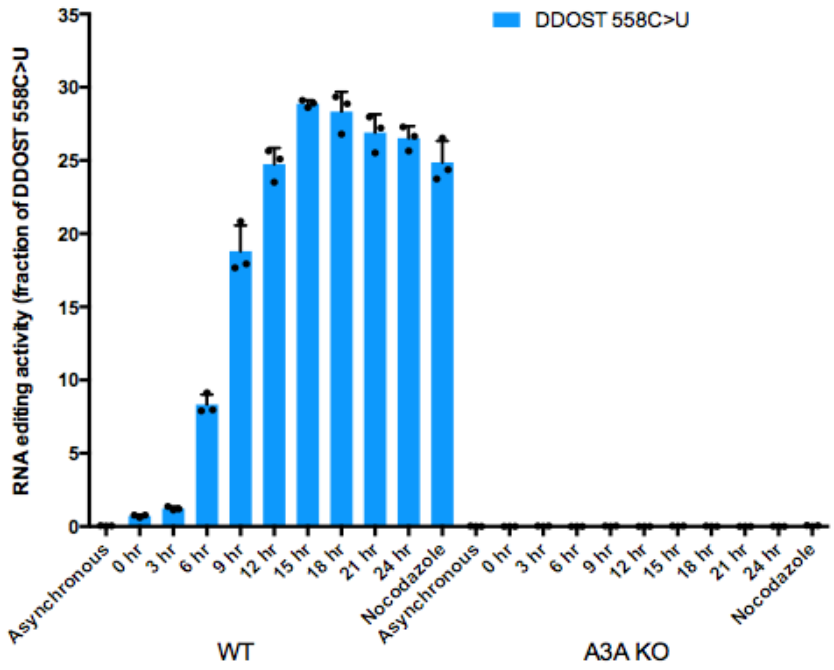

Figure 4-22 A3A induction leads to C-to-U editing of DDOST transcripts.
A3A induction in WT-NIKS leads to up to 30% of 558C>U edited DDOST RNA. WT and A3A KO NIKS were serum starved for 40 hrs, then re-stimulated with FC media. Asynchronous cells were 18 hr post-media change. 100 ng/ml of nocodazole (NZ) was added at 8 hr post-release for a further 6 hrs to arrest cells in G2/M. RNA was extracted from 3 biological repeats and reverse transcribed for ddPCR analysis at University of California Irvine. Droplets were generated using a QX200 Droplet Generator (Bio-Rad) and analysed with a QX200 Droplet Reader (Bio-Rad) for fluorescent measurement of fluorescein amidite and hexachloro-fluorescein probes (n=3).

Robust C-to-U editing of DDOST at position 558 (generating a synonymous change) was found in the WT but not A3A KO NIKS (Figure 4-22), showing that this activity was specific to A3A. DDOST editing was not found in asynchronous cells but was evident at low levels in starved cells (0 hr) and at 3 hr post-release. The incremental increase over subsequent time-points correlates to that of A3A protein expression (Figure 4-5), and the maximum level of RNA editing at 15 hr post-release (~30%) far exceeds that previously found in A3A positive tumour samples (~8%).

4.5 A3A induction in normal epithelial and cancer cell lines

4.5.1 A3A is induced in primary keratinocytes

We have found that A3A is upregulated during G0/quiescence, and is highly expressed following the re-stimulation of near-normal spontaneously immortalised keratinocyte (NIKS) cells. To validate whether this is also an occurrence in normal keratinocytes of the epithelium and therefore whether it could be of physiological relevance, we next tested A3A induction in primary keratinocytes.

Early passage (p2) normal human epidermal keratinocyte (NHEK) cells arising from pooled adult donors were cultured under the same conditions as NIKS: with 3T3 feeder cells and FC media. For quiescence induction, cells were incubated for 1 to 3 days in either: DMEM containing 0.3% FBS, or NIKS starvation media (F12:DMEM, 0.3% FBS, 0.4 μg/ml hydrocortisone, 8.3 ng/ml cholera toxin).

For re-stimulation, starvation media was replaced with FC media and cells were collected after 3 hr for RNA extraction and qPCR analysis; asynchronous cells were collected 18 hr post-media change. Basal levels of A3A were much higher than previously seen in NIKS under the same conditions: 3.259 copies/copy TBP (as compared to 0.01 copies/copy TBP in NIKS). This decreased through serum starvation with DMEM (0 hr), but increased using NIKS starve media: 4.469, 4.654, and 6.108 on days 1, 2 and 3 respectively (Figure 4-23).

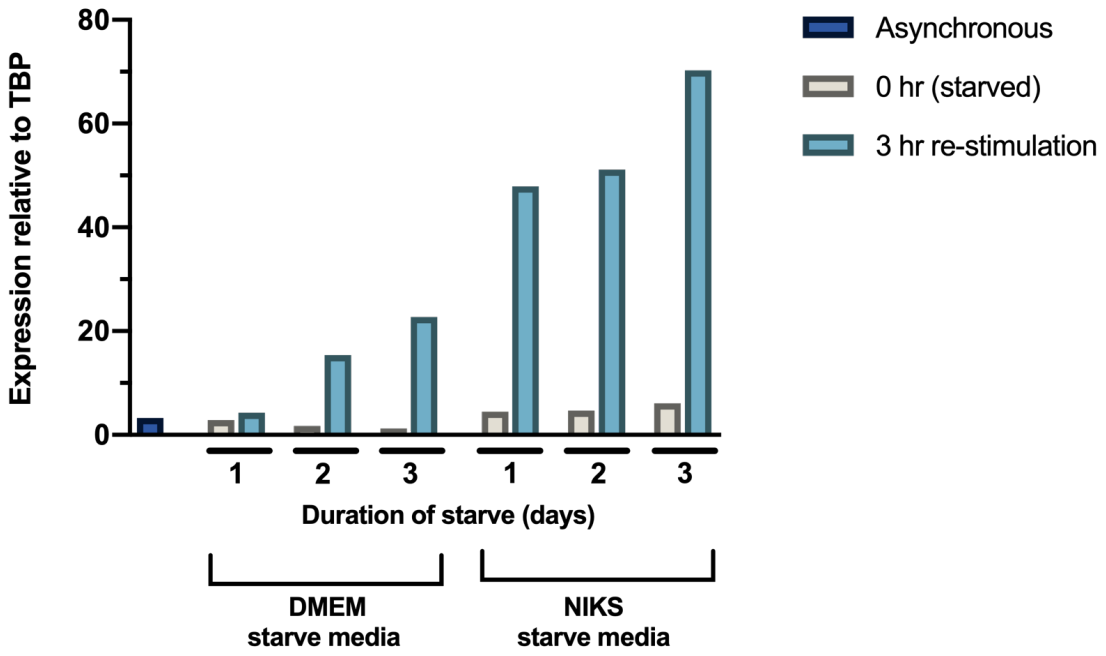

Figure 4-23 A3A is robustly induced through re-stimulation of primary keratinocytes.
Normal human epidermal keratinocytes (NHEK) cells were cultured in FC media together with 3T3-feeder cells. These were plated at a density of 2 x 10^6 per well in 6-well plates and the next day, media was removed, cells washed twice with PBS then incubated in starvation media for 1-3 days. Either: DMEM with 0.3% FBS; or F12:DMEM containing 0.3% FBS, 0.4 μg/ml hydrocortisone, and 8.3 ng/ml cholera toxin. Cells were re-stimulated for 3 hr with FC media and collected for RNA extraction. A3A copy numbers were calculated relative to TBP copies (n=1).

Following 3 hr re-stimulation of cells starved in DMEM, there was a 1.3-fold, 4.7-fold, and 7-fold induction of A3A (days 1-3) compared to asynchronous cells. However, this induction was far greater in NHEK cells starved in NIKS starve media: 14.7-fold, 15.7-fold, and 21.6-fold on days 1-3 respectively. The maximum copy number/copy TBP achieved upon starvation in NIKS starve media (70.273), was comparable to the induction shown previously in NIKS.

We additionally cultured NHEK cells in a serum-free, feeder-free system (in which they are supplied): in keratinocyte growth media containing 0.4% bovine pituitary extract, 0.125 ng/ml human EGF, 5 μg/ml insulin, 0.33 μg/ml hydrocortisone, 0.39 μg/ml epinephrine, 10 μg/ml transferrin and 0.06 mM $CaCl_2$. For quiescence induction, they were incubated for either 18 hr, 24 hr or 48 hr in three alternative starvation media: DMEM containing 0.3% FBS; NIKS starvation media (as above); or keratinocyte growth media containing 0.3% FBS, 0.33 μg/ml hydrocortisone and 0.39 μg/ml epinephrine. For re-stimulation, starvation media was replaced with their keratinocyte growth media containing either 0.125 ng/ml or 10 ng/ml of EGF.

As seen in Figure 4-24 (A-C), A3A mRNA was increased in both starved and re-stimulated NHEK cells compared to asynchronous levels. However, this induction was far less (~650-fold) than when cultured under the same conditions as NIKS. Basal A3A (asynchronous) levels were 0.019 copies/copy TBP (similar to NIKS); this increased ~4-fold in cells starved for 18/24 hr in DMEM (0 hr), and ~5.6-fold in starved and re-stimulated with 0.125 ng/ml EGF (3 hr), decreasing upon the higher concentration of EGF. Though 10 ng/ml EGF led to a greater induction in NHEK cells starved for 48 hr in NIKS starve media and the NHEK equivalent.

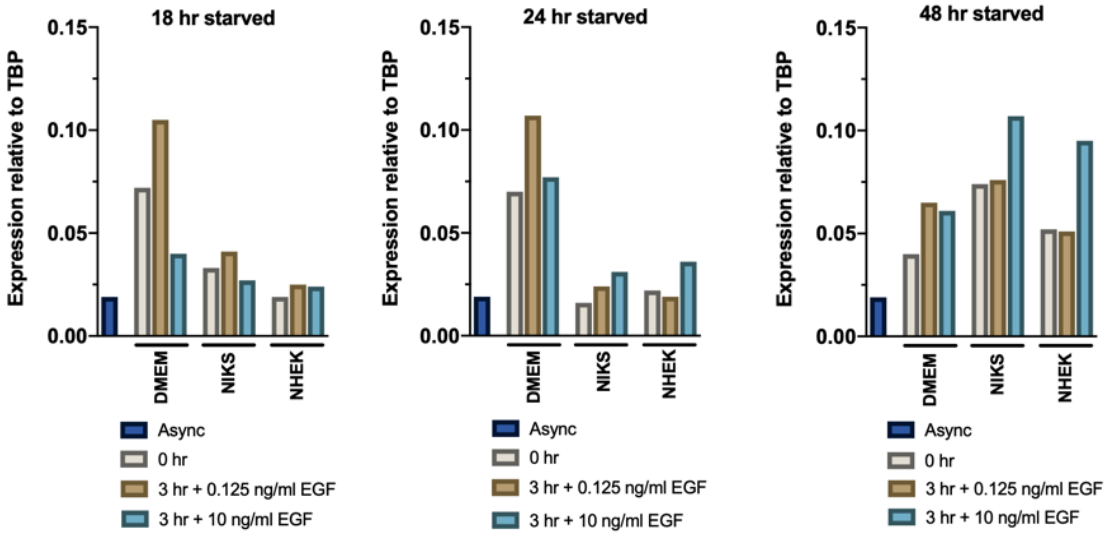

Figure 4-24 A3A induction is less in feeder-free, serum free cultured primary keratinocytes. Normal human epidermal keratinocytes (NHEK) cells were cultured serum-free, feeder-free in keratinocyte growth media (containing 0.4% bovine pituitary extract, 0.125 ng/ml human EGF, 5 μg/ml insulin, 0.33 μg/ml hydrocortisone, 0.39 μg/ml epinephrine, 10 μg/ml transferrin, and 0.06 mM $CaCl_2$). These were plated at a density of 2 x 10^6 per well in 6-well plates and the next day, media was removed, cells washed twice with PBS then incubated in the following starvation media for 18, 24, or 48 hr; either: DMEM with 0.3% FBS (DMEM); F12:DMEM containing 0.3% FBS, 0.4 μg/ml hydrocortisone, and 8.3 ng/ml cholera toxin (NIKS); or F12:DMEM containing 0.3% FBS, 0.33 μg/ml hydrocortisone and 0.39 μg/ml epinephrine (NHEK). Cells were re-stimulated for 3 hr with keratinocyte media containing either 0.125 ng/ml or 10 ng/ml of EGF and collected for RNA extraction. A3A copy numbers were calculated relative to TBP copies (n=1).

4.5.2 A3A is induced in normal breast epithelial cells (MCF-10A)

To determine whether A3A induction is analogous in other epithelial tissues, we employed a similar protocol in normal breast epithelial cells. These are cultured in MCF-10A specific growth media (F12:DMEM (1:1), supplemented with 5% horse serum, 20 ng/ml of recombinant human EGF, 100 ng/ml cholera toxin, 10 μg/ml insulin, and 0.5 μg/ml hydrocortisone).

For optimisation of quiescence induction they were incubated in starvation media for 24 hr or 48 hr, in either: DMEM containing 0.3% FBS; or F12:DMEM containing 0.3% FBS, 100 ng/ml cholera toxin, and 0.5 μg/ml hydrocortisone (similar to the NIKS starvation media yet at the concentrations of MCF-10A media). For re-stimulation, starvation media was replaced with their MCF-10A growth media containing either 0, 20, 50, or 100 ng/ml of EGF. In addition, to determine whether A3A induction in MCF-10A cells also occurred via EGF/EGFR signalling pathways, cells were pre-incubated with inhibitor before re-stimulation with media containing 100 ng/ml of EGF and 10 μM erlotinib.

As seen in Figure 4-25 (A), A3A was induced by starvation and re-stimulation using the NIKS/MCF-10A equivalent starvation media, yet much more so through re-stimulation following 48 hr incubation in DMEM. Furthermore, this was more robust using 100 ng/ml of EGF than 20 or 50 ng/ml of EGF. Shown on a Log 10 scale in Figure 4-25 (B), basal A3A (asynchronous) levels were 0.005-0.007 copies/copy TBP; this increased ~4-fold after 48 hr starvation in DMEM (0 hr) to 0.029, and a further ~230-fold increase between starved cells and those re-stimulated for 3 hr with 100 ng/ml EGF (6.809 copies/copy TBP).

Re-stimulation of MCF-10A cells with media without EGF (starved in DMEM for 48 hr) led to ~90-fold increase compared to starved levels (2.582 copies/copy TBP, Figure 4-25 (C)), though this was ~190-fold, ~140-fold, and ~230-fold through the addition of 20, 50, and 100 ng/ml EGF respectively. The EGFR inhibitor, erlotinib, reduced this to 1.265 copies/copy TBP (to less than re-stimulation without EGF).

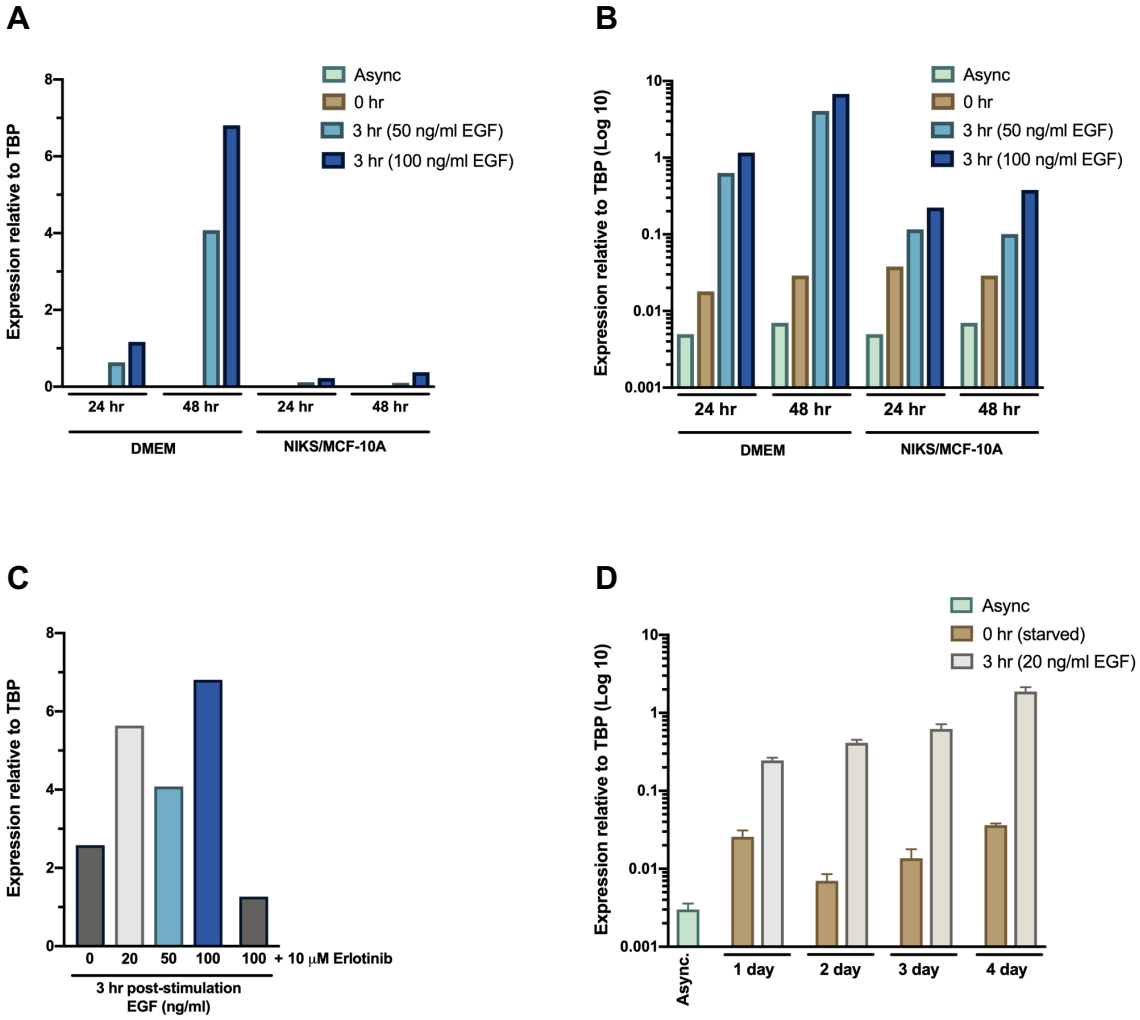

Figure 4-25 A3A is induced in normal breast epithelial cells in an EGF-dependent manner.
(A-B) MCF-10A cells starved for 24-48 hr in DMEM or NIKS equivalent starve media (NIKS/MCF-10A), and re-stimulated with 50 or 100 ng/ml EGF. (**C)** 48 hr starve in DMEM with 0.3% FBS, and 3 hr re-stimulation with 0 – 100 ng/ml EGF, or 100 ng/ml EGF together with 10 μM Erlotinib**.** **(D)** 1-4 day starve in DMEM with 0.3% FBS, and 3 hr re-stimulation with MCF-10A media (20 ng/ml EGF). MCF-10A cells were plated at a density of 2 x 10^6 per well in 6-well plates and the next day, media was removed, cells washed twice with PBS then incubated in starvation media for 1-4 day. Either: DMEM with 0.3% FBS (DMEM); or F12:DMEM containing 0.3% FBS, 0.5 μg/ml hydrocortisone, and 100 ng/ml cholera toxin (NIKS/MCF-10A). Cells were re-stimulated for 3 hr with MCF-10A media containing either 0, 20, 50, or 100 ng/ml of EGF and collected for RNA extraction. A3A copy numbers were calculated relative to TBP copies (A-C: n=1; D: n=3).

Finally, we wanted to establish whether a longer starvation period would increase A3A induction, therefore this was repeated with incremental starvation periods of 1-4 days (using DMEM containing 0.3% FBS). Seen in Figure 4-25 (D), although the absolute level upon re-stimulation was less on this occasion, there was incremental increases of A3A induction with increased starvation duration.

4.5.3 APOBEC3 induction in retinal pigment epithelial cells (RPE-1)

While nearly all cell types express multiple APOBEC3s, some immune privileged organs have very low levels (Refsland *et al.*, 2010), and A3A is not induced by IFN-γ in human retinal capillary endothelial cells, a component of the blood-retinal barrier (Lin *et al.*, 2009). Having established conditions in which A3A is induced far more robustly than ever previously reported (by PMA or type-1 IFNs), we were interested to see whether A3A could similarly be induced in retinal pigment epithelial cells (RPE-1) using this method.

RPE-1 cells are not dependent on EGF, insulin, adenine, cholera toxin or adenine supplementation for culturing, and were maintained in F12:DMEM supplemented with 10% FBS (RPE-1 media). These were then incubated in a starvation media for 40 hr (F12:DMEM containing 0.3% FBS) to induce quiescence, then re-stimulated with RPE-1 media for 3 hr. Samples were collected for RNA extraction and qPCR analysis of all seven APOBEC3 family transcripts, and though further optimisation may be necessary with duration and alternative starvation media (additionally +/- EGF upon re-stimulation), A3A (and A3D) were both undetectable at basal levels and following starvation or re-stimulation.

Basal levels of A3B expression, as well starved (0 hr) and 3 hr re-stimulated were similar to that seen previously in NIKS (Figure 4-14). Basal levels of A3C (0.868 copies/copy TBP) were a lot lower than NIKS (4.60), as were A3F (0.06 compared to 0.310), A3G (0.0003 compared to 0.032), and A3H (0.006 compared to 0.041).

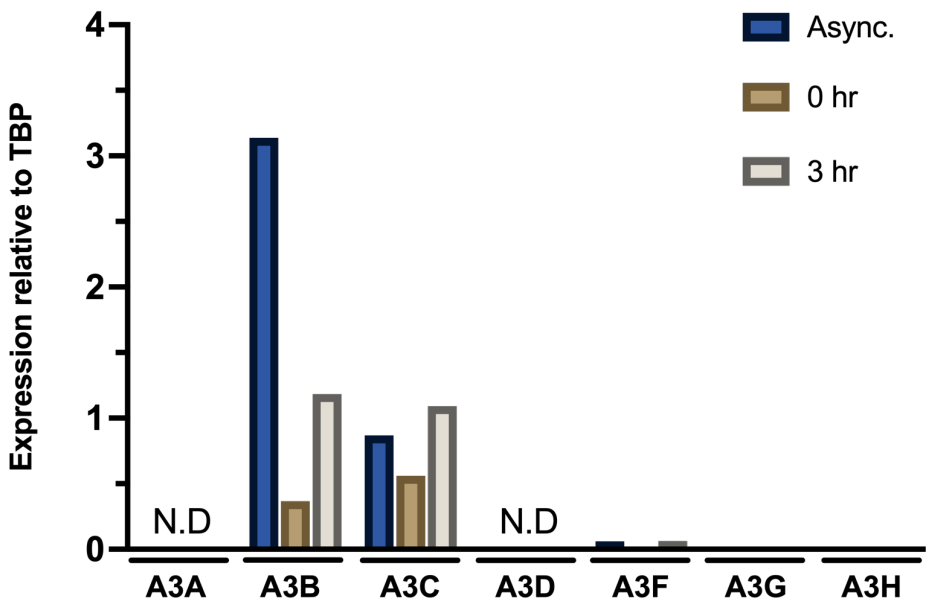

Figure 4-26 APOBEC3 expression in retinal epithelial cells.
RPE-1 cells were plated at a density of 2 x 10^6 per well in 6-well plates and the next day, media was removed, cells washed twice with PBS then incubated in starvation media (F12:DMEM containing 0.3% FBS) for 40 hr. Starved cells (0 hr) and those re-stimulated for 3 hr with RPE-1 media (F12:DMEM containing 10% FBS) were collected for RNA extraction. Asynchronous (async.) cells were 17 hr post media-change. A3A-A3H copy numbers were calculated relative to TBP copies (n=1).

4.5.4 A3A is not induced in HPV positive cervical cancer cell lines

Whilst HPV-positive cervical tissues show elevated expression of A3A and A3B during early stages of cancer progression, their mRNA expression is low in established cervical cancers and we have shown that NIKS expressing HPV16 oncoproteins or the whole HPV16 genome have reduced A3A expression upon starvation and re-stimulation (Figure 4-12). SiHa and HeLa cells are derived from cancerous tissues of the cervix and have integrated copies of HPV-16 and -18 respectively. Similar to RPE-1 cells, they are not dependent on complex exogenous growth factors (EGF, insulin, hydrocortisone, cholera toxin, adenine) and are maintained in DMEM media with 10% FBS.

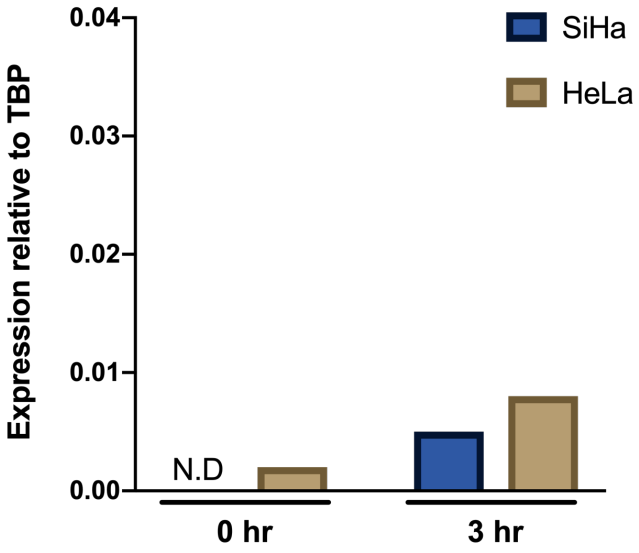

Figure 4-27 A3A is not induced by serum starvation/stimulation in HPV positive cervical cancer cells.
HPV-16$^+$ SiHa and HPV-18$^+$ HeLa cells were plated at a density of 5 x 10^4 per well in 12-well plates. The next day, media was removed, cells washed twice with PBS then incubated in starvation media (DMEM containing 0.3% FBS) for 40 hr. Starved cells (0 hr) and those re-stimulated for 3 hr with DMEM containing 10% FBS were collected for RNA extraction. A3A copy numbers were calculated relative to TBP copies (n=1).

To induce quiescence, SiHa and HeLa cells were incubated in DMEM containing 0.3% FBS for 40 hr, following which they were re-stimulated with DMEM containing 10% FBS and collected at 3 hr post-release for RNA extraction and qPCR analysis of A3A mRNA levels. Shown in Figure 4-27, A3A was not detected in starved SiHa cells (0 hr) and was barely detectable in HeLa cells (0.002 copies/copy TBP). Upon re-stimulation, A3A was detected in SiHa cells (albeit very low at 0.005 copies/copy TBP), and 0.008 in HeLa cells. Further optimisation with duration / alternative starvation media / EGF induction may be of interest.

4.5.5 EGF-dependent A3A induction in urinary bladder carcinoma cells

We were next interested to see whether A3A could be induced in HPV-negative cancer cell lines; APOBEC3 signature mutations are high in bladder cancers (Alexandrov *et al.*, 2013), therefore we chose urinary bladder carcinoma cells (BFTC-905) for this purpose. Furthermore, BFTC-905 are cultured in IMDM supplemented with 5% FBS, allowing a comparison against the non-complex growth factor dependent cell lines (EGF and other NIKS growth supplements).

BFTC-905 cells were serum starved in IMDM containing 0.3% FBS for 48 hr, then re-stimulated with IMDM containing 5% FBS together with either 0 or 10 ng/ml of EGF. In addition, cells were pre-incubated with inhibitor before re-stimulation with media containing 10 ng/ml of EGF and 10 μM erlotinib. To investigate whether 3T3 feeder cells influence A3A induction in BFTC-905 cells, they were starved and re-stimulated either on their own, or with 3T3 feeders at the same density as co-cultured with NIKS.

Finally, asynchronously growing cells were collected 18 hr post media change, or treated with PMA and IFN-α for 6 and 24 hr (24 hr post-media change) with DMSO used at equal volumes as a vehicle-only control for PMA. There was an ~11-fold increase in A3A in starved (0 hr) BFTC-905 cells (0.102 copies/copy TBP) as compared to asynchronous cells (0.009) (Figure 4-28 (A)). Re-stimulation with IMDM and 5% FBS (no EGF) for 3 hr increased this a further ~5-fold compared to starved cells.

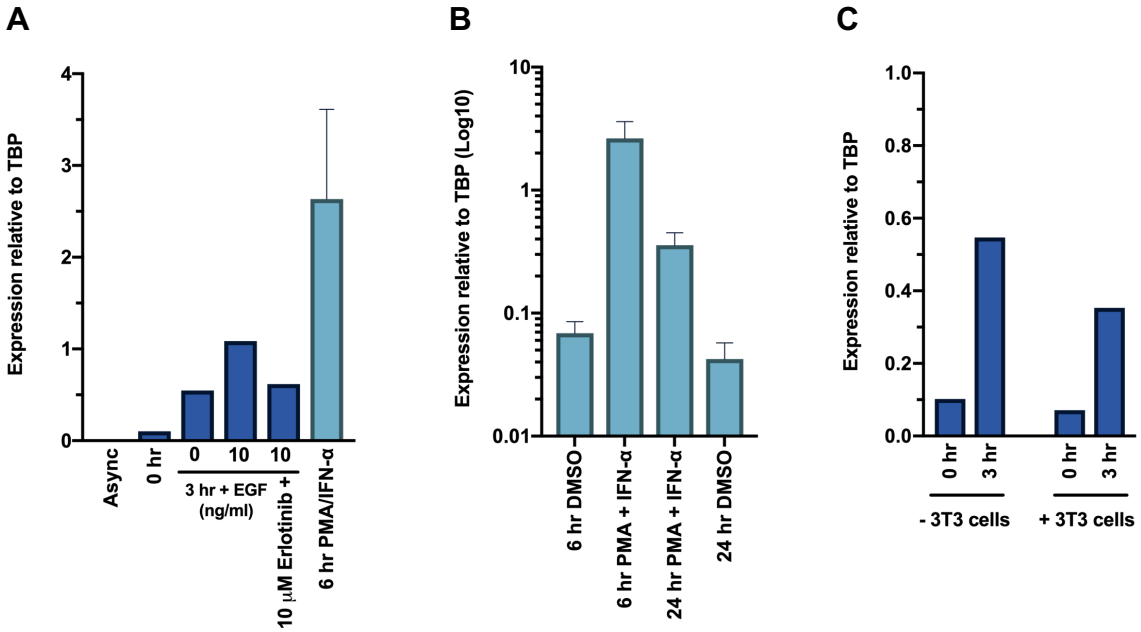

Figure 4-28 A3A is EGF inducible in bladder carcinoma cells.
(A) BFTC-905 cells starved for 48 hr in IMDM containing 0.3% FBS (0 hr) and re-stimulated for 3 hr with 5% serum +/- 10 ng/ml EGF, +/- 10 μM Erlotinib (n=1). PMA/IFN-α treated cells from (B) shown as a comparison (n=3). (**B)** Asynchronously growing cells were treated with 100 ng/ml of PMA and 1000 IU/ml IFN-α for 6 and 24 hr (DMSO control) (n=3)**. (C)** BFTC-905 cells were cultured individually, or co-cultured with 3T3-feeder cells. These were starved for 48 hr in IMDM containing 0.3% FBS (0 hr) and re-stimulated with IMDM containing 5% serum for 3 hr. RNA was extracted for qPCR analysis and A3A copy numbers are shown relative to TBP copies.

Despite a lack of EGF-dependency for culturing, A3A induction was 2-fold greater with the addition of 10 ng/ml of EGF; an increase that could be abrogated by 10 μM of erlotinib (Figure 4-28 (A)). However, PMA and IFN-α treatment of asynchronous populations led to a more robust induction of A3A: 2.634 ± 0.978 copies/copy TBP. And as shown in Figure 4-28 (C), there was no increase in A3A expression through co-culturing BFTC-905 cells with 3T3-feeder cells.

4.6 Discussion / Conclusions

Having established conditions in which we could induce endogenous A3A expression with PMA (± IFN-α) we observed through western blot analysis that this was restricted to sub-confluent populations, and through immunofluorescent imaging that expression was restricted to a subset of cells. This was investigated using cell synchronisation methods, in which A3A was found to increase at the protein level shortly after release from a thymidine block (G1/S), though this was small in comparison to that observed in the subsequent G1-phase (between 24 hr and 30 hr), which was greater still when the media was replenished at 24 hr post-release: a point at which we suspected a portion of cells may have exited the cell cycle. Furthermore, we found that basal levels of A3A expression, as well as those induced by PMA and IFN-α were less at 18 hr post-media change than those seen previously when cells were treated 48 hr post-media change (again, when a proportion are likely to have exited the cell cycle).

Through withdrawal of growth factors, the cells entered the resting state of quiescence which was validated by flow cytometry analysis of the DNA content.

By doing so, it was found that as little as 6 hr withdrawal from growth factors led to a ~7-fold increase in A3A transcripts, though this increased to ~50-fold after 40 hr incubation in starvation media. Preliminary ChIP-qPCR analysis revealed increased transcriptional activity at the A3A promoter and enhancer in starved cells, consistent with promoter-proximal pausing; this may be mediated through the p38 MAPK signalling pathway as inhibition of the p38α/β isoforms largely abolished the rise in A3A transcripts. Interestingly, inhibiting MEK or ERK in starved cells led to an increase in transcripts.

Treatment of starved cells with A3A inducers (PMA $\pm$ IFN-α) activated a far stronger response than seen previously in asynchronous cells (with or without re-stimulation into the cell cycle by growth factors), supporting a hypothesis that A3A induction may be “primed” during quiescence for rapid activation from multiple stimuli. Through re-stimulating quiescent cells with growth factors that activate cell-cycle re-entry, A3A was rapidly and robustly amplified a further ~100-fold from starved levels, with peak mRNA expression seen by 3 hr post-stimulation, and an increase in H3K4me3 that correlated with activation of transcription.

Using a specific A3A antibody (zero background in the A3A KO cells), endogenous A3A protein could be readily detected between 6 hr and 24 hr; A3A protein levels remain high as cells transit through S-phase (and ssDNA is a substrate for A3A-mediated deamination), yet despite this increase and in contrast to that found through exogenous A3A expression, we found no evidence that this caused an increase in DNA DSBs or abasic (AP) sites.

This suggests that A3A may either be excluded from the nucleus during S-phase or that it is normally tightly regulated in such a way that it is non-genotoxic under these conditions (as is suggested in monocytes where it is both abundantly expressed and highly inducible). We also found that in contrast to a previous report that describes A3A protein stabilisation by HPV16 E7 (Westrich *et al.*, 2018), there was less A3A detected by western blot analysis in NIKS stably transfected with E6, E7, both E6 and E7, or the whole HPV16 genome. Furthermore, A3A was not induced upon starvation/re-stimulation of HPV-16 (SiHa) and -18 (HeLa) positive cervical cancer cells, though this appeared to be due to reduced levels of A3A mRNA, as evidenced by qPCR analysis.

Importantly, given the aberrant EGF/EGFR signalling in many cancers, is that EGF was found to cause the most significant induction upon re-stimulation (of the individual FC media growth factors). Existing A3A transcripts in starved cells could be increased ~13-fold or ~70-fold through the addition of F12:DMEM containing 0.3% or 5% FBS respectively, though by including 10 ng/ml of EGF this was elevated to ~50-fold and ~180 fold respectively. This was corroborated using EGFR inhibitors, which almost completely abrogated A3A induction. Additionally, EGF activation was found to be through canonical signalling (RAS/MAPK) as opposed to via the PI3K/AKT/mTOR cascade. EGFR signalling is a potent inducer of cell migration, critical to the wound healing response in epithelial cells (Egan *et al.*, 2003). Though the function of A3A induction is yet to be elucidated, this mechanism of starvation/re-stimulation potentially simulates the re-activation of keratinocytes during a wound healing response in which the innate immune response would also be activated and thus the activation of A3A.

Contradicting this is that A3A was the only APOBEC3 family member that was robustly induced. However, we additionally found that A3A edits DDOST RNA transcript (and potentially others). DDOST is a component of the glycosylation machinery and its down-regulation has been found to inhibit the replication of flaviviruses (Petrova *et al.*, 2019). Though the RNA editing creates a synonymous mutation and the downstream effect of this needs further investigation, A3A editing may affect DDOST RNA folding or stability, or the rate/preference of translation, and thus may mediate viral inhibition indirectly.

A3A induction upon starvation/re-stimulation was not detected in retinal pigment epithelial cells *in vitro*, though this may be due to them residing within an immune privileged site *in vivo*. Yet A3A was also robustly induced in normal primary keratinocyte (NHEK) cells (when cultured in FC media with 3T3 feeder cells, but not in a feeder-free, serum-free system, that has very low EGF supplementation (and no cholera toxin)). Therefore, it remains to be established whether the differential expression is attributable to growth factors from the feeder cells (such as FGF (Llames *et al.*, 2015)), or rather due to media differences (serum / EGF / cholera toxin). Furthermore, A3A induction was robust in normal breast epithelial cells (feeder-free) which was augmented with increasing concentrations of EGF. Likewise, A3A was induced in starved and re-stimulated bladder carcinoma cells (feeder-free, and not increased in the presence of feeder cells), though was increasingly stimulated with a higher concentration of EGF; indicating that the same underlying mechanism of A3A induction exists in these cells yet at significantly lower levels than arise in the normal cell lines (NIKS, NHEK, MCF-10A).

5 Phenotypic alterations in A3A deletion NIKS

5.1 Introduction

Cell growth and division are highly coordinated, regulated events involving multiple signalling pathways to maintain tissue homeostasis and prevent aberrant growth. Growth factor stimulation activates multiple pathways including PI3K/AKT/mTOR and RAS/MAPK (Palm and Thompson, 2017); mTOR coordinates nutrient and growth factor sensing with cell growth, metabolism and proliferation (reviewed by Saxton and Sabatini, 2017). Irreversible commitment to mitosis occurs at the “restriction point” (or R) in G1-phase, although there are two distinct R points: one growth-factor dependent in early G1, and one cell growth-dependent in late G1 (Foster *et al*., 2010). More recently it has been proposed that this decision is also influenced during the previous G2-phase (reviewed by Matson and Cook, 2017).

Cells maintain size uniformity through selectively adjusting their growth rates, and Ginzberg *et al.* demonstrated that cells need to reach a minimum size to progress through a G1/S size checkpoint (smaller cells will spend longer growing in G1 to reach the size threshold before starting replication). Furthermore, that cell size directly correlates with nucleus size (independent of DNA replication) (Ginzberg *et al.*, 2018). A small molecule screen by Liu *et al.* (2018) found that although the PI3K/AKT/mTOR regulates cell size, it does not coordinate it with G1 length and instead that correlation is regulated by p38 MAPK activity, and demonstrated in that its inhibition abrogated the compensatory G1 length extension, resulting in increased proliferation of cells of an overall smaller size.

5.2 A3A KO NIKS are highly proliferative

It was observed through sub-culturing A3A KO cells that they grow at an increased rate, becoming confluent much more quickly than WT-NIKS. The cell growth of three separate clones of A3A KO NIKS and three clones of mock-transfected NIKS were therefore quantified with a colorimetric MTS assay, in which the reduction of MTS tetrazolium by viable and metabolically active cells is measured by absorbance.

Each clone was plated on day one in sextuplicate at a density of 3×10^3 per well of a 96-well plates with 1×10^3 of 3T3 feeder cells. Media was replenished every second day and absorbance following the addition of MTS was measured on day two; the mean absorbance of each clone was then used as a baseline to calculate the accumulative fold-change of each repeat over the subsequent three days. Shown in Figure 5-1 (A), the absorbance at day two was similar between the WT-NIKS and A3A KO clones, though by day three the KO clones started to show an increased rate of growth which was more significant by day four and five: a mean fold-change of 37.61 ± 8.31 SEM in the KO as compared to 9.78 ± 1.11 in the mock-transfected (WT-NIKS) cells. The increased proliferation of A3A KO cells throughout the whole time-period was statistically significant (two-way ANOVA $p<0.0002$).

Total cell counts were also performed with the same three clones of A3A KO cells and three clones of mock-transfected (WT)-NIKS. For this, cells were plated at a density of 1.5×10^5 per well of a 6-well plates together with 1×10^5 per well of 3T3 feeder cells, and half of the total media volume was replenished daily.

Following removal of feeder cells, cell numbers of each clone were quantified on a CellDrop automated cell counter over the subsequent six days. Shown in Figure 5-1 (B), the growth kinetics followed very similar kinetics to the MTS assay absorbance: by day seven, there was ~2.3-fold increase in the number of A3A KO NIKS ($8.93 \times 10^6 \pm 0.41$) as compared to WT-NIKS ($3.95 \times 10^6 \pm 0.3$).

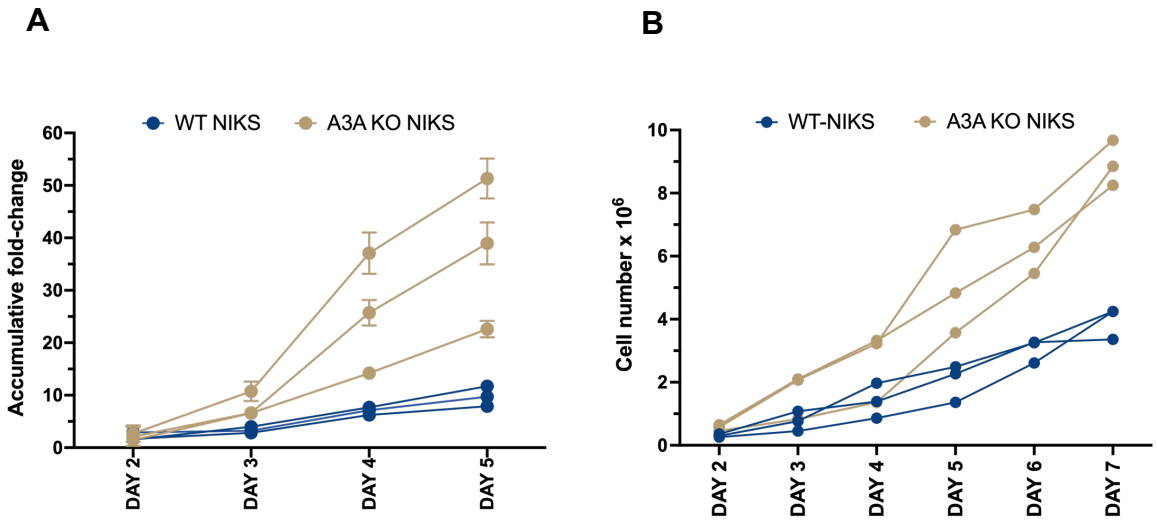

Figure 5-1 A3A deletion cells proliferate significantly faster than WT-NIKS.
(A) A3A KO NIKS proliferate significantly faster than WT-NIKS, measured by MTS assay. **(B)** Total cell counts of WT-NIKS and A3A KO NIKS over a seven day period. For MTS assay, three clones of mock-transfected NIKS and three clones of A3A KO NIKS were plated with six technical repeats on day 1 at a density of 3×10^3/well in 96-well plates, with 1×10^3 3T3 feeder cells. MTS was added on days 1-5 and absorbance measured as a quantification of viable cells; media was refreshed every 2nd day. The accumulative fold-change of each technical repeat was calculated relative to the mean absorbance reading on day 1. Error bars represent the SEM for each clone. For cell counting, cells were plated at a density of 1.5×10^6 per well of a 6-well plate and half of the media was changed daily. One count of each clone was completed daily counting using a CellDrop™ automated cell counter.

5.3 A3A KO NIKS proliferate faster following starvation/re-stimulation

We previously found that A3A was less strongly induced following starvation / re-stimulation in HPV16 oncogene containing NIKS (Figure 4-12), though the fold-change between asynchronous or starved levels was greater in all (except NIKS-E7) (Figure 4-13); we additionally observed that A3A KO NIKS proliferate significantly faster than WT-NIKS (Figure 5-1). We were therefore interested to compare their relative proliferation rates following starvation / re-stimulation, which was measured by MTS assay. These were performed on day one (at the start of the starvation period), and subsequently at 24 hr and 4 days post-release. Cell proliferation was then quantified as a fold-change of the absorbance relative to day one.

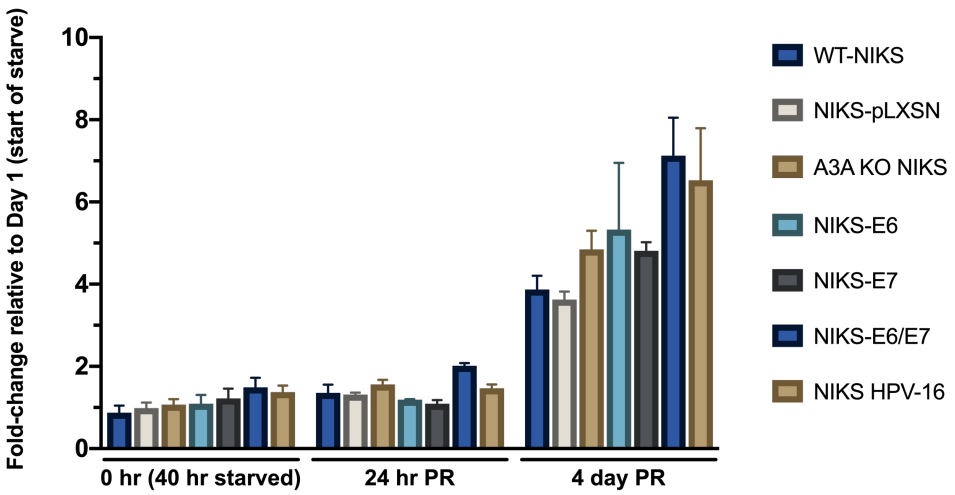

Figure 5-2 NIKS continue to proliferate following starvation/re-stimulation.
Cell proliferation of WT-NIKS and HPV16 oncoprotein expressing NIKS, measured by MTS assay. Cells were plated in triplicate in 96-well plates, at a density of 4 x 10^3 cells/well together with 1 x 10^3 3T3-feeder cells. The next day (day 1), media was removed, the cells washed twice with PBS, then incubated for 40 hr in starvation media. At which point (0 hr), cells were released from quiescence through the addition of FC media. MTS was added on day 1, and the fold-change of absorbance at 24 hr and 4 day post-release (PR) calculated relative to day 1. The mean of each triplicate was calculated (errror bars represent the SEM).

As seen in Figure 5-2, each cell line resumed proliferation following re-stimulation, indicating that there was no significantly detrimental effect from the starvation (or from the induction of A3A in those expressing it). As expected, WT-NIKS and NIKS-pLXSN had the lowest accumulative fold-changes after four days (~3.9 and ~3.6-fold). A3A KO NIKS and those expressing HPV-E7 were both equally more proliferative (~4.8-fold); more highly so were NIKS-E6, NIKS-E6/E7, and NIKS-HPV16 at ~5.3, ~7.1, and ~6.5-fold changes respectively.

5.4 A3A KO NIKS are smaller than WT-NIKS

In addition to increased proliferation, A3A KO cells are significantly smaller than WT-NIKS. Cells were detached and their mean cell diameter recorded using a CellDrop automated cell counter over a seven-day period; cells were plated on day one (from sub-confluent dishes which had a recent media change and were therefore actively growing), they then either received a daily replenishment (of half of the total media volume) or were incubated in the same media for the duration. Mean cell sizes are shown in Figure 5-3, and the distribution of each cell size in the supplementary material (Figure 8-4): WT-NIKS had a mean size of 16.62 μm ± 0.24 SEM on day one, as compared to a A3A KO that had a mean size of 15.73 μm ± 0.72 (~5% smaller). Calculating cell volume based on an assumption that a detached cell is roughly spherical ($V = \frac{4}{3}\pi r^3$), this equates to a ~15% smaller mean cell volume in A3A KO cells. Cells cultured in the same media for the duration failed to reach full confluency (WT- or A3A KO), and their mean cell size became increasing smaller (Figure 5-3 (A)).

A3A KO cells had a mean size of 11.45 μm ± 0.26 on day seven as compared to 13 μm ± 0.52 in the WT-NIKS (~12% smaller diameter / ~30% smaller volume, two-way ANOVA p<0.0001), however A3A KO cells also appeared to have a visible increase in apoptotic cells which may in part account for some of the reduction in size. The increased apoptosis in A3A KO may arise from faster exhaustion of nutrients due to their increased proliferation rate, or may suggest that they are more sensitive to cellular stresses experienced in the absence of regular media changes). Cells that received daily media replenishment decreased in size over the duration though the difference between WT- and A3A KO at day seven was less pronounced: A3A KO mean of 13.04 μm ± 0.17, WT-NIKS mean of 13.69 μm ± 0.18 (~5% smaller diameter / ~15% smaller volume) (Figure 5-3 (B), two-way ANOVA p<0.0001).

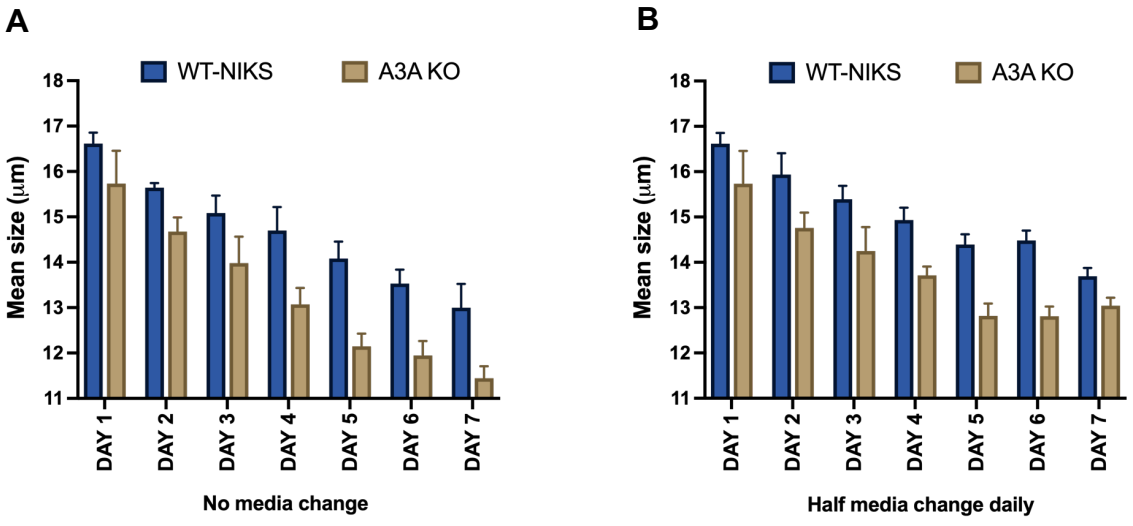

Figure 5-3 A3A deletion NIKS have a significantly smaller mean diameter.
(A) A3A KO NIKS are significantly smaller than WT-NIKS, as quantified over a 7-day period (without media change). **(B)** A3A KO NIKS are smaller than WT-NIKS (half media changed daily). For cell size analysis, three clones of mock-transfected (WT)-NIKS and three clones of A3A KO NIKS cells were plated at a density of 1.5 x 10^6 per well of a 6-well plate. One count of each clone was completed daily counting using a CellDrop™ automated cell counter. Error bars represent the SEM.

5.5 Proliferating A3A KO NIKS are more sensitive to DNA damaging drugs

A3A-mediated deamination events can activate the DNA damage response, consequently repairing lesions caused by DNA damaging agents that may drive therapeutic resistance (Landry *et al.*, 2011); we therefore wanted to compare cell survival (measured by metabolic activity through MTS assay) in three clones of A3A KO and three clones of mock-transfected (WT)-NIKS following treatment with either: bleomycin, an agent that causes DNA single- and double-strand breaks; cisplatin, a standard platinum based drug; or the thymidine analogue, 5-ethynyl-2´-deoxyuridine (EdU), which affects viability in a cell-type dependent manner (Diermeier-Daucher *et al.*, 2009).

Cells were either incubated in the same media (and drug) for the duration, or half the media (with fresh drug) was replenished daily. A3A KO cells are more proliferative than WT-NIKS which makes a direct comparison of drug sensitivity difficult; therefore, the effective concentration that elicited 50% response (EC50) was calculated from the absorbance relative to untreated cells (shown as 0.0001 μM) using a three-parameter logistic regression model.

As seen in Figure 5-4, A3A KO cells were more sensitive to these drugs than WT-NIKS when cultured under proliferative conditions (following half daily media changes): bleomycin [WT-NIKS 0.341 μM, A3A KO 0.018 μM]; cisplatin [WT-NIKS 4.066 μM, A3A KO 2.449 μM]; EdU [WT-NIKS 5.083 μM, A3A KO 1.707 μM].

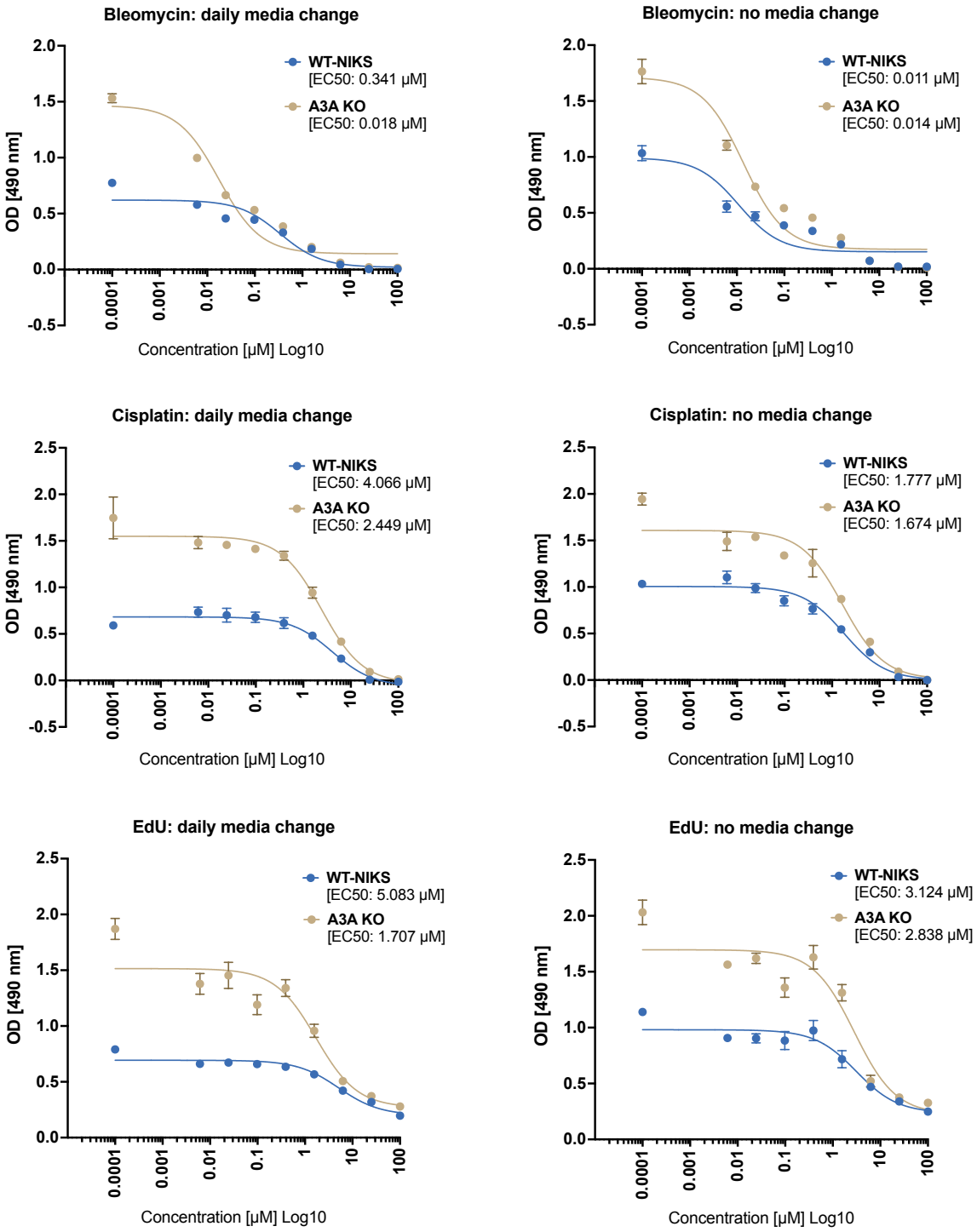

Figure 5-4 A3A deletion NIKS are more sensitive to DNA damaging drugs.
Three clones each of mock-transfected NIKS and A3A KO NIKS were either: plated with drug on 1st day, then half of the media removed each subsequent day and replaced with media containing fresh drug (4 days total); or plated with drug on the 1st day and incubated in the same media for the duration (no media change). Each clone was plated in triplicate with J2-3T3 feeder cells. Cell viability was measured by MTS assay through absorbance measured at 490 nm. SEM calculated from three technical repeats.

5.6 Discussion / Conclusions

A3A is robustly induced following growth factor withdrawal and re-stimulation in NIKS, primary keratinocytes (NHEK), and normal breast epithelial cells (MCF-10A), and may potentially occur in other normal cell types. Yet A3A induction was much weaker in a urinary bladder cancer cell line (BFTC-905), in HPV-positive NIKS (NIKS-E6, NIKS-E7, NIKS-E6/E7, and NIKS-HPV-16), and barely detectable in cervical cancer cells (SiHa and HeLa).

Basal levels of A3A mRNA are low in most cell types (other than monocytes/macrophages) and were not upregulated following media replacement in asynchronous populations, yet despite the apparent low abundance of A3A in asynchronously growing cells we observed (through MTS assay and cell-counting) that A3A KO NIKS had significantly increased proliferation. Thus, it appears that even low levels of A3A can exert anti-proliferative, cell-cycle functions in the absence of stimulation (known inducers or starvation/re-stimulation) and thus selection against A3A could potentially be favourable for driving or contributing to the increased proliferation rates of cancer cells.

A3A KO cells were more sensitive to the DNA damaging drugs (bleomycin, cisplatin, EdU) when cultured under more proliferative conditions in which A3A expression is expected to be very low, though this could be due to the mode of action of DNA damaging drugs being more toxic to actively growing cells.

Serum sensing is a means by which cell size and proliferation are controlled and we previously found A3A to be sensitive to growth factor stimulation in quiescent NIKS; we also found that deletion of A3A also leads to a decrease in cell size: asynchronously growing A3A KO NIKS have a ~5% smaller mean cell diameter than WT-NIKS, and at the conclusion of a seven-day period (in which they had a daily media replenishment and so A3A levels were likely to be low), the ~5% difference in mean cell diameter was maintained. Through growth factor depletion (keeping cells in the same media for seven days without refreshment), conditions in which we predict A3A levels will be increased in line with our observations from starved cells, the difference in size increased: A3A KO cells were ~12% smaller on day seven.

Thus, conditions in which A3A is upregulated may contribute to an increase (or maintenance) of cell size which might also reconcile our findings that inhibition of mTOR (which favours increased growth and cell size) had no inhibitory effect on A3A induction following starvation/re-stimulation. Alternatively, the increase in cell size might again arise from a greater population of larger, differentiating cells in the WT-NIKS.

6 Discussion

6.1 Characterisation of APOBEC3 expression in NIKS

The APOBEC3 family of enzymes have prominent roles in innate immunity against viruses, though their deregulation or off-target effects lead to an accumulation of signature mutations that form the second-most prominent source of DNA mutagenesis (in ~15% of all sequenced tumours), and are present in 50% or more of certain cancer types including breast, lung, and HPV associated cervix and HNSCC.

A3A and A3B were first discovered through PMA induction of normal keratinocytes and were also found to be present within tissues from the hyperproliferative, inflammatory skin disease, psoriasis (Rasmussen and Celis, 1993). Basal levels of A3A are very low in most normal cells (other than monocytes/macrophages), thus most studies of its activity rely on exogenous overexpression; for this study we used CRISPR/Cas9 gene edited NIKS that express an HA-epitope tag on A3A and A3B to firstly characterise their endogenous expression and activity in normal keratinocytes following stimulation with known inducers.

PMA is a mimic of DAG and its mechanism for A3B upregulation has been shown to be via PKC/NF-κB signalling, with the recruitment of transcriptional activators to the A3B promoter, either: RelB/p52 (the non-canonical NF-κB pathway) (Leonard *et al.*, 2015), or p65/p50 and p65/c-Rel (the classical NF-κB pathway) (Maruyama *et al.,* 2016).

IFN-stimulated response elements have been found in the promoter regions of A3F and A3G, and in a putative promoter region of A3A (Peng *et al.,* 2006). A3A is induced by IFN-α in activated and quiescent PBLs, monocytes, MDMs and DCs (Berger *et al.*, 2011), and peripheral blood mononuclear cells (PBMLs) (Refsland *et al.*, 2010; Aynaud *et al.*, 2012). Type I IFN strongly upregulates A3A in monocytes leading to multiple RNA editing events (Sharma *et al.*, 2015), and IFNAR/PKC/STAT1 signalling was shown to mediate mA3 upregulation (Mehta *et al.*, 2012).

A3A has the highest catalytic activity of the APOBEC3 family and co-treatment of PMA with TNF-α has been shown to greatly enhance A3A, but not A3B upregulation (Siriwardena *et al.*, 2018). We initially compared the induction of all seven APOBEC3 genes in NIKS using plasmid DNA standards for specific and quantitative detection, and found that there was slight upregulation of A3A and A3B by IFN-α, though a greater fold-change of induction of A3F and A3G (Figure 3-7). PMA treatment more substantially increased both A3A and A3B expression.

We also found that A3A induction by PMA could be greatly amplified in NIKS through co-treatment with IFN-α. Moreover, it was the most strongly expressed APOBEC3 enzyme under these conditions (and the only one in which the synergistic induction occurred). A3B mRNA was also increased by co-treatment of PMA/IFN-α, though far less than A3A by qPCR, and was not initially detected by western blot under the same conditions that induced strong A3A protein expression (Figure 3-3).

We additionally compared the expression in WT-NIKS against three clones of A3A KO NIKS and found induction to be very similar (Figure 3-8) which verified there was no disruption to the gene expression of the remaining APOBEC3s and was therefore a useful model for the comparison of A3A activity in WT-NIKS.

6.2 A3B is specifically upregulated during G2/M phase

We saw a slight increase in A3B mRNA in the A3A KO NIKS (Figure 3-8) following PMA or PMA/IFN-α treatment though the basal level was also slightly higher and so the relative fold-change of induction remained similar. However, we subsequently found that A3B protein was specifically upregulated during the G2/M phase of the cell-cycle and by PMA/IFN-α in actively proliferating (media enriched) cells (Figure 3-9), and also that A3A KO cells grow significantly faster than WT-NIKS (Figure 5-1); findings which therefore likely reconcile these differences.

A3B is upregulated by the HR-HPV E6 oncogene in NIKS and HPV-positive cancer cell lines (Vieira *et al.*, 2014) and is consistently elevated in HPV-associated cancers compared to normal tissue (Chakravarthy *et al.*, 2016). Though A3B levels do not correlate with A3 signature mutations in HPV-associated cancers (Roberts *et al.*, 2013; Henderson *et al.*, 2014; Ojesina *et al.*, 2014), suggesting that A3B may instead have an important role in the viral life cycle. Consistent with previous findings, we see that A3B mRNA and protein is upregulated in NIKS that stably express HPV16 E6 (Figure 3-9), again preferentially so during G2/M (and PMA/IFN-α induction).

The function of A3B expression in G2/M and by HPV16 upregulation is yet to be elucidated (A3B KO NIKS have proven difficult to generate). Although non-synonymous A3B-mediated mutations in the HPV genome may promote genetic diversity that could aid evasion of host adaptive immune responses (Hirose *et al.*, 2018), we can also speculate that the fact it is preferentially expressed in actively growing/media enriched cells may relate to positive reinforcement of proliferation and thus favourable to the HPV life cycle. Its elevated expression could alternatively arise as a consequence of the increased proliferative potential that is facilitated by E6-mediated p53 degradation (Scheffner *et al.*, 1990) and by the E7-mediated disruption of Rb (Dyson *et al*., 1989).

6.3 A3A and A3B are induced under opposing cell culture conditions

Importantly, we also found that A3A and A3B have opposing cell culture conditions that are most conducive to their induction in NIKS, which suggests that they may also have opposing roles. For example: A3B mRNA was lower than basal levels in serum starved/re-stimulated cells (Figure 4-14) and was not detected at the protein level by PMA/IFN-α induction in cells that had been incubated in the same media for 48 hr prior to treatment (Figure 3-3). Though A3B protein could be induced by PMA/IFN-α in media enriched, asynchronous populations following multiple media changes prior to treatment (Figure 3-9 (C)), in which a larger population are more likely to still be actively proliferating (though the cell-cycle status under the different conditions needs to be confirmed by flow cytometry analysis).

In contrast, basal levels of A3A mRNA are very low but increase in serum starved cells (Figure 4-5) and dramatically so in those subsequently induced back into the cell-cycle through media replenishment; hence PMA/IFN-α treatment after 48 hr incubation in the same media (in which a proportion of cells may have exited the cell-cycle and then subsequently re-stimulated by the fresh media/treatment) would be favourable for A3A, but not A3B induction. Thus, some caution may be necessary when interpreting A3A/A3B levels directly relative to each other under the same experimental conditions as the conditions that favour the induction of one are likely detrimental to the other, and one interesting possibility is that there could be reciprocal regulation of A3A/A3B gene transcription.

These findings also likely resolve the discrepancies between the levels of A3A and A3B induction in different cell-types. For example, only A3B had detectable upregulation following PMA treatment across a panel of cell lines, particularly MCF-10As (Leonard *et al.*, 2015); whereas upon PMA treatment of normal human oral keratinocytes, induction of A3A mRNA and protein were more than 2-fold greater than that of A3B (Siriwardena *et al*., 2018). By applying the same principle as seen in NIKS, these differences might be explained if the cell lines in the Leonard *et al.* study were treated with PMA within 24 hr of a media change, and the oral keratinocytes in the Siriwardena *et al.* study were treated 48 hr or more after a media change, for example. Our findings may also explain why basal levels of A3A are reported as being very low in most cell types when proliferative cells are commonly used for assays, if its expression is specific to quiescent and re-stimulated cells.

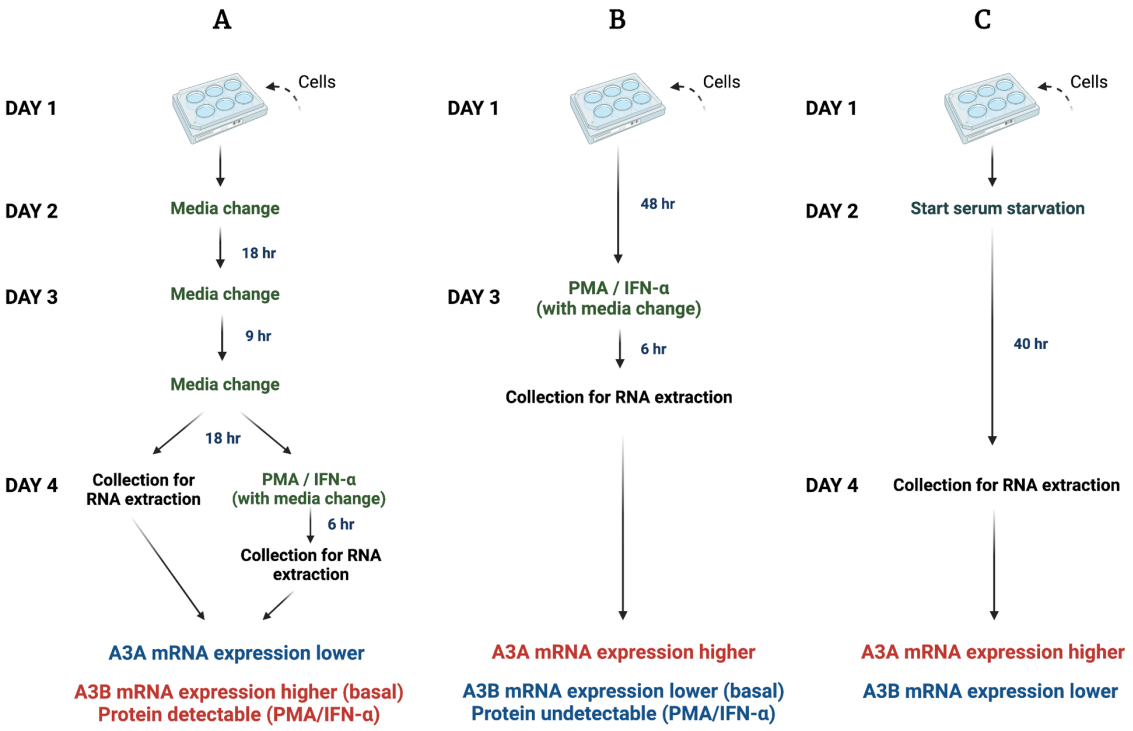

Figure 6-1 A3A and A3B have opposing culture conditions most favourable to their expression. **(A**) Conditions corresponding with the double thymidine block protocol. **(B)** Conditions used for characterisation of all APOBEC3 expression by PMA/IFN-α (following 48 hr incubation in the same media). **(C)** Serum starvation protocol.

We additionally found that the basal levels of all APOBEC3 enzymes (except A3A and A3H) were higher in sub-confluent, actively proliferating cells that were collected at 18 hr post-media change (Figure 4-14) compared to seen previously (Figure 3-7). Furthermore, A3C is widely considered to be the most abundantly expressed member in both basal and suprabasal keratinocytes (the Human Protein Atlas). This was initially corroborated in NIKS (48 hr post-media change) though A3B and A3C were subsequently found to be equally the most abundantly expressed at 18 hr post-media change. This is attributable to a ~12-fold increase in expression of A3B in the media enriched cells as opposed to only a ~ 2-fold increase in A3C.

Interestingly, A3A was only detected at 28 hr post-release from G1/S synchronisation (with thymidine) when cells were cultured in lower media volumes (114 μl cm^{-2}, Figure 4-3) though we were unable to detect A3A protein when this was repeated using higher volumes (208 μl cm^{-2}, data not shown). There are a number of possibilities that could account for this discrepancy: the lower volume was tested due to suggestion in literature that it helps facilitate cell-cycle re-entry (as it takes longer for cells to condition the media in larger volumes), therefore one possibility is that there is an accumulation of an A3A-promoting factor in the media that doesn't accumulate sufficiently in larger volumes. Alternatively, there may be greater acidification of media through metabolic activity in the lower media volumes, which could be consistent with our finding that induction of A3A was mediated through the p38 pathway: p38 has also been found to respond to extracellular pH changes (Stathopoulou, Gaitanaki and Beis, 2006).

Another hypothesis, which resonates more closely with our observations from serum starvation, is that there is faster depletion of nutrients/growth factors in the lower media volume (particularly as a large proportion of cells are transiting though a growth phase simultaneously, which does not occur in asynchronous populations), and therefore serum sensing signalling would induce a larger proportion to exit the cell cycle into quiescence following completion of mitosis, rather than continuing to cycle: as A3A appears to be specific to quiescence and re-stimulation, this would account for A3A induction in the absence of a media change, and the robust induction observed through media refreshment at this point.

Finally, A3A-mediated RNA editing in monocyte-enriched PBMCs is upregulated by hypoxia treatment (Sharma *et al.*, 2015) and we additionally observed that there was slightly greater A3A induction when cells were re-stimulated from quiescence for 3 hr in the higher media volume (in Supplementary Figure 8-2). This is intriguing as it seems unlikely that there would be either nutrient depletion, pH changes, or media conditioning within that time-frame that could account for the increased induction. Therefore, an alternative possibility is that the increased media depth may induce a transient hypoxic state that increases the A3A response: this is because oxygen has low solubility therefore would require twice as long to diffuse through the larger volume of media (Al-Ani *et al.*, 2018).

It would therefore also be interesting to establish which cell culture conditions most closely represent different physiological environments to gain a better understanding of their role/activity in normal vs cancer tissues. Serum starvation combined with hypoxia and/or decreased glucose content is used experimentally to mimic the nutrient, growth factor and oxygen deficient environment of tumour cell cells (Tavaluc *et al.*, 2007; Levin *et al.*, 2010; Sánchez *et al.*, 2011) and interestingly, A3A was also induced ~2-fold more by DMEM (with 0.3% FBS) that did not contain glucose than that which did (in Supplementary Figure 8-3). On the other hand, basal cells in a normal epithelial are mostly quiescent and can be re-stimulated upon wound injury or for normal tissue turnover (Le Roy *et al.*, 2010; Schlüter *et al.*, 2011). Therefore, it is possible that either or both represent conditions that may favour A3A expression.

6.4 Conceptual basis of starvation and re-stimulation

Unlike senescence or terminal differentiation, quiescence is a reversible non-proliferative state that exists in certain cells and is critical for tissue regeneration and repair, as well as being a protective mechanism against cellular stresses (Yao, 2014). In the absence of growth factor signalling, cells exit the cell-cycle (normally in G0), a process that is tightly regulated through expression of the CDK inhibitors p21, p27, and p57 (Marescal and Cheeseman, 2020); maintenance of quiescence also involves soluble quiescence-inducing factors such as TGF-β1 (Batard *et al.*, 2000).

The p38-MAPK pathway was originally identified as a mechanism of cell defence following extracellular changes in osmolarity (Han *et al.*, 1994) though since is shown to respond to a variety of stress-related stimuli (Rouse *et al.*, 1994), including serum starvation (Lu *et al.*, 2008). It has further been shown to be important for quiescence maintenance: quiescent leukemic cells become proliferative through its inhibition (an effect that is abrogated through MEK inhibition) (Vaidya, Sharma and Kale, 2008).

Rather than being a dormant state, quiescent cells remain transcriptionally active to suppress apoptosis and terminal differentiation, but it also facilitates the rapid re-entry to the cell-cycle upon growth factor signalling (Cheung and Rando, 2013). The quiescence–proliferation balance is controlled by an Rb-E2F1 bistable switch (Yao *et al.*, 2008): the E2F1 transcriptional activator is required for S-phase entry and is inactivated by Rb binding (Marescal and Cheeseman, 2020).

Growth factor signalling decreases CDK inhibitor expression and increases levels of cyclins; the cyclin D-CDK4/6 complex phosphorylates and inactivates Rb, leading to depression of E2F1 and inducing cell-cycle re-entry (Marescal and Cheeseman, 2020).

Wound healing stages consist of inflammation, re-epithelialisation, and tissue remodelling. Macrophages are critical to the inflammatory phase, including their switch to M1 polarisation (Landén, Li and Ståhle, 2016) which is also shown to be promoted by the RNA-editing activity of A3A (Sharma *et al.*, 2015, 2017; Alqassim *et al.*, 2021). During the inflammatory phase, DAMPS and PAMPS are recognised by TLRs and initiate signalling via NF-κB and MAPK pathways (Landén, Li and Ståhle, 2016). The re-epithelisation overlaps with the inflammatory phase and occurs through the proliferatory and migratory action of keratinocytes, mediated in part by a subset of stem cells (Levy *et al.*, 2005).

Serum is added to culture medium to provide essential components for cell proliferation such as growth factors, vitamins, hormones, carrier and macromolecular proteins (van der Valk *et al.*, 2018). Serum starvation elicits cell-type dependent effects though can be used to induce cellular quiescence (alternative methods include contact-inhibition or loss of adhesion). As we wanted to investigate cell-cycle re-entry, we used serum starvation followed by re-stimulation with full media components to establish a synchronised population, though this method also potentially mimics the re-activation of quiescent cells during a wound healing response.

However, the term serum starvation has been used to denote serum-free or low serum concentrations, with or without BSA or specific growth factors. NIKS complex growth media is required for proliferation and to prevent terminal differentiation (Esteban-Vives *et al.*, 2015) and studies for synchronising NIKS using serum starvation are limited; Matrka *et al*. serum starved NIKS for 48 hr in serum-free F-media media with no insulin, adenine or EGF, and though the rationale for including cholera toxin and hydrocortisone was not discussed, this method resulted in ~70% G0/G1, and ~15% each of S- and G2/M phase cells and was therefore adopted with moderations (40 hr starvation, with 0.3% FBS).

Growth-promoting effects of different factors vary between cell type and culture conditions and the contributions of NIKS growth supplementation has been explored in several studies: cholera toxin in the range of 10 fM to 10 nM was found to increase the growth rate and colony formation of epidermal keratinocytes through increasing cyclic AMP concentrations (Okada, Kitano and Ichihara, 1982), the effect of which was greater in the presence of feeder cells than without (Green, 1978). Feeder cells are growth arrested (by mitomycin C treatment) though remain viable and secrete many soluble factors (including IL-2, fibrinogen, vascular endothelial growth factor (VEGF), fibroblast growth factor-2 (FGF2), and leukaemia inhibitory factor (LIF)) that support NIKS growth, without which they eventually terminally differentiate (Fleischmann *et al.*, 2009; Llames *et al.*, 2015). Notably, FGF receptors regulate keratinocyte migration following wounding, controlling re-epithelialisation (Meyer *et al.*, 2012). Furthermore, keratinocytes constitutively express LIF-receptors (Paglia *et al.*, 1996) and LIF/receptor binding activates the JAK-STAT3 pathway (Tang and Tian, 2013).

NIKS are supplemented with 8.3 ng/ml (0.1 nM) of cholera toxin whereas primary keratinocyte (NHEK) cells grown in a serum-free feeder-free system are alternatively supplemented with epinephrine (0.39 μg/ml) in place of cholera toxin. They have the same concentration of insulin as FC media, though a lot lower concentration of EGF (0.125 ng/ml compared to 10 ng/ml), a lower Ca^{2+} concentration (0.06 mM compared to 1.8 mM), and adenine is replaced with transferrin.

We found that A3A induction following starvation/re-stimulation was detectable in the serum-free feeder-free model (Figure 4-24) though at very low levels (regardless of the different starvation media formulas), and whilst re-stimulation with FC media was not investigated, induction with 10 ng/ml of EGF (the primary stimulant in NIKS) yielded only slightly greater induction.

Whereas there was robust induction using the FC media/feeder cell system (Figure 4-23) that was similar in expression to found in NIKS (Figure 4-5). Furthermore, the cell morphology differed greatly between the two systems: feeder-free serum-free NHEKs grew in individual cells or in small loosely connected groups, as opposed to FC media/feeder grown NHEK cells that grew in distinct colonies (resembling NIKS). Lamb and Ambler (2013) also saw similar effects of feeder-free serum-free systems on keratinocyte colony formation in that they failed to form stratified epidermis in an *in vitro* skin equivalent model. This effect was reversed when re-introduced to 1.4 mM of Ca^{2+} and 10% serum-containing media.

It would therefore be interesting to establish whether the differences are due to a) the feeder cells: either through assisting colony formation and/or growth factors that they excrete, and/or b) differential expression of EGFR in cells that are cultured in either low or high EGF concentrations, and/or c) a consequence of the cholera toxin supplementation, and/or d) the cells being more viable under different conditions therefore entering quiescence as opposed to inducing apoptosis as well as influencing their ability to re-enter the cell-cycle. Of note, cell-cycle distribution upon starvation (other than NIKS) has not been verified by flow cytometry analysis.

In regards to clinical applications of cultured skin, efforts to find suitable replacements for 3T3 feeder cells found that two laminin substrates (LN-511 and LN-421) supported comparable proliferative and colony-forming capabilities to 3T3 feeder cells and facilitated formation of a normal stratified epidermal structure (Tjin *et al.*, 2018), thus could potentially be a means to dissect the contribution of the feeder cells in A3As expression.

A3A induction in BFTC-905 cells was not increased by co-culturing them with feeder cells (Figure 4-28) though they also lack a dependency on EGF supplementation for proliferation (which may not necessarily reflect physiological environments). Though A3A was induced through starvation/re-stimulation in BFTC-905 cells, and increasingly so through EGF stimulation. However, induction was far less than by PMA/IFN-α treatment and therefore may be a mechanism that is selected against during oncogenesis in bladder carcinoma cells. It would therefore be interesting to compare A3A induction in normal bladder epithelial cells.

Similarly, the cervical cancer cell-lines (SiHa and HeLa) did not induce A3A upon starvation/re-stimulation (Figure 4-27), though would also be of interest to investigate alternative culture conditions in addition to re-stimulation with/without EGF.

MCF-10A cells are cultured with 2-fold the concentration of EGF (as NIKS), and ~12-fold more cholera toxin (100 ng/ml (1.2 nM)) but do not require feeder cells. They showed robust induction of A3A upon starvation/re-stimulation (Figure 4-25), though the maximum achieved was ~12-fold less than the mean induction in NIKS. Moreover, induction was only robust when starved in DMEM (with 0.3% FBS) and not when starved in NIKS equivalent media (with cholera toxin (at concentration they are cultured: ~12-fold more than NIKS), and hydrocortisone). Whereas NIKS induction was less in starved cells in DMEM (with 0.3% FBS) than through using the NIKS starve media (data not shown). Thus, there are disparities between cell-type and culture conditions that influence A3A induction upon re-stimulation and establishing the source of these might help to reveal the nature of A3As induction.

6.5 Is A3A specific to cell cycle arrest in G1 or does it occur in other cell cycle phases?

Immunofluorescent staining revealed that A3A induction by PMA (± IFN-α) results in a pan-cellular localisation of A3A (Figure 3-5), though surprisingly this was restricted to a minority of cells, and its induction did not correlate with DNA DSB formation (Figure 3-6).

This led us to hypothesise that A3A was cell-phase specific and we subsequently found through G1/S synchronisation (with thymidine) that A3A protein may correspond with G1-phases (Figure 4-3). Contradicting that, however, is that the majority of cells within an asynchronous population reside in G1-phase. Therefore, if A3A were G1-specific per se, you might expect to see a much larger proportion of cells staining strongly for A3A protein following PMA/IFN-α in an asynchronous population.

Unlike A3B, A3A is not expressed in G2/M immediately following release from G1/S or by nocodazole treatment (Figure 4-3), though it did increase at 34 hr post-release which corresponded with an increase in the G2-specific cyclin B1 (Figure 4-4), and has been shown to be co-expressed with mitotic genes at the protein level in a breast invasive carcinoma dataset (TCGA Firehose Legacy). However, the expression at 26 hr / 28 hr / 34 hr only occurred when cells were cultured in lower volumes of media (114 $\mu l/cm^2$) and was not detected in any samples when cells were cultured in higher media volumes (208 $\mu l/cm^2$), therefore may be either a G1 or G2/M response that occurs as a consequence of nutrient depletion/starvation conditions.

When robustly induced following starvation/re-stimulation, a subset strongly expressing A3A were seen by immunofluorescence at 8 hr (Figure 4-7). However, it additionally appeared that A3A protein was expressed in the majority of cells, yet at a lot lower level, though this was variable (and dependent on microscope threshold settings, gain and exposure times) and requires further investigation.

Supporting the hypothesis that A3A induction likely occurs in the majority of cells following starvation/re-stimulation (albeit less strongly) is that A3A protein is robustly induced (Figure 4-5 (B)) and this persists as the majority of cells proceed through the cell-cycle (Figure 4-6). Furthermore, by treating asynchronous cells with the CDK4/6 inhibitor, palbociclib, for 18 hr, there was an enrichment of G1-phase cells and this corresponded with a slight enrichment of A3A mRNA (Figure 4-8). Moreover, the absolute value of A3A mRNA at 8 hr post-release is approximately equal to GAPDH mRNA (used as an additional house-keeping gene for each sample). Therefore, it seems improbable (but not impossible) that a small fraction of cells express equal quantities of A3A mRNA as that of the abundantly expressed GAPDH (within an entire population).

Keratinocytes are able to initiate terminal differentiation from any point within the cell cycle, retaining the ability to replicate DNA as they do so, and G2/M arresting cells can undergo endoreplication which results in polyploid or multinucleated cells (Gandarillas, Davies and Blanchard, 2000). The flow cytometry analysis additionally showed that there was a smaller population of cells that were in G2/M at 0 hr/starved (Figure 4-6, Figure 4-8), and that 36-46% remained in G1 by 18 hr post-release. ssDNA during S-phase is vulnerable to A3A deaminase activity, though the apparent lack of DNA DBSs or accumulation of abasic sites suggests that it is either not expressed in S-phase cells or is tightly regulated to protect host-DNA; human tribbles 3 and the chaperon-containing TCP-1 complex are potential candidates for its regulation, both found to interact with A3A and may prevent nuclear transportation/accumulation (Aynaud *et al.*, 2012; Green *et al.*, 2021).

An alternative possibility is that A3A is strongly expressed in those cells that have alternatively arrested in G2/M, or in G1-phase cells that may not re-enter the cell cycle (methods for further investigation of this are discussed in future directions, in section 6.8.2).

Furthermore, mRNA levels were lower in sub-confluent starved, than confluent starved NIKS (Figure 4-15) though the fold-change of subsequent induction was less in the contact-inhibited cells. On the other hand, we saw that A3A was induced by PMA/IFN-α in sub-confluent but not confluent unstarved NIKS (Figure 3-4). However, confluent cells had received a daily media change prior to treatment (and we do not have a comparison of mRNA basal levels under the different conditions), thus comparing mRNA and protein levels in both conditions might help establish whether cell cycle exit as opposed to stress caused by starvation induces A3A.

In addition to stress-related stimulation, p38 additionally regulates the G1/S and G2/M cell cycle checkpoints, coordinating cell size with a G1 length extension (smaller cells will spend longer growing in G1 to reach the size threshold before starting replication) (Liu *et al.*, 2018) and p38 inhibition in corneal endothelial cells increased proliferation of cells of a smaller size (Nakahara *et al.*, 2018). We found that A3A was upregulated in starved cells via p38 signalling, and that A3A KO cells grow significantly faster and are smaller than WT-NIKS (Figure 5-1), potentially linking A3A induction to a p38-mediated role in regulating cell size/proliferation. Thus cell-cycle arrest through exogenous A3A expression, proposed to be a consequence of DNA DSBs, might rather be an A3A-mediated cell-cycle control mechanism.

Preliminary investigations were made into the rate at which WT-NIKS and A3A KO NIKS proceed through the cell cycle following release from starvation (through EdU incorporation, data not shown) as well as comparison of cyclin B1 and p21 mRNA expression (shown in the Supplementary material, Figure 8-5), and they appear to proceed at very similar rates. This might suggest that there are no alterations to cell-phase length, though this could be affected by observations that A3A KO NIKS appear to be recover / proliferate more slowly following serum starvation than an unperturbed population (Figure 5-1, Figure 5-2) and so requires further investigation.

Smaller keratinocytes are also associated with being in a less advanced stage of differentiation (Barrandon and Green, 1985); moreover A3A has been shown to be upregulated in differentiating cells (Wakae *et al.*, 2018). A3A KO NIKS have a ~12% smaller mean diameter / 30% smaller cell volume under nutrient poor conditions compared to WT-NIKS (Figure 5-3) which could arise from either a greater quantity of larger, differentiating cells in the WT-NIKS, or a larger population of smaller cells in the A3A KO NIKS. Shown in the supplementary material (Figure 8-4), cell sizes in NIKS ranged between ~10 - 20 μm, and there appears to be a shift towards the left (decreased cell size) in A3A KO cells. However, preliminary work with keratin-10 (a marker of late keratinocyte differentiation) showed no increase in WT-NIKS (by western blot or immunofluorescent staining following PMA/IFN-α induction, data not shown) which suggests it is may not be directly related to differentiation status.

6.6 Signalling pathways and transcriptional activity mediating A3A induction during starvation/re-stimulation

A3A is transcriptionally activated in NIKS (~50-fold, Figure 4-5) through serum starvation (referred to as Signal 1 in Figure 6-2): upregulation occurred within 6 hr but increases with the length of starvation (Figure 4-16) though it would additionally be of interest to look at earlier time-points (in addition to earlier time-points upon re-stimulation). This could support the hypothesis that A3A is specifically primed in quiescent cells (as opposed to a stress response) for the following reason: at the commencement of growth factor withdrawal, cells that have already passed the G1 restriction point are committed to complete the cell cycle; after 6 hr starvation, only the cells that were within reach of completing mitosis within that time-frame are then able to enter quiescence. A greater proportion would reach cell-cycle exit following 18 hr starvation, with the remainder doing so by 36 hr to 40 hr. This would result in incremental increases in A3A transcriptional activity due to incremental increases in quiescent cells (hence maximum induction reached following 36 hr to 40 hr starvation that we observed). After 60 hr of starvation, cell viability was also less (by visible inspection) and correspondingly the fold-change of A3A induction starts to decline, which suggests that A3A is not being induced in a pro-apoptotic manner.

Transcriptional activation of “Signal 1” was found to be via p38α/β-MAPK signalling and A3A was almost completely abrogated by its inhibition (Figure 4-18). Transient p38 activation promotes cell survival signalling (Puri *et al.*, 2000) thus p38-mediated A3A upregulation may also be related to pro-survival signalling within starved cells.

Supporting this, we found that A3A KO cells also appear to be more sensitive to the stress of serum starvation (more visibly apoptotic cells). Furthermore, p38 regulates the EGF-mediated proliferation/migration balance via the Src kinase signalling pathway (Frey, Golovin and Brent Polk, 2004) and A3A transcripts increased ~2-fold through Src (SU-6656) inhibition (Figure 4-20).

Though this only occurred at high concentration (5 μM) whereas they decreased at 500 nM. Of note, SU-6656 is also a potent inhibitor of the platelet derived growth factor (PDGF) receptor and fibroblast growth factor receptors (FGFR1) (Blake *et al.*, 2000).

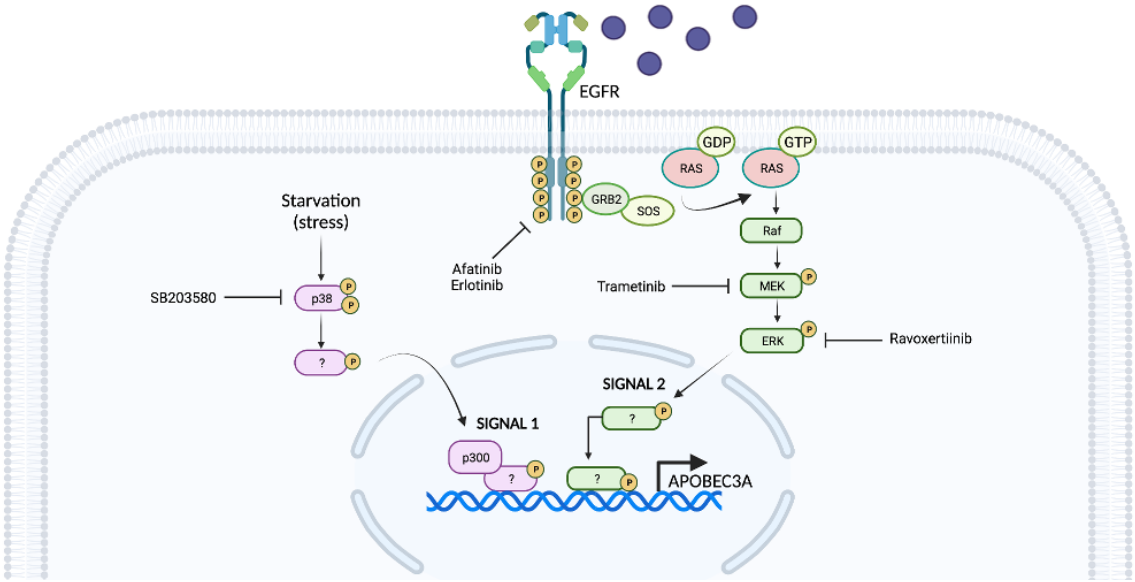

Figure 6-2 Signal transduction mediating A3A expression in starved and re-stimulated NIKS. A3A is upregulated during starvation by the p38-MAPK signalling pathway (Signal 1) through as yet unknown transcriptional activators and is consistent with proximal pausing. This would facilitate rapid transcriptional activity upon Signal 2, received from growth factor stimulation via EGFR/RAS/MAPK signalling.

MEK and ERK inhibitors both significantly increased A3A transcripts in starved cells (Figure 4-18); these MAPKs are activated by receptor tyrosine kinase (RTK) signalling from growth factors and cytokines, and have roles including proliferation, migration, and differentiation (Cargnello and Roux, 2011). Pulsatile ERK activity additionally regulates exit from the stem cell compartment in epithelial cells, with its inhibition favouring differentiation (Cargnello and Roux, 2011). Suppression of A3A in quiescence may therefore be required to suppress terminal differentiation, or rather arise though stress-related cross-talk signalling as a result of MAPK inhibition.

Upon re-stimulation with growth factor signalling (referred to as Signal 2, in Figure 6-2), MEK and ERK inhibitors instead reduced A3A transcription. EGFR (1 μM afatinib) and PI3K (10 μM pictilisib) inhibitors reduced A3A expression by ~75% in starved cells, though there was also a high proportion of detached, apoptotic cells in those samples. The PI3K/AKT/mTOR pathway is necessary for quiescence exit (Wang *et al.*, 2018) and is also a key component of the wound healing process (Squarize *et al.*, 2010).

EGFR signalling promotes proliferation, inhibits apoptosis, and is commonly upregulated in multiple cancer types (Wee and Wang, 2017). The second-generation tyrosine kinase inhibitor (TKI) afatinib is a potent and irreversible inhibitor of EGFR (ErbB1/HER), ErbB2 and ErbB4 (Roskoski, 2019). Our findings suggest there is a requirement for EGFR and PI3K signalling to maintain viability in starved NIKS (despite exogenous EGF not being included in the starvation media).

Furthermore, we have found that the rapid and robust transcriptional activity of A3A upon re-stimulation is also mediated through EGFR/RAS/MAPK signalling, therefore it is possible that EGFR signalling may also play a role in A3A induction during quiescence (thus A3A downregulated by EGFR inhibition in starved cells).

Keratinocytes release the pro-inflammatory TNF-α cytokine in response to stress (including oxidative stress and UV radiation) which activates the NF-κB signalling pathway (Yarosh *et al.*, 2000; Young *et al.*, 2008). TNF-α additionally induces TGF-α expression in mouse fibroblast cells (Sullivan *et al.*, 2005). Moreover, TGF-α is a ligand for EGFR (Dlugosz *et al.*, 1994) and therefore autocrine / paracrine signalling may directly or indirectly (via feeder cells) activate EGFR signalling and contribute to the upregulation of A3A in starved cells. This could be investigated using TGF-α and/or TNF-α neutralising antibodies.

EGF was the primary media component (other than serum) to induce A3A in starved cells (Figure 4-19 (A-B)), though at concentrations higher than 10 ng/ml (in which they are cultured) A3A expression decreased (Figure 4-19 (D)). After activation, EGFR is ubiquitinated and internalised (Capuani *et al.*, 2015) therefore there may be faster turnover and downregulation of EGFR at higher concentrations (50 – 100 ng/ml). Though this also was complicated in that the vehicle-only control (HBES) shows similar inhibition at higher volumes and so should be verified with alternatively suspended EGF (as should the inhibition by HBES components). Likewise, EGF stimulated A3A induction in normal breast epithelial cells (Figure 4-25) and bladder carcinoma cells (Figure 4-28), which was abrogated using 10 μM of the first-generation EGFR inhibitor, erlotinib.

However, 1 μM of erlotinib was less effective than 1 μM of afatinib in inhibiting the potent induction of A3A in NIKS (Figure 4-20) which may be due to erlotinib being a reversible TKI inhibitor. Though A3A is not induced by EGF/EGFR under all circumstances as there is no increase (by FC media) in nutrient-rich proliferating cells (Figure 4-16), therefore, it appears to be specifically cell-cycle related and restricted to those that have exited the cell-cycle either through media exhaustion or stress/serum starvation.

Absolute values of A3A induction by starvation/re-stimulation was far less in the HPV-16 oncogene containing NIKS (Figure 4-12), though this is not through disruption of “Signal 2” upon re-stimulation as the fold-change was greater in all (except E7) (Figure 4-13) and instead appears to depend on basal levels before starvation (all were lower than WT-NIKS (NIKS-pLXSN)). HR-HPV suppresses NF-kB signalling (Karim *et al.*, 2013) which could indicate that A3A induction is also mediated through the NF-kB pathway downstream of EGFR. This may be suppressed by HPV under basal conditions but overcome by the robust growth factor signalling upon re-stimulation.

An alternative hypothesis for the downregulation of A3A at basal levels could be that a smaller proportion of cells exit the cell-cycle in the HPV-NIKS under the same conditions that prompt cell-cycle exit in WT-NIKS; this would be consistent with that they are more proliferative (Figure 5-2) and could be verified by flow cytometry analysis, though would require quiescence specific markers. It would also be interesting to compare NF-kB protein expression.

Our preliminary analysis of chromatin modifications (ChIP-qPCR in Figure 4-21) showed thar there is increased transcriptional activity at the A3A promoter and the -33 kb upstream enhancer in starved/quiescent NIKS. Though this does not increase upon re-stimulation despite the robust increase in A3A transcripts and protein and we speculate that promoter-proximal pausing of RNA pol II in starved cells may “prime” cells for the rapid transcription of A3A from multiple stimuli. This mechanism would support our findings that A3A is more robustly induced by various stimuli (individual growth factors (Figure 4-19), or PMA/IFN-α (Figure 4-17)) in starved cells that may be poised for rapid transcriptional activation, and potentially simulates an immune response that would be activated following wound/injury.

Promoter-proximal pausing was discovered in a study of heat-shock protein genes, in which Pol II was recruited to the gene promoter region of *hsp*70 prior to heat stress (Gilmour and Lis, 1986). After transcription of a short, nascent RNA, it remains tightly associated with the DNA:RNA hybrid until transitioning into productive elongation under the appropriate stimuli (Rougvie and Lis, 1988). It has since been shown to be a hallmark of Pol II transcription in many genes, and that the efficiency of pause-release is a key determinant of subsequent gene expression (Jonkers, Kwak and Lis, 2014). Pause release is initiated by the positive transcription elongation factor b (P-TEFb) (Lu *et al.*, 2016) and impacted by various factors including pause position (Kwak *et al.*, 2013). Furthermore, pausing is enriched in early mediators of the inflammatory response, including TNF-α (Adelman *et al.*, 2009).

A3A is rapidly induced upon re-stimulation (Figure 4-16: ~6-fold by 1 hr and ~90-fold by 2 hr). The earliest time-point quantified by ChIP-qPCR was at 3 hr therefore potentially there is earlier activity that has since subsided. As such, chromatin preparations have been prepared for further investigation (0 hr, 30 min, 1 hr, 2 hr, 3 hr) which may hopefully also reveal A3A transcriptional activators.

The delay between peak A3A mRNA and protein expression is in contrast to that seen previously through thymidine synchronisation, in which upregulation of both coincided in the majority of cases. This suggests that A3A protein may either be rapidly translated, and/or stabilised, in actively cycling cells. Whereas A3A protein translation may be less rapid in cells recently released from quiescence, which could be due to a lower abundance of translation synthesis proteins in these conditions.

This disparity between transcription/translation was also seen with A3B, whereby strong protein upregulation in G2/M (Figure 3-9 (A)) following either thymidine synchronisation or nocodazole arrest was coupled to only a modest increase in mRNA (Figure 3-9 (B)). Whereas a larger increase in mRNA through PMA/IFN-α treatment led to undetectable protein levels (in less actively cycling cells). Furthermore, whilst A3B protein was detected following PMA/IFN-α in more actively cycling cells, the 2-fold greater abundance of mRNA (than 8 hr to 10 hr post-release) yielded less protein (Figure 3-9 (C, E)). This would suggest that A3B protein is stabilised at G2/M, but not following PMA/IFN-α treatment.

6.7 Implications of A3A-mediated RNA editing activity in NIKS

RNA editing can aid proteomic adaptation to various stimuli though is also implicated in neurological diseases and cancer (Christofi and Zaravinos, 2019); and whilst the APOBEC3 family are primarily known as DNA editors, mutating sequences in viral DNA that limits their replicative ability (Koito and Ikeda, 2013; Harris and Dudley, 2015), some APOBEC members have additional roles in editing host-RNA: APOBEC1 edits and truncates apoB, a component of lipid transportation (Chen *et al.*, 1987; Powell *et al.*, 1987); AID RNA editing has important roles in antibody diversification (Muramatsu *et al.*, 2000; Revy *et al.*, 2000); A3G edits RNA which encodes proteins that may impact viral pathogenesis (Sharma *et al.*, 2016); and A3A edits numerous RNA transcripts in macrophages during M1 polarisation, favourable to the immune response (Sharma *et al.*, 2015).

RNA editing also increases transcript and protein diversity and can serve as a source of self-generated auto-antigens in normal tissue, as well as tumour neo-antigens that are presented on the major histocompatibility complex (MHC) for immune activation (Roth *et al.*, 2018; Zhang *et al.*, 2018). Hence RNA editing is a means by which some APOBEC family members may complement their antiviral activity and enhance immune activation. However, A3A may also contribute towards immune evasion through upregulation of PD-L1 (a negative regulator of T-cell activity) expression on the cell-surface, though this did not occur via interferon signalling and may instead be on dependent on replication-associated DNA damage (Zhao *et al.*, 2021).

Whole exome and mRNA sequencing data found high frequency of APOBEC3-mediated RNA editing in both breast tumours and normal adjacent tissue, of which SERPINA1 and DDOST were the most frequently edited; additionally, RNA editing correlated with increased immune activity and improved patient survival (Asaoka *et al.*, 2019). Specifically, A3A was found to be responsible for DDOST RNA editing in tumour samples (Jalili *et al.*, 2020). DDOST is a component of the N-glycosylation machinery in the endoplasmic reticulum and has important roles including signal transduction and protein folding (Jones *et al.*, 2012), and many viruses are dependent on glycosylation for both immune evasion and to modify their viral proteins (Vigerust and Shepherd, 2007). Moreover, DDOST down-regulation has been found to inhibit the replication of flaviviruses (Petrova *et al.*, 2019).

We found that A3A also robustly edits DDOST RNA upon release from quiescence (at a far higher frequency), indicating that A3A is catalytically active under these conditions. Editing occurred most robustly after 18 hr re-stimulation and followed similar kinetics to A3A protein expression (with zero editing in the A3A KO NIKS). A3A-mediated editing of DDOST RNA (at position 558) generates a synonymous change: AUC-to-AUU (both isoleucine). Codons can be categorised as rare or common and the rate of translation elongation is dependent on the abundance of their cognate tRNA (Richter and Coller, 2015). Furthermore, RT-PCR of tRNAs in S. *cerevisiae* found that UAG (tRNA for AUC) is upregulated by cellular stresses, and UAA (tRNA for AUU) is downregulated (Torrent *et al.*, 2018).

Additionally, Guimaraes *et al.* (2020) found that mRNA of proliferative genes are enriched in rare codons which confers differential expression potential at different stages of the cell-cycle: particularly AUC is a G1-preferred codon, whereas AUU is G2/M preferred.

Whilst the downstream effect of DDOST RNA editing is not yet known, we can speculate that it may impact the rate/preference of translation in a cell-phase specific manner. Whilst investigating the downstream effect on protein expression we may first need to establish whether A3A is being expressed in all cells following re-stimulation or restricted to cells within specific cell-cycle phases (hence whether A3A-mediated RNA editing is occurring in all cells). If A3A is specific to G1-phase for example, RNA editing would change the DDOST codon to a less preferentially translated version and thus may slow down rate of translation.

However, if A3A KO NIKS have a greater percentage of G2/M-phase (due to their increased proliferation) their original AUC codon would not be favoured, hence total DDOST might also appear relatively less across an entire population. Furthermore, the assay explicitly quantifies DDOST RNA editing, therefore A3A potentially edits many additional transcripts under these conditions.

6.8 Future work

6.8.1 Elucidating mechanisms of A3A activation

A3A induction is sensitive to EGFR and downstream MAPK (MEK, ERK) inhibition, but not PI3K/AKT/mTOR inhibition. Further investigation is required (including varying concentrations, drugs, and biological repeats) to build a comprehensive understanding of the upstream pathways of activation.

Increased transcriptional activity was found in starved cells though without additional increase upon activation (at 3 hr); therefore further ChIP-qPCR will be performed (on earlier time-points) to both investigate whether there is earlier increased transcriptional activity and to potentially identify transcriptional activators. Promoter-proximal pausing can be further investigated using 5' RACE to identify active A3A promoter and enhancer interactions and mapped using circularised-chromatin-conformation-capture-sequencing (4C-seq), comparing architecture changes with A3A gene expression changes.

6.8.2 A3A cell-phase specific subcellular localisation

To elucidate whether A3A is expressed in all cells during cell-cycle re-entry: co-staining A3A with a DNA stain followed by flow cytometry analysis would establish which phase-specific populations A3A expressing cells exist. Alternatively, cells can be sorted based on their DNA content followed by qPCR analysis to establish A3A relative quantity within distinct cell-cycle phase cells.

Super-resolution imaging (such as STORM) would further the investigation into A3As sub-cellular localisation; and combined with cell-cycle specific markers (such as geminin) could help validate in which cells A3A expression occurs. Conducted over a time-course would also allow us to assess if there are any changes to the subcellular localisation (during S-phase for example).

6.8.3 A3A-mediated RNA deamination events

A3A edits DDOST RNA, however further validation of its catalytic activity will be performed with quantitative and qualitative deaminase assays. Additionally, validation of whether DDOST editing also occurs in MCF-10A and primary (NHEK) keratinocytes following A3A activation (by ddPCR).

Other A3A-mediated RNA editing events upon re-stimulation of NIKS can be identified using RNA-sequencing (compared against the A3A KO NIKS), following which, investigation of downstream protein expression changes may link A3A activity to cellular function.

6.9 Summary

We have found that endogenous A3B is differentially expressed during G2/M of the cell-cycle (in proliferating NIKS) and whilst the mechanism and function has not been explored further, this is potentially favourable to cell-cycle progression.

Exogenous overexpression of A3A causes cell-cycle arrest and this was attributed to its genotoxic effects, however we found striking A3A induction upon cell cycle re-entry induced by EGF (at far greater abundance than with known inducers) with no overt genotoxic effects and propose that A3A performs an important function that is tightly regulated. Furthermore, deletion of A3A causes a significant increase in cell proliferation and therefore may have a previously unappreciated physiological role in cell-cycle control during the re-activation of quiescent cells.

As summarised in Figure 6-3, A3A transcription increases in quiescent cells through starvation or stress, and we propose that proximal promoter pausing facilitates the rapid transcriptional activation upon growth factor re-stimulation.

A3A induction leads to robust editing of host-RNA DDOST (and potentially others) which may confer antiviral activity and immune activation. A3A is similarly induced in primary keratinocytes (NHEK), normal breast epithelial cells (MCF-10A), and potentially other normal epithelial cells; though is down-regulated in bladder carcinoma (BFTC-905) cells, cervical cancer (SiHa and HeLa) cells, and in NIKS stably expressing HPV16 oncogenes or the whole HPV16 genome.

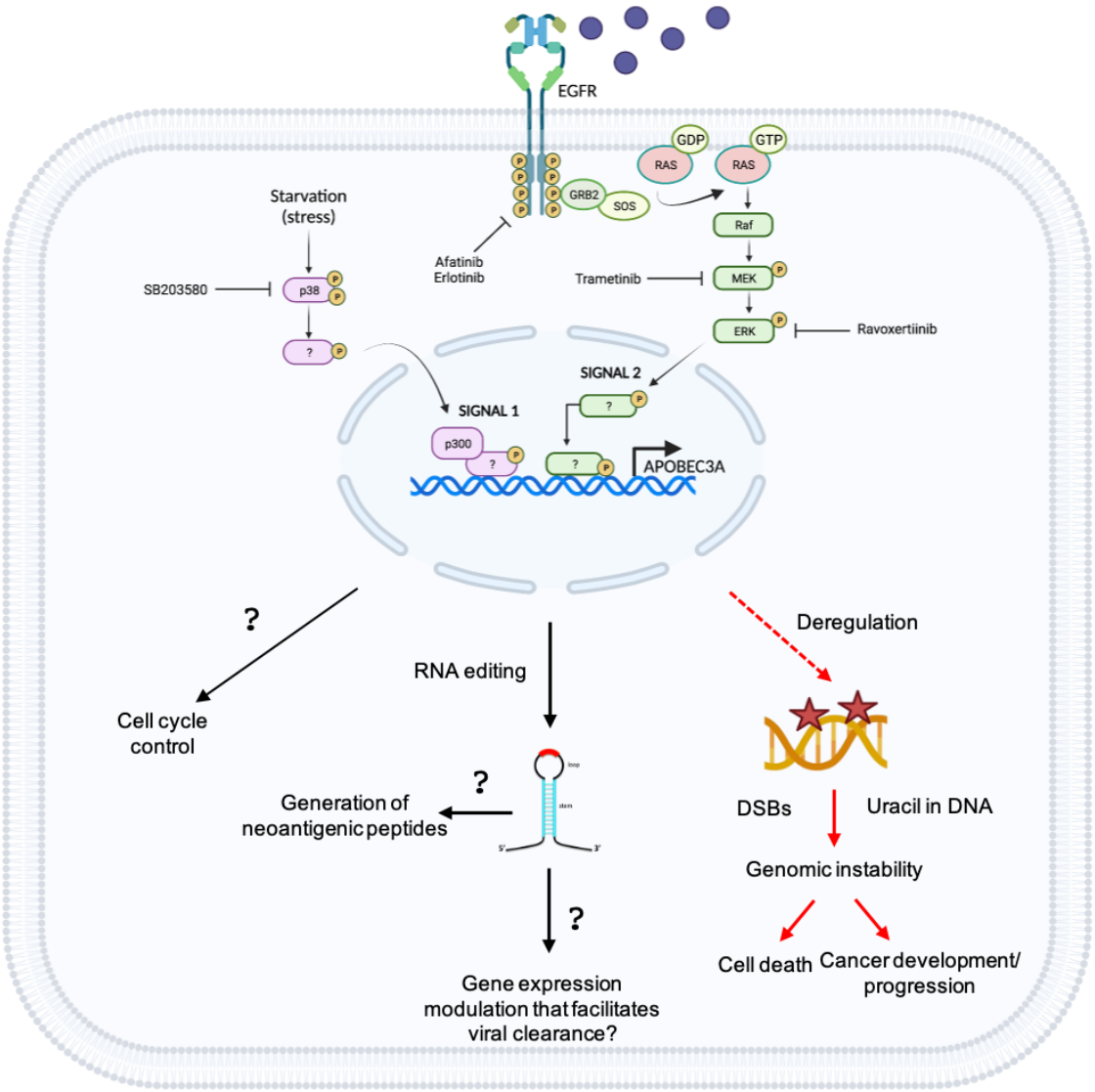

Figure 6-3 A3A transcriptional activation and potential downstream effects.
A3A is transcriptionally upregulated during starvation, mediated through the p38-MAPK pathway (Signal 1). Rapid transcriptional upregulation occurs through growth factor stimulation via EGFR/RAS/MAPK signalling (Signal 2). A3A activity suppresses cell proliferation through an unknown mechanism. Upregulation following re-stimulation leads to robust editing of host-RNA DDOST and potentially others, which may generate antigenic peptides and/or facilitate gene modulation that aids immune responses and viral clearance. Though there were no overt genotoxic effects (DNA DSB or abasic site formation), the regulation of A3A is unknown and deregulation of this mechanism could potentially lead to cell death, or cancer development/progression.

7 References

Abe, T. and Barber, G. N. (2014) ‘Cytosolic-DNA-mediated, STING-dependent proinflammatory gene induction necessitates canonical NF-κB activation through TBK1.’, *Journal of virology*, 88(10), pp. 5328–5341. doi: 10.1128/JVI.00037-14.

Adelman, K. *et al.* (2009) ‘Immediate mediators of the inflammatory response are poised for gene activation through RNA polymerase II stalling.’, *Proceedings of the National Academy of Sciences of the United States of America*, 106(43), pp. 18207–18212. doi: 10.1073/pnas.0910177106.

Aderem, A. and Underhill, D. M. (1999) ‘Mechanisms of phagocytosis in macrophages’, *Annual Review of Immunology*. Annual Reviews, 17(1), pp. 593–623. doi: 10.1146/annurev.immunol.17.1.593.

Adolph, M. B. *et al.* (2017) ‘Enzyme cycling contributes to efficient induction of genome mutagenesis by the cytidine deaminase APOBEC3B’, *Nucleic Acids Research*, 45(20), pp. 11925–11940. doi: 10.1093/nar/gkx832.

Ahasan, M. M. *et al.* (2015) ‘APOBEC3A and 3C decrease human papillomavirus 16 pseudovirion infectivity’, *Biochemical and Biophysical Research Communications*, 457(3), pp. 295–299. doi: 10.1016/j.bbrc.2014.12.103.

Al-Ani, A. *et al*., 'Oxygenation in cell culture: Critical parameters for reproducibility are routinely not reported.” *PloS one* vol. 13,10 e0204269. 16 Oct. 2018, doi:10.1371/journal.pone.0204269

Alexandrov, L. B. *et al.* (2013) ‘Signatures of mutational processes in human cancer’, *Nature*, 500(7463), pp. 415–421. doi: 10.1038/nature12477.

Alexandrov, L. B. *et al.* (2020) ‘The repertoire of mutational signatures in human cancer’, *Nature*, 578(7793), pp. 94–101. doi: 10.1038/s41586-020-1943-3.

Allen-Hoffmann, B. L. *et al.* (2000) ‘Normal Growth and Differentiation in a Spontaneously Immortalized Near-Diploid Human Keratinocyte Cell Line, NIKS’, *Journal of Investigative Dermatology*, 114(3), pp. 444–455. doi: 10.1046/j.1523-1747.2000.00869.x.

Almine, J. F. *et al.* (2017) ‘IFI16 and cGAS cooperate in the activation of STING during DNA sensing in human keratinocytes’, *Nature Communications*, 8(1), pp. 1–15. doi: 10.1038/ncomms14392.

Alqassim, E. Y. *et al.* (2021) ‘RNA editing enzyme APOBEC3A promotes pro-inflammatory M1 macrophage polarization’, *Communications Biology*. Nature Research, 4(1), pp. 1–11. doi: 10.1038/s42003-020-01620-x.

Anant, S. and Davidson, N. O. (2000) ‘An AU-Rich Sequence Element (UUUN[A/U]U) Downstream of the Edited C in Apolipoprotein B mRNA Is a High-Affinity Binding Site for Apobec-1: Binding of Apobec-1 to This Motif in the 3’ Untranslated Region of c-myc Increases mRNA Stability’, *Molecular and Cellular Biology*, 20(6), pp. 1982–1992. doi: 10.1128/mcb.20.6.1982-1992.2000.

Anant, S., MacGinnitie, A. J. and Davidson, N. O. (1995) 'apobec-1, the catalytic subunit of the mammalian apolipoprotein B mRNA editing enzyme, is a novel RNA-binding protein', *Journal of Biological Chemistry*, 270(24), pp. 14762–14767. doi: 10.1074/jbc.270.24.14762.

Argyris, E. G. *et al.* (2007) 'The interferon-induced expression of APOBEC3G in human blood-brain barrier exerts a potent intrinsic immunity to block HIV-1 entry to central nervous system', *Virology*, 367(2), pp. 440–451. doi: 10.1016/j.virol.2007.06.010.

Asaoka, M. *et al.* (2019) 'APOBEC3-Mediated RNA Editing in Breast Cancer is Associated with Heightened Immune Activity and Improved Survival', *International Journal of Molecular Sciences*. doi: 10.3390/ijms20225621.

Aynaud, M.-M. *et al.* (2012) 'Human Tribbles 3 protects nuclear DNA from cytidine deamination by APOBEC3A.', *The Journal of biological chemistry*, 287(46), pp. 39182–39192. doi: 10.1074/jbc.M112.372722.

Baeuerle, P. A. and Baltimore, D. (1989) 'A 65-kappaD subunit of active NF-kappaB is required for inhibition of NF-kappaB by I kappaB.', *Genes & development*, 3(11), pp. 1689–1698. doi: 10.1101/gad.3.11.1689.

Ballard, D. W. *et al.* (1990) 'The v-rel oncogene encodes a κB enhancer binding protein that inhibits NF-κB function', *Cell*, 63(4), pp. 803–814. doi: 10.1016/0092-8674(90)90146-6.

Barrandon, Y. and Green, H. (1985) 'Cell size as a determinant of the clone-forming ability of human keratinocytes', *Proceedings of the National Academy of Sciences of the United States of America*, 82(16), pp. 5390–5394. doi: 10.1073/pnas.82.16.5390.

Batard, P. *et al.* (2000) 'TGF-β1 maintains hematopoietic immaturity by a reversible negative control of cell cycle and induces CD34 antigen up-modulation', *Journal of Cell Science*, 113(3), pp. 383–390. doi: 10.1242/jcs.113.3.383.

Baum, A. and García-Sastre, A. (2011) 'Differential recognition of viral RNA by RIG-I', *Virulence*, 2(2), pp. 166–169. doi: 10.4161/viru.2.2.15481.

Beger, R. D. and Bolton, P. H. (1998) 'Structures of apurinic and apyrimidinic sites in duplex DNAS', *Journal of Biological Chemistry*, 273(25), pp. 15565–15573. doi: 10.1074/jbc.273.25.15565.

Berger, G. *et al.* (2011) 'APOBEC3A Is a Specific Inhibitor of the Early Phases of HIV-1 Infection in Myeloid Cells', *PLoS Pathogens*, 7(9), p. e1002221. doi: 10.1371/journal.ppat.1002221.

Bertoli, C., Skotheim, J. M. and de Bruin, R. A. M. (2013) 'Control of cell cycle transcription during G1 and S phases', *Nature reviews. Molecular cell biology*, 14(8), pp. 518–528. doi: 10.1038/nrm3629.

Betts, J. C. and Nabel, G. J. (1996) 'Differential regulation of NF-kappaB2(p100) processing and control by amino-terminal sequences.', *Molecular and Cellular Biology*, 16(11), pp. 6363–6371. doi: 10.1128/mcb.16.11.6363.

Betts, L. *et al.* (1994) 'Cytidine deaminase. the 2.3 Å crystal structure of an enzyme: Transition-state analog complex', *Journal of Molecular Biology*, 235(2), pp. 635–656. doi: 10.1006/jmbi.1994.1018.

Beyazit, F. *et al.* (2018) 'The prevelance of human papillomavirus (HPV) genotypes detected by PCR in women with normal and abnormal cervico-vaginal cytology', *Ginekologia Polska*, 89(2), pp. 62–67. doi: 10.5603/GP.A2018.0011.

Bishop, K. N. *et al.* (2004) 'APOBEC-mediated editing of viral RNA', *Science*, 305(5684), p. 645. doi: 10.1126/science.1100658.

Blake, R. A. *et al.* (2000) 'SU6656, a selective src family kinase inhibitor, used to probe growth factor signaling', *Molecular and cellular biology*, 20(23), pp. 9018–9027. doi: 10.1128/MCB.20.23.9018-9027.2000.

Blanc, V. *et al.* (2001) 'Mutagenesis of Apobec-1 Complementation Factor Reveals Distinct Domains That Modulate RNA Binding, Protein-Protein Interaction with Apobec-1, and Complementation of C to U RNA-editing Activity', *Journal of Biological Chemistry*, 276(49), pp. 46386–46393. doi: 10.1074/jbc.M107654200.

Blanc, V., Kennedy, S. and Davidson, N. O. (2003) 'A Novel Nuclear Localization Signal in the Auxiliary Domain of Apobec-1 Complementation Factor Regulates Nucleocytoplasmic Import and Shuttling', *Journal of Biological Chemistry*, 278(42), pp. 41198–41204. doi: 10.1074/jbc.M302951200.

Blank, C. *et al.* (2006) 'Blockade of PD-L1 (B7-H1) augments human tumor-specific T cell responses iin vitro/i', *International Journal of Cancer*, 119(2), pp. 317–327. doi: 10.1002/ijc.21775.

Bockstaele, L. *et al.* (2006) 'Regulation of CDK4', *Cell Division*, p. 25. doi: 10.1186/1747-1028-1-25.

Bodily, J. and Laimins, L. A. (2011) 'Persistence of human papillomavirus infection: keys to malignant progression', *Trends in Microbiology*, 19(1), pp. 33–39. doi:10.1016/j.tim.2010.10.002.

Bogerd, H. P. *et al.* (2006) 'Cellular inhibitors of long interspersed element 1 and Alu retrotransposition', *Proceedings of the National Academy of Sciences*, 103(23), pp. 8780–8785. doi: 10.1073/pnas.0603313103.

Bogerd, H. P. *et al.* (2007) 'The intrinsic antiretroviral factor APOBEC3B contains two enzymatically active cytidine deaminase domains', *Virology*, 364(2), pp. 486–493. doi: 10.1016/j.virol.2007.03.019.

Bohn, M.-F. *et al.* (2015) 'The ssDNA Mutator APOBEC3A Is Regulated by Cooperative Dimerization', *Structure*, 23(5), pp. 903–911. doi: 10.1016/j.str.2015.03.016.

Boichard, A., Tsigelny, I. F. and Kurzrock, R. (2017) 'High expression of PD-1 ligands is associated with kataegis mutational signature and APOBEC3 alterations'. doi: 10.1080/2162402X.2017.1284719.

Bonvin, M. *et al.* (2006) 'Interferon-inducible expression of APOBEC3 editing enzymes in human hepatocytes and inhibition of hepatitis B virus replication', *Hepatology*. John Wiley & Sons, Ltd, 43(6), pp. 1364–1374. doi: 10.1002/hep.21187.

Bross, L. *et al.* (2002) 'DNA double-strand breaks: Prior to but not sufficient in targeting hypermutation', *Journal of Experimental Medicine*, 195(9), pp. 1187–1192. doi: 10.1084/jem.20011749.

Brouha, B. *et al.* (2003) 'Hot L1s account for the bulk of retrotransposition in the human population', *Proceedings of the National Academy of Sciences of the United States of America*, 100(9), pp. 5280–5285. doi: 10.1073/pnas.0831042100.

Bruns, A. M. *et al.* (2014) 'The Innate Immune Sensor LGP2 Activates Antiviral Signaling by Regulating MDA5-RNA Interaction and Filament Assembly', *Molecular Cell*, 55(5), pp. 771–781. doi: 10.1016/j.molcel.2014.07.003.

Buisson, R. *et al.* (2019) 'Passenger hotspot mutations in cancer driven by APOBEC3A and mesoscale genomic features', *Science*, 364(6447). doi: 10.1126/science.aaw2872.

Burns, K. *et al.* (1998) 'MyD88, an adapter protein involved in interleukin-1 signaling', *Journal of Biological Chemistry*, 273(20), pp. 12203–12209. doi: 10.1074/jbc.273.20.12203.

Burns, M. B. *et al.* (2013) 'APOBEC3B is an enzymatic source of mutation in breast cancer', *Nature*, 494(7437), pp. 366–370. doi: 10.1038/nature11881.

Burns, M. B., Temiz, N. A. and Harris, R. S. (2013) 'Evidence for APOBEC3B mutagenesis in multiple human cancers', *Nature Genetics*, 45(9), pp. 977–983. doi: 10.1038/ng.2701.

Byeon, I.-J. L. J. L. *et al.* (2013) 'NMR structure of human restriction factor APOBEC3A reveals substrate binding and enzyme specificity', *Nature Communications*, 4, p. 1890. doi: 10.1038/ncomms2883.

Capuani, F. *et al.* (2015) 'Quantitative analysis reveals how EGFR activation and downregulation are coupled in normal but not in cancer cells', *Nature Communications*, 6. doi: 10.1038/ncomms8999.

Cargnello, M. and Roux, P. P. (2011) 'Activation and function of the MAPKs and their substrates, the MAPK-activated protein kinases.', *Microbiology and molecular biology reviews*, 75(1), pp. 50–83. doi: 10.1128/MMBR.00031-10.

Carpenter, M. A. *et al.* (2012) 'Methylcytosine and normal cytosine deamination by the foreign DNA restriction enzyme APOBEC3A.', *The Journal of biological chemistry*, 287(41), pp. 34801–34808. doi: 10.1074/jbc.M112.385161.

Caval, V. *et al.* (2019) 'Mouse APOBEC1 cytidine deaminase can induce somatic mutations in chromosomal DNA', *BMC Genomics*, 20(1), p. 858. doi: 10.1186/s12864-019-6216-x.

Cescon, D. W., Haibe-Kains, B. and Mak, T. W. (2015) 'APOBEC3B expression in breast cancer reflects cellular proliferation, while a deletion polymorphism is associated with immune activation', *Proceedings of the National Academy of Sciences of the United States of America*, 112(9), pp. 2841–2846. doi: 10.1073/pnas.1424869112.

Chakravarthy, A. *et al.* (2016) 'Human Papillomavirus Drives Tumor Development Throughout the Head and Neck: Improved Prognosis Is Associated With an Immune Response Largely Restricted to the Oropharynx', *Journal of Clinical Oncology*, 34(34), pp. 4132–4141. doi: 10.1200/JCO.2016.68.2955.

Chan, K. *et al.* (2015) 'An APOBEC3A hypermutation signature is distinguishable from the signature of background mutagenesis by APOBEC3B in human cancers', *Nature Genetics*, 47(9), pp. 1067–1072. doi: 10.1038/ng.3378.

Chan, K., Resnick, M. A. and Gordenin, D. A. (2013) 'The choice of nucleotide inserted opposite abasic sites formed within chromosomal DNA reveals the polymerase activities participating in translesion DNA synthesis', *DNA Repair*, 12(11), pp. 878–889. doi: 10.1016/j.dnarep.2013.07.008.

Chassot, A.-A. *et al.* (2008) 'Confluence-induced cell cycle exit involves pre-mitotic CDK inhibition by p27Kip1 and cyclin D1 downregulation', *Cell Cycle*, 7(13), pp. 2038–2046. doi: 10.4161/CC.7.13.6233.

Chen, H. *et al.* (2006) 'APOBEC3A Is a Potent Inhibitor of Adeno-Associated Virus and Retrotransposons', *Current Biology*, 16(5), pp. 480–485. doi: 10.1016/j.cub.2006.01.031.

Chen, K. *et al.* (2006) 'Alpha Interferon Potently Enhances the Anti-Human Immunodeficiency Virus Type 1 Activity of APOBEC3G in Resting Primary CD4 T Cells', *Journal of Virology*, 80(15), pp. 7645–7657. doi: 10.1128/jvi.00206-06.

Chen, S. *et al.* (2015) 'APOBEC3A possesses anticancer and antiviral effects by differential inhibition of HPV E6 and E7 expression on cervical cancer.', *International journal of clinical and experimental medicine*, 8(7), pp. 10548–10557.http://www.ncbi.nlm.nih.gov/pubmed/26379844.

Chen, S. H. *et al.* (1987) 'Apolipoprotein B-48 is the product of a messenger RNA with an organ-specific in-frame stop codon', *Science*, 238(4825), pp. 363–366. doi: 10.1126/science.3659919.

Chen, Y. *et al.* (2018) 'APOBEC3B edits HBV DNA and inhibits HBV replication during reverse transcription', *Antiviral Research*, 149, pp. 16–25. doi: 10.1016/j.antiviral.2017.11.006.

Cheng, A. Z., Moraes, S. N., *et al.* (2019) 'A Conserved Mechanism of APOBEC3 Relocalization by Herpesviral Ribonucleotide Reductase Large Subunits', *Journal of Virology*, 93(23), pp. e01539-19. doi: 10.1128/jvi.01539-19.

Cheng, A. Z., Yockteng-Melgar, J., *et al.* (2019) 'Epstein-Barr virus BORF2 inhibits cellular APOBEC3B to preserve viral genome integrity', *Nature microbiology*, 4(1), p. 78. doi: 10.1038/S41564-018-0284-6.

Cheng, A. Z. *et al.* (2021) 'APOBECs and herpesviruses', *Viruses*. doi: 10.3390/v13030390.

Cheung, T. H. and Rando, T. A. (2013) 'Molecular regulation of stem cell quiescence', *Nature reviews*, 14(6), pp. 329–340. doi: 10.1038/nrm3591.

Chi, X., Li, Y. and Qiu, X. (2020) 'V(D)J recombination, somatic hypermutation and class switch recombination of immunoglobulins: mechanism and regulation', *Immunology*. doi: 10.1111/imm.13176.

Chiu, Y. H., MacMillan, J. B. and Chen, Z. J. (2009) 'RNA Polymerase III Detects Cytosolic DNA and Induces Type I Interferons through the RIG-I Pathway', *Cell*, 138(3), pp. 576–591. doi: 10.1016/j.cell.2009.06.015.

Chiu, Y. L. and Greene, W. C. (2008) 'The APOBEC3 cytidine deaminases: An innate defensive network opposing exogenous retroviruses and endogenous retroelements', *Annual Review of Immunology*, pp. 317–353. doi: 10.1146/annurev.immunol.26.021607.090350.

Chow, J. C. *et al.* (1999) 'Toll-like receptor-4 mediates lipopolysaccharide-induced signal transduction', *Journal of Biological Chemistry*, 274(16), pp. 10689–10692. doi: 10.1074/jbc.274.16.10689.

Christofi, T. and Zaravinos, A. (2019) 'RNA editing in the forefront of epitranscriptomics and human health', *Journal of Translational Medicine*, 17(1), p. 319. doi: 10.1186/s12967-019-2071-4.

Clijsters, L. *et al.* (2014) 'Inefficient degradation of cyclin B1 re-activates the spindle checkpoint right after sister chromatid disjunction.', *Cell cycle,* 13(15), pp. 2370–2378. doi: 10.4161/cc.29336.

Cohen, B. *et al.* (1995) 'Ligand-induced association of the type I interferon receptor components.', *Molecular and Cellular Biology*, 15(8), pp. 4208–4214. doi: 10.1128/mcb.15.8.4208.

Conticello, S. G. *et al.* (2005) 'Evolution of the AID/APOBEC Family of Polynucleotide (Deoxy)cytidine Deaminases', *Molecular Biology and Evolution*, 22(2), pp. 367–377. doi: 10.1093/molbev/msi026.

Cordaux, R. and Batzer, M. A. (2009) 'The impact of retrotransposons on human genome evolution', *Nature Reviews Genetics*, pp. 691–703. doi: 10.1038/nrg2640.

Core, L. and Adelman, K. (2019) 'Promoter-proximal pausing of RNA polymerase II: a nexus of gene regulation', *Genes & development*. 2019/05/23, 33(15–16), pp. 960–982. doi: 10.1101/gad.325142.119.

Cortez, L. M. *et al.* (2019) 'APOBEC3A is a prominent cytidine deaminase in breast cancer', *PLoS Genetics*, 15(12), p. e1008545. doi: 10.1371/journal.pgen.1008545.

Da Costa, R. M. G. *et al.* (2016) 'The NFkB signaling pathway in papillomavirus-induced lesions: Friend or foe?', *Anticancer Research*, 36(5), pp. 2073–2083.

Craig Venter, J. *et al.* (2001) 'The sequence of the human genome', *Science*, 291(5507), pp. 1304–1351. doi: 10.1126/science.1058040.

Creyghton, M. P. *et al.* (2010) 'Histone H3K27ac separates active from poised enhancers and predicts developmental state', *Proceedings of the National Academy of Sciences of the United States of America*, 107(50), pp. 21931–21936. doi: 10.1073/pnas.1016071107.

Crusius, K. *et al.* (1999) 'The human papillomavirus type 16 E5 protein modulates phospholipase C-gamma-1 activity and phosphatidyl inositol turnover in mouse fibroblasts', *Oncogene*, 18(48), pp. 6714–6718. doi: 10.1038/sj.onc.1203075.

D'Souza, G. and Dempsey, A. (2011) 'The role of HPV in head and neck cancer and review of the HPV vaccine.', *Preventive medicine*, 53 Suppl 1(Suppl 1), pp. S5–S11. doi: 10.1016/j.ypmed.2011.08.001.

Darnell, J. E., Kerr, I. M. and Stark, G. R. (1994) 'Jak-STAT pathways and transcriptional activation in response to IFNs and other extracellular signaling proteins', *Science*, 264(5164), pp. 1415–1421. doi: 10.1126/science.8197455.

Davidson, N. O. *et al.* (1995) 'Proposed nomenclature for the catalytic subunit of the mammalian apolipoprotein B mRNA editing enzyme: APOBEC-1.', *RNA*, p. 3.

Denli, A. M. *et al.* (2015) 'Primate-Specific ORF0 Contributes to Retrotransposon-Mediated Diversity', *Cell*, 163(3), pp. 583–593. doi: 10.1016/j.cell.2015.09.025.

Denning, M. F. *et al.* (1995) 'Cholesterol sulfate activates multiple protein kinase C isoenzymes and induces granular cell differentiation in cultured murine keratinocytes.', *Cell growth & differentiation : the molecular biology journal of the American Association for Cancer Research*, pp. 1619–1626. Available at: http://www.ncbi.nlm.nih.gov/pubmed/9019167.

Diermeier-Daucher, S. *et al.* (2009) 'Cell type specific applicability of 5-ethynyl-2′-deoxyuridine (EDU) for dynamic proliferation assessment in flow cytometry', *Cytometry Part A*, 75(6), pp. 535–546. doi: 10.1002/cyto.a.20712.

Dlugosz, A. A. *et al.* (1994) 'Keratinocyte growth factor receptor ligands induce transforming growth factor alpha expression and activate the epidermal growth factor receptor signaling pathway in cultured epidermal keratinocytes.', *Cell growth & differentiation : the molecular biology journal of the American Association for Cancer Research*, 5(12), pp. 1283–1292.

Dlugosz, A. A. and Yuspa, S. H. (1993) 'Coordinate changes in gene expression which Mark the spinous to granular cell transition in epidermis are regulated by protein kinase C', *Journal of Cell Biology*, 120(1), pp. 217–225. doi: 10.1083/jcb.120.1.217.

Doehle, B. P., Schäfer, A. and Cullen, B. R. (2005) 'Human APOBEC3B is a potent inhibitor of HIV-1 infectivity and is resistant to HIV-1 Vif', *Virology*, 339(2), pp. 281–288. doi: 10.1016/j.virol.2005.06.005.

Domanski, P. *et al.* (1995) 'Cloning and expression of a long form of the β subunit of the interferon αβ receptor that is required for signaling', *Journal of Biological Chemistry*, 270(37), pp. 21606–21611. doi: 10.1074/jbc.270.37.21606.

Dombroski, B. A. *et al.* (1991) 'Isolation of an active human transposable element', *Science*, 254(5039), pp. 1805–1808. doi: 10.1126/science.1662412.

Dyson, N. *et al.* (1989) 'The human papilloma virus-16 E7 oncoprotein is able to bind to the retinoblastoma gene product', *Science*, 243(4893), pp. 934–937. doi: 10.1126/science.2537532.

Egan, L. J. *et al.* (2003) 'Nuclear factor-κB activation promotes restitution of wounded intestinal epithelial monolayers', *American Journal of Physiology-Cell Physiology*, 285(5), pp. C1028–C1035. doi: 10.1152/ajpcell.00167.2003.

Eppihimer, M. J. *et al.* (2002) 'Expression and Regulation of the PD-L1 Immunoinhibitory Molecule on Microvascular Endothelial Cells', *Microcirculation*, 9(2), pp. 133–145. doi: 10.1038/sj.mn.7800123.

Esteban-Vives, R. *et al.* (2015) 'In vitro keratinocyte expansion for cell transplantation therapy is associated with differentiation and loss of basal layer derived progenitor population', *Differentiation*, 89(5), pp. 137–145. doi: https://doi.org/10.1016/j.diff.2015.05.002.

Falck, J. *et al.* (2001) 'The ATM-Chk2-Cdc25A checkpoint pathway guards against radioresistant DNA synthesis.', *Nature*, 410(6830), pp. 842–847. doi: 10.1038/35071124.

Faust, D. *et al.* (2012) 'Differential p38-dependent signalling in response to cellular stress and mitogenic stimulation in fibroblasts', *Cell Communication and Signaling*, 10(1), p. 6. doi: 10.1186/1478-811X-10-6.

Feng, Y. *et al.* (2017) 'Deamination-independent restriction of LINE-1 retrotransposition by APOBEC3H', *Scientific Reports*, 7(1), p. 10881. doi: 10.1038/s41598-017-11344-4.

Fitzgerald, K. A. *et al.* (2003) 'LPS-TLR4 signaling to IRF-3/7 and NF-κB involves the toll adapters TRAM and TRIF', *Journal of Experimental Medicine*, 198(7), pp. 1043–1055. doi: 10.1084/jem.20031023.

Fleischmann, G. *et al.* (2009) 'Growth characteristics of the nonhuman primate embryonic stem cell line cjes001 depending on feeder cell treatment.', *Cloning and stem cells*, 11(2), pp. 225–233. doi: 10.1089/clo.2008.0064.

Forman, D. *et al.* (2012) 'Global Burden of Human Papillomavirus and Related Diseases', *Vaccine*, 30, pp. F12–F23. doi: 10.1016/j.vaccine.2012.07.055.

Fortunel, N. O. *et al.* (2003) 'Long-term expansion of human functional epidermal precursor cells: Promotion of extensive amplification by low TGF-β1 concentrations', *Journal of Cell Science*, 116(19), pp. 4043–4052. doi: 10.1242/jcs.00702.

Fossat, N. *et al.* (2014) ' C to U RNA editing mediated by APOBEC 1 requires RNA - binding protein RBM 47 ', *EMBO reports*, 15(8), pp. 903–910. doi: 10.15252/embr.201438450.

Foster, D. A. *et al.* (2010) 'Regulation of G1 cell cycle progression: Distinguishing the restriction point from a nutrient-sensing cell growth checkpoint(s)', *Genes and Cancer*, 1(11), pp. 1124–1131. doi: 10.1177/1947601910392989.

Frey, M. R., Golovin, A. and Brent Polk, D. (2004) 'Epidermal Growth Factor-stimulated Intestinal Epithelial Cell Migration Requires Src Family Kinase-dependent p38 MAPK Signaling*'. JBC. doi: 10.1074/jbc.M406253200.

Fu, Yang *et al.* (2015) 'DNA cytosine and methylcytosine deamination by APOBEC3B: enhancing methylcytosine deamination by engineering APOBEC3B', *Biochemical Journal*, 471(Pt 1), p. 25. doi: 10.1042/BJ20150382.

Fu, Y *et al.* (2015) 'DNA cytosine and methylcytosine deamination by APOBEC3B: enhancing methylcytosine deamination by engineering APOBEC3B', *Biochemical Journal*, 471(1), pp. 25–35. doi: 10.1042/BJ20150382.

Furuno, N., den Elzen, N. and Pines, J. (1999) 'Human Cyclin a Is Required for Mitosis until Mid Prophase', *Journal of Cell Biology*, 147(2), pp. 295–306. doi: 10.1083/jcb.147.2.295.

Galavazi, G., Schenk, H. and Bootsma, D. (1966) 'Synchronization of mammalian cells in vitro by inhibition of the DNA synthesis. I. Optimal conditions', *Experimental Cell Research*, 41(2), pp. 428–437. doi: 10.1016/S0014-4827(66)80149-0.

Gallois-Montbrun, S. *et al.* (2007) 'Antiviral Protein APOBEC3G Localizes to Ribonucleoprotein Complexes Found in P Bodies and Stress Granules', *Journal of Virology*, 81(5), pp. 2165–2178. doi: 10.1128/jvi.02287-06.

Gandarillas, A., Davies, D. and Blanchard, J. M. (2000) 'Normal and c-Myc-promoted human keratinocyte differentiation both occur via a novel cell cycle involving cellular growth and endoreplication', *Oncogene*, 19(29), pp. 3278–3289. doi: 10.1038/sj.onc.1203630.

Gansmo, L. B. *et al.* (2017) 'APOBEC3A/B deletion polymorphism and cancer risk', *Carcinogenesis*. doi: 10.1093/carcin/bgx131.

Garcia-Diaz, A. *et al.* (2017) 'Interferon Receptor Signaling Pathways Regulating PD-L1 and PD-L2 Expression', *Cell Reports*, 19(6), pp. 1189–1201. doi: 10.1016/j.celrep.2017.04.031.

Ghosh, S. *et al.* (1990) 'Cloning of the p50 DNA binding subunit of NF-κB: Homology to rel and dorsal', *Cell*, 62(5), pp. 1019–1029. doi: 10.1016/0092-8674(90)90276-K.

Gilmour, D. S. and Lis, J. T. (1986) 'RNA polymerase II interacts with the promoter region of the noninduced hsp70 gene in Drosophila melanogaster cells.', *Molecular and cellular biology*, 6(11), pp. 3984–3989. doi: 10.1128/mcb.6.11.3984-3989.1986.

Ginzberg, M. B. *et al.* (2018) 'Cell size sensing in animal cells coordinates anabolic growth rates and cell cycle progression to maintain cell size uniformity', *eLife*, 7, pp. 1–27. doi: 10.7554/eLife.26957.

Goel, S. *et al.* (2018) 'CDK4/6 Inhibition in Cancer: Beyond Cell Cycle Arrest', *Trends in Cell Biology*, pp. 911–925. doi: 10.1016/j.tcb.2018.07.002.

Goila-Gaur, R. *et al.* (2007) 'Targeting APOBEC3A to the viral nucleoprotein complex confers antiviral activity', *Retrovirology*, 4(1), p. 61. doi: 10.1186/1742-4690-4-61.

Gong, D. and Ferrell, J. E. J. (2010) 'The roles of cyclin A2, B1, and B2 in early and late mitotic events.', *Molecular biology of the cell*, 21(18), pp. 3149–3161. doi: 10.1091/mbc.E10-05-0393.

Görlich, D. and Kutay, U. (1999) 'Transport between the cell nucleus and the cytoplasm', *Annual Review of Cell and Developmental Biology*, pp. 607–660. doi: 10.1146/annurev.cellbio.15.1.607.

Gowrishankar, K. *et al.* (2015) 'Inducible but not constitutive expression of PD-L1 in human melanoma cells is dependent on activation of NF-κB', *PLoS ONE*, 10(4). doi: 10.1371/journal.pone.0123410.

Green, A. M. *et al.* (2016) 'APOBEC3A damages the cellular genome during DNA replication', *Cell Cycle*, 15(7), pp. 998–1008. doi: 10.1080/15384101.2016.1152426.

Green, A. M. *et al.* (2021) 'Interaction with the CCT chaperonin complex limits APOBEC3A cytidine deaminase cytotoxicity', *EMBO reports*, 22(9), p. e52145. doi: https://doi.org/10.15252/embr.202052145.

Green, H. (1978) 'Cyclic AMP in relation to proliferation of the epidermal cell: a new view.', *Cell*, 15(3), pp. 801–811. doi: 10.1016/0092-8674(78)90265-9.

Griffiths, G. M. *et al.* (1984) 'Somatic mutation and the maturation of immune response to 2-phenyl oxazolone', *Nature*, 312(5991), pp. 271–275. doi: 10.1038/312271a0.

Guimaraes, J. C. *et al.* (2020) 'A rare codon-based translational program of cell proliferation', *Genome Biology*, 21(1), p. 44. doi: 10.1186/s13059-020-1943-5.

Hammouda, M. B. *et al.* (2020) 'The JNK Signaling Pathway in Inflammatory Skin Disorders and Cancer', *Cells*, 9(4), p. 857. doi: 10.3390/cells9040857.

Han, J. *et al.* (1994) 'A MAP kinase targeted by endotoxin and hyperosmolarity in mammalian cells', *Science*, 265(5173), pp. 808–811. doi: 10.1126/science.7914033.

Hanson, K. D. *et al.* (1994) 'Effects of c-myc expression on cell cycle progression.', *Molecular and cellular biology*, 14(9), pp. 5748–5755. doi: 10.1128/mcb.14.9.5748-5755.1994.

Haradhvala, N. J. *et al.* (2016) 'Mutational Strand Asymmetries in Cancer Genomes Reveal Mechanisms of DNA Damage and Repair', *Cell*, 164, pp. 538–549. doi: 10.1016/j.cell.2015.12.050.

Harper, E. G., Alvares, S. M. and Carter, W. G. (2005) 'Wounding activates p38 map kinase and activation transcription factor 3 in leading keratinocytes', *Journal of Cell Science*, 118(15), pp. 3471–3485. doi: 10.1242/jcs.02475.

Harris, R. S. *et al.* (2002) 'AID Is Essential for Immunoglobulin V Gene Conversion in a Cultured B Cell Line' *Current Biology*. Mar 5;12(5):435-8. doi: 10.1016/s0960-9822(02)00717-0. PMID: 11882297.

Harris, R. S. (2015) 'Molecular mechanism and clinical impact of APOBEC3B-catalyzed mutagenesis in breast cancer', *Breast Cancer Research*, pp. 1–10. doi: 10.1186/s13058-014.

Harris, R. S. and Dudley, J. P. (2015) 'APOBECs and virus restriction', *Virology*, pp. 131–145. doi: 10.1016/j.virol.2015.03.012.

Harris, R. S., Petersen-Mahrt, S. K. and Neuberger, M. S. (2002) 'RNA editing enzyme APOBEC1 and some of its homologs can act as DNA mutators', *Molecular Cell*, 10(5), pp. 1247–1253. doi: 10.1016/S1097-2765(02)00742-6.

Hasan, U. A. *et al.* (2007) 'TLR9 Expression and Function Is Abolished by the Cervical Cancer-Associated Human Papillomavirus Type 16', *The Journal of Immunology*, 178(5), pp. 3186–3197. doi: 10.4049/jimmunol.178.5.3186.

Haug, T. *et al.* (1998) 'Regulation of expression of nuclear and mitochondrial forms of human uracil-DNA glycosylase', *Nucleic Acids Research*, 26(6), pp. 1449–1457. doi: 10.1093/nar/26.6.1449.

Helleday, T., Eshtad, S. and Nik-Zainal, S. (2014) 'Mechanisms underlying mutational signatures in human cancers', *Nature Reviews Genetics*, pp. 585–598. doi: 10.1038/nrg3729.

Henderson, S. *et al.* (2014) 'APOBEC-Mediated Cytosine Deamination Links PIK3CA Helical Domain Mutations to Human Papillomavirus-Driven Tumor Development', *Cell Reports*, 7(6), pp. 1833–1841. doi: 10.1016/j.celrep.2014.05.012.

Henderson, S. and Fenton, T. (2015) 'APOBEC3 genes: Retroviral restriction factors to cancer drivers', *Trends in Molecular Medicine*, pp. 274–284. doi: 10.1016/j.molmed.2015.02.007.

Hirose, Y. *et al.* (2018) 'Within-Host Variations of Human Papillomavirus Reveal APOBEC Signature Mutagenesis in the Viral Genome.', *Journal of virology*, 92(12). doi: 10.1128/JVI.00017-18.

Holden, N. S. *et al.* (2008) 'Phorbol ester-stimulated NF-κB-dependent transcription: Roles for isoforms of novel protein kinase C', *Cellular Signalling*, 20(7), pp. 1338–1348. Available at: https://www.sciencedirect.com/science/article/pii/S0898656808000909 via%3Dihub.

Holder, J., Mohammed, S. and Barr, F. A. (2020) 'Ordered dephosphorylation initiated by the selective proteolysis of cyclin B drives mitotic exit', *eLife*, 9, p. e59885. doi: 10.7554/eLife.59885.

Honda, K., Takaoka, A. and Taniguchi, T. (2006) 'Type I interferon [corrected] gene induction by the interferon regulatory factor family of transcription factors.', *Immunity*. Elsevier, pp. 349–360. doi: 10.1016/j.immuni.2006.08.009.

Hong, H. S. *et al.* (2020) 'Proinflammatory cytokine TNFα promotes HPV-associated oral carcinogenesis by increasing cancer stemness', *International Journal of Oral Science*, 12(1), pp. 1–10. doi: 10.1038/s41368-019-0069-7.

Huff, A. L. *et al.* (2018) 'APOBEC3 Mediates Resistance to Oncolytic Viral Therapy', *Molecular Therapy - Oncolytics*, 11, pp. 1–13. doi: 10.1016/j.omto.2018.08.003.

Huibregtse, J. M., Scheffner, M. and Howley, P. M. (1991) 'A cellular protein mediates association of p53 with the E6 oncoprotein of human papillomavirus types 16 or 18', *Embo J*, 10(13), pp. 4129–4135. doi: 10.1002/j.1460-2075.1991.tb04990.x.

Hultquist, J. F. *et al.* (2011) 'Human and Rhesus APOBEC3D, APOBEC3F, APOBEC3G, and APOBEC3H Demonstrate a Conserved Capacity To Restrict Vif-Deficient HIV-1', *Journal of Virology*, 85(21), pp. 11220–11234. doi: 10.1128/JVI.05238-11.

Huthoff, H. *et al.* (2009) 'RNA-dependent oligomerization of APOBEC3G Is required for restriction of HIV-1', *PLoS Pathogens*, 5(3). doi: 10.1371/journal.ppat.1000330.

Ikeda, T. *et al.* (2008) 'The antiretroviral potency of APOBEC1 deaminase from small animal species', *Nucleic Acids Research*, 36, pp. 6859–6871. doi: 10.1093/nar/gkn802.

Ikeda, T. *et al.* (2011) 'Intrinsic restriction activity by apolipoprotein B mRNA editing enzyme APOBEC1 against the mobility of autonomous retrotransposons', *Nucleic Acids Research*, 39(13), pp. 5538–5554. doi: 10.1093/nar/gkr124.

Ito, S. *et al.* (2004) 'Activation-induced cytidine deaminase shuttles between nucleus and cytoplasm like apolipoprotein B mRNA editing catalytic polypeptide 1', *Proceedings of the National Academy of Sciences of the United States of America*, 101(7), pp. 1975–1980. doi: 10.1073/pnas.0307335101.

Ivanova, I. A., D'Souza, S. J. A. and Dagnino, L. (2006) 'E2F1 stability is regulated by a novel-PKC/p38β MAP kinase signaling pathway during keratinocyte differentiation', *Oncogene*, 25(3), pp. 430–437. doi: 10.1038/sj.onc.1208999.

Iwatani, Y. *et al.* (2006) 'Biochemical Activities of Highly Purified, Catalytically Active Human APOBEC3G: Correlation with Antiviral Effect', *Journal of Virology*, 80(12), pp. 5992–6002. doi: 10.1128/jvi.02680-05.

Jackson, P. K. *et al.* (1995) 'Early events in DNA replication require cyclin E and are blocked by p21CIP1', *The Journal of cell biology*, 130(4), pp. 755–769. doi: 10.1083/jcb.130.4.755.

Jacquemin, P. *et al.* (1996) 'A Novel Family of Developmentally Regulated Mammalian Transcription Factors Containing the TEA / ATTS DNA Binding Domain', *Journal of Biological Chemistry*, 271(36), pp. 21775–21785.

Jalili, P. *et al.* (2020) 'Quantification of ongoing APOBEC3A activity in tumor cells by monitoring RNA editing at hotspots', *Nature Communications*, 11(1), pp. 1–13. doi: 10.1038/s41467-020-16802-8.

James, M. A., Lee, J. H. and Klingelhutz, A. J. (2006) 'Human Papillomavirus Type 16 E6 Activates NF-B, Induces cIAP-2 Expression, and Protects against Apoptosis in a PDZ Binding Motif-Dependent Manner', *Journal of Virolgy*, 80(11), pp. 5301–5307. doi: 10.1128/JVI.01942-05.

Jarmuz, A. *et al.* (2002) 'An anthropoid-specific locus of orphan C to U RNA-editing enzymes on chromosome 22', *Genomics*. doi: 10.1006/geno.2002.6718.

Jones, M. A. *et al.* (2012) 'DDOST mutations identified by whole-exome sequencing are implicated in congenital disorders of glycosylation', *American journal of human genetics*, 90(2), pp. 363–368. doi: 10.1016/j.ajhg.2011.12.024.

Jonkers, I., Kwak, H. and Lis, J. T. (2014) 'Genome-wide dynamics of Pol II elongation and its interplay with promoter proximal pausing, chromatin, and exons.', *eLife*, 3, p. e02407. doi: 10.7554/eLife.02407.

Kanu, N. *et al.* (2016) 'DNA replication stress mediates APOBEC3 family mutagenesis in breast cancer', *Genome Biology*, 17(1), p. 185. doi: 10.1186/s13059-016-1042-9.

Karim, R. *et al.* (2013) 'Human Papillomavirus (HPV) Upregulates the Cellular Deubiquitinase UCHL1 to Suppress the Keratinocyte's Innate Immune Response', *PLoS Pathogens*, 9(5)..

Karwacz, K. *et al.* (2011) 'PD-L1 co-stimulation contributes to ligand-induced T cell receptor down-modulation on CD8 sup+/sup T cells', *EMBO Molecular Medicine*, 3(10), pp. 581–592. doi: 10.1002/emmm.201100165.

Kashem, S. W., Haniffa, M. and Kaplan, D. H. (2017) 'Antigen-Presenting Cells in the Skin'. *Annual Review of Immunology*, Apr 26;35:469-499. doi: 10.1146/annurev-immunol.

Kato, H. *et al.* (2006) 'Differential roles of MDA5 and RIG-I helicases in the recognition of RNA viruses', *Nature*, 441(1), pp. 101–105. doi: 10.1038/nature04734.

Kazanietz, M. G. *et al.* (2000) 'Pharmacology of the receptors for the phorbol ester tumor promoters: Multiple receptors with different biochemical properties', *Biochemical Pharmacology*, 60(10), pp. 1417–1424. doi: 10.1016/S0006-2952(00)00470-6.

Keir, M. E. *et al.* (2008) 'PD-1 and Its Ligands in Tolerance and Immunity', *Annual Review of Immunology*, 26(1), pp. 677–704. doi: 10.1146/annurev.immunol.26.021607.090331.

Kerur, N. *et al.* (2011) 'IFI16 acts as a nuclear pathogen sensor to induce the inflammasome in response to Kaposi Sarcoma-associated herpesvirus infection', *Cell Host and Microbe*, 9(5), pp. 363–375. doi: 10.1016/j.chom.2011.04.008.

Kim, H. and Seed, B. (2010) 'The transcription factor MafB antagonizes antiviral responses by blocking recruitment of coactivators to the transcription factor IRF3', *Nature Immunology*, 11(8), pp. 743–750. doi: 10.1038/ni.1897.

Kinomoto, M. *et al.* (2007) 'All APOBEC3 family proteins differentially inhibit LINE-1 retrotransposition', *Nucleic Acids Research*, 35(9), pp. 2955–2964. doi: 10.1093/nar/gkm181.

Klonowska, K. *et al.* (2017) 'The 30 kb deletion in the APOBEC3 cluster decreases APOBEC3A and APOBEC3B expression and creates a transcriptionally active hybrid gene but does not associate with breast cancer in the European population.', *Oncotarget*, 8(44), pp. 76357–76374. doi: 10.18632/oncotarget.19400.

Knudsen, E. S. *et al.* (2017) 'Biological specificity of CDK4/6 inhibitors: Dose response relationship, in vivo signaling, and composite response signatures', *Oncotarget*, 8(27), pp. 43678–43691. doi: 10.18632/oncotarget.18435.

Ko, R. and Bennett, S. E. (2005) 'Physical and functional interaction of human nuclear uracil-DNA glycosylase with proliferating cell nuclear antigen', in *DNA Repair*, pp. 1421–1431. doi: 10.1016/j.dnarep.2005.08.006.

Koito, A. and Ikeda, T. (2013) 'Intrinsic immunity against retrotransposons by APOBEC cytidine deaminases', *Frontiers in Microbiology*. doi: 10.3389/fmicb.2013.00028.

Koning, Fransje A *et al.* (2009) 'Defining APOBEC3 Expression Patterns in Human Tissues and Hematopoietic Cell Subsets', *Journal of Virology*, 83(18), pp. 9474–9485. doi: 10.1128/JVI.01089-09.

Koning, F A *et al.* (2009) 'Defining APOBEC3 Expression Patterns in Human Tissues and Hematopoietic Cell Subsets', *Journal of Virology*, 83(18), pp. 9474–9485. doi: 10.1128/JVI.01089-09.

Koning, F. A. *et al.* (2011) 'Target Cell-Mediated Editing of HIV-1 cDNA by APOBEC3 Proteins in Human Macrophages', *Journal of Virology*, 85(24), pp. 13448–13452. doi: 10.1128/JVI.00775-11.

Kornbluth, R. S. *et al.* (1989) 'Interferons and bacterial lipopolysaccharide protect macrophages from productive infection by human immunodeficiency virus in vitro.', *The Journal of experimental medicine*, 169(3), pp. 1137–1151. doi: 10.1084/JEM.169.3.1137.

Kwak, H. *et al.* (2013) 'Precise maps of RNA polymerase reveal how promoters direct initiation and pausing.', *Science*, 339(6122), pp. 950–953. doi: 10.1126/science.1229386.

Lackey, L. *et al.* (2012) 'APOBEC3B and AID Have Similar Nuclear Import Mechanisms', *Journal of Molecular Biology*, 419(5), pp. 301–314. doi: 10.1016/j.jmb.2012.03.011.

Lackey, L. *et al.* (2013) 'Subcellular localization of the APOBEC3 proteins during mitosis and implications for genomic DNA deamination', *Cell Cycle*, 12(5), pp. 762–772. doi: 10.4161/cc.23713.

Lada, A. G. *et al.* (2011) 'Mutator effects and mutation signatures of editing deaminases produced in bacteria and yeast.', *Biochemistry*, 76(1), pp. 131–146. doi: 10.1134/s0006297911010135.

Lamb, R. and Ambler, C. A. (2013) 'Keratinocytes propagated in serum-free, feeder-free culture conditions fail to form stratified epidermis in a reconstituted skin model', *PloS one*, 8(1), pp. e52494–e52494. doi: 10.1371/journal.pone.0052494.

Land, A. M. *et al.* (2013) 'Endogenous APOBEC3A DNA Cytosine Deaminase Is Cytoplasmic and Nongenotoxic', *Journal of Biological Chemistry*. J Biol Chem, 288(24), pp. 17253–17260. doi: 10.1074/jbc.M113.458661.

Landén, N. X., Li, D. and Ståhle, M. (2016) 'Transition from inflammation to proliferation: a critical step during wound healing.', *Cellular and molecular life sciences*, 73(20), pp. 3861–3885. doi: 10.1007/s00018-016-2268-0.

Lander, E. S. *et al.* (2001) 'Initial sequencing and analysis of the human genome', *Nature*, 409(6822), pp. 860–921. doi: 10.1038/35057062.

Landry, S. *et al.* (2011) 'APOBEC3A can activate the DNA damage response and cause cell-cycle arrest', *EMBO Reports*, 12(5), pp. 444–450. doi: 10.1038/embor.2011.46.

LaRue, R. S. *et al.* (2009) 'Guidelines for Naming Nonprimate APOBEC3 Genes and Proteins', *Journal of Virology*, 83(2), pp. 494–497. doi: 10.1128/jvi.01976-08.

Lau, A. W. Y. and Brink, R. (2020) 'Selection in the germinal center', *Current Opinion in Immunology*, pp. 29–34. doi: 10.1016/j.coi.2019.11.001.

Lau, P. P. *et al.* (1991) 'Apolipoprotein B mRNA editing is an intranuclear event that occurs posttranscriptionally coincident with splicing and polyadenylation', *Journal of Biological Chemistry*, 266(30), pp. 20550–20554. doi: 10.1016/S0021-9258(18)54960-7.

Lauberth, S. M. *et al.* (2013) 'H3K4me3 interactions with TAF3 regulate preinitiation complex assembly and selective gene activation', *Cell*, 152(5), pp. 1021–1036. doi: 10.1016/j.cell.2013.01.052.

Law, E. K. *et al.* (2016) 'The DNA cytosine deaminase APOBEC3B promotes tamoxifen resistance in ER-positive breast cancer', *Science Advances*, 2(10), pp. e1601737–e1601737. doi: 10.1126/sciadv.1601737.

Lebre, M. C. *et al.* (2007) 'Human keratinocytes express functional Toll-like receptor 3, 4, 5, and 9.', *Journal of Investigative Dermatology*, 127(2), pp. 331–341. doi: 10.1038/sj.jid.5700530.

Lee, S. W. S. J. *et al.* (2006) 'Interferon regulatory factor-1 is prerequisite to the constitutive expression and IFN-γ-induced upregulation of B7-H1 (CD274)', *FEBS Letters*, 580(3), pp. 755–762. doi: 10.1016/j.febslet.2005.12.093.

Leonard, B. *et al.* (2015) 'The PKC/NF-κB signaling pathway induces APOBEC3B expression in multiple human cancers.', *Cancer research*, 75(21), pp. 4538–4547. doi: 10.1158/0008-5472.CAN-15-2171-T.

Levin, V. A. *et al.* (2010) 'Different changes in protein and phosphoprotein levels result from serum starvation of high-grade glioma and adenocarcinoma cell lines.', *Journal of proteome research*, 9(1), pp. 179–191. doi: 10.1021/pr900392b.

Levy, D. E. *et al.* (1989) 'Cytoplasmic activation of ISGF3, the positive regulator of interferon-alpha-stimulated transcription, reconstituted in vitro.', *Genes & development*, 3(9), pp. 1362–1371. doi: 10.1101/gad.3.9.1362.

Levy, V. *et al.* (2005) 'Distinct stem cell populations regenerate the follicle and interfollicular epidermis.', *Developmental cell*, 9(6), pp. 855–861. doi: 10.1016/j.devcel.2005.11.003.

Lew, D. J. and Kornbluth, S. (1996) 'Regulatory roles of cyclin dependent kinase phosphorylation in cell cycle control.', *Current opinion in cell biology*, 8(6), pp. 795–804. doi: 10.1016/s0955-0674(96)80080-9.

Li, D. *et al.* (2019) 'STING-Mediated IFI16 Degradation Negatively Controls Type I Interferon Production', *Cell Reports*, 29(5), pp. 1249–1260.e4. doi: 10.1016/j.celrep.2019.09.069.

Li, J. *et al.* (2014) 'APOBEC3 Multimerization Correlates with HIV-1 Packaging and Restriction Activity in Living Cells', *Journal of Molecular Biology*, 426(6), pp. 1296–1307. doi: 10.1016/j.jmb.2013.12.014.

Li, J. and Gilmour, D. S. (2011) 'Promoter proximal pausing and the control of gene expression', *Current Opinion in Genetics and Development*, 21(2), pp. 231–235. doi: 10.1016/j.gde.2011.01.010.

Li, Z. *et al.* (2017) 'APOBEC signature mutation generates an oncogenic enhancer that drives LMO1 expression in T-ALL.', *Leukemia*, 31(10), pp. 2057–2064. doi: 10.1038/leu.2017.75.

Lian, L. H. *et al.* (2012) 'The double-stranded RNA analogue polyinosinic-polycytidylic acid induces keratinocyte pyroptosis and release of IL-36γ', *Journal of Investigative Dermatology*, 132(5), pp. 1346–1353. doi: 10.1038/jid.2011.482.

Liao, W. *et al.* (1999) 'APOBEC-2, a cardiac- and skeletal muscle-specific member of the cytidine deaminase supergene family', *Biochemical and Biophysical Research Communications*, 260(2), pp. 398–404. doi: 10.1006/bbrc.1999.0925.

Lin, H. *et al.* (2009) 'Primary Culture of Human Blood–Retinal Barrier Cells and Preliminary Study of APOBEC3 Expression: An In Vitro Study', *Investigative Opthalmology & Visual Science*, 50(9), p. 4436. doi: 10.1167/iovs.08-3169.

Lindahl, T. (1982) 'DNA repair enzymes.', *Annual review of biochemistry*, pp. 61–87. doi: 10.1146/annurev.bi.51.070182.000425.

Liu, S. *et al.* (2015) 'Phosphorylation of innate immune adaptor proteins MAVS, STING, and TRIF induces IRF3 activation', *Science*, 347(6227), pp. aaa2630–aaa2630. doi: 10.1126/science.aaa2630.

Liu, S. *et al.* (2018) 'Size uniformity of animal cells is actively maintained by a p38 MAPK-dependent regulation of G1-length', *eLife*, 7, p. e26947. doi: 10.7554/eLife.26947.

Liu, T.-M. *et al.* (2019) 'Transcription Factor MafB Suppresses Type I Interferon Production by CD14+ Monocytes in Patients With Chronic Hepatitis C', *Frontiers in Microbiology*, 10, p. 1814. doi: 10.3389/fmicb.2019.01814.

Llames, S. *et al.* (2015) 'Feeder Layer Cell Actions and Applications.', *Tissue engineering. Part B, Reviews*, 21(4), pp. 345–353. doi: 10.1089/ten.TEB.2014.0547.

Logue, E. C. *et al.* (2014) 'A DNA Sequence Recognition Loop on APOBEC3A Controls Substrate Specificity', *PLoS ONE*, 9(5), p. e97062. doi: 10.1371/journal.pone.0097062.

Lolli, G. and Johnson, L. N. (2005) 'CAK-Cyclin-dependent Activating Kinase: a key kinase in cell cycle control and a target for drugs?', *Cell cycle*, 4(4), pp. 572–577.

Love, R. P., Xu, H. and Chelico, L. (2012) 'Biochemical Analysis of Hypermutation by the Deoxycytidine Deaminase APOBEC3A', *Journal of Biological Chemistry*, 287(36), pp. 30812–30822. doi: 10.1074/jbc.M112.393181.

Lu, C. *et al.* (2008) 'Serum starvation induces H2AX phosphorylation to regulate apoptosis via p38 MAPK pathway', *FEBS Letters*, 582(18), pp. 2703–2708. doi: 10.1016/j.febslet.2008.06.051.

Lu, X. *et al.* (2016) 'Multiple P-TEFbs cooperatively regulate the release of promoter-proximally paused RNA polymerase II.', *Nucleic acids research*, 44(14), pp. 6853–6867. doi: 10.1093/nar/gkw571.

Lucifora, J. *et al.* (2014) 'Specific and Nonhepatotoxic Degradation of Nuclear Hepatitis B Virus cccDNA', *Science*, 343(6176), pp. 1221–1228. doi: 10.1126/science.1243462.

Lulli, D., Carbone, M. L. and Pastore, S. (2017) 'The MEK Inhibitors Trametinib and Cobimetinib Induce a Type I Interferon Response in Human Keratinocytes', *International journal of molecular sciences*, 18(10), p. 2227. doi: 10.3390/ijms18102227.

Luo, Y., Na, Z. and Slavoff, S. A. (2018) 'P-Bodies: Composition, Properties, and Functions', *Biochemistry*, pp. 2424–2431. doi: 10.1021/acs.biochem.7b01162.

Madsen, P. *et al.* (1999) 'Psoriasis Upregulated Phorbolin-1 Shares Structural but not Functional Similarity to the mRNA-Editing Protein Apobec-1', *Journal of Investigative Dermatology*, 113(2), pp. 162–169. doi: 10.1046/j.1523-1747.1999.00682.x.

Mangeat, B. *et al.* (2003) 'Broad antiretroviral defence by human APOBEC3G through lethal editing of nascent reverse transcripts', *Nature*, 424(6944), pp. 99–103. doi: 10.1038/nature01709.

Mankan, A. K. *et al.* (2014) ' Cytosolic RNA:DNA hybrids activate the cGAS –STING axis', *The EMBO Journal*, 33(24), pp. 2937–2946. doi: 10.15252/embj.201488726.

Marescal, O. and Cheeseman, I. M. (2020) 'Cellular Mechanisms and Regulation of Quiescence', *Developmental Cell*, 55(3), pp. 259–271. doi: https://doi.org/10.1016/j.devcel.2020.09.029.

Marin, M. *et al.* (2008) 'Human Immunodeficiency Virus Type 1 Vif Functionally Interacts with Diverse APOBEC3 Cytidine Deaminases and Moves with Them between Cytoplasmic Sites of mRNA Metabolism', *Journal of Virology*, 82(2), pp. 987–998. doi: 10.1128/JVI.01078-07.

Marino, D. *et al.* (2016) 'APOBEC4 Enhances the Replication of HIV-1', *PLoS ONE*, 11(6). doi: 10.1371/journal.pone.0155422.

Martinez-Zapien, D. *et al.* (2016) 'Structure of the E6/E6AP/p53 complex required for HPV-mediated degradation of p53', *Nature*, 529(7587), pp. 541–545. doi: 10.1038/nature16481.

Maruyama, W. *et al.* (2016) 'Classical NF-κB pathway is responsible for APOBEC3B expression in cancer cells', *Biochemical and Biophysical Research Communications*, 478(3), pp. 1466–1471. doi: 10.1016/j.bbrc.2016.08.148.

Masani, S., Han, L. and Yu, K. (2013) 'Apurinic/Apyrimidinic Endonuclease 1 Is the Essential Nuclease during Immunoglobulin Class Switch Recombination', *Molecular and Cellular Biology*, 33(7), pp. 1468–1473. doi: 10.1128/mcb.00026-13.

Matrka, M. C. *et al.* (2015) 'DEK over-expression promotes mitotic defects and micronucleus formation.', *Cell cycle*, 14(24), pp. 3939–3953. doi: 10.1080/15384101.2015.1044177.

Matson, J. P. and Cook, J. G. (2017) 'Cell cycle proliferation decisions: the impact of single cell analyses', *FEBS Journal*, 284(3), pp. 362–375. doi: 10.1111/febs.13898.

Matsumoto, Y. *et al.* (2007) 'Helicobacter pylori infection triggers aberrant expression of activation-induced cytidine deaminase in gastric epithelium', *Nature Medicine*, 13(4), pp. 470–476. doi: 10.1038/nm1566.

Matsumoto, Y. *et al.* (2010) 'Up-regulation of activation-induced cytidine deaminase causes genetic aberrations at the CDKN2b-CDKN2a in gastric cancer', *Gastroenterology*, 139(6), pp. 1984–1994. doi: 10.1053/j.gastro.2010.07.010.

Matsuoka, S., Huang, M. and Elledge, S. J. (1998) 'Linkage of ATM to cell cycle regulation by the Chk2 protein kinase.', *Science*, 282(5395), pp. 1893–1897. doi: 10.1126/science.282.5395.1893.

Matthews, J. R. *et al.* (1993) 'Interaction of the C-terminal region of p105 with the nuclear localisation signal of p50 is required for inhibition of NF-xB DNA binding activity', *Nucleic Acids Research*, *21*(19), 4516–4523. https://doi.org/10.1093/nar/21.19.4516.

Mehta, A. *et al.* (2000) 'Molecular Cloning of Apobec-1 Complementation Factor, a Novel RNA-Binding Protein Involved in the Editing of Apolipoprotein B mRNA', *Molecular and Cellular Biology*, 20(5), pp. 1846–1854. doi: 10.1128/mcb.20.5.1846-1854.2000.

Mehta, H V *et al.* (2012) 'IFN- and Lipopolysaccharide Upregulate APOBEC3 mRNA through Different Signaling Pathways', *The Journal of Immunology*, 189(8), pp. 4088–4103. doi: 10.4049/jimmunol.1200777.

Mehta, Harshini V *et al.* (2012) 'IFN-α and Lipopolysaccharide Upregulate APOBEC3 mRNA through Different Signaling Pathways', *The Journal of Immunology*, 189(8), pp. 4088–4103. doi: 10.4049/jimmunol.1200777.

Meng, X. *et al.* (2018) 'MAPK Pathway Involved in Epidermal Terminal Differentiation of Normal Human Epidermal Keratinocytes', *Open medicine*, 13, pp. 189–195. doi: 10.1515/med-2018-0029.

Meshcheryakova, A. *et al.* (2021) 'AID and APOBECs as Multifaceted Intrinsic Virus-Restricting Factors: Emerging Concepts in the Light of COVID-19.', *Frontiers in immunology*, 12, p. 690416. doi: 10.3389/fimmu.2021.690416.

Meyer, M. *et al.* (2012) 'FGF receptors 1 and 2 are key regulators of keratinocyte migration in vitro and in wounded skin', *Journal of cell science*, 125(Pt 23), pp. 5690–5701. doi: 10.1242/jcs.108167.

Mi, B. *et al.* (2018) 'Icariin promotes wound healing by enhancing the migration and proliferation of keratinocytes via the AKT and ERK signaling pathway', *International journal of molecular medicine*, 42(2), pp. 831–838. doi: 10.3892/ijmm.2018.3676.

Mikl, M. C. *et al.* (2005) 'Mice Deficient in APOBEC2 and APOBEC3', *Molecular and cellular biology*, 25(16), pp. 7270–7277. doi: 10.1128/MCB.25.16.7270-7277.2005.

Milstein, C. and Neuberger, M. S. (1996) 'Maturation of the Immune Response', *Academic Press*, pp. 451–485. doi: 10.1016/S0065-3233(08)60494-5.

Mitra, M. *et al.* (2014) 'Structural determinants of human APOBEC3A enzymatic and nucleic acid binding properties', *Nucleic Acids Research*, 42(2), pp. 1095–1110. doi: 10.1093/nar/gkt945.

Miyazaki, T. and Arai, S. (2007) 'Two distinct controls of mitotic Cdk1/cyclin B1 activity requisite for cell growth prior to cell division', *Cell Cycle*, 6(12), pp. 1418–1424. doi: 10.4161/cc.6.12.4409.

Mognato, M., Burdak-Rothkamm, S. and Rothkamm, K. (2021) 'Interplay between DNA replication stress, chromatin dynamics and DNA-damage response for the maintenance of genome stability', *Mutation Research - Reviews in Mutation Research*, p. 108346. doi: 10.1016/j.mrrev.2020.108346.

Mohanram, V. *et al.* (2013) 'IFN- Induces APOBEC3G, F, and A in Immature Dendritic Cells and Limits HIV-1 Spread to CD4+ T Cells', *The Journal of Immunology*, 190(7), pp. 3346–3353. doi: 10.4049/jimmunol.1201184.

Montagnoli, A. *et al.* (1999) 'Ubiquitination of p27 is regulated by Cdk-dependent phosphorylation and trimeric complex formation.', *Genes & development*, 13(9), pp. 1181–1189. doi: 10.1101/gad.13.9.1181.

Mori, S. *et al.* (2015) 'Identification of APOBEC3B promoter elements responsible for activation by human papillomavirus type 16 E6', *Biochemical and Biophysical Research Communications*, 460(3), pp. 555–560. doi: 10.1016/j.bbrc.2015.03.068.

Mori, S. *et al.* (2017) 'Human Papillomavirus 16 E6 Upregulates APOBEC3B via the TEAD Transcription Factor', *Journal of Virology*, 91(6), pp. e02413–16. doi: 10.1128/JVI.02413-16.

Muckenfuss, H. *et al.* (2006) 'APOBEC3 Proteins Inhibit Human LINE-1 Retrotransposition', *Journal of Biological Chemistry*, 281(31), pp. 22161–22172. doi: 10.1074/jbc.M601716200.

Mullane, S. A. *et al.* (2016) 'Correlation of Apobec mRNA Expression with overall Survival and pd-l1 Expression in Urothelial Carcinoma', 6. doi: 10.1038/srep27702.

Münger, K. *et al.* (2004) 'Mechanisms of human papillomavirus-induced oncogenesis.', *Journal of virology*, 78(21), pp. 11451–11460. doi: 10.1128/JVI.78.21.11451-11460.2004.

Muramatsu, M. *et al.* (1999) 'Specific Expression of Activation-induced Cytidine Deaminase (AID), a Novel Member of the RNA-editing Deaminase Family in Germinal Center B Cells', *Journal of Biological Chemistry*. Available at: http://www.jbc.org/.

Muramatsu, M. *et al.* (2000) 'Class switch recombination and hypermutation require activation-induced cytidine deaminase (AID), a potential RNA editing enzyme', *Cell*, 102(5), pp. 553–563. doi: 10.1016/S0092-8674(00)00078-7.

Mussil, B. *et al.* (2013) 'Human APOBEC3A Isoforms Translocate to the Nucleus and Induce DNA Double Strand Breaks Leading to Cell Stress and Death', *PLoS ONE*, 8(8), p. e73641. doi: 10.1371/journal.pone.0073641.

Muto, T. *et al.* (2000) 'Isolation, tissue distribution, and chromosomal localization of the human activation-induced cytidine deaminase (AID) gene', *Genomics*, 68(1), pp. 85–88. doi: 10.1006/geno.2000.6268.

Nagelhus, T. A. *et al.* (1997) 'A sequence in the N-terminal region of human uracil-DNA glycosylase with homology to XPA interacts with the C-terminal part of the 34-kDa subunit of replication protein A', *Journal of Biological Chemistry*, 272(10), pp. 6561–6566. doi: 10.1074/jbc.272.10.6561.

Nair, S. and Zlotnick, A. (2018) 'Asymmetric Modification of Hepatitis B Virus (HBV) Genomes by an Endogenous Cytidine Deaminase inside HBV Cores Informs a Model of Reverse Transcription', *Journal of Virology*, 92(10). doi: 10.1128/jvi.02190-17.

Nakahara, M. *et al.* (2018) 'Effect of a p38 mitogen-activated protein kinase inhibitor on corneal endothelial cell proliferation', *Investigative Ophthalmology and Visual Science*, 59(10), pp. 4218–4227. doi: 10.1167/iovs.18-24394.

Nakaya, Y. *et al.* (2016) 'In Vivo Examination of Mouse APOBEC3- and Human APOBEC3A- and APOBEC3G-Mediated Restriction of Parvovirus and Herpesvirus Infection in Mouse Models', *Journal of Virology*, 90(17), pp. 8005–8012. doi: 10.1128/JVI.00973-16.

Narasimha, A. M. *et al.* (2014) 'Cyclin D activates the Rb tumor suppressor by mono-phosphorylation', *eLife*, Jun 4;3:e02872. doi: 10.7554/eLife.02872. PMID: 24876129; PMCID: PMC4076869.

Narvaiza, I. *et al.* (2009) 'Deaminase-Independent Inhibition of Parvoviruses by the APOBEC3A Cytidine Deaminase', *PLoS Pathogens*, 5(5), p. e1000439. doi: 10.1371/journal.ppat.1000439.

Navaratnam, N. *et al.* (1993) 'The p27 Catalytic Subunit of the Apolipoprotein B mRNA Editing Enzyme Is a Cytidine Deaminase', *The Journal of Biological Chemistry,* Oct 5;268(28):20709-12. PMID: 8407891.

Nees, M. *et al.* (2001) 'Papillomavirus Type 16 Oncogenes Downregulate Expression of Interferon-Responsive Genes and Upregulate Proliferation-Associated and NF-B-Responsive Genes in Cervical Keratinocytes', *Journal of Virology*, 75(9), pp. 4283–4296. doi: 10.1128/JVI.75.9.4283-4296.2001.

Newton, A. C. (2003) 'Regulation of the ABC kinases by phosphorylation: protein kinase C as a paradigm.', *The Biochemical journal*, 370(Pt 2), pp. 361–371. doi: 10.1042/BJ20021626.

Ng, J.C and Fraternali, F. (2020) 'Understanding the structural details of APOBEC3-DNA interactions using graph-based representations', *Current Research in Structural Biology*, 2, pp. 130–143. doi: https://doi.org/10.1016/j.crstbi.2020.07.001.

Ng, J. C. F. *et al.* (2019) 'Pan-cancer transcriptomic analysis dissects immune and proliferative functions of APOBEC3 cytidine deaminases', *Nucleic Acids Research*, 47(3), pp. 1178–1194. doi: 10.1093/nar/gky1316.

Niewiadomska, A. M. *et al.* (2007) 'Differential Inhibition of Long Interspersed Element 1 by APOBEC3 Does Not Correlate with High-Molecular-Mass-Complex Formation or P-Body Association', *Journal of Virology*, 81(17), pp. 9577–9583. doi: 10.1128/jvi.02800-06.

Nik-Zainal, S. *et al.* (2012) 'Mutational Processes Molding the Genomes of 21 Breast Cancers', *Cell*, 149(5), pp. 979–993. doi: 10.1016/j.cell.2012.04.024.

Nik-Zainal, S. *et al.* (2014) 'Association of a germline copy number polymorphism of APOBEC3A and APOBEC3B with burden of putative APOBEC-dependent mutations in breast cancer', *Nature Genetics*, 46(5), pp. 487–491. doi: 10.1038/ng.2955.

Nishikura, K. (2016) 'A-to-I editing of coding and non-coding RNAs by ADARs', *Nature Reviews Molecular Cell Biology*, pp. 83–96. doi: 10.1038/nrm.2015.4.

Nishizuka, Y. (1988) 'The molecular heterogeneity of protein kinase C and its implications for cellular regulation', *Nature*, pp. 661–665. doi: 10.1038/334661a0.

Novick, D., Cohen, B. and Rubinstein, M. (1994) 'The human interferon α β receptor: Characterization and molecular cloning', *Cell*, 77(3), pp. 391–400. doi: 10.1016/0092-8674(94)90154-6.

Novoa, E. M. and Ribas de Pouplana, L. (2012) 'Speeding with control: Codon usage, tRNAs, and ribosomes', *Trends in Genetics*, pp. 574–581. doi: 10.1016/j.tig.2012.07.006.

Nurse, P. (1994) 'Ordering S phase and M phase in the cell cycle.', *Cell*, 79(4), pp. 547–550. doi: 10.1016/0092-8674(94)90539-8.

Oh, S. *et al.* (2021) 'Genotoxic stress and viral infection induce transient expression of APOBEC3A and pro-inflammatory genes through two distinct pathways.', *Nature communications*, 12(1), p. 4917. doi: 10.1038/s41467-021-25203-4.

Ohba, K. *et al.* (2014) 'In Vivo and In Vitro Studies Suggest a Possible Involvement of HPV Infection in the Early Stage of Breast Carcinogenesis via APOBEC3B Induction', *PLoS ONE*, 9(5), p. e97787. doi: 10.1371/journal.pone.0097787.

Ohtsubo, M. *et al.* (1995) 'Human cyclin E, a nuclear protein essential for the G1-to-S phase transition.', *Molecular and cellular biology*, 15(5), pp. 2612–2624. doi: 10.1128/MCB.15.5.2612.

Ojesina, A. I. *et al.* (2014) 'Landscape of genomic alterations in cervical carcinomas.', *Nature*, 506(7488), pp. 371–375. doi: 10.1038/nature12881.

Okada, N., Kitano, Y. and Ichihara, K. (1982) 'Effects of cholera toxin on proliferation of cultured human keratinocytes in relation to intracellular cyclic AMP levels', *Journal of Investigative Dermatology*, 79(1), pp. 42–47. doi: 10.1111/1523-1747.ep12510580.

Okazaki, I. M. *et al.* (2003) 'Constitutive expression of AID leads to tumorigenesis', *Journal of Experimental Medicine*, 197(9), pp. 1173–1181. doi: 10.1084/jem.20030275.

Okazaki, R. *et al.* (1968) 'Mechanism of DNA chain growth. I. Possible discontinuity and unusual secondary structure of newly synthesized chains.', *Proceedings of the National Academy of Sciences of the United States of America*, 59(2), pp. 598–605. doi: 10.1073/pnas.59.2.598.

Okeoma, C. M. *et al.* (2009) 'Induction of APOBEC3 In Vivo Causes Increased Restriction of Retrovirus Infection', *Journal of Virology*, 83(8), pp. 3486–3495. doi: 10.1128/JVI.02347-08.

Ooms, M. *et al.* (2012) 'APOBEC3A, APOBEC3B, and APOBEC3H Haplotype 2 Restrict Human T-Lymphotropic Virus Type 1', *Journal of Virology*, 86(11), pp. 6097–6108. doi: 10.1128/JVI.06570-11.

Otterlei, M. *et al.* (1999) 'Post-replicative base excision repair in replication foci', *EMBO Journal*, 18(13), pp. 3834–3844. doi: 10.1093/emboj/18.13.3834.

Pagano, M. *et al.* (1992) 'Cyclin A is required at two points in the human cell cycle.', *The EMBO Journal*, 11(3), pp. 961–971. doi: https://doi.org/10.1002/j.1460-2075.1992.tb05135.x.

Paglia, D. *et al.* (1996) 'Leukaemia inhibitory factor is expressed by normal human keratinocytes in vitro and in vivo.', *The British journal of dermatology*, 134(5), pp. 817–823.

Pak, V. *et al.* (2011) 'The Role of Amino-Terminal Sequences in Cellular Localization and Antiviral Activity of APOBEC3B', *Journal of Virology*, 85(17), pp. 8538–8547. doi: 10.1128/JVI.02645-10.

Palm, W. and Thompson, C. B. (2017) 'Nutrient acquisition strategies of mammalian cells', *Nature*, 546(7657), pp. 234–242. doi: 10.1038/nature22379.

Papp, H. *et al.* (2003) 'Protein kinase C isozymes regulate proliferation and high cell density-mediated differentiation in HaCaT keratinocytes', *Experimental Dermatology*, pp. 811–824. doi: 10.1111/j.0906-6705.2003.00097.x.

Peisley, A. *et al.* (2013) 'RIG-I Forms Signaling-Competent Filaments in an ATP-Dependent, Ubiquitin-Independent Manner', *Molecular Cell*, 51(5), pp. 573–583. doi: 10.1016/j.molcel.2013.07.024.

Peng, G. *et al.* (2006) 'Induction of APOBEC3 family proteins, a defensive maneuver underlying interferon-induced anti-HIV-1 activity', *Journal of Experimental Medicine*, 203(1), pp. 41–46. doi: 10.1084/jem.20051512.

Periyasamy, M. *et al.* (2017) 'p53 controls expression of the DNA deaminase APOBEC3B to limit its potential mutagenic activity in cancer cells', *Nucleic Acids Research*. doi: 10.1093/nar/gkx721.

Petersen-Mahrt, S. K. and Neuberger, M. S. (2003) 'In vitro deamination of cytosine to uracil in single-stranded DNA by apolipoprotein B editing complex catalytic subunit 1 (APOBEC1)', *Journal of Biological Chemistry*, 278(22), pp. 19583–19586. doi: 10.1074/jbc.C300114200.

Petljak, M. *et al.* (2019) 'Characterizing Mutational Signatures in Human Cancer Cell Lines Reveals Episodic APOBEC Mutagenesis', *Cell*, 176(6), pp. 1282-1294.e20. doi: 10.1016/j.cell.2019.02.012.

Petrova, E. *et al.* (2019) 'Uncovering Flavivirus Host Dependency Factors through a Genome-Wide Gain-of-Function Screen', *Viruses* . doi: 10.3390/v11010068.

Pham, P. *et al.* (2003) 'Processive AID-catalysed cytosine deamination on single-stranded DNA simulates somatic hypermutation', *Nature*, 424(6944), pp. 103–107. doi: 10.1038/nature01760.

Pines, J. and Hunter, T. (1994) 'The differential localization of human cyclins A and B is due to a cytoplasmic retention signal in cyclin B', *The EMBO journal*, 13(16), pp. 3772–3781. Available at: https://pubmed.ncbi.nlm.nih.gov/8070405.

Pirkmajer, S. and Chibalin, A. V (2011) 'Serum starvation: caveat emptor', *American Journal of Physiology-Cell Physiology*, 301(2), pp. C272–C279. doi: 10.1152/ajpcell.00091.2011.

Plaksin, D., Baeuerle, P. A. and Eisenbach, L. (1993) 'KBF1 (p50 NF-kappa B homodimer) acts as a repressor of H-2Kb gene expression in metastatic tumor cells.', *The Journal of experimental medicine*, 177(6), pp. 1651–1662. doi: 10.1084/jem.177.6.1651.

Plataniassj, L. C., Uddins, S. and Colamonicin, O. R. (1994) 'Tyrosine Phosphorylation of the a and p Subunits of the Type I Interferon Receptor', *The Journal of Biological Chemistry*, 269(27), pp. 17761-17764.

Pouplard, C. *et al.* (2013) 'Risk of cancer in psoriasis: a systematic review and meta-analysis of epidemiological studies', *Journal of the European Academy of Dermatology and Venereology*, 27(SUPPL.3), pp. 36–46. doi: 10.1111/jdv.12165.

Powell, C., Cornblath, E. and Goldman, D. (2014) 'Zinc-binding domain-dependent, deaminase-independent actions of apolipoprotein B mRNA-editing enzyme, catalytic polypeptide 2 (apobec2), mediate its effect on zebrafish retina regeneration', *Journal of Biological Chemistry*, 289(42), pp. 28924–28941. doi: 10.1074/jbc.M114.603043.

Powell, C., Elsaeidi, F. and Goldman, D. (2012) 'Injury-dependent Müller Glia and Ganglion cell reprogramming during tissue regeneration requires Apobec2a and Apobec2b', *Journal of Neuroscience*, 32(3), pp. 1096–1109. doi: 10.1523/JNEUROSCI.5603-11.2012.

Powell, L. M. *et al.* (1987) 'A novel form of tissue-specific RNA processing produces apolipoprotein-B48 in intestine', *Cell*, 50(6), pp. 831–840. doi: 10.1016/0092-8674(87)90510-1.

Protter, D. S. W. and Parker, R. (2016) 'Principles and Properties of Stress Granules', *Trends in Cell Biology*, pp. 668–679. doi: 10.1016/j.tcb.2016.05.004.

Puri, P. L. *et al.* (2000) 'Induction of terminal differentiation by constitutive activation of p38 MAP kinase in human rhabdomyosarcoma cells', *Genes and Development*, 14(5), pp. 574–584. doi: 10.1101/gad.14.5.574.

Rada, C. *et al.* (2002) 'Immunoglobulin isotype switching is inhibited and somatic hypermutation perturbed in UNG-deficient mice', *Current Biology*. Curr Biol, 12(20), pp. 1748–1755. doi: 10.1016/S0960-9822(02)01215-0.

Ramiro, A. R. *et al.* (2004) 'AID is required for c-myc/IgH chromosome translocations in vivo', *Cell*, 118(4), pp. 431–438. doi: 10.1016/j.cell.2004.08.006.

Ran, F. A. *et al.* (2013) 'Double nicking by RNA-guided CRISPR Cas9 for enhanced genome editing specificity', *Cell*, 155(2), pp. 479–480. doi: 10.1016/j.cell.2013.09.040.

Rasmussen, H. H. and Celis, J. E. (1993) 'Evidence for an altered protein kinase C (PKC) signaling pathway in psoriasis', *Journal of Investigative Dermatology,* 101(4), pp. 560–566. doi: 10.1111/1523-1747.ep12365986.

Raynaud, F. and Evain-Brion, D. (1991) 'Protein kinase C activity in normal and psoriatic cells: cultures of fibroblasts and lymphocytes', *British Journal of Dermatology*, 124(6), pp. 542–546. doi: 10.1111/j.1365-2133.1991.tb04947.x.

Refsland, E. W. *et al.* (2010) 'Quantitative profiling of the full APOBEC3 mRNA repertoire in lymphocytes and tissues: implications for HIV-1 restriction', *Nucleic Acids Research*, 38(13), pp. 4274–4284. doi: 10.1093/nar/gkq174.

Renner, T. M. *et al.* (2018) 'Characterization of molecular attributes that influence LINE-1 restriction by all seven human APOBEC3 proteins', *Virology*, 520, pp. 127–136. doi: 10.1016/j.virol.2018.05.015.

Revy, P. *et al.* (2000) 'Activation-Induced Cytidine Deaminase (AID) Deficiency Causes the Autosomal Recessive Form of the Hyper-IgM Syndrome (HIGM2)' *Cell,* Sep 1;102(5):565-75. doi: 10.1016/s0092-8674(00)00079-9. PMID: 11007475.

Richardson, H. *et al.* (2003) 'The natural history of type-specific human papillomavirus infections in female university students.', *Cancer epidemiology, biomarkers & prevention*, 12(6), pp. 485–490. Available at: http://www.ncbi.nlm.nih.gov/pubmed/12814991.

Richardson, S. R. *et al.* (2014) 'APOBEC3A deaminates transiently exposed single-strand DNA during LINE-1 retrotransposition.', *eLife*, 3, p. e02008. Available at: http://www.ncbi.nlm.nih.gov/pubmed/24843014.

Richter, J. D. and Coller, J. (2015) 'Pausing on Polyribosomes: Make Way for Elongation in Translational Control.', *Cell*, 163(2), pp. 292–300. doi: 10.1016/j.cell.2015.09.041.

Roberts, S. A. *et al.* (2013) 'An APOBEC cytidine deaminase mutagenesis pattern is widespread in human cancers', *Nature Genetics*, 45(9), pp. 970–976. doi: 10.1038/ng.2702.

Robinson, A. *et al.* (2021) 'Monocyte Regulation in Homeostasis and Malignancy', *Trends in Immunology*, pp. 104–119. doi: 10.1016/j.it.2020.12.001.

Roelofs, P. A. *et al.* (2020) 'Characterization of the mechanism by which the rb/e2f pathway controls expression of the cancer genomic dna deaminase apobec3b', *eLife*, 9, pp. 1–64. doi: 10.7554/ELIFE.61287.

Rogozin, I. B. *et al.* (2005) 'APOBEC4, a new member of the AID/APOBEC family of polynucleotide (deoxy)cytidine deaminases predicted by computational analysis', *Cell Cycle*, 4(9), pp. 1281–1285. doi: 10.4161/cc.4.9.1994.

Rose, K. M. *et al.* (2004) 'Transcriptional regulation of APOBEC3G, a cytidine deaminase that hypermutates human immunodeficiency virus', *Journal of Biological Chemistry*, 279(40), pp. 41744–41749. doi: 10.1074/jbc.M406760200.

Rosenberg, B. R. *et al.* (2011) 'Transcriptome-wide sequencing reveals numerous APOBEC1 mRNA-editing targets in transcript 3′ UTRs', *Nature Structural and Molecular Biology*, 18(2), pp. 230–238. doi: 10.1038/nsmb.1975.

Roskoski, R. J. (2019) ‘Small molecule inhibitors targeting the EGFR/ErbB family of protein-tyrosine kinases in human cancers.’, *Pharmacological research*, 139, pp. 395–411. doi: 10.1016/j.phrs.2018.11.014.

Roth, S. H. *et al.* (2018) ‘Increased RNA Editing May Provide a Source for Autoantigens in Systemic Lupus Erythematosus’, *Cell Reports*, 23(1), pp. 50–57. doi: 10.1016/j.celrep.2018.03.036.

Rougvie, A. E. and Lis, J. T. (1988) ‘The RNA polymerase II molecule at the 5’ end of the uninduced hsp70 gene of D. melanogaster is transcriptionally engaged.’, *Cell*, 54(6), pp. 795–804. doi: 10.1016/s0092-8674(88)91087-2.

Rouse, J. *et al.* (1994) ‘A novel kinase cascade triggered by stress and heat shock that stimulates MAPKAP kinase-2 and phosphorylation of the small heat shock proteins’, *Cell*, 78(6), pp. 1027–1037. doi: 10.1016/0092-8674(94)90277-1.

Le Roy, H. *et al.* (2010) ‘Asymmetric Distribution of Epidermal Growth Factor Receptor Directs the Fate of Normal and Cancer Keratinocytes In Vitro’, *Stem Cells and Development*, 19(2), pp. 209–220. doi: 10.1089/scd.2009.0150.

Rundhaug, J. E. and Fischer, S. M. (2010) ‘Molecular Mechanisms of Mouse Skin Tumor Promotion’, *Cancers*, 2(2), pp. 436–482. doi: 10.3390/cancers2020436.

Saitoh, T. *et al.* (2009) ‘Atg9a controls dsDNA-driven dynamic translocation of STING and the innate immune response’, *Proceedings of the National Academy of Sciences of the United States of America*, 106(49), pp. 20842–20846. doi: 10.1073/pnas.0911267106.

Salamango, D. J. *et al.* (2018) ‘APOBEC3B Nuclear Localization Requires Two Distinct N-Terminal Domain Surfaces.’, *Journal of molecular biology*, 430(17), pp. 2695–2708. doi: 10.1016/j.jmb.2018.04.044.

Salvadori, G. *et al.* (2021) ‘Article Fasting-mimicking diet blocks triple-negative breast cancer and cancer stem cell escape Fasting-mimicking diet blocks triple-negative breast cancer and cancer stem cell escape’, *Cell Metabolism*, 33(11), pp. 2247-2259.e6. doi: 10.1016/j.cmet.2021.10.008.

Sánchez, C. *et al.* (2011) ‘Activation of autophagy in mesenchymal stem cells provides tumor stromal support.’, *Carcinogenesis*, 32 7, pp. 964–972.

Saraconi, G. *et al.* (2014) ‘The RNA editing enzyme APOBEC1 induces somatic mutations and a compatible mutational signature is present in esophageal adenocarcinomas’, *Genome Biology*, 15(7), p. 417. doi: 10.1186/s13059-014-0417-z.

Saxton, R. A. and Sabatini, D. M. (2017) ‘mTOR Signaling in Growth, Metabolism, and Disease’, *Cell*, 168(6), pp. 960–976. doi: 10.1016/j.cell.2017.02.004.

Scheffner, M. *et al.* (1990) ‘The E6 oncoprotein encoded by human papillomavirus types 16 and 18 promotes the dagradation of p53’, *Cell*, 63, pp. 1129–1136.

Schlüter, H. *et al.* (2011) ‘Functional Characterization of Quiescent Keratinocyte Stem Cells and Their Progeny Reveals a Hierarchical Organization in Human Skin Epidermis’, *Stem Cells*, 29(8), pp. 1256–1268. doi: 10.1002/stem.675.

Schmidt, A., Caron, E. and Hall, A. (2001) 'Lipopolysaccharide-Induced Activation of β2-Integrin Function in Macrophages Requires Irak Kinase Activity, p38 Mitogen- Activated Protein Kinase, and the Rap1 GTPase', *Molecular and Cellular Biology*, 21(2), pp. 438–448. doi: 10.1128/mcb.21.2.438-448.2001.

Schreiner, B. *et al.* (2004) 'Interferon-β enhances monocyte and dendritic cell expression of B7-H1 (PD-L1), a strong inhibitor of autologous T-cell activation: Relevance for the immune modulatory effect in multiple sclerosis', *Journal of Neuroimmunology*, 155(1–2), pp. 172–182. doi: 10.1016/j.jneuroim.2004.06.013.

Schwartz, T. *et al.* (2001) 'Structure of the DLM-1-Z-DNA complex reveals a conserved family of Z-DNA-binding proteins', *Nature Structural Biology*, 8(9), pp. 761–765. doi: 10.1038/nsb0901-761.

Sen, R. and Baltimore, D. (1986) 'Multiple nuclear factors interact with the immunoglobulin enhancer sequences', *Cell*, 46(5), pp. 705–716. doi: 10.1016/0092-8674(86)90346-6.

Seplyarskiy, V. B. *et al.* (2016) 'APOBEC-induced mutations in human cancers are strongly enriched on the lagging DNA strand during replication', *Genome Research*, 26(2), pp. 174–182. doi: 10.1101/gr.197046.115.

Shandilya, S. M. D., Bohn, M. F. and Schiffer, C. A. (2014) 'A computational analysis of the structural determinants of APOBEC3's catalytic activity and vulnerability to HIV-1 Vif', *Virology*, 471–473, pp. 105–116. doi: 10.1016/j.virol.2014.09.023.

Sharma, S. *et al.* (2015) 'APOBEC3A cytidine deaminase induces RNA editing in monocytes and macrophages', *Nature Communications*, 6(1), pp. 1–15. doi: 10.1038/ncomms7881.

Sharma, S. *et al.* (2016) 'The double-domain cytidine deaminase APOBEC3G is a cellular site-specific RNA editing enzyme', *Scientific Reports*, 6(1), p. 39100. doi: 10.1038/srep39100.

Sharma, S. *et al.* (2017) 'Transient overexpression of exogenous APOBEC3A causes C-to-U RNA editing of thousands of genes', *RNA Biology*, 14(5), pp. 603–610. doi: 10.1080/15476286.2016.1184387.

Sharma, S. and Baysal, B. E. (2017) 'Stem-loop structure preference for site-specific RNA editing by APOBEC3A and APOBEC3G', *PeerJ*, 5, p. e4136. doi: 10.7717/peerj.4136.

Sheehy, A. M. *et al.* (2002) 'Isolation of a human gene that inhibits HIV-1 infection and is suppressed by the viral Vif protein', *Nature*, 418(6898), pp. 646–650. doi: 10.1038/nature00939.

Sherr, C. J. (1994) 'G1 phase progression: cycling on cue.', *Cell*, 79(4), pp. 551–555. doi: 10.1016/0092-8674(94)90540-1.

Sherr, C. and Roberts, J. (1999) 'CDK inhibitors: positive and negative regulators of G1-phase progression', *Genes & development*, 13(12), pp. 1501–1512. doi: 10.1101/GAD.13.12.1501.

Shi, K. *et al.* (2015) 'Crystal Structure of the DNA Deaminase APOBEC3B Catalytic Domain', *Journal of Biological Chemistry*, 290(47), pp. 28120–28130. doi: 10.1074/jbc.M115.679951.

Shieh, S. Y. *et al.* (1997) 'DNA damage-induced phosphorylation of p53 alleviates inhibition by MDM2.', *Cell*, 91(3), pp. 325–334. doi: 10.1016/s0092-8674(00)80416-x.

Shuai, K. *et al.* (1994) 'Interferon activation of the transcription factor Stat91 involves dimerization through SH2-phosphotyrosyl peptide interactions', *Cell*, 76(5), pp. 821–828. doi: 10.1016/0092-8674(94)90357-3.

Sieuwerts, A. M. *et al.* (2014) 'Elevated APOBEC3B Correlates with Poor Outcomes for Estrogen-Receptor-Positive Breast Cancers', *Hormones and Cancer*, 5(6), pp. 405–413. doi: 10.1007/s12672-014-0196-8.

Siriwardena, S. U. *et al.* (2018) 'A Tumor-Promoting Phorbol Ester Causes a Large Increase in APOBEC3A Expression and a Moderate Increase in APOBEC3B Expression in a Normal Human Keratinocyte Cell Line without Increasing Genomic Uracils', *Molecular and Cellular Biology*, 39(1). doi: 10.1128/mcb.00238-18.

Siriwardena, S. U., Guruge, T. A. and Bhagwat, A. S. (2015) 'Characterization of the Catalytic Domain of Human APOBEC3B and the Critical Structural Role for a Conserved Methionine', *Journal of Molecular Biology*, 427(19), pp. 3042–3055. doi: 10.1016/j.jmb.2015.08.006.

Skuse, G. R. *et al.* (1996) 'The neurofibromatosis type I messenger RNA undergoes base-modification RNA editing', *Nucleic Acids Research*, 1;24(3):478-85. doi: 10.1093/nar/24.3.478. PMID: 8602361; PMCID: PMC145654.

Smith, H. L. *et al.* (2020) 'DNA damage checkpoint kinases in cancer.', *Expert reviews in molecular medicine*, 22, p. e2. doi: 10.1017/erm.2020.3.

Smith, N. J. and Fenton, T. R. (2019) 'The APOBEC3 genes and their role in cancer: Insights from human papillomavirus', *Journal of Molecular Endocrinology*, pp. R269–R287. doi: 10.1530/JME-19-0011.

Smits, V. A. and Medema, R. H. (2001) 'Checking out the G(2)/M transition.', *Biochimica et biophysica acta*, 1519(1–2), pp. 1–12. doi: 10.1016/s0167-4781(01)00204-4.

Solca, F. *et al.* (2012) 'Target binding properties and cellular activity of afatinib (BIBW 2992), an irreversible ErbB family blocker.', *The Journal of pharmacology and experimental therapeutics*, 343(2), pp. 342–350. doi: 10.1124/jpet.112.197756.

Squarize, C. H. *et al.* (2010) 'Accelerated wound healing by mTOR activation in genetically defined mouse models.', *PloS one*, 5(5), p. e10643. doi: 10.1371/journal.pone.0010643.

Stanley, M. A. *et al.* (1989) 'Properties of a non-tumorigenic human cervical keratinocyte cell line', *International Journal of Cancer*, 43(4), pp. 672–676. doi: 10.1002/ijc.2910430422.

Starrett, G. J. *et al.* (2019) 'Polyomavirus T Antigen Induces APOBEC3B Expression Usingan LXCXE-Dependent and TP53-Independent Mechanism', *American Society for Microbiology*, 10(1), pp. 1–14.

Stathopoulou, K., Gaitanaki, C. and Beis, I. (2006) 'Extracellular pH changes activate the p38-MAPK signalling pathway in the amphibian heart', *Journal of Experimental Biology*, 209(7), pp. 1344–1354. doi: 10.1242/jeb.02134.

Stenglein, M. D. *et al.* (2010) 'APOBEC3 proteins mediate the clearance of foreign DNA from human cells', *Nature Structural & Molecular Biology*, 17(2), pp. 222–229. doi: 10.1038/nsmb.1744.

Stetson, D. B. *et al.* (2008) 'Trex1 Prevents Cell-Intrinsic Initiation of Autoimmunity', *Cell*, 134(4), pp. 587–598. doi: 10.1016/j.cell.2008.06.032.

Stopak, K. S. *et al.* (2007) 'Distinct patterns of cytokine regulation of APOBEC3G expression and activity in primary lymphocytes, macrophages, and dendritic cells', *Journal of Biological Chemistry*, 282(6), pp. 3539–3546. doi: 10.1074/jbc.M610138200.

Su, A. I. *et al.* (2004) 'A gene atlas of the mouse and human protein-encoding transcriptomes', *Proceedings of the National Academy of Sciences of the United States of America*, 101(16), pp. 6062–6067. doi: 10.1073/pnas.0400782101.

Sullivan, D. E. *et al.* (2005) 'Tumor necrosis factor-alpha induces transforming growth factor-beta1 expression in lung fibroblasts through the extracellular signal-regulated kinase pathway.', *American journal of respiratory cell and molecular biology*, 32(4), pp. 342–349. doi: 10.1165/rcmb.2004-0288OC.

Sun, L. *et al.* (2013) 'Cyclic GMP-AMP synthase is a cytosolic DNA sensor that activates the type I interferon pathway', *Science*, 339(6121), pp. 786–791. doi: 10.1126/science.1232458.

Sun, S. C. (2011) 'Non-canonical NF-κB signaling pathway', *Cell Research*, 21(1), pp. 71–85. doi: 10.1038/cr.2010.177.

Suri, B. K., Verma, N. K. and Schmidtchen, A. (2018) 'Toll-like receptor 3 agonist, polyinosinic-polycytidylic acid, upregulates carbonic anhydrase ii in human keratinocytes', *Acta Dermato-Venereologica*, 98(8), pp. 762–765. doi: 10.2340/00015555-2963.

Suspene, R. *et al.* (2011) 'Genetic Editing of Herpes Simplex Virus 1 and Epstein-Barr Herpesvirus Genomes by Human APOBEC3 Cytidine Deaminases in Culture and In Vivo', *Journal of Virology*, 85(15), pp. 7594–7602. doi: 10.1128/jvi.00290-11.

Suspène, R. *et al.* (2011) 'Somatic hypermutation of human mitochondrial and nuclear DNA by APOBEC3 cytidine deaminases, a pathway for DNA catabolism.', *Proceedings of the National Academy of Sciences of the United States of America*, 108(12), pp. 4858–4863. doi: 10.1073/pnas.1009687108.

Suspène, R. *et al.* (2017) 'Self-cytoplasmic DNA upregulates the mutator enzyme APOBEC3A leading to chromosomal DNA damage', *Nucleic Acids Research*, 45(6), p. gkx001. doi: 10.1093/nar/gkx001.

Swanton, C. *et al.* (2015) 'APOBEC Enzymes: Mutagenic Fuel for Cancer Evolution and Heterogeneity.', *Cancer discovery*, 5(7), pp. 704–712. doi: 10.1158/2159-8290.CD-15-0344.

Takaoka, A. *et al.* (2007) 'DAI (DLM-1/ZBP1) is a cytosolic DNA sensor and an activator of innate immune response', *Nature*, 448(7152), pp. 501–505. doi: 10.1038/nature06013.

Takatsuki, K. (2005) 'Discovery of adult T-cell leukemia', *Retrovirology*, p. 16. doi: 10.1186/1742-4690-2-16.

Takizawa, C. G. and Morgan, D. O. (2000) 'Control of mitosis by changes in the subcellular location of cyclin-B1-Cdk1 and Cdc25C.', *Current opinion in cell biology*, 12(6), pp. 658–665. doi: 10.1016/s0955-0674(00)00149-6.

Takizawa, C. G., Weis, K. and Morgan, D. O. (1999) 'Ran-independent nuclear import of cyclin B1-Cdc2 by importin beta.', *Proceedings of the National Academy of Sciences of the United States of America*, 96(14), pp. 7938–7943. doi: 10.1073/pnas.96.14.7938.

Tanaka, T. *et al.* (2006) 'Phosphorylation of histone H2AX on Ser 139 and activation of ATM during oxidative burst in phorbol ester-treated human leukocytes.', *Cell cycle*, 5(22), pp. 2671–2675. doi: 10.4161/cc.5.22.3472.

Tanaka, Y. *et al.* (2006) 'Anti-viral protein APOBEC3G is induced by interferon-α stimulation in human hepatocytes', *Biochemical and Biophysical Research Communications*, 341(2), pp. 314–319. doi: 10.1016/j.bbrc.2005.12.192.

Tang, Y. and Tian, X. (Cindy) (2013) 'JAK-STAT3 and somatic cell reprogramming', *Jak-Stat*, 2(4), p. e24935. doi: 10.4161/jkst.24935.

Tasker, C. *et al.* (2016) 'IFN-ε protects primary macrophages against HIV infection', *JCI Insight*, 1(20), p. e88255. doi: 10.1172/jci.insight.88255.

Taura, M. *et al.* (2019) 'Apobec3A maintains HIV-1 latency through recruitment of epigenetic silencing machinery to the long terminal repeat', *Proceedings of the National Academy of Sciences of the United States of America*, 116(6), pp. 2282–2289. doi: 10.1073/pnas.1819386116.

Tavaluc, R. T. *et al.* (2007) 'Effects of low confluency, serum starvation and hypoxia on the side population of cancer cell lines.', *Cell cycle*, 6(20), pp. 2554–2562. doi: 10.4161/cc.6.20.4911.

Taylor, B. J. M. *et al.* (2013) 'DNA deaminases induce break-associated mutation showers with implication of APOBEC3B and 3A in breast cancer kataegis', *eLife*, 2(2), p. e00534. doi: 10.7554/eLife.00534.

Thielen, B. K. *et al.* (2010) 'Innate immune signaling induces high levels of TC-specific deaminase activity in primary monocyte-derived cells through expression of APOBEC3A isoforms', *Journal of Biological Chemistry*, 285(36), pp. 27753–27766. doi: 10.1074/jbc.M110.102822.

Tilborghs, S. *et al.* (2017) 'The role of Nuclear Factor-kappa B signaling in human cervical cancer', *Critical Reviews in Oncology / Hematol*ogy pp. 120:141-150. doi: 10.1016 /j.critrevonc.2017.11.001.

Tjin, M. S. *et al.* (2018) 'Biologically relevant laminin as chemically defined and fully human platform for human epidermal keratinocyte culture', *Nature Communications*, 9(1). doi: 10.1038/s41467-018-06934-3.

Torrent, M. *et al.* (2018) 'Cells alter their tRNA abundance to selectively regulate protein synthesis during stress conditions', *Science Signaling*, 11(546), p. eaat6409. doi: 10.1126/scisignal.aat6409.

Toshchakov, V. *et al.* (2002) 'TLR4, but not TLR2, mediates IFN-β-induced STATIα/β-dependent gene expression in macrophages', *Nature Immunology*, 3(4), pp. 392–398. doi: 10.1038/ni774.

Trapp, S. *et al.* (2009) 'Double-Stranded RNA Analog Poly(I:C) Inhibits Human Immunodeficiency Virus Amplification in Dendritic Cells via Type I Interferon-Mediated Activation of APOBEC3G', *Journal of Virology*, 83(2), pp. 884–895. doi: 10.1128/jvi.00023-08.

Trotter, E. W. and Hagan, I. M. (2020) 'Release from cell cycle arrest with Cdk4/6 inhibitors generates highly synchronized cell cycle progression in human cell culture: Cdk4/6 Induction Synchronisation', *Open Biology*, 10(10). doi: 10.1098/rsob.200200rsob200200.

Tuller, T. *et al.* (2010) 'An evolutionarily conserved mechanism for controlling the efficiency of protein translation', *Cell*, 141(2), pp. 344–354. doi: 10.1016/j.cell.2010.03.031.

Tzenov, Y. R. *et al.* (2013) 'Human Papilloma Virus (HPV) E7-Mediated Attenuation of Retinoblastoma (Rb) Induces hPygopus2 Expression via Elf-1 in Cervical Cancer', *Molecular Cancer Research*, 11(1), pp. 19–30. doi: 10.1158/1541-7786.MCR-12-0510.

Uddin, S. *et al.* (1999) 'Activation of the p38 mitogen-activated protein kinase by type I interferons', *Journal of Biological Chemistry*, 274(42), pp. 30127–30131. doi: 10.1074/jbc.274.42.30127.

Upton, J. W., Kaiser, W. J. and Mocarski, E. S. (2012) 'DAI/ZBP1/DLM-1 complexes with RIP3 to mediate virus-induced programmed necrosis that is targeted by murine cytomegalovirus vIRA', *Cell Host and Microbe*, 11(3), pp. 290–297. doi: 10.1016/j.chom.2012.01.016.

Uzé, G., Lutfalla, G. and Gresser, I. (1990) 'Genetic transfer of a functional human interferon α receptor into mouse cells: Cloning and expression of its c-DNA', *Cell*, 60(2), pp. 225–234. doi: 10.1016/0092-8674(90)90738-Z.

Vaidya, A. A., Sharma, M. B. and Kale, V. P. (2008) 'Suppression of p38-stress kinase sensitizes quiescent leukemic cells to anti-mitotic drugs by inducing proliferative responses in them', *Cancer Biology and Therapy*, 7(8), pp. 1232–1240. doi: 10.4161/cbt.7.8.6262.

Vaidyanathan, S. *et al.* (2021) 'Thermoplastic nanofluidic devices for identifying abasic sites in single DNA molecules', *Lab on a Chip*, 21(8), pp. 1579–1589. doi: 10.1039/d0lc01038c.

van der Valk, J. *et al.* (2018) 'Fetal Bovine Serum (FBS): Past - Present - Future.', *ALTEX*, 35(1), pp. 99–118. doi: 10.14573/altex.1705101.

Vartanian, J.-P. *et al.* (2008) 'Evidence for editing of human papillomavirus DNA by APOBEC3 in benign and precancerous lesions.', *Science*, 320(5873), pp. 230–233. doi: 10.1126/science.1153201.

Vasquez, R. J. *et al.* (1997) 'Nanornolar Concentrations of Nocodazole Alter Microtubule Dynamic Instability In Vivo and In Vitro', *Molecular Biology of the Cell*, pp. 973–985.

Vermeulen, K., Van Bockstaele, D. R. and Berneman, Z. N. (2003) 'The cell cycle: a review of regulation, deregulation and therapeutic targets in cancer', *Cell proliferation*, 36(3), pp. 131–149. doi: 10.1046/j.1365-2184.2003.00266.x.

Vieira, V. C. *et al.* (2014) 'Human papillomavirus E6 triggers upregulation of the antiviral and cancer genomic DNA deaminase APOBEC3B', *mBio*, 5(6). doi: 10.1128/mBio.02234-14.

Vigerust, D. J. and Shepherd, V. L. (2007) 'Virus glycosylation: role in virulence and immune interactions', *Trends in microbiology*, 15(5), pp. 211–218. doi: 10.1016/j.tim.2007.03.003.

Voccola, S. *et al.* (2020) 'CARD14/CARMA2sh and TANK differentially regulate poly(I:C)–induced inflammatory reaction in keratinocytes', *Journal of Cellular Physiology*, 235(3), pp. 1895–1902. doi: 10.1002/jcp.29161.

Wakae, K. *et al.* (2018) 'Keratinocyte differentiation induces APOBEC3A, 3B, and mitochondrial DNA hypermutation', *Scientific Reports*, 8(1), pp. 1–11. doi: 10.1038/s41598-018-27930-z.

Walker, B. A. *et al.* (2015) 'APOBEC family mutational signatures are associated with poor prognosis translocations in multiple myeloma', *Nature Communications*, 6, p. 6997. doi: 10.1038/ncomms7997.

Wang, G. *et al.* (2018) 'p110α of PI3K is necessary and sufficient for quiescence exit in adult muscle satellite cells.', *The EMBO journal*, 37(8). doi: 10.15252/embj.201798239.

Wang, J. *et al.* (2002) 'MyD88 is involved in the signalling pathway for Taxol-induced apoptosis and TNF-alpha expression in human myelomonocytic cells', *British Journal of Haematology*, 118(2), pp. 638–645. doi: 10.1046/j.1365-2141.2002.03645.x.

Wang, Y. *et al.* (2017) 'HPV11 E6 mutation by overexpression of APOBEC3A and effects of interferon-ω on APOBEC3s and HPV11 E6 expression in HPV11.HaCaT cells', *Virology Journal*, 14(1). doi: 10.1186/s12985-017-0878-2.

Wang, Z. *et al.* (2014) 'APOBEC3 Deaminases Induce Hypermutation in Human Papillomavirus 16 DNA upon Beta Interferon Stimulation', *Journal of Virology*, 88(2), pp. 1308–1317. Available at: http://www.ncbi.nlm.nih.gov/pubmed/24227842.

Warren, C. J. *et al.* (2015) 'APOBEC3A Functions as a Restriction Factor of Human Papillomavirus', *Journal of Virology*, 89(1), pp. 688–702. Available at: http://www.ncbi.nlm.nih.gov/pubmed/25355878.

Warren, C. J. *et al.* (2017) 'Roles of APOBEC3A and APOBEC3B in Human Papillomavirus Infection and Disease Progression.', *Viruses*, 9(8). doi: 10.3390/v9080233.

Wedekind, J. E. *et al.* (2003) 'Messenger RNA editing in mammals: New members of the APOBEC family seeking roles in the family business', *Trends in Genetics*, pp. 207–216. doi: 10.1016/S0168-9525(03)00054-4.

Wee, P. and Wang, Z. (2017) 'Epidermal Growth Factor Receptor Cell Proliferation Signaling Pathways', *Cancers*, 9(5), p. 52. doi: 10.3390/cancers9050052.

Weisblum, Y. *et al.* (2017) 'APOBEC3A Is Upregulated by Human Cytomegalovirus (HCMV) in the Maternal-Fetal Interface, Acting as an Innate Anti-HCMV Effector', *Journal of Virology*, 91(23), pp. e01296–17. doi: 10.1128/JVI.01296-17.

Westrich, J. A. *et al.* (2018) 'Human Papillomavirus 16 E7 Stabilizes APOBEC3A Protein by Inhibiting Cullin 2-Dependent Protein Degradation', *Journal of Virology*, 92(7), pp. e01318-17. doi: 10.1128/JVI.01318-17.

Wiegand, H. L. and Cullen, B. R. (2007) 'Inhibition of Alpharetrovirus Replication by a Range of Human APOBEC3 Proteins', *Journal of Virology*, 81(24), pp. 13694–13699. doi: 10.1128/JVI.01646-07.

Wijesinghe, P. and Bhagwat, A. S. (2012) 'Efficient deamination of 5-methylcytosines in DNA by human APOBEC3A, but not by AID or APOBEC3G.', *Nucleic acids research*, 40(18), pp. 9206–9217. doi: 10.1093/nar/gks685.

Woodworth, C. D. *et al.* (1995) 'Interleukin 1α and tumor necrosis factor α stimulate autocrine amphiregulin expression and proliferation of human papillomavirus-immortalized and carcinoma-derived cervical epithelial cells', *Proceedings of the National Academy of Sciences of the United States of America*, 92(7), pp. 2840–2844. doi: 10.1073/pnas.92.7.2840.

Xiao, X. *et al.* (2017) 'Structural determinants of APOBEC3B non-catalytic domain for molecular assembly and catalytic regulation', *Nucleic Acids Research*, 45(12), pp. 7494–7506. doi: 10.1093/nar/gkx362.

Xiao, Z. *et al.* (2003) 'Chk1 mediates S and G2 arrests through Cdc25A degradation in response to DNA-damaging agents.', *The Journal of Biological Chemistry*, 278(24), pp. 21767–21773. doi: 10.1074/jbc.M300229200.

Xu, H. *et al.* (2003) 'Ras participates in CpG oligodeoxynucleotide signaling through association with toll-like receptor 9 and promotion of interleukin-1 receptor-associated kinase/tumor necrosis factor receptor-associated factor 6 complex formation in macrophages', *Journal of Biological Chemistry*, 278(38), pp. 36334–36340. doi: 10.1074/jbc.M305698200.

Xu, L. *et al.* (2015) 'High APOBEC3B expression is a predictor of recurrence in patients with low-risk clear cell renal cell carcinoma', *Urologic Oncology: Seminars and Original Investigations*, 33(8), pp. 340.e1–340.e8. doi: 10.1016/j.urolonc.2015.05.009.

Yablonovitch, A. L. *et al.* (2017) 'The evolution and adaptation of A-to-I RNA editing', *PLoS Genetics*. doi: 10.1371/journal.pgen.1007064.

Yamamoto, M. *et al.* (2002) 'Essential role for TIRAP in activation of the signalling cascade shared by TLR2 and TLR4', *Nature*, 420(6913), pp. 324–329. doi: 10.1038/nature01182.

Yamanaka, S. *et al.* (1995) 'Apolipoprotein B mRNA-editing protein induces hepatocellular carcinoma and dysplasia in transgenic animals', *Proceedings of the National Academy of Sciences of the United States of America*, 92(18), pp. 8483–8487. doi: 10.1073/pnas.92.18.8483.

Yamaoka, S. *et al.* (1998) 'Complementation cloning of NEMO, a component of the IκB kinase complex essential for NF-κB activation', *Cell*, 93(7), pp. 1231–1240. doi: 10.1016/S0092-8674(00)81466-X.

Yan, L., Zheng, D. and Xu, R. H. (2018) 'Critical role of tumor necrosis factor signaling in mesenchymal stem cell-based therapy for autoimmune and inflammatory diseases', *Frontiers in Immunology*. doi: 10.3389/fimmu.2018.01658.

Yan, N. *et al.* (2010) 'The cytosolic exonuclease TREX1 inhibits the innate immune response to human immunodeficiency virus type 1', *Nature Immunology*, 11(11), pp. 1005–1013. doi: 10.1038/ni.1941.

Yang, Y., Sowden, M. P. and Smith, H. C. (2000) 'Induction of cytidine to uridine editing on cytoplasmic apolipoprotein B mRNA by overexpressing APOBEC-1', *Journal of Biological Chemistry*, 275(30), pp. 22663–22669. doi: 10.1074/jbc.M910406199.

Yang, Y. Y., Yang, Y. Y. and Smith, H. C. (1997) 'Multiple protein domains determine the cell type-specific nuclear distribution of the catalytic subunit required for apolipoprotein B mRNA editing', *Proceedings of the National Academy of Sciences of the United States of America*, 94(24), pp. 13075–13080. doi: 10.1073/pnas.94.24.13075.

Yao, G. *et al.* (2008) 'A bistable Rb–E2F switch underlies the restriction point', *Nature Cell Biology*, 10(4), pp. 476–482. doi: 10.1038/ncb1711.

Yao, G. (2014) 'Modelling mammalian cellular quiescence', *Interface focus*, 4(3), p. 20130074. doi: 10.1098/rsfs.2013.0074.

Yao, J. *et al.* (2019) 'Induction of APOBEC3B cytidine deaminase in HTLV-1-infected humanized mice', *Experimental and therapeutic medicine*, 17(5), pp. 3701–3708. doi: 10.3892/etm.2019.7375.

Yarilina, A. *et al.* (2008) 'TNF activates an IRF1-dependent autocrine loop leading to sustained expression of chemokines and STAT1-dependent type I interferon–response genes', *Nature Immunology*, 9(4), pp. 378–387. doi: 10.1038/ni1576.

Yarosh, D. *et al.* (2000) 'Regulation of TNFalpha production and release in human and mouse keratinocytes and mouse skin after UV-B irradiation.', *Photodermatology, photoimmunology & photomedicine*, 16(6), pp. 263–270. doi: 10.1034/j.1600-0781.2000.160606.x.

Young, C. N. *et al.* (2008) 'Reactive oxygen species in tumor necrosis factor-alpha-activated primary human keratinocytes: implications for psoriasis and inflammatory skin disease', *The Journal of investigative dermatology*, 128(11), pp. 2606–2614. doi: 10.1038/jid.2008.122.

Zahoor, M. A. *et al.* (2014) 'HIV-1 Vpr Induces Interferon-Stimulated Genes in Human Monocyte-Derived Macrophages', *PLoS ONE*, 9(8), p. e106418. doi: 10.1371/journal.pone.0106418.

Zaiss, D. M. W. *et al.* (2015) 'Emerging functions of amphiregulin in orchestrating immunity, inflammation, and tissue repair', *Immunity*, pp. 216–226. doi: 10.1016/j.immuni.2015.01.020.

Zhang, H. *et al.* (2009) 'TEAD transcription factors mediate the function of TAZ in cell growth and epithelial-mesenchymal transition', *Journal of Biological Chemistry*, 284(20), pp. 13355–13362. doi: 10.1074/jbc.M900843200.

Zhang, H. S. *et al.* (2000) 'Exit from G1 and S phase of the cell cycle is regulated by repressor complexes containing HDAC-Rb-hSWI/SNF and Rb-hSWI/SNF.', *Cell*, 101(1), pp. 79–89. doi: 10.1016/S0092-8674(00)80625-X.

Zhang, M. *et al.* (2018) 'RNA editing derived epitopes function as cancer antigens to elicit immune responses', *Nature Communications*, 9(1). doi: 10.1038/s41467-018-06405-9.

Zhang, X., Zhang, R. and Yu, J. (2020) 'New Understanding of the Relevant Role of LINE-1 Retrotransposition in Human Disease and Immune Modulation', *Frontiers in Cell and Developmental Biology*, p. 657. doi: 10.3389/fcell.2020.00657.

Zhao, B. *et al.* (2008) 'TEAD mediates YAP-dependent gene induction and growth control', *Genes and Development*, 22(14), pp. 1962–1971. doi: 10.1101/gad.1664408.

Zhao, K. *et al.* (2021) 'Cytidine Deaminase APOBEC3A Regulates PD-L1 Expression in Cancer Cells in a JNK/c-JUN-dependent Manner', *Molecular Cancer Research*,.MCR-21-0219-A.2021. doi: 10.1158/1541-7786.MCR-21-0219.

Zhu, C., Li, L. and Zhao, B. 'The regulation and function of YAP transcription co-activator', *Acta Biochimica et Biophysica Sinica*, 47(1), pp. 16–28.

Zimmerman, E. S. *et al.* (2004) 'Human Immunodeficiency Virus Type 1 Vpr-Mediated G 2 Arrest Requires Rad17 and Hus1 and Induces Nuclear BRCA1 and γ-H2AX Focus Formation', *Molecular and Cellular Biology*, 24(21), pp. 9286–9294. doi: 10.1128/mcb.24.21.9286-9294.2004.

8 Supplementary

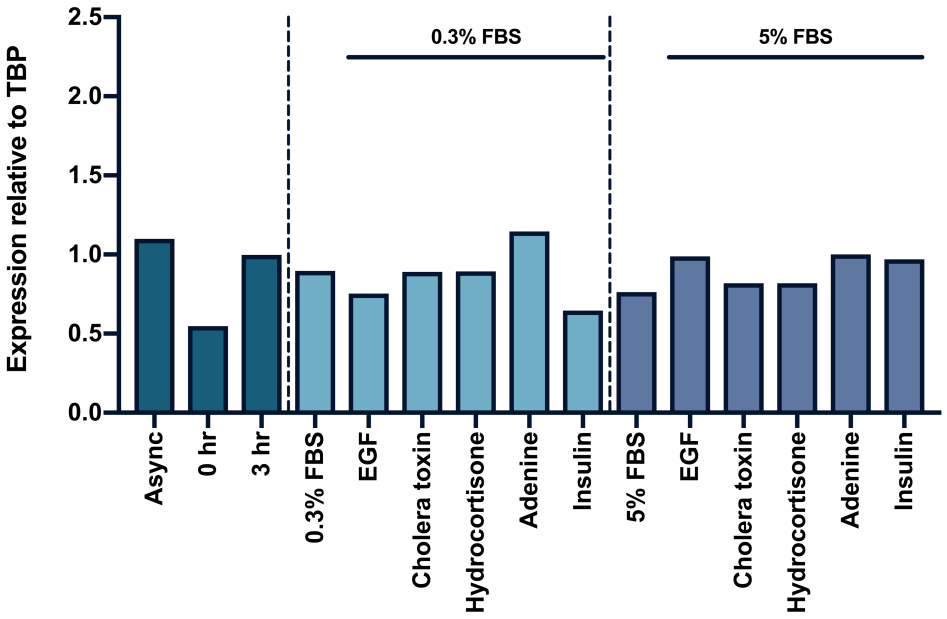

Figure 8-1 A3B is not induced by EGF in re-stimulated NIKS
WT-NIKS were serum starvation for 40 hr then re-stimulated for 3 hr with either F-12/DMEM (containing 0.3 or 5% FBS) plus either: 10 ng/ml EGF, 8.3 ng/ml cholera toxin, 0.4 μg/ml hydrocortisone, 24 μg/ml adenine, or 5 μg/ml insulin. A3B mRNA copy numbers are shown relative to TBP copies (n=1).

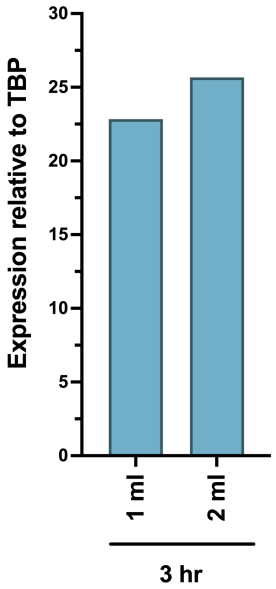

Figure 8-2 A3A induction is higher upon re-stimulation with increased media volume
WT-NIKS were serum starvation for 40 hr then re-stimulated for 3 hr with either 1 ml or 2 ml of FC media in 6-well plates. A3A mRNA levels detected by qPCR and copy numbers calculated relative to TBP copies (n=1).

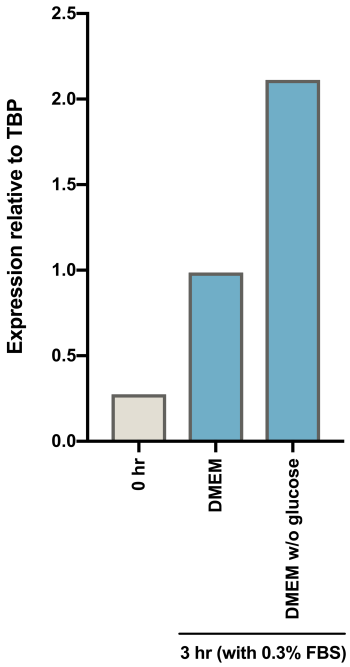

Figure 8-3 A3A induction is higher upon re-stimulation in glucose-free media
WT-NIKS were serum starvation for 40 hr then re-stimulated for 3 hr with either DMEM with 0.3% FBS, or glucose-free DMEM with 0.3% FBS. A3A mRNA levels detected by qPCR and copy numbers calculated relative to TBP copies (n=1).

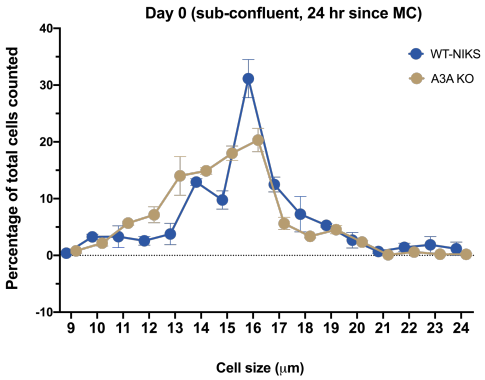
Day 0 (sub-confluent, 24 hr since MC)
WT-NIKS
A3A KO
Percentage of total cells counted
Cell size (μm)

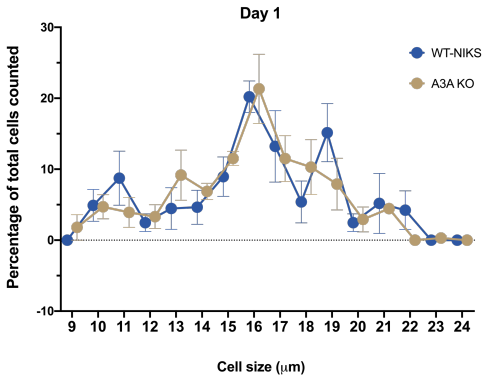
Day 1
WT-NIKS
A3A KO
Percentage of total cells counted
Cell size (μm)

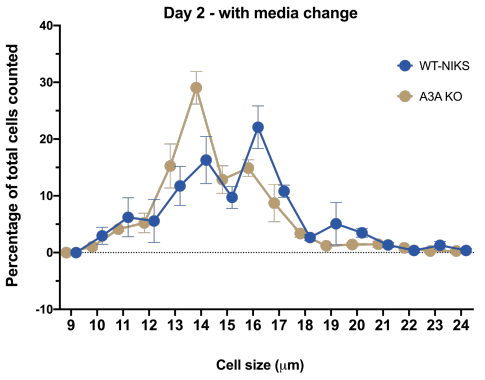
Day 2 - with media change
WT-NIKS
A3A KO
Percentage of total cells counted
Cell size (μm)

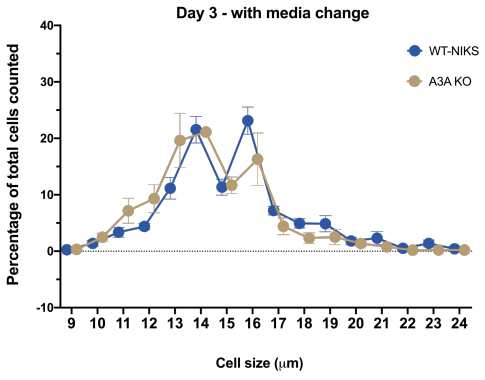
Day 3 - with media change
WT-NIKS
A3A KO
Percentage of total cells counted
Cell size (μm)

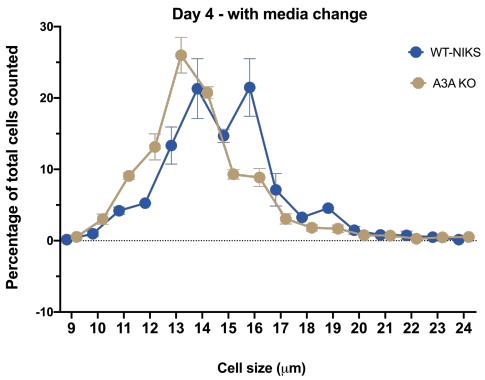
Day 4 - with media change
WT-NIKS
A3A KO
Percentage of total cells counted
Cell size (μm)

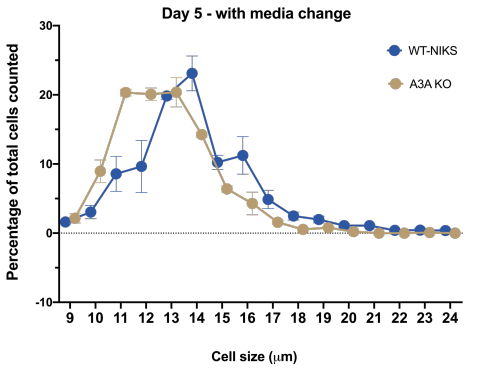
Day 5 - with media change
WT-NIKS
A3A KO
Percentage of total cells counted
Cell size (μm)

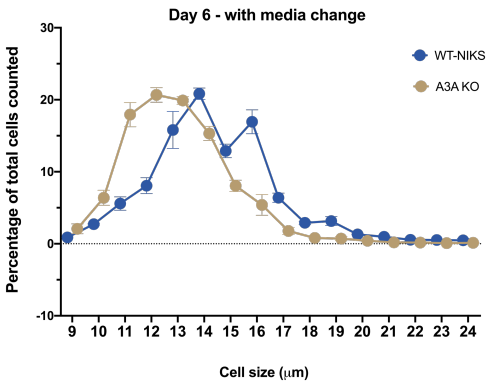
Day 6 - with media change
WT-NIKS
A3A KO
Percentage of total cells counted
Cell size (μm)

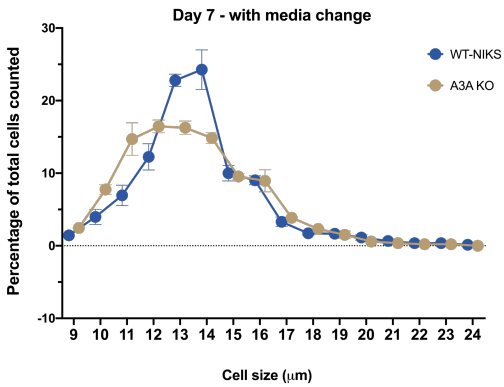
Day 7 - with media change
WT-NIKS
A3A KO
Percentage of total cells counted
Cell size (μm)

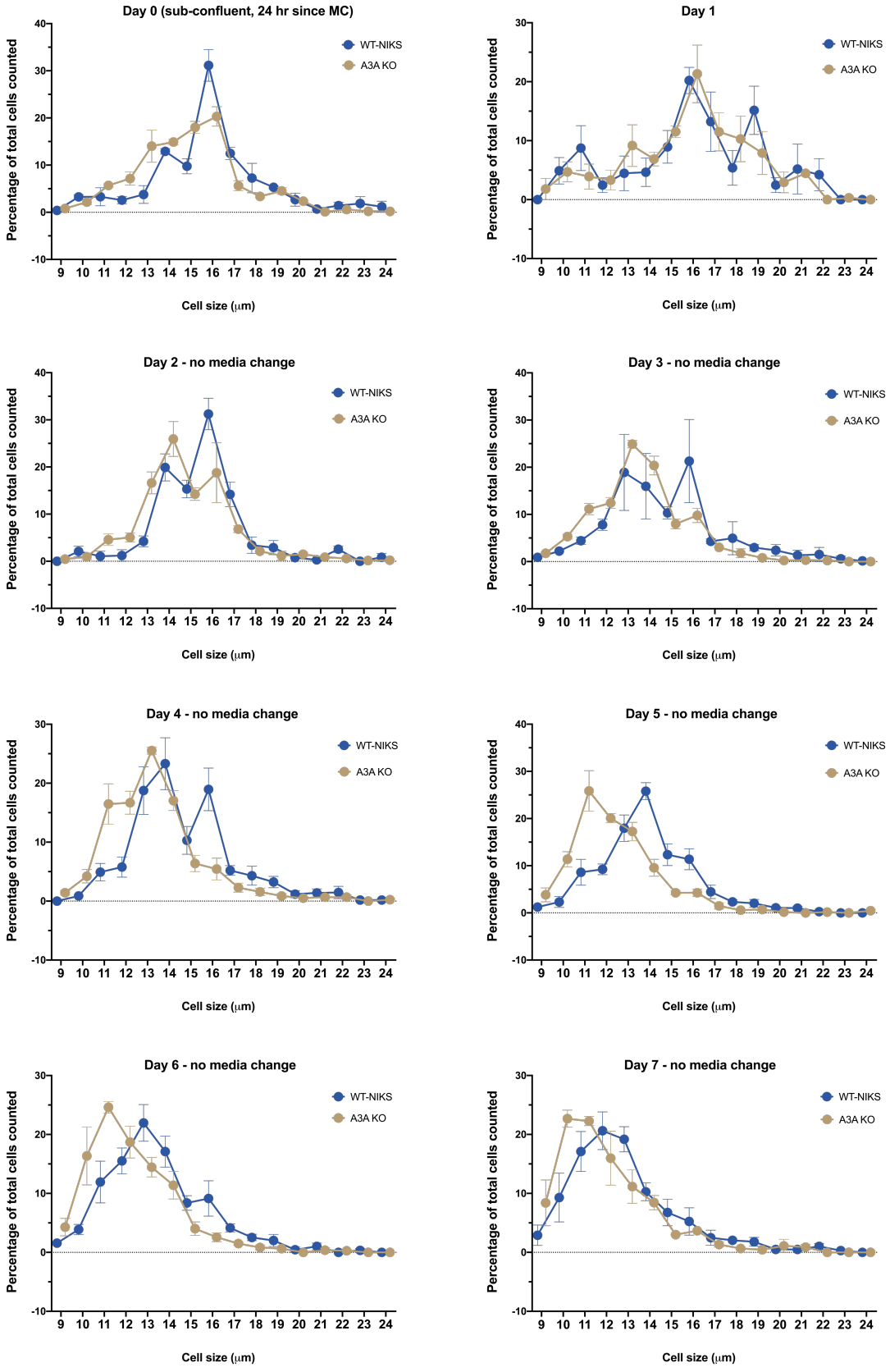

Figure 8-4 Cell size differences in WT-NIKS and A3A KO NIKS
Cell size measurements of each clone (three of A3A KO and three of mock-transfected NIKS were completed daily counting using a CellDrop™ automated cell counter. Error bars represent the SEM.

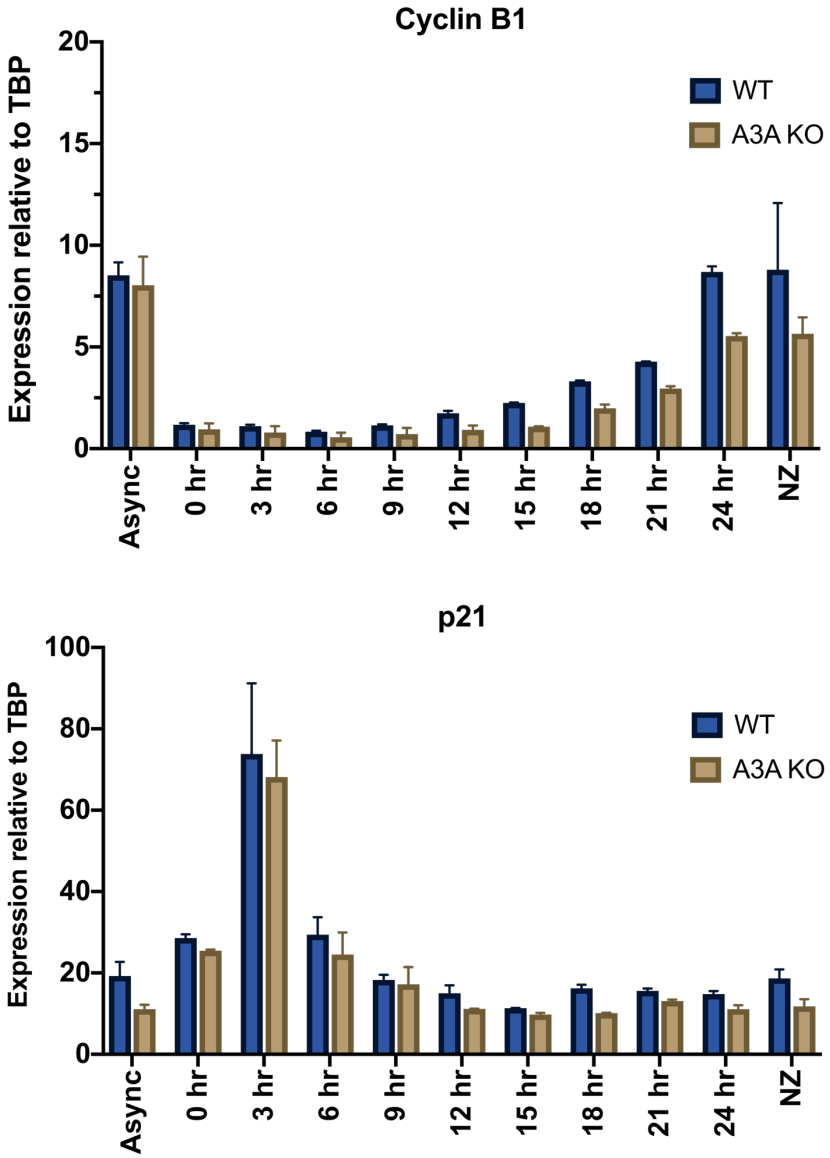

Figure 8-5 Cyclin B1 and p21 mRNA proceed similarly in WT-NIKS and A3A-KO NIKS following starvation / re-stimulation.
WT-NIKS and A3A KO NIKS were serum starved for 40 hrs then re-stimulated with FC media. Asynchronous cells were 18 hr post-media change. 100 ng/ml of nocodazole (NZ) was added at 18 hr post-release for a further 6 hrs to arrest cells in G2/M. mRNA copy numbers of p21 and cyclin B1 are shown relative to TBP copies (n=3).